

The chemotherapeutic effects of synthetic and natural compounds



Tshegofatso Harold Motau

A dissertation submitted to the Faculty of Health Sciences, University of the Witwatersrand, Johannesburg, in fulfilment of the requirements for the degree of Master of Science in Medicine.

Johannesburg, South Africa, 2015.

Declaration

I, Tshegofatso Harold Motau, declare that this dissertation is my own work. It is being submitted for the degree of Master of Science in Medicine at the University of the Witwatersrand, Johannesburg, South Africa. It has not been submitted before for any degree or examination at this or any other University.

.....

Tshegofatso Harold Motau

.....day of....., 2015.

Dedication

This work is dedicated to my loving family, colleagues and all the people who have contributed selflessly to my development and achievements. First and foremost to the remarkable women who nurtured and raised me with love and discipline: my aunts Maria and Dikeledi 'Musi, my mother Eusybia 'Musi and my grandmother Jeannette 'Musi. A special dedication to my children, Keratile, Bonisa and Litha for their love and patience, as well as to my siblings Jerry and Lerato 'Musi for their moral support

Last but not least, to my wife Dr Loyiso F. Mpuntsha-Motau, your support, encouragement and unconditional love have carried me throughout this journey.

Abstract

Plasmodium falciparum remains the most virulent cause of malaria. With increasing drug resistance to artemisinin and other antimalarial drugs, combined with an absence of an effective vaccine, there's a critical need for new agents to complement existing treatment and prophylaxis. Therefore, the aim of the study was to evaluate the *in vitro* antimalarial activity and potential toxicity to mammalian cells of select synthetic and natural colourants, nucleoside and imidazo[1,2a]pyridine (IP) analogues on the erythrocytic stages of the 3D7 chloroquine-sensitive strain of *P. falciparum*. The *P. falciparum* 3D7 strain was maintained *in vitro* according to standard methods. Quinine and chloroquine were used as positive controls. The tritiated hypoxanthine incorporation assay was used for evaluating the ability of test compounds to inhibit the growth of *P. falciparum*. Active test compounds were tested in combination studies with quinine. Uninfected human red blood cell (RBC) toxicity was analysed spectrophotometrically. The ability of test compounds to inhibit β -haematin formation, a metabolic pathway that sequesters toxic haem within the parasites, was determined. Cytotoxic activity of active compounds was evaluated on two human cell lines (HEK293 and K562) using the [³H]-thymidine incorporation assay. Data was analysed using the one-way ANOVA test and reported as the mean \pm standard deviation of at least triplicate experiments and significant difference when $p < 0.05$. Of the 56 compounds tested, the synthetic colourants showed the most potent antimalarial activity. Methylene blue and safranin O were most potent with IC₅₀ values of 4.19 ± 0.16 nM and 86.50 ± 2.61 nM, respectively, compared to quinine (IC₅₀: 103.90 ± 8.30 nM), and displayed negligible toxicity to uninfected human RBCs. Combination studies with methylene blue and quinine demonstrated a synergistic interaction. Methylene blue also demonstrated the highest selectivity indices (480 and 968) compared to quinine (180). Curcumin (diferuloylmethane), a natural extract was active (IC₅₀: 2.29 ± 0.18 μ g/ml) against *P. falciparum*, but significantly ($p < 0.05$) less potent than quinine. Curcumin was 78-fold more active in inhibiting β -haematin formation than quinine, indicating of a possible mechanism of action. The most active nucleoside analogue, JLP118.1 (IC₅₀: 1.79 ± 0.12 μ M), demonstrated inhibitory activity against the trophozoite stage of *P. falciparum*. The imidazopyridine analogue, IP-4, displayed the least potent antimalarial activity (IC₅₀: 15.3 ± 0.41 μ M) of the synthetic compounds tested, with low selectivity indices < 1 . The study has confirmed the potent antimalarial activity and relative safety of methylene blue as well as its potential as an antimalarial drug. The nucleoside and imidazopyridine analogues showed promising activity and with structural modification their potency and selectivity indices may be enhanced.

Acknowledgements

The author would like to thank supervisors Professor R.L. van Zyl and Dr L.J. Harmse for their outstanding academic support and mentorship. I am very grateful to the senior laboratory technician and my colleague, Mr Chieng-Teng Chen, for his expert technical support. Synthetic colourants were kindly donated by Dr Laurent Meijer (Station Biologique de Roscoff, France), and natural colourants were a gift from Phytone, Ltd. Professor Charles De Koning (School of Chemistry, University of the Witwatersrand) for providing novel nucleoside and imidazopyridine analogues compounds tested in the study.

Financial support:

National Research Foundation (NRF) Thutuka Fund, Belgium Technical Corporation (BTC), National Scheme for Financial Assistance (NSFAS), Research Committee of the Faculty of Health Sciences of the University of the Witwatersrand for funding this work and allowing me to further my studies.

Publications and presentations

Publications

- Motau, H., Van Zyl, R.L., and Harmse, L. (2010). The chemotherapeutic action of synthetic dyes against *Plasmodium falciparum*. *Basic & Clinical Pharmacology & Toxicology*, 107 (Suppl. 1), 472–473. (from conference proceedings)

Presentations

- Motau, H.T., Van Zyl, R.L., and Harmse, L.J. 2010.
The chemotherapeutic action of synthetic dyes against *Plasmodium falciparum*.
Poster presentation: The 5th International Conference on Pharmaceutical and Pharmacological Sciences, North-West University, Potchefstroom, South Africa, 23-26 September 2009.
- Motau, H.T., Van Zyl, R.L., and Harmse, L.J. 2010.
The chemotherapeutic action of synthetic dyes against *Plasmodium falciparum*.
Poster presentation: WorldPharma 2010, the 16th World Congress of Basic and Clinical Pharmacology, Copenhagen, Denmark, 17-23 July 2010.
- Motau, H.T., Van Zyl, R.L., and Harmse, L.J. 2010.
The chemotherapeutic action of synthetic dyes against *Plasmodium falciparum*.
Poster presentation: The University of the Witwatersrand, Faculty of Health Sciences Research Day, 22 September 2010.
- Motau, H.T., Van Zyl, R.L., and Harmse, L.J. 2010.
The chemotherapeutic action of synthetic dyes against *Plasmodium falciparum*.
Poster presentation: The 3rd Cross-Faculty Postgraduate Symposium, University of the Witwatersrand, Faculty of Health Sciences Research Day, 26-29 October 2010.
- Motau, H.T., Van Zyl, R.L., Harmse, L.J., Panayides, J., van Otterlo, W.AL. 2011.
The antimalarial activity and selectivity of novel nucleoside analogues for *Plasmodium falciparum*.
Poster presentation: 6th International Conference on Pharmaceutical and Pharmacological Sciences (ICPPS), Durban, South Africa, 25-28 September 2011:
2011. University of Kwa-Zulu Natal.

Table of contents

Declaration	ii
Dedication	iii
Abstract	iv
Acknowledgements	v
Publications and presentations	vi
List of figures	xii
List of tables	xvi
List of equations	xviii
List of abbreviations, acronyms and symbols	xix
Chapter 1 Introduction	1
1.1 The malaria epidemic	1
1.2 Malaria in South Africa.....	2
1.3 Clinical signs and symptoms of malaria	3
1.4 Drugs used in the management of malaria	4
1.4.1 Class I agents: blood schizontocides and gametocytocides	4
1.4.2 Class II agents: blood and liver schizontocides	5
1.4.3 Class III agents: liver schizontocides, hypnozoantocides and gametocytocides ..	5
1.5 Clinical management of <i>P. falciparum</i> infections.....	5
1.5.1 Management of severe malaria	5
1.5.2 Management of mixed <i>Plasmodium</i> infections.....	5
1.5.3 Chemoprophylaxis of malaria	6
1.6 Challenges in the management and eradication of malaria.....	6
1.6.1 Mechanism of chloroquine-resistance.....	6
1.6.2 Multi-drug resistance.....	7
1.6.3 Vaccine development	8
1.7 Malaria parasite developmental life-cycle	8
1.8 <i>Plasmodium</i> life-cycle regulatory protein kinases as drug targets	10
1.9 Targeting the nucleoside metabolic pathway in <i>P. falciparum</i> parasites.....	12
1.9.1 Nucleosides, nucleic acid precursors	13
1.9.2 Cellular nucleoside transport.....	14
1.9.3 <i>Plasmodium</i> nucleotide biosynthesis	15
1.10 CDK inhibition and antiprotozoal activity of imidazopyridines.....	17

1.11	Targeting the haemozoin formation pathway.....	18
1.12	Antimalarial activity of some colourants	20
1.12.1	General chemistry of colourants	20
1.12.2	Synthetic colourants	21
1.12.2.1.1	Discovery of sulfa drugs from azo dyes	22
1.12.2.1.2	Metabolism of food colourants	22
1.12.2.2.1	Methylene blue	23
1.12.3	Natural compounds as a source for antimalarial drugs	24
1.13	Problem statement	32
1.14	Aims and objectives of the study	33
Chapter 2	Antimalarial activity.....	34
2.1	Introduction	34
2.1.1	Approach to antimalarial drug screening	34
2.1.2	pH-Dependent sensitivity of <i>P. falciparum</i> parasites.....	34
2.1.3	pKa and degree of drug ionisation	36
2.1.4	Lipinski's Rule of 5 as a measure of 'drug-likeness'	37
2.2	Objectives.....	38
2.3	Methodology	39
2.3.1	Preparation of test compounds	39
2.3.2	<i>P. falciparum</i> parasite culture maintenance	39
2.3.3	Preparation of culture medium.....	40
2.3.4	Preparation of human plasma.....	40
2.3.5	Preparation of buffered solution.....	40
2.3.6	Preparation of red blood cells.....	40
2.3.7	Blood smear slide preparation and parasite assessment.....	41
2.3.8	Synchronisation of parasite culture	41
2.3.9	Tritiated hypoxanthine incorporation assay	41
2.3.10	Drug combination study	43
2.3.11	Haemolysis assay	45
2.3.12	Beta-haematin formation inhibition assay.....	46
2.3.13	Drug-sensitivity of erythrocytic stages of <i>P. falciparum</i>	47
2.3.14	Measurement of drug-likeness using physicochemical properties.....	48
2.4	Data analysis	49
2.5	Results	49
2.5.1	Antimalarial activity.....	49

2.5.2	Haemolytic activity	54
2.5.3	β -Haematin inhibition activity	55
2.5.4	Drug interactions	56
2.5.5	Morphology and drug-sensitivity of development stages	57
2.5.6	Structure-activity relationship of analogue compounds.....	60
2.5.7	Drug-like properties	63
2.5.8	Predicted ionisation and absorption as a function of pH.....	65
2.6	Discussion	67
2.6.1	Antimalarial activity of synthetic colourants	67
2.6.2	Antimalarial activity of natural colourants.....	76
2.6.3	Antimalarial activity of nucleoside and analogues	80
2.6.4	Antimalarial activity of imidazopyridine analogues	83
Chapter 3	Mammalian cell toxicity	85
3.1	Introduction	85
3.1.1	Selectivity index and <i>in vitro</i> toxicology	85
3.2	Objectives.....	86
3.3	Methods.....	86
3.3.1	Cell lines.....	86
3.3.2	Preparation of culture medium.....	86
3.3.3	Preparation of test compounds and control drugs	87
3.3.4	General cell culture maintenance	87
3.3.5	Sub-culturing of HEK293 monolayer cells.....	87
3.3.6	Sub-culturing of K562 suspension cells.....	88
3.3.7	Determination of cell number	88
3.3.8	Tritiated thymidine incorporation assay.....	88
3.4	Data analysis	89
3.5	Selectivity index.....	89
3.6	Results	90
3.6.1	Cytotoxic effect of synthetic colourants.....	90
3.6.2	Cytotoxic effect of natural colourants.....	91
3.6.3	Cytotoxicity of nucleoside and imidazopyridine analogues	92
3.6.4	Selectivity indices of most active test compounds for <i>P. falciparum</i>	93
3.7	Discussion	94
3.7.1	Selectivity of synthetic colourants for <i>P. falciparum</i>	94
3.7.2	Selectivity of natural colourants for <i>P. falciparum</i>	96

3.7.3	Selectivity of nucleoside analogues for <i>P. falciparum</i>	98
3.7.4	Selectivity of imidazopyridine analogues for <i>P. falciparum</i>	99
Chapter 4 Potential inhibition of PfNek-4 protein kinase by test compounds.....		100
4.1	Introduction	100
4.1.1	Catalytic activity of protein kinases	100
4.1.2	<i>PfNek-4</i> and the <i>P. falciparum</i> sexual cycle	101
4.1.3	<i>Plasmodium</i> NIMA-related kinases and the sexual cycle completion.....	102
4.2	Aim.....	103
4.3	Methodology	103
4.3.1	<i>PfNek-4</i> expression plasmid	103
4.3.2	2YT broth preparation.....	103
4.3.3	Preparation of carbenicillin selector agar plates	103
4.3.4	Expression of GST- <i>PfNek-4</i> fusion protein.....	104
4.3.5	Analysis of the GST- <i>PfNek-4</i> protein.....	106
4.3.6	Kinase assay	110
4.3.7	Plasmid isolation	112
4.3.8	Restriction digest of <i>PfNek-4</i> containing plasmids.....	112
4.3.9	Agarose gel electrophoresis of restriction products	112
4.3.10	DNA sequencing	113
4.3.11	Bioinformatics.....	113
4.4	Results	114
4.4.1	Expression of <i>PfNek4</i>	114
4.4.2	Western blot	115
4.4.3	Protein concentration.....	116
4.4.4	Kinase activity and inhibition	117
4.4.5	Plasmid isolation and restriction analysis of <i>PfNek4</i>	118
4.4.6	Nucleotide sequence analysis.....	119
4.4.7	Protein sequence analysis.....	121
4.5	Discussion	123
Chapter 5 Conclusions.....		126
5.1	Synthetic colourants	126
5.2	Curcumin.....	127
5.3	Nucleoside analogues.....	128
5.4	Imidazopyridine analogues	128
5.5	Potential inhibition of PfNek-4 protein kinase activity.....	129

References	131
Appendices	150
Appendix A Chemical structures of test compounds.....	150
Appendix A1 Nucleoside analogues.....	150
Appendix A2 Imidazopyridine analogues	151
Appendix A3 Least active synthetic colourants	152
Appendix B Biosafety and ethical clearances	154
Appendix B1 Biosafety clearance for use of <i>P. falciparum</i>	154
Appendix B2 Ethical clearance for use of human plasma.....	155
Appendix B3 Ethical clearance for drawing of human blood from volunteers.....	156
Appendix B4 Ethical clearance waiver for use of human cell lines	157
Appendix B5 Biosafety clearance for use of recombinant <i>PfNek-4</i> protein kinase	158
Appendix C pGEX 4T-3 Vector map	159
Appendix D <i>PfNek-4</i> nucleotide sequence chromatographs	160
Appendix D1 <i>PfNek-4</i> clone-A forward and reverse nucleotide sequences	160
Appendix D2 <i>PfNek-4</i> clone-B forward and reverse nucleotide sequences	164
Appendix E <i>PfNek-4</i> nucleotide sequence alignments	168
Appendix E1 <i>PfNek-4</i> clone-A consensus sequence alignment.....	168
Appendix E2 <i>PfNek-4</i> clone-B consensus sequence alignment.....	169
Appendix F Single-letter amino acid code	170

List of figures

Figure 1.1 Mechanism of <i>Pf</i> CRT-mediated chloroquine-resistance associated with hydrogen-ion leak in <i>P. falciparum</i> (adapted from Lehane <i>et al.</i> , 2008 and Fidock <i>et al.</i> , 2008).....	7
Figure 1.2 The malaria parasite life-cycle (Centers for Disease Control, 2011).....	10
Figure 1.3 The <i>P. falciparum</i> cell cycle in comparison to the mammalian cell cycle (adapted from Arnot <i>et al.</i> , 2011; www.usma.edu).....	11
Figure 1.4 Nucleotide structure (adapted from Alberts <i>et al.</i> , 2008b).	13
Figure 1.5 Nucleoside transporters and permeation pathways in the human RBC infected by <i>P. falciparum</i> during the parasite's trophozoite stage (adapted from Baldwin <i>et al.</i> , 2007).....	14
Figure 1.6 Enzymatic purine salvage and <i>de novo</i> pyrimidine metabolic pathways (adapted from Cassera <i>et al.</i> , 2011).....	16
Figure 1.7 Parent chemical structure of the imidazopyridine (imidazo[1,2- <i>a</i>]pyridines) analogues.	17
Figure 1.8 Haem metabolic pathway within a <i>P. falciparum</i> -infected RBC (adapted from Ginsburg, 2013)..	19
Figure 1.9 Chromophore and auxochromes of acid red azo compound (adapted from Verma <i>et al.</i> , 2012).....	21
Figure 1.10 Chemical structures of azo, di-azo and axozy compounds (Zollinger, 1987).....	22
Figure 1.11 Azoreduction of methyl red (adapted from Chen <i>et al.</i> , 2005).....	23
Figure 1.12 Redox reaction of methylene blue (adapted from Schirmer <i>et al.</i> , 2005).....	24
Figure 1.13 Chemical structure of safranin O (PubChem Compound, 2013c).	24
Figure 1.14 <i>Curcuma longa</i> plant and ground powder prepared from dried rhizomes (adapted from Goel <i>et al.</i> , 2008; Britannica, 2013c).....	26
Figure 1.15 Chemical structure of curcumin (Goel <i>et al.</i> , 2008; PubChem Compound, 2013b).	26
Figure 1.16 <i>Bixa orellana</i> plant seeds in an open seed pod (Brittanica, 2013c).	27
Figure 1.17 Chemical structures of the constituent of annatto namely, bixin (~80%) and its hydrolysed derivative, norbixin (adapted from Evans, 1996).	27
Figure 1.18 (a) Cochineal insects, (b) <i>Dactylopius coccus</i> , forming white clusters on <i>Opuntia</i> cactus (Brittanica, 2013b).....	28

Figure 1.19 Chemical structure of carminic acid (PubChem Compound, 2013a).	28
Figure 1.20 The (a) safflower (<i>Carthamus tinctorius</i> L.) plant, (b) seeds and (c) dried flowers (Van Wyk and Wink, 2004).	29
Figure 1.21 General chemical structures of (a) betalamic acid, (b) betacyanins and (c) betaxanthins (adapted from Strack <i>et al.</i> , 2003).	31
Figure 1.22 Ground red powder from the bulbs of the <i>Beta vulgaris</i> plant (Brittanica, 2013a). .	32
Figure 2.1 “Ion-trapping” of chloroquine within the malaria parasite digestive vacuole (adapted from O’Neill <i>et al.</i> , 2012).	35
Figure 2.2 Change in ionisation and relative solubility of weakly acidic and weakly basic drugs as a function of pH (adapted from Aulton, 2000).	37
Figure 2.3 Design of [³ H]-hypoxanthine assay in a 96-well microtitre plate (adapted from Desjardins <i>et al.</i> , 1979).	42
Figure 2.4 A general isobologram with classification of possible interactions between two drugs (adapted from Gupta <i>et al.</i> , 2002).	44
Figure 2.5 Workflow of <i>in silico</i> methodology applying the Lipinski Rule of 5 (adapted from Bhal <i>et al.</i> , 2007).	48
Figure 2.6 <i>In vitro</i> antimalarial activity of synthetic colourants on <i>P. falciparum</i>	51
Figure 2.7 Antimalarial activity of curcumin and carbon black on the growth of <i>P. falciparum</i> parasite compared to quinine.	52
Figure 2.8 Inhibitory activity of nucleoside analogues on the <i>P. falciparum</i> parasite growth compared to quinine.	53
Figure 2.9 Antimalarial activity of the most active imidazopyridine analogues on the <i>in vitro</i> growth of <i>P. falciparum</i> parasite compared to quinine.	54
Figure 2.10 Isobolograms showing the drug interactions between quinine and the most active (a) synthetic and (b) natural compounds.	57
Figure 2.11 Morphological changes and stage-sensitivity of the <i>P. falciparum</i> parasites to the most active compounds.	58
Figure 2.12 Effect of methylene blue, JLP118.1 and IP-4 in comparison to quinine at an IC ₉₀ value on <i>P. falciparum</i> parasite growth over a single 48 h-cycle.	59
Figure 2.13 Correlation between predicted log P values and antimalarial activity IC ₅₀ values. ...	65

Figure 2.14 Putative redox-cycling of methylene blue affecting anti-oxidant systems in <i>P. falciparum</i> -infected RBC attributed to antimalarial activity (adapted from Blank <i>et al.</i> 2012).	73
Figure 2.15 The hexose monophosphate pathway in <i>P. falciparum</i> (adapted from Preuss <i>et al.</i> 2012).	75
Figure 2.16 Regulation of gene activation and repression by acetylation of histones (adapted from Barnes <i>et al.</i> , 2005).	80
Figure 3.1 Cytotoxic effect of synthetic colourants on the HEK293 and K562 cell lines.	90
Figure 3.2 Cytotoxic effect of natural colourants on the HEK293 and K562 cell lines.	91
Figure 3.3 Cytotoxic effect of nucleoside and imidazopyridine analogues against the HEK293 and K562 cell lines.	92
Figure 3.4 Selectivity indices of the most active compounds for <i>P. falciparum</i> .	93
Figure 4.1 The catalytic domain of eukaryotic protein kinases consisting of 12 conserved subdomains (adapted from Hanks, 2003).	101
Figure 4.2 <i>P. falciparum</i> erythrocytic stage gametocytes development (adapted from Dixon <i>et al.</i> , 2008).	102
Figure 4.3 Assembly of the “gel-sandwich” for electrophoretic protein transfer to a PVDF membrane (Bio-Rad, 2013).	108
Figure 4.4 Chemiluminiscent visualisation of the GST-tagged proteins using horse-radish peroxidase conjugated primary antibodies.	109
Figure 4.5 Coomassie blue-stained SDS-PAGE gel depicting the isolated GST- <i>PfNek-4</i> (clone A) protein bands alongside molecular weight markers.	114
Figure 4.6 A linear curve of the log MW versus R_f values used to determine the MW of expressed proteins.	115
Figure 4.7 Western Blot of the GST- <i>PfNek4</i> (A) protein kinase.	116
Figure 4.8 Standard curve of BSA protein standard concentrations and absorbance _{595nm} values.	117
Figure 4.9 Kinase activity of various isolates of the recombinant GST- <i>PfNek-4</i> protein kinase.	117
Figure 4.10 The kinase assays with most active compounds.	118
Figure 4.11 Agarose gel electrophoresis of plasmid extracts fragmented with site-specific restriction digest enzymes, <i>BamHI</i> and <i>SalI</i> .	119

Figure 4.12 Nucleotide sequence alignment of <i>PfNek-4</i> (clone-A) consensus sequence.	120
Figure 4.13 Open Reading Frame showing the DNA insert of <i>PfNek-4</i> (clone-A) and restriction sites.	120
Figure 4.14 Nucleotide sequence alignment of <i>PfNek-4</i> (clone-B) consensus sequence.	121
Figure 4.15 Open Reading Frame showing the DNA insert of <i>PfNek-4</i> (clone-B) and restriction sites.	121
Figure 4.16 Alignment of translated amino acid sequence of clone-A to <i>PfNek-4</i>	122
Figure 4.17 Alignment of translated amino acid sequence of clone-B to <i>PfNek-4</i>	122

List of tables

Table 1.1 Signs and symptoms of malaria (National Department of Health, 2010).	3
Table 1.2 Currently available drug classes for treatment of malaria (Parkinson, 2010; Rossiter, 2012).	4
Table 2.1 The <i>in vitro</i> antimalarial activity of synthetic colourants and reference drugs chloroquine and quinine.	50
Table 2.2 Antimalarial activity of natural colourants on <i>P. falciparum</i>	52
Table 2.3 Antimalarial activity of nucleosides analogues.	53
Table 2.4 Antimalarial activity of imidazopyridine analogues on <i>P. falciparum</i>	54
Table 2.5 Haemolytic activity of the most active synthetic compounds.	55
Table 2.6 Haemolytic activity of natural colourants.	55
Table 2.7 β -Haematin formation inhibition of the most active synthetic compounds.	56
Table 2.8 β -Haematin formation inhibition activity of natural colourants.	56
Table 2.9 Drug interactions of the most active colourants in combination with quinine.	57
Table 2.10 Chemical structure and antimalarial activity of nucleoside analogues.	62
Table 2.11 Chemical structure and antimalarial activity of imidazopyridine analogues.	63
Table 2.12 Predicted solubility and permeability properties of most active synthetic test compounds based on the Lipinski's Rule of 5 (Lipinski, 2004).	64
Table 2.13 Predicted percentage ionisation of most active test compounds.	66
Table 2.14 Summary of antimalarial, haemolytic and β -haematin formation inhibitory activity of the most active synthetic colourants.	68
Table 2.15 Summary table showing antimalarial, haemolytic activity and β -haematin formation inhibition IC_{50} values of the most active natural compounds.	77
Table 2.16 Summary of antimalarial, haemolytic and β -haematin formation inhibitory activity of the most active nucleoside analogues.	82
Table 4.1 List of stock reagents and volumes of the 30 μ l single kinase reaction solution.	111
Table 4.2 Homologous protein sequences to <i>PfNek-4</i> (clone-A).	123
Table 5.1 Summarised results of the most active synthetic compounds.	130

Table 5.2 Summarised results of the natural curcumin colourant. 130

List of equations

Equation 2.1 The Henderson-Hasselbalch equation.....	36
Equation 2.2 Percentage parasite growth.	43
Equation 2.3 Fractional inhibitory concentrations.	44
Equation 2.4 Sum of mean fractional inhibitory concentrations.	45
Equation 2.5 Percentage haemolysis equation.	46
Equation 2.6 Modified % haemolysis equation for colourants.	46
Equation 2.7 Selectivity index for <i>P. falciparum</i> compared to uninfected human RBC.	46
Equation 2.8 Percentage β -haematin formation.	47
Equation 2.9 Percentage ionisation for weak acids and weak bases (pH-pK _a).	49
Equation 3.1 Cell density.	88
Equation 3.2 Percentage cell growth determination.....	89
Equation 3.3 Selectivity index for <i>P. falciparum</i> compared to human cancer cell lines.....	90

List of abbreviations, acronyms and symbols

A

Abs Absorbance
 ACT Artemisinin combined
 therapy
 ADME Absorption, distribution,
 metabolism and excretion

ADP Adenosine diphosphate

ATP Adenosine triphosphate

α Alpha

ANOVA Analysis of variance

B

β Beta

bp Base pairs

BSA Bovine serum albumin

BLAST Basic Logical Alignment-
 Search Tool

C

CAS Chemical abstract services

CDK Cyclin dependant kinase

CDKI Cyclin dependant kinase
 inhibitor

C.I. Colour index

cpm Counts per minute

D

$^{\circ}\text{C}$ Degrees celsius

DNA Deoxyribonucleic acid

DMEM Dulbecco's Modified Eagle's
 Medium

DMSO Dimethyl sulfoxide

dNTP Deoxyribonucleotide
 triphosphate

DTT Dithiothreitol

E

E. coli *Escherichia coli*

EDTA Ethylene diamine- tetracetic
 acid

et al. And others

ENT Equilibrative nucleoside
 transporter

ePK Eukaryotic protein kinase

EtBr Ethidium bromide

F

Fe^{3+} -PPIX Ferriprotoporphyrin IX
 (haematin)

FIC Fractional inhibitory
 concentration

FIC_{50} IC_{50} of drug A+B divided by
 IC_{50} of drug A

$\sum \text{FIC}_{50}$ Sum of FIC_{50} values

G

γ Gamma

g Gravity

Gly^- Glycine ions

G6PD Glucose-6-phosphate-
 dehydrogenase

GSSG Glutathione (oxidised form)

GSH Glutathione (reduced-form)

GST Glutathione S-transferase

H

HBA Hydrogen bond acceptors

Hb Haemoglobin

hENT	Human equilibrative nucleoside transporter	min	Minutes
		ml	Millilitre
hGR	Human glutathione reductase	mM	Millimolar
HIV	Human immunodeficiency virus	MW	Molecular weight
		N	
HLC ₅₀	Haemolytic concentration yielding 50% lysis	nm	Nanometre (micron)
		nM	Nanomolar
HMS	Hexose monophosphate shunt (same as PPS)	NCBI	National Centre for Biotechnology Information
HRP	Horse-radish peroxidase	ND	Not determined
HAT	Histone acetyltransferase	NADP	Nicotinamide adenine dinucleotide phosphate
I			
IC ₅₀	Inhibitory concentration yielding 50% response	NADPH	Nicotinamide adenine dinucleotide phosphate (reduced-form)
IRS	Indoor residual spraying		
IPTG	Isopropylthio-β-galactoside	NIMA	Never in mitosis <i>Aspergillus nidulans</i>
IARC	International Agency for Research on Cancer	P	
K		%	Percentage
kDa	Kilo Daltons	PAGE	Polyacrylamide gel electrophoresis
KZN	Kwa-Zulu Natal		
L		PBS	Phosphate-buffered saline
λ	Lambda (wavelength)	<i>PbNek</i>	<i>Plasmodium berghei</i> Never in mitosis gene A related kinase
LB	Luria Bertani (broth)	<i>PfENT</i>	<i>Plasmodium falciparum</i> -ENT
LSDI	Lubombo Spatial Development Initiative	<i>PfGR</i>	<i>Plasmodium falciparum</i> glutathione reductase
M		<i>PfNek</i>	<i>Plasmodium falciparum</i> Never in mitosis gene A related kinase
metHb	methaemoglobin		
mRNA	Messenger ribonucleic acid		
μCi/ml	Microcurie per ml		
μl	Microlitre	pKa	Acid dissociation constant (logarithmic scale)
μm	Micrometre (microns)		
μM	Micromolar	PlasmoDB	<i>Plasmodium</i> database
mg	Milligrams	PPM	Parasite plasma membrane

PPS	Pentose phosphate shunt
PVDF	Polyvinylidene fluoride
PVM	Parasitophorous vacuole Membrane
R	
RBC	Red blood cell
RNA	Ribonucleic acid
Ro5	Rule of five
rpm	Revolutions per minute
RPMI	Rosewell Park Memorial Institute
S	
SDS	Sodium dodecyl sulphate
S.I.	Selectivity index
T	
TB	Tuberculosis
TBST	Tris buffered saline and Tween-20
TEMED	N,N,N',N'- tetramethylenediamine
Tris	Tris (hydroxymethyl) aminomethane
U	
UV	Ultra-violet
V	
Vis	Visible
v/v	Volume per volume
W	
w/v	Weight per volume
WHO	World Health Organisation

Chapter 1 Introduction

1.1 The malaria epidemic

Malaria is a vector-borne parasitic disease that presents as a febrile illness and may cause dysfunction in organs such as the spleen, liver and the brain in its severe and chronic form (Miller *et al.*, 2002). Malaria parasites are transmitted to humans by the bite of infected female mosquito vectors of the *Anopheles* species (WHO, 2013). Malaria is caused by five species of parasites of the genus *Plasmodium* that affect humans: *P. falciparum*, *P. vivax*, *P. ovale*, *P. malariae* and *P. knowlesi* (WHO, 2013). Of these *Plasmodium* species, *P. falciparum* and *P. vivax* are the most prevalent and virulent, accounting for more than 95% of malaria in Africa, East Asia countries and India (Micale, 2012). In 2012, the global estimate of people at risk of malaria was 3.4 billion, with populations living in the African and South-East Asia regions having the highest risk of acquiring malaria (WHO, 2012). In addition the World Health Organisation (WHO) reported an estimate of 207 million cases of malaria globally, and 627 000 deaths worldwide in 2012 (WHO, 2013). Of the estimated deaths, most occurred in sub-Saharan Africa (90%) and mostly in children under 5 years of age (77%) (WHO, 2013). Globally, malaria is ranked fifth as a cause of death from an infectious disease after respiratory infections, human immuno-deficiency virus/acquired immuno-deficiency syndrome (HIV/AIDS), diarrhoeal diseases and tuberculosis (Centers for Disease Control, 2011).

The economic burden in Africa alone is estimated at 12 billion US dollars annually in direct losses due to morbidity and premature death (Roll Back Malaria Partnership, 2008). The disease burden especially in sub-Saharan African countries is compounded by poor socio-economic conditions and healthcare systems, migration to malarial regions, changing agricultural and environmental landscape (Sachs and Malaney, 2002). In addition, climate change may be considered a possible contributing factor particularly to the proliferation and spread of the mosquito vector (Sachs and Malaney, 2002). Provided the interventions currently recommended by the WHO are implemented, malaria can easily be prevented (WHO, 2012). These prevention interventions include vector control through the use of insecticide-treated nets and indoor residual spraying. Chemopreventative measures for the most vulnerable populations, particularly pregnant women and infants, as well as early malaria diagnosis and timely treatment, are critical (WHO, 2012).

1.2 Malaria in South Africa

Malaria risk areas in South Africa include north-eastern KwaZulu-Natal, the low altitude areas of Mpumalanga and Limpopo provinces, particularly those along the borders of Zimbabwe, Mozambique and Swaziland (National Department of Health, 2010). Only 4% of the population is at high risk of malaria and 6% at low risk, while 90% live in malaria-free areas (WHO, 2012). Between the year 2000 and 2011, steady progress has been made in controlling malaria. During this period the malaria cases in South Africa decreased by 85% (from 64,622 cases to 9,866) and the mortality rate greatly decreased by 81% (from 458 deaths to 89) (National Department of Health, 2012). Generally adults living in malaria endemic areas such Mozambique, Malawi and Tanzania may acquire partial immunity subsequent to long-term and repeated exposure to *P. falciparum* infection (Sachs and Malaney, 2002). However, South Africans are not immune to malaria and therefore at risk of developing cerebral malaria, which can be fatal (National Department of Health, 2010). In most cases, increased morbidity and mortality is a culmination of delayed diagnosis and inappropriate treatment (National Department of Health, 2010). In South Africa, malaria is a notifiable medical condition requiring health workers and local authority or hospitals to record cases and deaths for regional planning and monitoring of the disease (National Department of Health, 2010). Chloroquine, sulphadoxine or pyrimethamine monotherapies were used as first line of treatment for uncomplicated *P. falciparum* malaria until treatment failure rates above 10% were detected (Mullick *et al.*, 2011). In response to the increasing drug resistance, the WHO recommended the use of artemisinin-based combined therapy (ACT) (WHO, 2010). Chloroquine-resistance in South Africa was first observed in KwaZulu-Natal and later in Mpumalanga (National Department of Health, 2010). This resulted in a change in the treatment policy with the use of sulphadoxine-pyrimethamine as first line treatment for early stage or uncomplicated *P. falciparum* in KwaZulu-Natal in 1988 and Mpumalanga in 1997 (National Department of Health, 2010). The development of significant sulphadoxine-pyrimethamine resistance in KwaZulu-Natal led to a further policy change in 2001 with artemether-lumefantrine replacing sulphadoxine-pyrimethamine as first line treatment (National Department of Health, 2009). The increase in drug resistance initiated a successful inter-governmental initiative such as the Lubombo Spatial Development Initiative involving Mozambique, South Africa and Swaziland (Sharp *et al.*, 2007). This collaboration successfully resulted in a 78% reduction in malaria cases in Mpumalanga between 1999 and 2005 by reducing cross-border infections, implementing indoor residual spraying and first line therapy with ACT (Sharp *et al.*, 2007; National Department of Health, 2010).

1.3 Clinical signs and symptoms of malaria

The signs and symptoms of malaria are non-specific (Table 1.1) and malaria is clinically suspected on the basis of fever or a history of fever, as well as travelling to malaria endemic regions (WHO, 2010). Presentation of *P. falciparum* malaria mimics many other diseases including influenza, viral hepatitis, meningitis, septicaemia, typhoid, tick-bite fever, gastroenteritis, viral haemorrhagic fever, trypanosomiasis, HIV sero-conversion illness, urinary tract infection and relapsing fever (National Department of Health, 2010). Malaria symptoms may present as early as 7 days after exposure, usually 10-21 days after being bitten by an infected mosquito. Longer incubation periods may occur in patients who have failed chemoprophylaxis due to poor compliance or inappropriate prophylaxis regimen, or have been on an antibiotic course not prescribed for malaria. Malaria due to infections with *P. vivax*, *P. ovale*, or *P. malariae*, can take up to 12 months to first manifest clinically (National Department of Health, 2010). Another clinical manifestation of malaria is placental malaria. This is of particular danger for primigravidae (a woman pregnant for the first time) and is due to *P. falciparum* adherence to chondroitin sulphate-A in the placenta (Vinetz *et al.*, 2011). This often leads to severe complications, including miscarriage. When treated early, symptoms of malarial infection usually improve within 24-48 h (Vinetz *et al.*, 2011). Patients with uncomplicated malaria are at a risk of developing severe *P. falciparum* malaria with life-threatening complications as a result of delay in diagnosis and/or treatment of an uncomplicated infection, or the use of ineffective therapy (WHO, 2010).

Table 1.1 Signs and symptoms of malaria (National Department of Health, 2010).

Uncomplicated malaria:

- Fever
- Headache
- Rigors (cold and shiver or hot sweats)
- Myalgia
- Dizziness
- Loss of appetite (or poor feeding)
- Diarrhoea, nausea and vomiting
- Cough
- Splenomegaly

Severe malaria:

- Prostration
- Impaired consciousness
- Multiple convulsions
- Circulatory collapse
- Acute respiratory distress syndrome (ARDS); hypoxia
- Abnormal bleeding; Disseminated intravascular coagulation (DIC)
- Jaundice
- Haemoglobinuria
- Hypoglycaemia
- Renal and Hepatic impairment

1.4 Drugs used in the management of malaria

Currently available antimalarial drugs can be categorised according to their drug classes and into four groups according to their biological activity against specific developmental stages of the parasite (Vinetz *et al.*, 2011). These include drugs that eliminate liver tissue schizonts, dormant liver forms or hypnozoites (for casual prophylaxis and to prevent relapse), blood schizontocides and gametocytocides (Vinetz *et al.*, 2011). Currently there is no antimalarial drug that kills sporozoites, so drugs used for chemoprophylaxis can only prevent the development of symptomatic malaria caused by asexual erythrocytic forms. Patterns of clinically effective drugs can be categorised into three general classes based on the stages of the life-cycle they are active against, as well as their mechanism of action (Table 1.2) (Parkinson, 2010; Vinetz *et al.*, 2011).

Table 1.2 Currently available drug classes for treatment of malaria (Parkinson, 2010; Rossiter, 2012).

Drug class	Examples	Mechanism of action
4-Aminoquinolines	Chloroquine, amodiaquine,	Prevent detoxification of haem by the parasite
Quinoline methanol	Quinine, mefloquine, quinidine	
8-Aminoquinolines	Primaquine	
Bisquinoline	Piperaquine	
Amyl alcohol	Lumefantrine	
Anti-folates	Sulphadoxine, pyrimethamine, proguanil	Inhibit dihydrofolate reductase, interfering with <i>Plasmodium</i> pyrimidine synthesis
Napthoquinones	Atovaquone	Inhibit mitochondrial function of the parasite
Artemisinin derivatives	Artemisinin, dihydroartemisinin, artemether, artesunate, artemotil/arteether	Sesquiterpene lactone endoperoxides that produce free radicals in the parasite food vacuole
Antibiotics	Tetracycline, doxycycline, clindamycin	Inhibit parasite apicoplast organelle function

1.4.1 Class I agents: blood schizontocides and gametocytocides

The drug action of these antimalarial agents (artemisinin, chloroquine, mefloquine, quinine/quinidine, pyrimethamine, sulfadoxine and tetracyclines) is mainly directed against the asexual erythrocytic forms, except for artemisinin which acts as both a blood schizontocide and gametocytocide. Chloroquine, quinine or quinidine show low to moderate activity against gametocytes. This class of drugs treat, or prevent clinically symptomatic malaria (Vangapandu *et al.*, 2007; Rossiter, 2012).

1.4.2 Class II agents: blood and liver schizontocides

Typically atovaquone and proguanil target both the asexual erythrocytic forms and the liver tissue schizonts of *P. falciparum*. Their activity reduces the required period for post-exposure chemoprophylaxis from 4 to 1 week (Vinetz *et al.*, 2011).

1.4.3 Class III agents: liver schizontocides, hypnozoitocides and gametocytocides

This class currently comprises solely of primaquine, which is effective against liver schizonts and latent, hypnozoites liver stages as well as gametocytes. Primaquine is used most commonly to eradicate the intra-hepatic hypnozoites of *P. vivax* and *P. ovale* that are responsible for relapsing infections, but not used in the treatment of symptomatic malaria (Vangapandu *et al.*, 2007; Vinetz *et al.*, 2011).

1.5 Clinical management of *P. falciparum* infections

The differential diagnosis between uncomplicated and severe malaria is critical in selecting an appropriate therapeutic strategy for effective treatment; where severe malaria is characterised as having a parasitaemia > 4%, haematocrit < 20% and haemoglobin < 6 g/dl (National Department of Health, 2010). Artemisinin-based combination therapies are used for the treatment of uncomplicated *P. falciparum* malaria (National Department of Health, 2010; WHO, 2012). The recommended drug treatment for *P. falciparum* infections is the administration of an artemisinin-lumefantrine combination or alternatively, quinine plus either doxycycline or clindamycin for 7 days to avoid quinine-induced adverse effects (National Department of Health, 2010).

1.5.1 Management of severe malaria

Intravenous quinine is the preferred treatment for severe malaria in South African children and adults who have no immediate access to intravenous artesunate (National Department of Health, 2010). The WHO recommends intravenous artesunate as the treatment of choice for severe malaria in adults (WHO, 2012). Once the patient is able to tolerate oral therapy, artemether-lumefantrine or quinine plus either doxycycline or clindamycin, should be administered (National Department of Health, 2010).

1.5.2 Management of mixed *Plasmodium* infections

When a mixed infection of *P. falciparum* with either *P. vivax* or *P. ovale* is confirmed or suspected, the standard therapy for uncomplicated or severe *P. falciparum* malaria infection is recommended, along with a follow-up of course of primaquine (National Department of Health, 2010).

1.5.3 Chemoprophylaxis of malaria

In addition to preventative measures such as mosquito repellents and use of bed nets, prophylactic regimens using mefloquine, doxycycline and atovaquone are recommended by the South African Department of Health (Baker, 2009; National Department of Health, 2010).

1.6 Challenges in the management and eradication of malaria

Resistance to chloroquine is most prevalent, while resistance to other antimalarial drugs such as quinine, mefloquine, halofantrine, atovaquone, sulfadoxine and pyrimethamine have been progressively spreading (Vangapandu *et al.*, 2007; O'Neill *et al.*, 2012). The development of most of the vaccine candidates is still underway or in clinical trials. Given the complexity of the malaria parasite life-cycle, a malaria vaccine needs to encompass various strategies of stimulating the immune responses in order to achieve a high degree of efficacy (PATH, 2007; Birkett *et al.*, 2013; Riley and Stewart, 2013).

1.6.1 Mechanism of chloroquine-resistance

Chloroquine was first synthesised in 1934 and became the gold standard treatment by the 1940s for malaria with good clinical efficacy, limited toxicity at an affordable cost of treatment in Africa (O'Neill *et al.*, 2012). After about a decade of use, chloroquine-resistance emerged in South-East Asia, South America, and the Western Pacific region (Ecker *et al.*, 2012). The first incidences of malaria parasite resistance to chloroquine were reported in 1957 (O'Neill *et al.*, 2012). Chloroquine-resistance spread progressively throughout malaria endemic areas including Africa, where surges in mortality rate were reported (Ecker *et al.*, 2012). Chloroquine-resistance (mechanism model shown in Figure 1.1) is putatively acquired via mutations in the *P. falciparum* parasite that caused the efflux of chloroquine out of the digestive vacuole of the parasite, at a rate 40 to 50-fold faster compared to chloroquine-sensitive strains (Krogstad *et al.*, 1987; Ecker *et al.*, 2012).

A *P. falciparum* P-glycoprotein homologue-1 (Pgh-1), known as the chloroquine-resistant transporter (*PfCRT*), modulates drug uptake by transporting drugs in and out of the parasites' digestive vacuole (Vangapandu *et al.*, 2007). The major mutation (K76T) implicated in chloroquine-resistance is due to the lysine⁷⁶ (K76) amino acid substitution with threonine (T) (Ecker *et al.*, 2012). Moreover, *PfCRT* is a transmembrane protein localised within the digestive vacuole membrane and is expressed from the ring stage through to the trophozoite stage where there is maximal haemoglobin digestion (Ecker *et al.*, 2012). Thereby, preventing the accumulation of chloroquine within the digestive vacuole, via passive diffusion down the pH gradient (Ecker *et al.*, 2012). As a result, binding of chloroquine to the haemoglobin

breakdown product to form toxic drug-haem complexes is also reduced (Fidock *et al.*, 2000). However, chloroquine-resistance has been shown to be reversed to a certain degree by calcium-channel blockers such as verapamil, cyproheptadine and hydroxyzine by interfering with the efflux pump (Martin *et al.*, 1987).

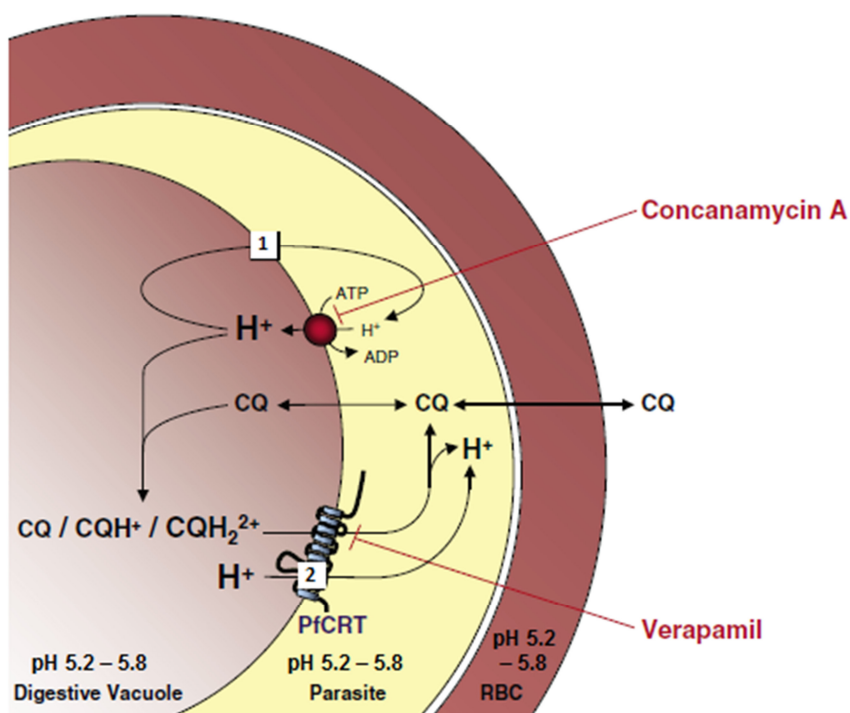


Figure 1.1 Mechanism of *PfCRT*-mediated chloroquine-resistance associated with hydrogen-ion leak in *P. falciparum* (adapted from Lehane *et al.*, 2008 and Fidock *et al.*, 2008). Uncharacterised outward leak pathway of H^+ (1), leads to alkalinisation of the digestive vacuole (DV) upon inhibition of V-type H^+ -ATPase pump by concanamycin A. Neutral form of chloroquine (CQ), diffuses through the RBC down the pH gradient into the DV. In CQ-sensitive strains di-protonated, less membrane-permeant CQ (CQH_2^{2+}) accumulates within the DV. Whereas in CQ-resistant strains, mutant *PfCRT*-mediated efflux of CQH_2^{2+} occurs in symport with H^+ ions. This efflux of CQH_2^{2+} can be reversed by verapamil. The H^+ leak pathway (2) would explain the higher rate of alkalinisation after *PfCRT* inhibition with verapamil observed in CQ-strains.

1.6.2 Multi-drug resistance

Although the presence of a *PfCRT* K76T mutation increases the risk of chloroquine treatment failure by 2.1-fold on day-14 post-treatment and by 7.2-fold on day-28, some patients in high-transmission areas infected with malaria parasite strains containing mutant *PfCRT*, seem to respond adequately to chloroquine perhaps partially due to acquired-immunity (Ecker *et al.*, 2012). However, a secondary determinant of chloroquine-resistance in *P. falciparum* has been attributed to a multidrug-resistance (*PfMDR1*) transmembrane localised within the digestive vacuole membrane. *PfMDR1* is an orthologue of mammalian P-glycoproteins that mediate verapamil-reversible tumour multidrug-resistance (Ecker *et al.*, 2012). However, although

PfMDR1 mutations alone appear to be insufficient to confer chloroquine-resistance, it is suggested they can modulate the degree of mutant *PfCRT*-mediated chloroquine-resistance, dependant on the parasite strain (Ecker *et al.*, 2012). *P. falciparum* resistance to sulfadoxine-pyrimethamine is associated with mutations in the dihydrofolate reductase (*PfDHFR*) gene and to a lesser extent in the dihydropteroate synthase (*PfDHPS*) (Wang *et al.*, 1997; Osman *et al.*, 2007). Reduced susceptibility of *P. falciparum* to the potent short-acting artemisinin derivatives has been observed in South-East Asia, Cambodia-Thailand region (Dondorp *et al.*, 2011).

1.6.3 Vaccine development

The strategic goals of current malaria vaccine initiatives are aimed at the induction of immunity to prevent clinical malaria, as well as the interruption of transmission, thereby supporting elimination and eradication efforts (Birkett *et al.*, 2013). Sustained immunity to *P. falciparum* infection has been induced in volunteers without prior exposure using live, attenuated sporozoites delivered by irradiated mosquitoes, while simultaneously preventing disease with chloroquine prophylaxis (Roestenberg *et al.*, 2011). Subunit vaccines (as opposed to attenuated whole-parasite vaccines), have previously shown lower efficacy than whole-parasite vaccines, but are simpler to clinically deliver (Greenwood *et al.*, 2008). However one subunit vaccine candidate RTS,S developed by GlaxoSmithKline Biologicals, has shown promising results in Phase IIb clinical trials and currently undergoing Phase III evaluation (Birkett *et al.*, 2013). However, following vaccination over the 12-month period during the clinical trials, RTS,S only conferred 50% protection in children aged 5-17 months and approximately 30% protection in children aged 6-12 weeks across 13 clinical sites in eight African countries (Birkett *et al.*, 2013). Key barriers to the development of more highly efficacious vaccines than RTS,S include: lack of well characterised target immunogens in all the stages of *P. falciparum* life-cycle, limited number of safe and effective delivery systems and adjuvants that induce potent long-lasting protective immunity, be it by antibody, CD4⁺ and/or CD8⁺ T-cell responses (Birkett *et al.*, 2013). These complexities in malaria vaccine development demonstrate the critical need for the development of new novel drugs that may be used in combination with existing drugs and even with a licensed vaccine candidate to control the malaria disease and even sensitise resistant strains.

1.7 Malaria parasite developmental life-cycle

The life-cycle of *P. falciparum* (Figure 1.2) is complex and characterised by developmental stages that have distinct morphological forms adapted to different microenvironments in the human and mosquito hosts (Arnot and Gull, 1998; Bannister *et al.*, 2005). The *Plasmodium*

sporozoites from the salivary glands of an infected female *Anopheles* mosquito are injected into the bloodstream of the human host during a blood meal ① and migrate to the liver where they invade hepatocytes and asexually multiply ② (Arnot *et al.*, 2011; Centers for Disease Control, 2011). This stage forms the exo-erythrocytic schizogony phase, which is asymptomatic. During the liver schizont stage ③, nuclear division completes and the parasite undergoes nuclear segmentation giving rise to daughter merozoites. Upon the rupture of the hepatocytes, the mature schizonts release several thousand merozoites ④ into the bloodstream where they rapidly invade red blood cells (RBCs) ⑤. Post-invasion, the parasite undergoes a 46-48 h intra-erythrocytic schizogony cycle with distinct morphological forms: the ring form, which matures into a trophozoite, which in turn forms a schizont that gives rise to 16-32 daughter merozoites. Deoxyribose nucleic acid (DNA) synthesis begins during the trophozoite stage after the appearance of the malaria pigment (haemozoin) from RBC haemoglobin digestion (Arnot *et al.*, 2011).

The schizont-infected RBC is ruptured, releasing the extracellular merozoites into the bloodstream where they infect new RBCs ⑥. This intra-erythrocytic cycle represents the pathogenic phase of the malaria disease (Bannister *et al.*, 2005; Arnot *et al.*, 2011). A fraction of the parasites within the RBCs undergo cell cycle arrest or differentiate into sexual erythrocytic stage known as gametocytes ⑦, which take approximately 8-12 days to mature (Bannister *et al.*, 2005; Dixon *et al.*, 2008). The gametocytes are ingested by the female mosquito vector when biting an infected human host ⑧. While in the mosquito's stomach, the microgametes penetrate the macrogametes generating zygotes ⑨. The zygotes develop into motile and elongated ookinetes ⑩, which invade the mid-gut epithelial wall of the mosquito and develop into oocysts ⑪. The oocysts grow, rupture, and release sporozoites, which migrate to the mosquito's salivary glands ⑫ and are inoculated into a new human host ①, thus perpetuating the malaria life-cycle (Bannister *et al.*, 2005).

The complex life-cycle of *P. falciparum*, proteomic expression and metabolic pathways are unique to that of the human host. These characteristics of the malaria parasite provide various targets for therapeutic intervention (Florens *et al.*, 2002; Doerig *et al.*, 2010). Therefore, the sections that follow evaluate the nucleotide synthesis and haemozoin formation metabolic pathways that are established drug targets and a literature review of some selected and structurally related test compounds on their putative antimalarial activity.

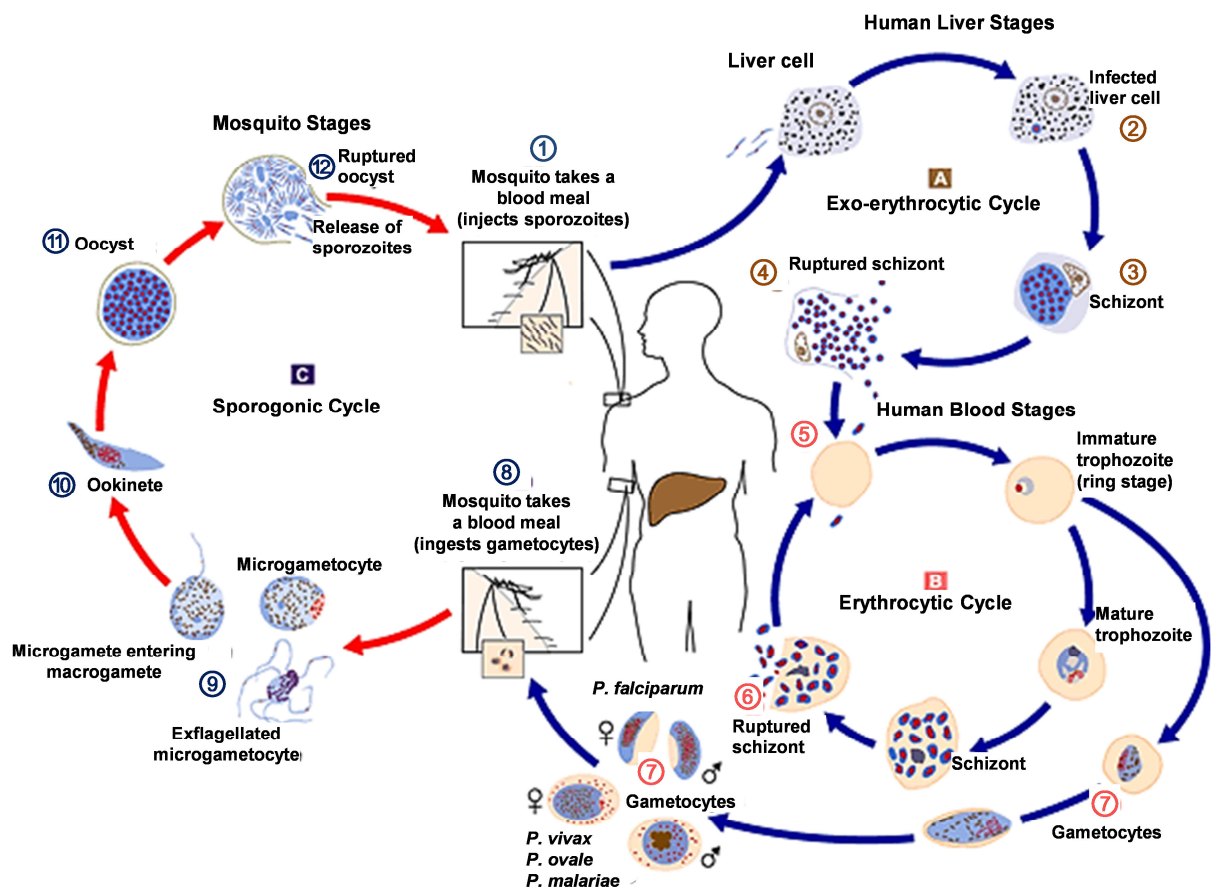


Figure 1.2 The malaria parasite life-cycle (Centers for Disease Control, 2011).

1.8 *Plasmodium* life-cycle regulatory protein kinases as drug targets

The intra-erythrocytic cycle of the *Plasmodium* parasite varies greatly from that of the typical cell cycle observed in higher eukaryotes. For instance, in higher eukaryotic cells, there is a single round of DNA replication per cell cycle, resulting in two identical daughter cells subsequent to mitosis (Geyer *et al.*, 2005). In contrast, the genome of the parasite undergoes multiple rounds of DNA replication and nuclear division, generating a single multinucleate cell called a schizont (Arnot *et al.*, 2011). At least five phases of DNA synthesis within the *P. falciparum* life-cycle have been identified. These occur during the micro-gametogenesis or male gametocytes formation, meiosis and sporogony (sexual cycle) within the mosquito vector, intra-hepatic schizogony in the liver and erythrocytic schizogony (asexual cycle) within the human host (Arnot and Gull, 1998). Higher eukaryotic cell cycle (Figure 1.3) is divided into the G1 (G-gap), S (DNA synthesis) and G2 phases that make up the interphase, as well as the mitotic (M) phase (Alberts *et al.*, 2008a). The majority of cells in living organisms are in a quiescent G0 phase (Donovan *et al.*, 2005). The transition between these phases is tightly regulated by positive effectors, cyclins and cyclin-dependent kinases (CDKs), and families of negative protein regulators that inhibit CDKs (Kong *et al.*, 2003;

Alberts *et al.*, 2008a). Mammalian CDKs comprise a family of 10 serine-threonine protein kinases (CDK1-10) that catalyse different cell cycle transitions. A CDK molecule binds to an activator molecule, a cyclin forming a protein complex (Donovan *et al.*, 2005; Alberts *et al.*, 2008a). This CDK-cyclin binding is a requisite for activation. Cell division cycle (Cdc) phosphatases, are responsible for removing phosphates from CDK binding sites to allow for further activation, thereby enabling the continuation of the cycle (Donovan *et al.*, 2005). Deregulation of the cell cycle marks the initiation and progression of cancer or neoplastic transformation of eukaryotic cells (Moniz *et al.*, 2011).

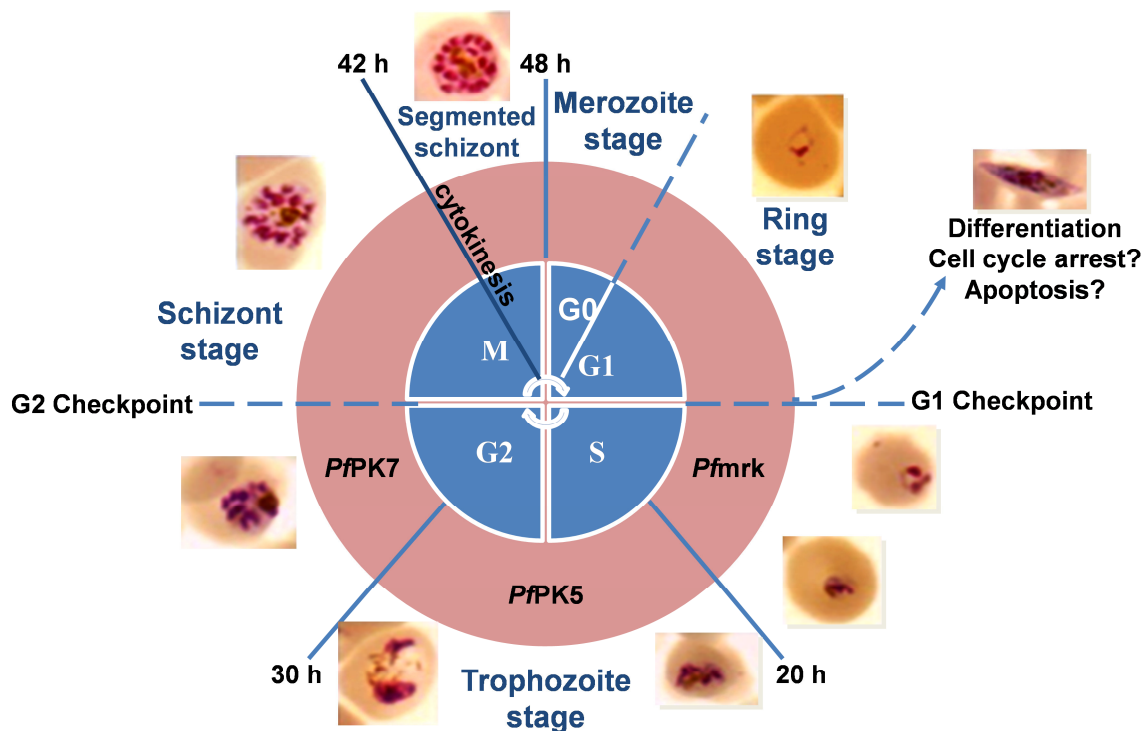


Figure 1.3 The *P. falciparum* cell cycle in comparison to the mammalian cell cycle (adapted from Arnot *et al.*, 2011; www.usma.edu). Mammalian cell cycle (inner blue circle) and *P. falciparum* (outer red circle). The free circulating haploid merozoites are in a G0-like state with condensed chromatin. The early trophozoite stage is similar to the G1-phase of mammalian cells. The S-like stage where DNA synthesis occurs begins soon after the appearance of malaria pigmentation (haemozoin) and continues throughout late trophozoite into the early schizont stage. Progression from G2-like stage to the mitotic-like stage is not discretely defined. Genomic segregation is rapid and may occur in 8-10 h. DNA segmentation occurs and merozoites are prominent in mature, late schizonts (Arnot and Gull, 1998; Arnot *et al.*, 2011).

P. falciparum homologues of several genes that encode critical regulators of DNA replication including CDKs and cyclins, have been identified (Doerig *et al.*, 2010). The first CDK-related protein kinase to be reported in *P. falciparum* was PfPK5 which showed homology to CDK1 (human cdc-2 protein) and CDK5 (Ross-Macdonald *et al.*, 1994; Doerig *et al.*, 2002). PfPK5 is putatively involved in the regulation of the S-like phase during trophozoite stage (Figure

1.3) in *P. falciparum* (Graeser *et al.*, 1996). *PfPK6* mRNA has been detected in parasites undergoing ring to schizont transition and showed homology to CDK1 and mitogen-activated protein kinases (Bracchi-Ricard *et al.*, 2000). *PfPK6* does not require cyclin binding for kinase activity *in vitro*, whilst *PfPK5* is able to autophosphorylate in the presence of a cyclin (Bracchi-Ricard *et al.*, 2000; Le Roch *et al.*, 2000). A MO15-related kinase, *Pfmrk*, has been detected in both asexual intra-erythrocytic forms and gametocytes (at higher levels), and is most closely related to CDK7, the kinase responsible for the activation of CDK1 (Li *et al.*, 1996). *PfPK7*, an orphan protein kinase with maximal homology to MEK3/6, has been shown to be involved in a pathway that regulates parasite asexual proliferation and sexual development. Genetically re-engineered clones without the *PfPK7* gene have shown a decrease in erythrocytic asexual growth associated with reduced number of daughter merozoites produced per schizont (Dorin-Semblat *et al.*, 2008). In addition, *PfPK7*-negative parasites have also shown a reduction in the ability to produce oocysts in the mosquito vector during the sexual developmental stages (Dorin-Semblat *et al.*, 2008). *Pfcrk-1* (*P. falciparum* cdc2-related protein kinase), closely related to the p58 gene subfamily, members of which are negative regulators of cell growth in vertebrates, has been detected in gametocytes (Doerig *et al.*, 1995). *PfNek-4*, a Never-in-mitosis *Aspergillus nidulans* (NIMA)-related kinase, has been detected and putatively involved in regulating gametocytogenesis and the maturation of the zygote of the *P. falciparum* parasite (Reininger *et al.*, 2012). Several compounds have been found to be selectively active against CDKs and other kinases. Purine analogues, which are structurally related to ATP, the natural substrate for kinases, are such a class of compounds (Harmse *et al.*, 2001).

1.9 Targeting the nucleoside metabolic pathway in *P. falciparum* parasites

Studies on the metabolism of pyrimidines nucleosides in humans started as early as 1927 (Rose and Coe, 2008). Research on the potential therapeutic role of nucleosides continued in 1929 focusing on the effects of purinergic compounds on the cardiovascular system (Rose and Coe, 2008). This interest in metabolism of nucleic acids combined with the discovery of the double helix structure of DNA led to studies in nucleoside analogues and anti-metabolite therapeutic agents. For instance, 6-mercaptopurine, a nucleoside analogue drug developed by Nobel Prize award recipients, Elion and Hitchings, is still an approved agent for human leukaemias (Bruce *et al.*, 2011). Elion and Hitchings work also led to the development of drugs for immunosuppression (azathioprine) and anti-viral chemotherapy (acyclovir, ganciclovir, vidarabine and zidovudine) (Bruce *et al.*, 2011). The development of allopurinol, a hypoxanthine analogue, was based on the same work. Allopurinol is used to treat

hyperuricaemia in patients with gout and acts by inhibiting xanthine oxidase, thus preventing the synthesis of urate from hypoxanthine and xanthine (Grosser *et al.*, 2011). In order to survive, the *P. falciparum* parasite has evolved and developed a unique life-cycle and metabolic pathways, different from that of its human host (Baldwin *et al.*, 2007). Therefore, these biochemical pathways such as energy metabolism, protein synthesis, lipid biosynthesis, nucleic acid synthesis and folate metabolism have been previously identified as drug targets (Mishra *et al.*, 2006). Nucleoside analogues are designed to interfere with the synthesis of nucleic acids in *P. falciparum* (Gero *et al.*, 2003). Some synthetic purine-derived CDK-inhibitors such as olomoucine and roscovotine show activity against *P. falciparum* (Harmse *et al.*, 2001).

1.9.1 Nucleosides, nucleic acid precursors

Nucleosides formed by the combination of a purine or pyrimidines nitrogenous base with a pentose sugar, either ribose or 2-deoxyribose, are critical in prokaryotic and eukaryotic cells as precursors of nucleotides (Figure 1.4) and nucleic acids for cell replication and survival (King *et al.*, 2006; Alberts *et al.*, 2008b). Nucleotides such as ATP provide cellular energy (King *et al.*, 2006). DNA is a double helix polymer structure with two antiparallel strands, sense strand in the 5-prime to 3-prime direction and the anti-sense strand in the opposite direction. The DNA chain is composed of four types of deoxyribonucleotide subunits containing bases adenine (A), cytosine (C), guanine (G) and thymine (T). In the ribonucleic acid (RNA) single strand chain, the thymine nucleotide subunit is substituted by uracil (U) (Alberts *et al.*, 2008b). According to the Watson-Crick base pair model, the purine bases (A and G) on one chain and pyrimidines bases (T or U and C) on the other chain pair in a complimentary manner (Alberts *et al.*, 2008b).

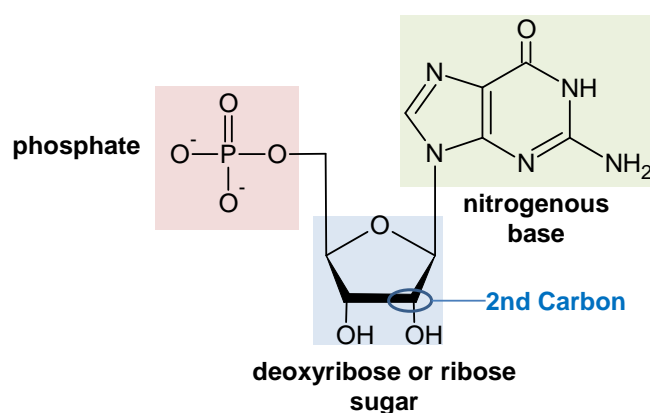


Figure 1.4 Nucleotide structure (adapted from Alberts *et al.*, 2008b). A nucleotide comprises a phosphate, sugar (deoxyribose or ribose) and a nitrogenous base, in this case guanine (a purine). In DNA the deoxyribose sugar lacks a hydroxyl (-OH) group on the second carbon atom. A nucleoside is a combination of the sugar and the base, a purine or pyrimidine (Alberts *et al.*, 2008b).

1.9.2 Cellular nucleoside transport

Plasma membrane transporters are specialised proteins that facilitate the movement of lipid-insoluble molecules with a large molecular size that cannot diffuse into prokaryotic or eukaryotic cells (Rose and Coe, 2008). Non-infected human RBCs express both the endogenous equilibrative nucleoside transporter (hENT1), encoded by SLC29A1 gene and facilitative nucleobase transporter (hFNT1) proteins (Quashie *et al.*, 2010). The ENT family of transporters is restricted to eukaryotes and hENT1 is found in the heart and central nervous system tissues (King *et al.*, 2006). Post-infection (10-20 h) during the trophozoite stage, the RBC expresses new permeation pathways (NPP) on the plasma membrane (Figure 1.5) (Baldwin *et al.*, 2007).

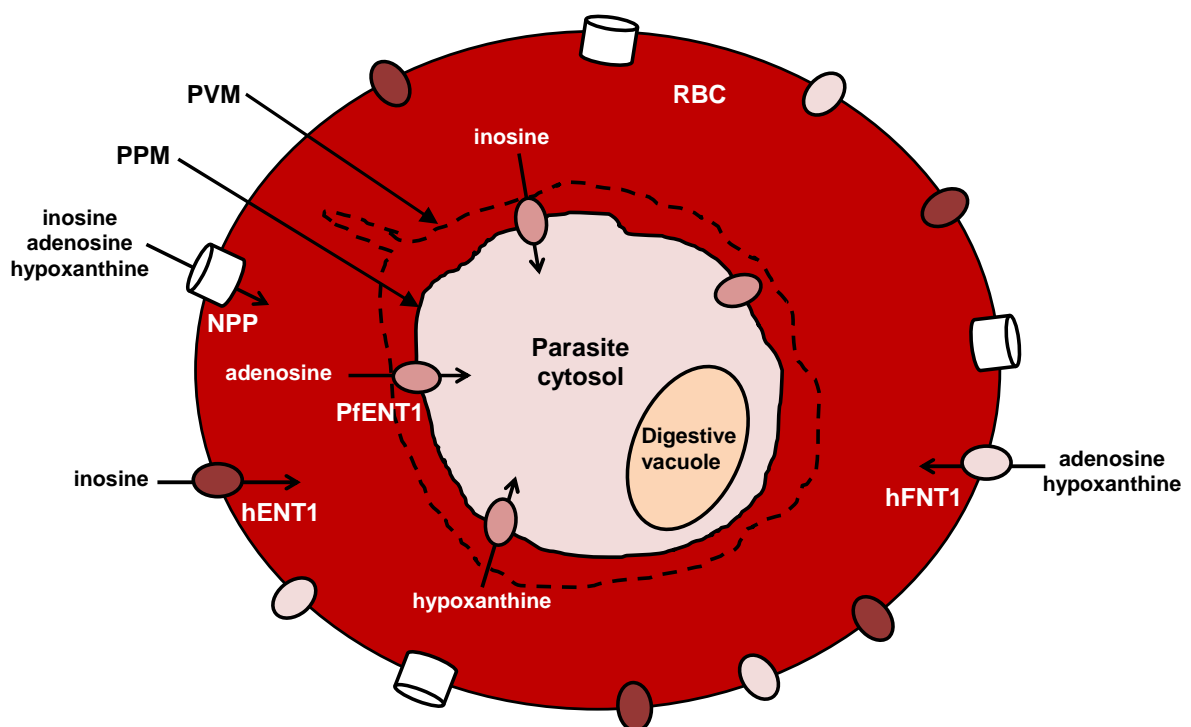


Figure 1.5 Nucleoside transporters and permeation pathways in the human RBC infected by *P. falciparum* during the parasite's trophozoite stage (adapted from Baldwin *et al.*, 2007). hENT1, human equilibrative nucleoside transporter 1; NPP, new permeation pathway; PVM, parasitophorous vacuole membrane; PPM, parasite plasma membrane; PfENT1, *P. falciparum* equilibrative nucleoside transporter 1.

NPPs are non-saturable channel-like systems that transport low molecular weight compounds including purines (Quashie *et al.*, 2010). The compounds moving between the RBC and the parasite have to cross a series of three membranes, the host RBC membrane, the parasitophorous vacuole membrane (PVM) and the parasite plasma membrane (PPM) (Figure 1.5) (Gero *et al.*, 2003; Baldwin *et al.*, 2007). Previous studies have demonstrated that NPPs are sensitive and may be inhibited by chloride-channel inhibitors such as furosemide and 5-

nitro-2-(4-phenylbutylamino) benzoic acid (Baldwin *et al.*, 2007). The parasitophorous vacuole membrane is proposed to possess non-selective channels. Permeation of nucleosides through the parasite plasma membrane is then mediated by *Pf*ENT1 transporter proteins into the parasite itself (Gero *et al.*, 2003). In addition to nucleosides, there is increased permeability of nutrients, such as carbohydrates, amino acids, cations: sodium (Na), potassium (K), zinc (Zn), iron (Fe), small peptides, several antimalarial drugs as well as an increased efflux of lactate (Gero *et al.*, 2003).

1.9.3 *Plasmodium* nucleotide biosynthesis

Nucleotides are either anionic or polyanionic and therefore are not permeable to cellular membranes (Gero *et al.*, 2003). However, nucleosides and their analogues are neutral molecules which can cross cell membranes and need to be intracellularly phosphorylated into their respective nucleotides (Gero *et al.*, 2003). *P. falciparum* is a purine auxotroph or lacks the ability to biosynthesize purine nucleotides *de novo* and instead relies upon the purine nucleosides and nucleobases salvaged from the host RBC (Baldwin *et al.*, 2007; Cassera *et al.*, 2011). Genomic sequencing of *P. falciparum* has shown that nine of the ten enzymes required for the biosynthesis of inosine monophosphate (IMP), a metabolic precursor for all purine nucleotides required for nucleic acid synthesis, are not encoded for (Baldwin *et al.*, 2007). Instead, hypoxanthine salvaged from the host is phosphorylated by a hypoxanthine-guanine-xanthine phosphoribosyl transferase (*Pf*HGXPRT) enzyme within the parasite to form IMP (Figure 1.6) (Cassera *et al.*, 2011). RBCs contain concentrations of ATP in equilibrium with adenosine diphosphate (ADP) and adenosine monophosphate (AMP), which placed no evolutionary pressure on the parasite to retain its *de novo* purine synthetic pathways (Cassera *et al.*, 2011).

1.9.3.1 Purine salvage and metabolic pathway

Hypoxanthine is the key precursor for all purine synthesis in *Plasmodium* metabolism, which is another reason why hypoxanthine is commonly added as a nutritional supplement in malaria parasite culture media (Cassera *et al.*, 2011). The source of hypoxanthine *in vivo* is the RBC purine pool where ATP is metabolically exchanged with hypoxanthine (Figure 1.6) (Cassera *et al.*, 2011). Human RBCs lack *de novo* purine biosynthesis, but maintain low concentrations of adenine nucleotide by salvaging adenosine via human adenosine kinase (hAK) enzyme (Cassera *et al.*, 2011). *P. falciparum* lacks adenosine kinase activity, but can salvage adenosine by conversion to inosine by adenosine deaminase (*Pf*ADA) and subsequently to hypoxanthine by purine nucleoside phosphorylase (*Pf*PNP) kinase activities (Figure 1.6) (Cassera *et al.*, 2011). Hypoxanthine is then converted to IMP by *Pf*HGXPRT.

Since *P. falciparum* cannot convert adenosine to AMP, it takes up AMP synthesised in the RBC, inducing more RBC AMP production (Cassera *et al.*, 2011).

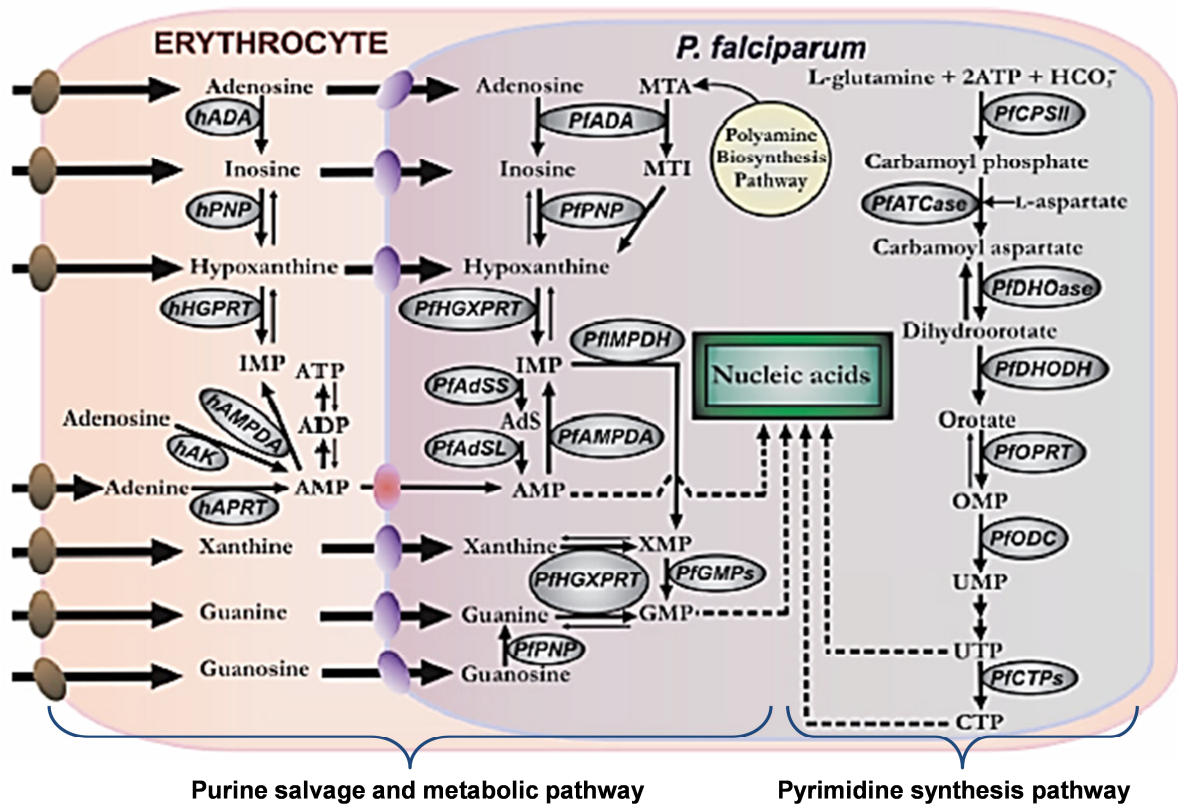


Figure 1.6 Enzymatic purine salvage and *de novo* pyrimidine metabolic pathways (adapted from Cassera *et al.*, 2011). Purine pathway: AMP, adenosine 5'-monophosphate; ADP, adenosine 5'-diphosphate; ATP, adenosine 5'-triphosphate; IMP, inosine 5'-monophosphate; XMP, xanthosine 5'-monophosphate; GMP, guanosine 5'-monophosphate; hADA, human adenosine deaminase; MTA, methylthioadenosine; MTI, methylthioinosine; AdS, adenylosuccinate; hPNP, human purine nucleoside phosphorylase; hHGPRT, human hypoxanthine-guanine phosphoribosyl transferase; hAK, human adenosine kinase; hAMPDA, human adenosine 5'-monophosphatedeaminase; hAPRT, human adenine phosphoribosyl transferase; *Pf*ADA, *P. falciparum* adenosine deaminase; *Pf*PNP, purine nucleoside phosphorylase; *Pf*HGPRT, hypoxanthine-guanine-xanthine phosphoribosyl transferase; *Pf*AMPDA, adenosine 5'-monophosphatedeaminase; *Pf*IMPDH, inosine 5'-monophosphate dehydrogenase; *Pf*GMPs, guanosine 5'-monophosphate synthase; *Pf*AdSS, adenylosuccinate synthetase; *Pf*AdSL, adenylosuccinate lyase. Pyrimidine pathway: OMP, orotidine 5'-monophosphate; UMP, uridine 5'-monophosphate; UTP, uridine 5'-triphosphate; CTP, cytidine 5'-triphosphate; *Pf*CPSII, carbamoyl phosphate synthetase II; *Pf*ATCase, aspartate carbamoyltransferase; *Pf*DHOase, dihydroorotase; *Pf*DHODH, dihydroorotate dehydrogenase; *Pf*OPRT, orotate phosphoribosyltransferase; *Pf*ODC, orotidine 5'-monophosphate decarboxylase; *Pf*CTPs, cytidine 5'-triphosphate synthase. The bold arrows on reversible steps, indicate the metabolically favoured direction. Nucleoside/nucleobase transporters are indicated on each membrane: hENT, human erythrocyte nucleoside transporter (brown); *Pf*NT1, *P. falciparum* nucleoside transporter 1 (purple) and adenosine 5'-monophosphate transporter (red) (Cassera *et al.*, 2011).

1.9.3.2 *De novo* pyrimidine synthesis pathway

Unlike purines that are in abundance in human RBCs, pyrimidines exist in small concentrations (Cassera *et al.*, 2011). As a result *P. falciparum* has retained its capacity for *de novo* synthesis of pyrimidines and therefore lacks pathways for the salvage of pyrimidines from the host RBC (Reyes *et al.*, 1982; Cassera *et al.*, 2011). Instead, the *de novo* pathway is the only route available for the synthesis of pyrimidine nucleotides (Figure 1.6), as well as synthesis from pyrimidine substrates such as thymidine, cytidine, deoxycytidine, uridine and uracil (Reyes *et al.*, 1982). The *de novo* synthesis of pyrimidines from carbamoyl phosphate and aspartic acid follows the same metabolic pathway found in other eukaryotic cells and the human host RBC (Cassera *et al.*, 2011). *P. falciparum* cell growth and division demand sufficient purine and pyrimidine supplies, in particular deoxyadenosine triphosphate (dATP) and deoxythymidine triphosphate (dTTP), since the parasite contains the most (A+T)-rich (approximately 80%) genome sequenced to date (Cassera *et al.*, 2011).

1.10 CDK inhibition and antiprotozoal activity of imidazopyridines

Imidazo[1,2-*a*]pyridine is a bicyclic system with a bridgehead nitrogen atom (Figure 1.7), first described by Chichibabin in 1925 (Enguehard-Gueiffier and Gueiffier, 2007).

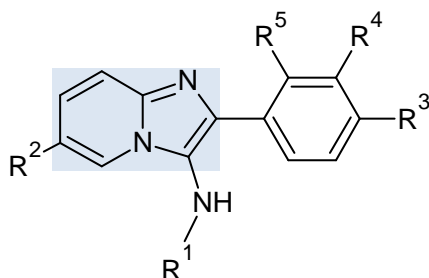


Figure 1.7 Parent chemical structure of the imidazopyridine (imidazo[1,2-*a*]pyridines) analogues. The imidazopyridine group is boxed.

Some imidazole pyrimidine analogues described by Enguehard-Gueiffier & Gueiffier (2007) demonstrated diverse pharmacological activities, including inhibition of enzymes involved in cell cycle regulation, receptor ligands of eukaryotic cells, anti-viral and antiprotozoal activity (Enguehard-Gueiffier and Gueiffier, 2007; Jones *et al.*, 2008). Other drug formulations containing imidazo[1,2-*a*]pyridines currently available on the market include alpidem (anxiolytic), zolpidem (hypnotic) and zolimidine (anti-ulcer) (Rousseau *et al.*, 2007). Antiprotozoal activity demonstrated by imidazopyridine analogues includes *Trypanosoma brucei rhodesiense*, *Trypanosoma cruzi*, *Plasmodium falciparum*, *Toxoplasma gondii* and coccidiosis (Enguehard-Gueiffier and Gueiffier, 2007). The suggested mechanism of action of

these imidazo[1,2-*a*]pyridine analogues involved the inhibition of parasite specific cyclic guanosine monophosphate (cGMP)-dependant protein kinase, although the parasites tested positive for mutagenesis (Enguehard-Gueiffier and Gueiffier, 2007). In the field of anti-cancer drugs, development of a series of imidazopyridine analogues targeting cyclin-dependant kinases has led to the discovery of drugs with anti-proliferative activity against various cell cancer lines. The proposed *in vitro* antiproliferative mechanism of action of 6-substituted imidazo[1,2-*a*]pyridines on HT-29 and Caco-2 cancer cell lines has been proposed to be mediated via the intrinsic apoptotic pathway (Dahan-Farkas *et al.*, 2011). Several other imidazo[1,2-*a*]pyridines and related imidazo[1,2-*a*]pyrimidines have been reported to be selective CDK-inhibitors, bradykinin B₂ receptor antagonists, gamma-aminobutyric acid and benzodiazepine receptor agonists (Rousseau *et al.*, 2007). In addition, a high-throughput screen of the AstraZeneca compound library identified a series of imidazo[1,2-*a*]pyridines as potent inhibitors of CDK2 and CDK4 (Anderson *et al.*, 2003; Enguehard-Gueiffier and Gueiffier, 2007).

1.11 Targeting the haemozoin formation pathway

Since the discovery of the malaria parasite in the 18th century, the malaria pigment (haemozoin), observed during the trophozoite stage, has played a role in revealing the life-cycle of the parasite (Ross and Smyth, 1897; Egan, 2008a). Slater *et al.* (1991) confirmed that indeed haemozoin consists of ferriprotoporphyrin-IX (Fe³⁺-PPIX) and that it is identical to synthetic β -haematin (Slater *et al.*, 1991). During its pathogenic asexual erythrocytic stage, the RBC cytoplasm is ingested into the parasite by a cytostome and transported to the digestive vacuole by double membrane bound transport vesicles (Figure 1.8) (Egan, 2008a). The *P. falciparum* parasite degrades up to 65-75% of the hosts' RBC haemoglobin during intra-erythrocytic growth (Skinner-Adams *et al.*, 2010). Inside the digestive vacuole, haemoglobin is digested by proteolytic enzymes; namely aspartic proteases (plasmepsins I, II, IV and histo-aspartic protease), cysteine proteinases (falcipains 2, 2' and 3), metallo-protease (falcilysin), dipeptidyl aminopeptidases I or cathepsin c to small peptides (Figure 1.8) (Skinner-Adams *et al.*, 2010). These small peptides are then exported to the parasite cytosol and finally degraded to amino acids by aminopeptidases (Skinner-Adams *et al.*, 2010). Free haem containing Fe²⁺-PPIX is released following haemoglobin digestion, and is spontaneously oxidised to form haematin, Fe³⁺-PPIX and toxic hydrogen peroxide (H₂O₂) by-products, capable of destroying the parasite membrane through oxidative stress, resulting in parasite death (Egan, 2003). In order to sequester and protect itself from this free toxic haematin, the parasite polymerises up to 95% of the haematin into the inert, microcrystal

structure known as haemozoin or malaria pigment. Haemozoin is a yellow-brown water-insoluble crystal, that is clearly visible, within the digestive vacuole (Egan, 2003; Egan, 2008b).

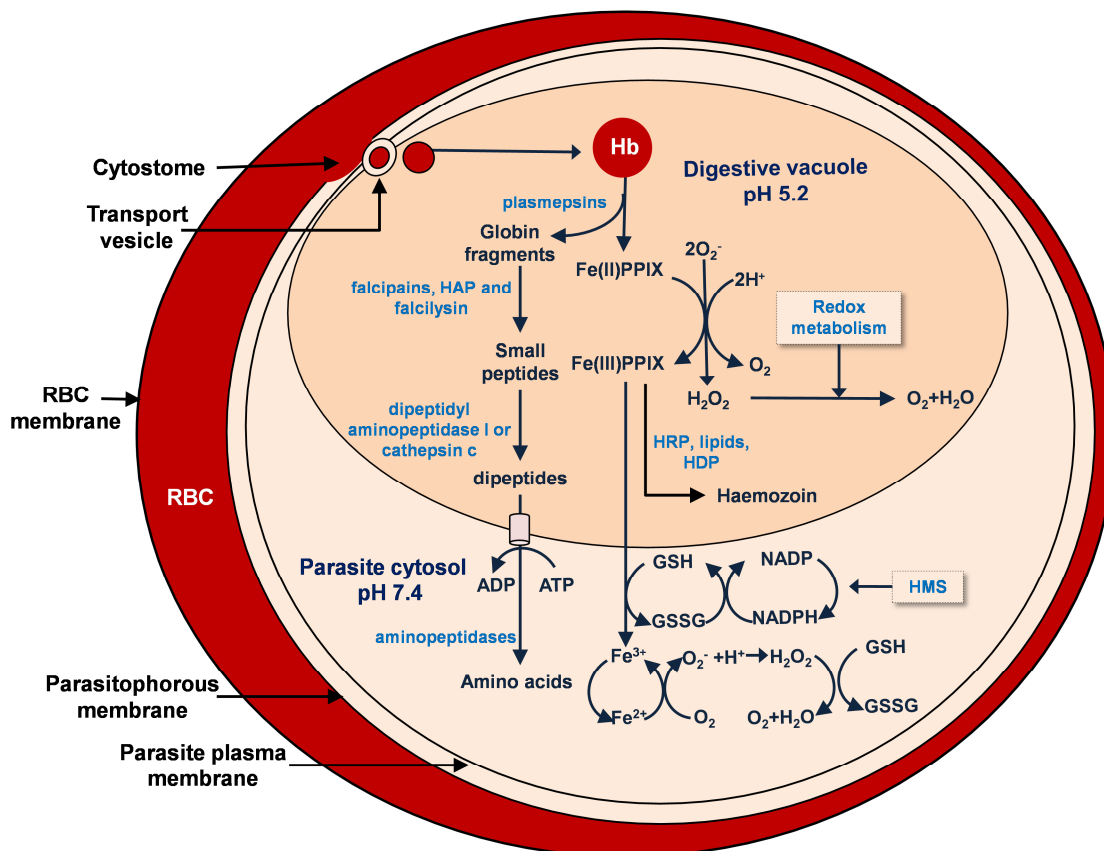


Figure 1.8 Haem metabolic pathway within a *P. falciparum*-infected RBC (adapted from Ginsburg, 2013). Hb, haemoglobin; Fe^{2+} -PPIX, ferriprotoporphyrin-IX or haem; Fe^{3+} -PPIX, haematin; H_2O_2 , hydrogen peroxides; O_2^- , superoxide anion; HRP, histidine-rich protein; HDP, haem detoxification protein; GSH, reduced glutathione; GSSG, oxidised glutathione; HMS, hexose monophosphate shunt; NADPH, nicotinamide adenine dinucleotide phosphate (Müller, 2004; Egan, 2008a; Skinner-Adams *et al.*, 2010; Ginsburg, 2013).

Haemozoin formation is susceptible to numerous therapeutic drugs. Quinolines and 4-aminoquinolines, such as quinine and chloroquine, respectively, are known to act by inhibiting the haemozoin formation pathway by forming haem-drug complexes, thus preventing the polymerisation of haem into haemozoin (Kumar *et al.*, 2007; O'Neill *et al.*, 2012). For instance, chloroquine is a weak base and in its non-ionised form can readily traverse down the pH gradient, from the RBC cytosol across the membranes into the acidic digestive vacuole where it is ionised (O'Neill *et al.*, 2012). In its ionised form, chloroquine then becomes less lipophilic and becomes trapped inside the digestive vacuole where it accumulates - a phenomenon called “ion-trapping” (Section 2.1.2) (Krogstad *et al.*, 1987; O'Neill *et al.*, 2012). Ionised chloroquine then pharmacologically acts by binding to monomeric units of haematin and preventing it from polymerising into haemozoin (Egan,

2006; O'Neill *et al.*, 2012). As a result the amount of free toxic haematin increases, generating reactive oxygen species which in turn causes oxidative stress to the parasite. Oxidative stress may lead to lipid peroxidation of cell membranes, DNA damage and protein-carbonyl formation, which could eventually lead to parasite death (Kumar *et al.*, 2007). The first synthetic antimalarial drug, methylene blue, a phenothiazinium dye and related synthetic colourants, and natural colourants such as curcumin have been shown to possess antimalarial activity, possibly by inhibiting haemozoin formation by complexation with haem, in a similar manner to chloroquine (Vennerstrom *et al.*, 1995).

1.12 Antimalarial activity of some colourants

Methylene blue, a phenothiazinium dye, is commonly used as a dye in various biological staining procedures in bacteriology and cytological studies. The components of the blood stain, eosin and methylene blue, were introduced by Baeyer and Caro, respectively (Krafts *et al.*, 2011). Methylene blue was used primarily for detecting *Mycobacterium tuberculosis*, until Ehrlich, in 1880, mixed methylene blue with acid fuchsin to produce a stain which allowed differentiation of blood cells (Krafts *et al.*, 2011).

Colourants are widely used in various industries including the textile, printing, pharmaceutical, cosmetic and food industries, as well as in laboratories as biological staining agents and pH indicators (Chung *et al.*, 1992). Scientists soon realised that some dye derivatives could selectively stain different cell types (Wainwright, 2008). In addition, these dyes could modify physiological processes like motility of microorganisms such as bacteria and protozoa. Ehrlich and Guttman (1891) introduced the idea that these compounds could be used in chemotherapy when they successfully treated a patient infected with malaria with methylene blue (Wainwright and Amaral, 2005; Wainwright, 2008).

1.12.1 General chemistry of colourants

Colourants possess colour due to the following chemical properties: (i) absorb light in the visible range (400 – 700 nm) of the electromagnetic spectrum; (ii) have at least one colour-bearing group (chromophore); (iii) have a conjugated system of alternating double and single bonds, and (iv) exhibit resonance of electrons, which provide stability in organic compounds (IARC, 2010). In addition to chromophores, most colourants contain auxochrome groups (Figure 1.9) which act as electron donors (Zollinger, 1987). Chromophores are a group of atoms in a molecule responsible for the absorption of radiation, such as carbonyl groups, nitriles and azo groups. Auxochromes (colour helpers) on the other hand enhance or even shift the colour of a colourant, but do not impart colour and include carboxylic acid, sulfonic acid,

amino and hydroxyl groups (Zollinger, 1987). Auxochromes are most often used to influence dye solubility (IARC, 2010).

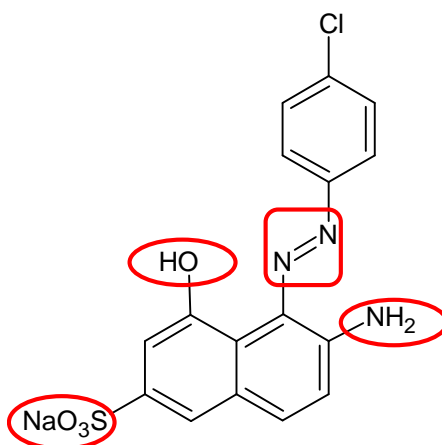


Figure 1.9 Chromophore and auxochromes of acid red azo compound (adapted from Verma *et al.*, 2012). The boxed azo group gives the acid red colourant its red colour. The circled functional groups are auxochromes that intensify the colour of the chromophore (Verma *et al.*, 2012).

Organic and inorganic colourants can be subdivided into natural and synthetic colourants (Zollinger, 1987). The majority of natural colourants used prior to the 19th century have been replaced by synthetic dyes due to the cost-effectiveness of production and stability of synthetic dyes (Gordon and Gregory, 1983).

1.12.2 Synthetic colourants

Synthetic dyes can be generally classified into eight main groups: (i) azo, (ii) anthroquinone, (iii) vat, (iv) indigoid, (v) polymethine, (vi) aryl-carbonium, (vii) phthalocyanine and (viii) nitro dyes (Gordon and Gregory, 1983). A prominent class of synthetic dyes, namely the azo dyes make up over 50% of the total dyes used worldwide (Gordon and Gregory, 1983; Zollinger, 1987). This can be largely attributed to the low cost production technique (azo coupling) that allows for a wide variation of di-azo compounds (Gordon and Gregory, 1983).

1.12.2.1 Azo dyes

Azo dyes are widely used in various industries such as textile, printing, pharmaceutical, cosmetic and food industries, and in research laboratories as previously indicated (Zollinger, 1987; Tsuda *et al.*, 2000). Azo dyes contain an azo group (Figure 1.10) that consists of two nitrogen atoms linked by a double bond ($R-N=N-R'$) with mostly aromatic side chains, either benzene or naphthalene rings (Zollinger, 1987). The azo group appears to be an electron acceptor. These can be further classified according to the number of azo groups, for example diazos (Figure 1.10) have two linked nitrogen atoms as a terminal reactive group ($R_2C=N_2$) (Zollinger, 1987). Since the discovery of macrozamin in 1951, a number of natural occurring

azoxy ($R-N=N(O)-R'$) compounds such as cycasin, elaiomycin, maniwamycin, azoxybacillin and valanimycin have been discovered (Zollinger, 1987; Engel *et al.*, 2003).

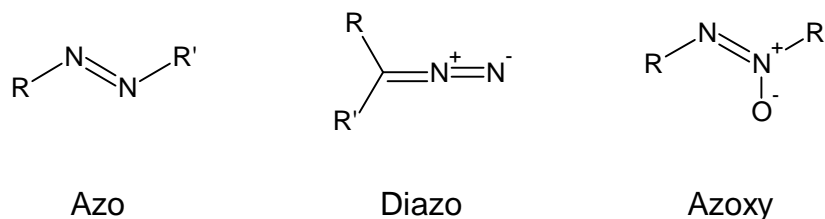


Figure 1.10 Chemical structures of azo, di-azo and axozy compounds (Zollinger, 1987).

1.12.2.1.1 Discovery of sulfa drugs from azo dyes

Sulfadiazine is indicated for treatment of burns, while sulfadoxine in combination with pyrimethamine has antimalarial activity, although wide-spread parasite resistance has been associated with the latter combined drug therapy (Shapiro and Goldberg, 2006; Wainwright, 2008). Azo-polymers have been utilised in the design of drug delivery systems for localised therapy. Pro-drugs such as sulfasalazine were developed for delivery of 5-aminosalicylic acid specifically to the colon for localised effect in inflammatory bowel disease (Jain *et al.*, 2006).

1.12.2.1.2 Metabolism of food colourants

Colourants are added to various types of foodstuffs including beverages, confectioneries and processed meats in order to increase their appeal (Zollinger, 1987). Most food colourants have no nutritional value and their use is regulated in most countries to prevent food toxicity. The concentration of dyes in coloured foods is usually only 0.005 to 0.03% by weight (Zollinger, 1987). Natural food dyes either extracted from plants or synthesised chemically as natural by-products are an expensive alternative and are usually unstable, thus making synthetic dyes more attractive from a manufacturing perspective (Zollinger, 1987). Ingested azo dye compounds are metabolised in humans by azoreductase enzymes found in the liver, gastrointestinal microflora and eliminated by renal excretion (Golka *et al.*, 2004). Intestinal azoreductase activity has however been found to be reduced by various dietary factors such as fibre, *Lactobacilli* live culture supplements and antibiotics (Chung *et al.*, 1992). The azoreductase reaction (Figure 1.11) may yield active and carcinogenic metabolites such as benzene and naphthol depending on the azo dye's chemical structure (Li *et al.*, 2007).

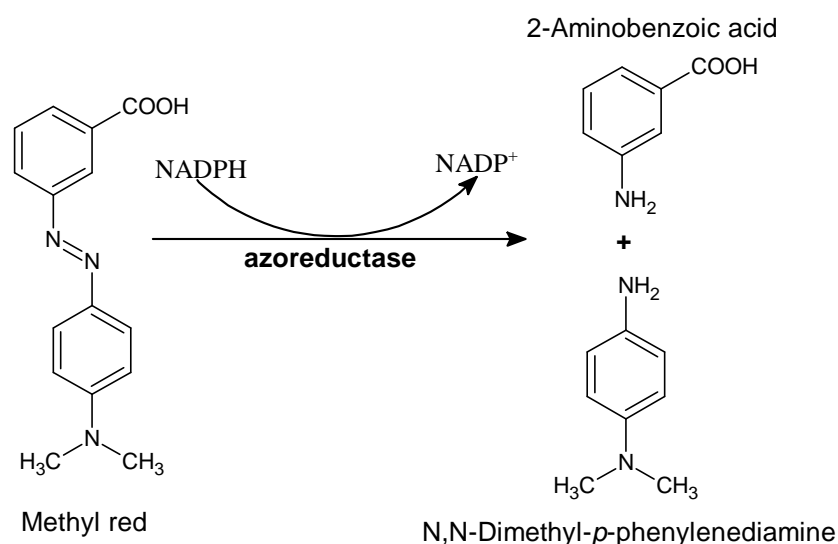


Figure 1.11 Azoreduction of methyl red (adapted from Chen *et al.*, 2005). The mechanism of action of azoreductase in the reduction of methyl red involves oxidation of NADPH, which acts as an electron donor and reductive agent. The reaction results in metabolites, *N,N*-dimethyl-*p*-phenylenediamine and 2-aminobenzoic acid.

1.12.2.2 Phenothiazinium and related dyes

In 1891, Ehrlich and Guttman reported antimalarial activity of a synthetic phenothiazinium dye, methylene blue, after oral administration to two patients who were clinically cured. The only side-effect was described as “spastic irritation of the bladder” (Vennerstrom *et al.*, 1995). Previous to this, Ehrlich had successfully treated neuralgias with methylene blue, but this was the first documented cure of malaria with a synthetic chemical. Although methylene blue itself was not as efficient a stain for normal RBCs as its derivatives, it had previously demonstrated specific staining of *Plasmodium* species (Vennerstrom *et al.*, 1995; Wainwright and Amaral, 2005).

1.12.2.2.1 Methylene blue

Methylene blue (CAS 61-73-4) is a phenothiazinium salt and the earliest reported synthetic antimalarial drug (Wainwright and Amaral, 2005). At room temperature it appears as a solid dark green powder, but turns blue when in solution. In its reduced-form, methylene blue appears colourless (Figure 1.12) (Schirmer *et al.*, 2003). It is suggested that it is the spontaneous cycling between the oxidised and reduced forms of methylene blue (or leucomethylene blue) (Figure 1.12) that make it an effective reduction-oxidation (redox) reagent (Atamna and Kumar, 2010). Methylene blue is clinically indicated for methaemoglobinaemia therapy, the prevention of ifosfamide-induced encephalopathy and has demonstrated neuroprotective activity in Alzheimer’s disease (Schirmer *et al.*, 2003; Atamna and Kumar, 2010).

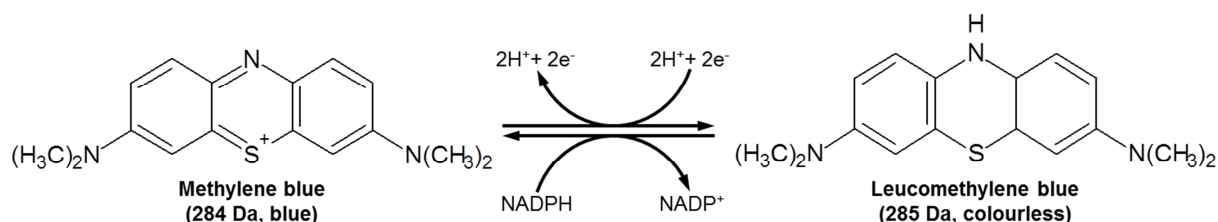


Figure 1.12 Redox reaction of methylene blue (adapted from Schirmer *et al.*, 2005). The redox reaction of methylene blue involves the oxidation of riboflavins, flavin adenine dinucleotide (FADH₂) and nicotinamide adenine dinucleotide (NADPH).

1.12.2.2.2 Safranin O

Safranin O (CAS 477-73-6; Figure 1.13), a cationic phenazinium dye structurally related to methylene blue, is commonly used in histochemical staining (Rosenberg, 1971). In its application it has been used in combination with fast green as a counterstain and with iron-haematoxylin to stain nuclei (Rosenberg, 1971). It has been particularly useful in differential staining of tissue polyanions in pathological studies of articular cartilage degradation such as in rheumatoid arthritis (Rosenberg, 1971). The antimalarial activity of phenazinium dyes such as Janus green B, phenosafranin, methylene violet 3RAX and indoine blue, safranin O and its analogues were reinvestigated for their *in vitro* inhibitory effect on the D6 and chloroquine-resistant W2 strains of *P. falciparum* parasite growth (Vennerstrom *et al.*, 1995).

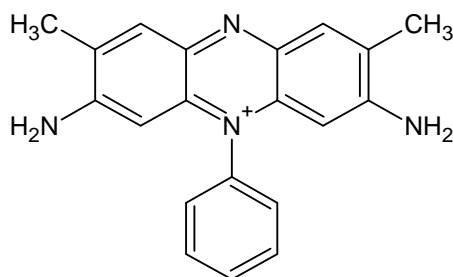


Figure 1.13 Chemical structure of safranin O (PubChem Compound, 2013c).

1.12.3 Natural compounds as a source for antimalarial drugs

Plants have been a source of medicine throughout history and continue to serve as a source for many pharmaceutical agents today (Ginsburg and Deharo, 2011). The medicinal properties of plants have been described as early as 2000 B.C. and documented in early Egyptian, Ayurvedic, Chinese traditional medicine, and various European documents and pharmacopoeia (Patwardhan, 2005; Kong *et al.*, 2009). The medicinal use of the cinchona tree (*Cinchona ledgeriana*) from South America, Peru, dates back more than 350 years, for curing fever and shivers. Only in 1820, the antimalarial drug quinine was isolated from the powdered

bark of the cinchona tree by Pelletier and Caventou (Vinetz *et al.*, 2011). Another potent antimalarial drug, artemisinin (qinghaosu) was derived from the plant *qing hao* (*Artemisia annua*) and has been recognised for its medicinal properties for more than 2000 years by the Chinese (Vinetz *et al.*, 2011). In some Asian and African countries, 80% of the population relies on traditional medicine for primary health care (Ginsburg and Deharo, 2011). Authorities have also raised concerns regarding counterfeit, contaminated herbal products with insufficient toxicity data that pose serious patient safety threats (Newton *et al.*, 2010). Whilst the WHO and its Member States are co-operating in promoting the use of traditional medicine, the African Network for Drugs and Diagnostics Innovation seems to be poised to address toxicity testing protocols, as well as preserving knowledge of indigenous medicinal herbs (Nwaka *et al.*, 2010).

1.12.3.1 Therapeutic activity of some natural colourants

Certain plant and animal colour extracts are not only used as food additives, but have been used in traditional medicine as well. For instance, the chemotherapeutic properties of the active constituent in turmeric, curcumin (diferuloylmethane), has been extensively investigated and published in 6,360 papers (Shishodia *et al.*, 2007; PubMed, 2014). Among its numerous therapeutic roles, curcumin has demonstrated activity against chloroquine-resistant *P. falciparum*, various cancers and tumours, ulcerative colitis, hypercholesterolaemia, atherosclerosis, pancreatitis and Alzheimer's disease in various clinical trials (Lim *et al.*, 2001; Duvoix *et al.*, 2003; Reddy *et al.*, 2005; Goel *et al.*, 2008). *In vivo* studies have indicated that an artemisinin or arteether combination therapy with curcumin has the potential to prevent parasite recrudescence and relapse of *P. berghei*-infected mice, as well as provide protection against cerebral malaria (Reddy *et al.*, 2005; Nandakumar *et al.*, 2006; Padmanaban *et al.*, 2012; Vathsala *et al.*, 2012). In addition, *in vitro* studies by Reddy *et al.* (2005) and Nandakumar *et al.* (2006) demonstrated the inhibitory activity of curcumin against the chloroquine-resistant *P. falciparum* strains.

1.12.3.1.1 Curcumin

Curcumin (diferuloylmethane; CAS 458-37-7; food additive E100) is found in turmeric (*Curcuma longa*) powder (Goel *et al.*, 2008). The turmeric plant (Figure 1.14) is a stemless, leafy perennial herb of the ginger (*Zingiberaceae*) family (Van Wyk and Wink, 2004; Brittanica, 2013c). The plant has broad hairless leaves arising from near ground level with white and yellow flowers borne in oblong spikes. The rhizomes are fleshy, smooth and bright orange inside and are the source of turmeric (Van Wyk and Wink, 2004). Turmeric is an ancient spice and vegetable dye thought to have originated in India (Van Wyk and Wink,

2004; Goel *et al.*, 2008). In addition, *Curcuma* species are widely used for their benefits in stimulating bile secretion, the healing of peptic ulcers and carminative (release of gastric gas) effects (Van Wyk and Wink, 2004; Goel *et al.*, 2008). A daily intake of 2 g of dried rhizome and up to 9 g of fresh rhizome is recommended (Van Wyk and Wink, 2004). The yellow, non-volatile pigments (3-5% of dry weight) in turmeric are called curcuminoids and include curcumin, monodesmethoxycurcumin and bisdesmethoxycurcumin, of which curcumin is predominant (Lucas *et al.*, 2001; Van Wyk and Wink, 2004). The essential oil (2-7% dry weight) is rich in bisabolane, guaiane and several germacrane-type sesquiterpenes including ar-turmerone, α -turmerone, β -turmerone, carlone and zingiberene (Van Wyk and Wink, 2004; Funk *et al.*, 2009). Curcumin was first isolated in 1815, obtained in crystalline form in 1870 and ultimately identified as diferuloylmethane (Figure 1.15) (Goel *et al.*, 2008). In 1910, the feruloylmethane skeleton of curcumin was confirmed and synthesised. (Goel *et al.*, 2008). Curcumin has a chemical formula of $C_{21}H_{20}O_6$, and a molecular weight of 368.37 g/mol.

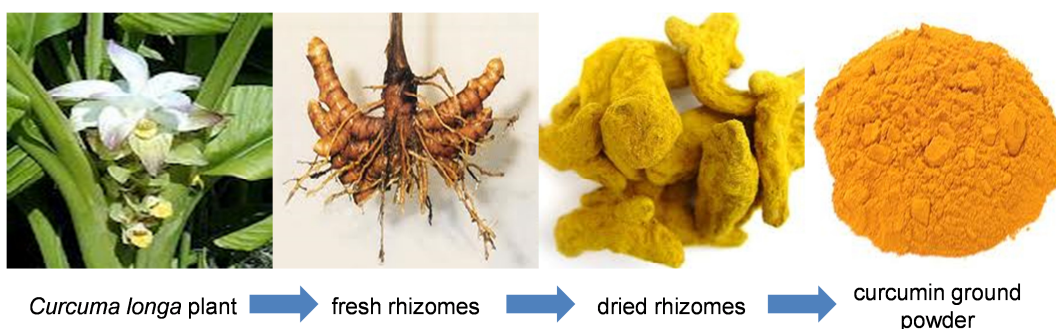


Figure 1.14 *Curcuma longa* plant and ground powder prepared from dried rhizomes (adapted from Goel *et al.*, 2008; Britannica, 2013c).

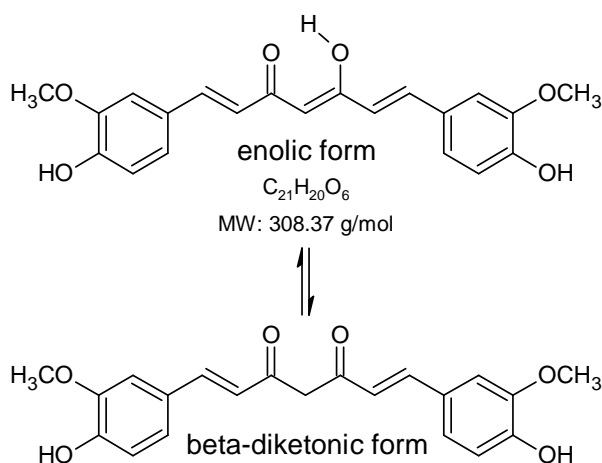


Figure 1.15 Chemical structure of curcumin (Goel *et al.*, 2008; PubChem Compound, 2013b). In solution, curcumin exists in enolic and β -diketonic forms, but primarily exists in enolic form.

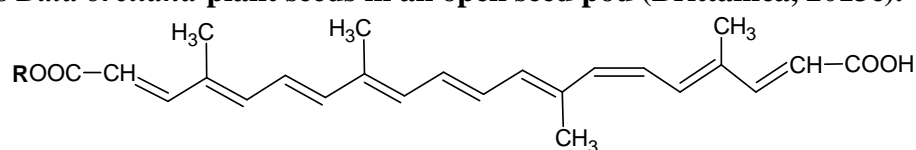
Pharmacological activity of curcumin and related compounds include anti-inflammatory, anti-oxidative, anti-microbial, anti-plasmodial and cytotoxicity toward tumour cells, but is contraindicated in cases of bile duct obstruction or gallstones (Van Wyk and Wink, 2004; Shishodia *et al.*, 2007; Goel *et al.*, 2008). In a study by Funk *et al.* (2009), turmeric essential oils demonstrated potent anti-inflammatory activity. As an anti-oxidant, curcumin is suggested to be even more potent than Vitamin E (Lim *et al.*, 2001). These anti-inflammatory and free radical scavenging properties were demonstrated in inhibiting inflammatory and oxidative damage that occur as a response to β -amyloid plaques in the transgenic mouse model carrying a human familial Alzheimer's disease gene (Lim *et al.*, 2001). Of greater importance to the current study, curcumin has previously demonstrated antiprotozoal effects against *Leishmania*, *Trypanosoma*, *P. falciparum* and *P. berghei* (Reddy *et al.*, 2005).

1.12.3.1.2 Annatto

Annatto (CAS 6983-79-5, food additive E160b) is red-yellow colourant extract from mature, dry seed pericarp (Figure 1.16) of the achiote tree, *Bixa orellana* (Bautista *et al.*, 2004). Annatto extract contains 80% bixin (Figure 1.17), a lipid-soluble carotenoid along with norbixin (Figure 1.17) which is a water-soluble hydrolysed derivative of bixin (Bautista *et al.*, 2004). In 1982, the WHO Expert Committee on Food Additives reduced the acceptable daily intake (ADI) of bixin (27%) from 1.25 mg/kg to 0.065 mg/kg body weight, which is significantly lower than the ADI of most synthetic colourants which is set at 0.5 mg/kg body weight due to insufficient toxicity data (Bautista *et al.*, 2004). Annatto (E160b) is a permitted food colorant under the European Community guidelines (Lucas *et al.*, 2001).



Figure 1.16 *Bixa orellana* plant seeds in an open seed pod (Brittanica, 2013c).



Bixin $R = CH_3$
Norbixin (annatto) $R = H$

Figure 1.17 Chemical structures of the constituent of annatto namely, bixin (~80%) and its hydrolysed derivative, norbixin (adapted from Evans, 1996).

1.12.3.1.3 Cochineal

Cochineal (CAS 1260-17-9, food additive E120) is extracted from a dried female insect, *Dactylopius coccus* (formerly called *Coccuss cacti*) which contains red pigmented eggs and larvae (Figure 1.18) (Evans, 1996). Cochineal was historically used as a dye in England as early as the 15th century. The *D. coccus* insects are indigenous to Central America and are usually found on cactus plants of the genus *Opuntia*, where they normally breed (Evans, 1996). Following fertilisation, the female insect swells up to double its former size due to the eggs (60 to 450 eggs) and developing larvae (Evans, 1996). The red-coloured larvae mature in 14 days and escape the body of the dead female insect. The insects are harvested by brushing the cacti plants. The red pigment is obtained by boiling the insects in water, or by exposure to the fumes of burning sulphur or charcoal (Evans, 1996). Cochineal contains about 10% carminic acid (Figure 1.19), a brilliant purple, water-soluble colouring matter, which is a C-glycoside anthroquinone derivative. The insects contain about 10% fat and 2% wax (Evans, 1996).

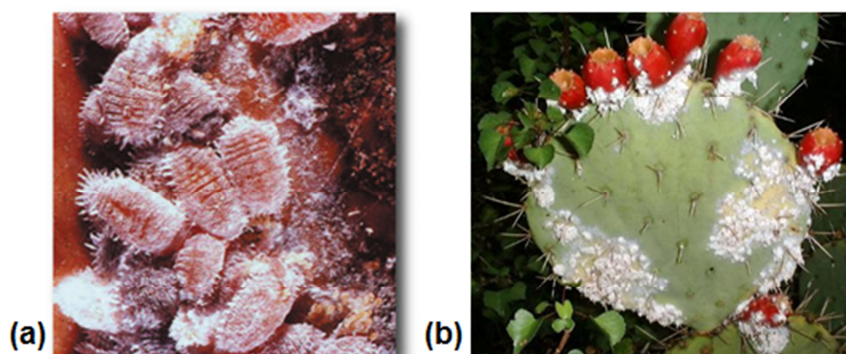


Figure 1.18 (a) Cochineal insects, (b) *Dactylopius coccus*, forming white clusters on *Opuntia* cactus (Brittanica, 2013b).

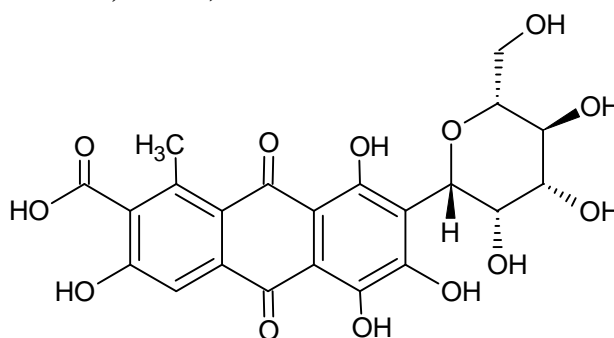


Figure 1.19 Chemical structure of carminic acid (PubChem Compound, 2013a).

1.12.3.1.4 Carmine

Carmine (food additive E120) is a purplish-red dye with an aluminium mordant, prepared from cochineal insects and contain about 50% carminic acid (Evans, 1996). The food

colourant carminic acid produces free radicals and in the presence of iron salts, readily damage membrane lipid and degrade carbohydrate deoxyribose (Gutteridge and Quinlan, 1986). A case of anaphylactic reaction was reported in a patient after ingestion of a generic carmine-coated azithromycin tablets suggesting carmine hypersensitivity in some patients (Greenhawt *et al.*, 2009). In the latter study, a skin-prick test including two brands of uncoated zithromax and azithromycin, isolated carmine-coating, commercial grade carmine and cochineal insect extract controls, showed reactivity to both the isolated carmine-coating and carmine solution within 30 min (Greenhawt *et al.*, 2009). In contrast, the patient showed no significant reaction to the cochineal insect extract control. Subsequently the patient took the zithromax tablet (without carmine coating) orally without adverse reactions (Greenhawt *et al.*, 2009).

1.12.3.1.5 Safflower

Safflower (CAS 8001-23-8) or *Carthamus tinctorius* L. is a member of the family Compositae (Dajue and Mündel, 1996). The safflower plant (Figure 1.20a) is an annual herb with toothed leaves and yellow flower heads (Van Wyk and Wink, 2004). The fruits are small, white nuts (achenes) that contain a single seed (Figure 1.20b).



Figure 1.20 The (a) safflower (*Carthamus tinctorius* L.) plant, (b) seeds and (c) dried flowers (Van Wyk and Wink, 2004).

Traditional uses of the flower extracts in Chinese medicine include the treatment of gynaecological ailments, inflammation, heart disorders and fever. Other uses of the flower extracts include relief of lower abdominal pain, to clean and treat wounds, scars, swellings and sprains. Dried flowers (Figure 1.20c) are prepared as tea infusions and tinctures or alcohol extracts (Van Wyk and Wink, 2004). The yellow pigments in the flowers are glycosylated dichalcones such as carthamin, safflower yellow B, safflornin C, hydroxysafflor

yellow A, and tinctormine (Van Wyk and Wink, 2004). Present in the flowers are numerous flavonoids (mainly quercetin and luteolin), α -tocopherol, triterpene alcohols (mainly helianol) and polysaccharides. The flowers are a source of yellow or red dye used to colour butter, liqueurs, confectionery and cosmetics (Van Wyk and Wink, 2004).

Pharmacologically, both the flowers and the oil have cholesterol lowering effects, while the polysaccharides are reported to act as immune stimulants (Van Wyk and Wink, 2004). The flavonoids and α -tocopherol possess anti-oxidant effects, whilst the triterpene alcohols are reported to be anti-inflammatory (Van Wyk and Wink, 2004). Alpha-tocopherol is reported to possess a vitamin E-like effect that is not only limited to protection against oxidative stress, but plays a role in cellular signalling functions in vascular smooth muscle and generates a metabolite that facilitates natriuresis (Brigelius-Flohe and Traber, 1999). The seed oil extract has the highest linoleic acid content of any seed oil and is used as a source of this acid in the health food industry (Van Wyk and Wink, 2004). Conjugated linoleic acid has been reported to have anti-carcinogenic, anti-obese, anti-diabetic and anti-cancer effects (Nagao and Yanagita, 2005).

1.12.3.1.6 Carbon black

Carbon black or vegetable black (CAS 1333-86-4, food additive E163) is a black powder of elemental carbon usually manufactured by the combustion of vegetable material at a high temperature to produce a black powder for food use (Wellmann *et al.*, 2006). However, oils with high aromatic hydrocarbon content are the preferred raw material for high production of carbon black (Wellmann *et al.*, 2006). Carbon black as a food additive is used in sugar and flour confectioneries (European Food Safety Authority, 2012). The IARC categorised carbon black as a Group 2B (meaning it is possibly carcinogenic to humans) colouring agent in 1995 (Wellmann *et al.*, 2006). Benzo[α]pyrene, a polycyclic aromatic hydrocarbon found in charbroiled food, environmental and tobacco smoke can be enzymatically metabolised into mutagenic and highly carcinogenic metabolites possibly associated with colon and lung cancers (Denissenko *et al.*, 1996; Le Marchand *et al.*, 2002; Jiang *et al.*, 2007). However, use of vegetable-derived carbon black (E153) containing 0.1-1 $\mu\text{g}/\text{kg}$ of residual carcinogenic polycyclic aromatic hydrocarbon, expressed as benzo[α]pyrene, has not been a safety concern (European Food Safety Authority, 2012).

1.12.3.1.7 Beetroot

The plant order, *Centrospermae* consists of ten families which produce red and yellow pigments collectively known as betalains (Harmer, 1980; Britton, 1983). Betalains include

two pigment classes, the red-violet betacyanins and the yellow betaxanthins (Strack *et al.*, 2003). Betalamic acid (Figure 1.21a) is the chromophore common to all betalain pigments (Strack *et al.*, 2003). Betalains are water-soluble and show some similarity to anthocyanins, however both pigment groups occur mutually exclusive to plants (Harmer, 1980; Britton, 1983). Most natural betacyanins (Figure 1.21b) are structurally based on two aglycones, namely betanidin and its epimer (different chirality at one carbon), isobetanidin (Britton, 1983). The addition of certain residues to betalamic acid determines whether the pigment may be classified as a betacyanin or betaxanthin (Figure 1.21c). Betalains are mostly restricted to higher plants in certain families of the *Centrospermae* including cacti, and are present in flowers, leaves and fruits or roots (Britton, 1983). The most commercially exploited betalain crop is red beetroot (food additive E162), *Beta vulgaris* (Figure 1.22a), which contains two major soluble pigments, betanin (red in colour) and vulgaxanthine I (yellow) (Azeredo, 2009).

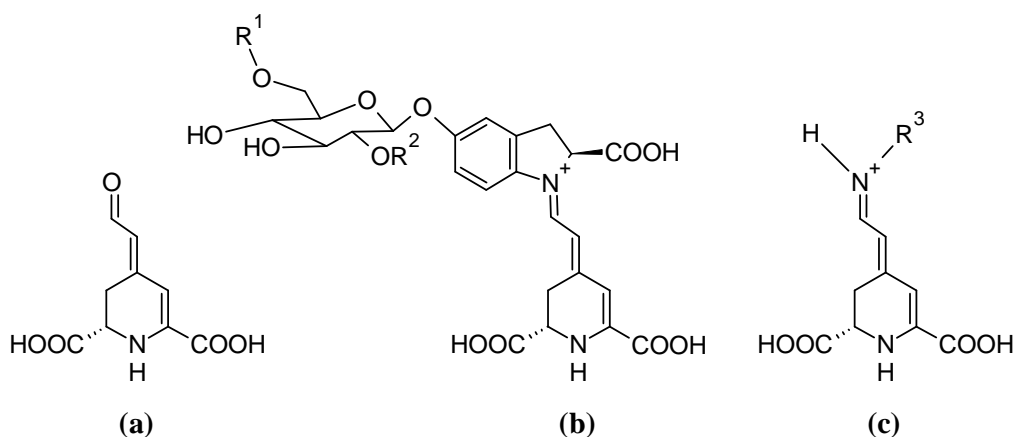


Figure 1.21 General chemical structures of (a) betalamic acid, (b) betacyanins and (c) betaxanthins (adapted from Strack *et al.*, 2003). Betanin: $R^1 = R^2 = H$. Betaxanthine: $R^3 =$ amine or amino acid group.

Betalains are added to foods such as desserts, confectioneries, dry mixes, dairy and meat products, and used as a pharmaceutical colourant (Evans, 1996; Azeredo, 2009). The spray-drying method used to obtain powdered beetroot (Figure 1.22c) yields approximately 1% betanin, whereas spray-drying which involves prior aerobic fermentation of the aqueous extraction may yield up to 8% betanin (Harmer, 1980).



Figure 1.22 Ground red powder from the bulbs of the *Beta vulgaris* plant (Brittanica, 2013a).

The potent free radical scavenging activity of betalains is well known and based on *in vitro* tests, some reports rank beets among the ten most potent vegetables with respect to their antioxidant activity (Azeredo, 2009). Betanin has demonstrated efficacy in the suppression of skin and liver tumours induced by different chemical carcinogens in mice (Kapadia *et al.*, 2003). Both betanin and betanidin have shown the ability to inhibit lipid peroxidation and haem decomposition *in vitro* (Kanner *et al.*, 2001). Interestingly, human RBCs incorporate dietary betalains which may protect the cells and avoid oxidative haemolysis (Tesoriere *et al.*, 2005). Betanin has shown to be effective in scavenging hypochlorous acid, the most powerful oxidant produced by human neutrophils. In addition, betanin acts as a reducing agent of the redox intermediates of myeloperoxidase, which catalyses the production of hypochlorous acid (Allegra *et al.*, 2005).

1.13 Problem statement

The drug research and development (R&D) process from compound screening to commercialisation and ultimate health impact is typically 10 to 15 years and costs ranging between 500 and 800 million US dollars (Nwaka *et al.*, 2009). Research and new drug development appears to be bias towards ailments such as hypertension, depression, tuberculosis and HIV/AIDS. Malaria is often regarded as one of the neglected diseases afflicting poor populations in developing countries (Nwaka *et al.*, 2009). Although malaria has in recent years received significant funding, the drugs expected from the existing R&D portfolio are a combination of current drugs such as the potent artemisinin derivatives, along with new novel agents. But even artemisinin-based drugs are threatened by resistance (Nwaka *et al.*, 2009; Dondorp *et al.*, 2011). Therefore, with the increasing resistance of *P. falciparum* to classical drugs such as mefloquine and artemisinin, and with the absence of a malaria vaccine that can deliver effective protection, there is a critical need in identifying new drugs with novel mechanism of actions. In addition, combination studies involving existing

effective drugs with these new drugs, is essential to delay or prevent the evolution of new resistance pathways (WHO, 2012).

1.14 Aims and objectives of the study

To this end, the aim of the study was to investigate the *in vitro* antimalarial activity of 56 select compounds (synthetic and natural colourants, novel nucleoside analogues and imidazopyridine analogues), taking into account the selectivity index (for malaria) of the most active test compounds, as well as elucidate a potential drug target such as haemozoin formation or the NIMA-related *PfNek-4* protein kinase enzyme.

In order to accomplish this, the main objectives of the study were as follows:

- Determine the anti-plasmodial activity of the test compounds on the asexual, intra-erythrocytic stages of *P. falciparum* over a single 48 h developmental cell-cycle.
- Analyse drug combination interactions of the most active compounds and classical antimalarial agent, quinine.
- Determine the selectivity index of most active compounds for *P. falciparum* parasites compared to transformed human epithelial cells and cancer cell line.
- Evaluate the ability of the lead compounds to inhibit haemozoin formation.
- Study the developmental stage-sensitivity of the asexual forms of the *P. falciparum* parasites to lead compounds.
- Express *PfNek-4*, a NIMA-related protein kinase putatively involved in the formation of gametocytes or conversion to the sexual stages of *P. falciparum*; as well as determine the inhibitory effects of most active compounds on the protein kinase activity of *PfNek-4*.

Chapter 2 Antimalarial activity

2.1 Introduction

New drugs for *P. falciparum* malaria infections should ideally be efficacious against drug-resistant strains and eliminate the disease within a reasonable time to ensure good compliance (Fidock *et al.*, 2004). Although, efficacy cannot be at the expense of toxicity, therefore the drugs need to be safe, suitable for small children and pregnant women and have appropriate formulations for oral use. In addition, these new drugs must be affordable so that they may be accessible to many who desperately need them, especially in Africa where most people must survive on less than 15 US dollars per month (Winstanley, 2000; Fidock *et al.*, 2004). However, the challenge of any drug discovery effort is to identify and develop compounds with properties that have predictive efficacy and safety in humans (Winstanley, 2000; Fidock *et al.*, 2004).

2.1.1 Approach to antimalarial drug screening

Screening of compounds may involve computational assessment of their physicochemical properties against molecular targets, *in vitro* or *in vivo* activity against the malaria parasite (Lipinski *et al.*, 2001; Fidock *et al.*, 2004). The compounds' *in vitro* activity may be measured by determining the concentration of the compound required for 50% inhibition (IC₅₀) of malaria parasite growth or survival (Fidock *et al.*, 2004). In order to ensure efficacy early on in the development of a drug, cut-off concentration values are used to narrow the search during high-throughput screening of compounds. These cut-off values vary depending on the class of the compounds or computational decisions, which should be in the range of less than 1 to 5 μM for *in vitro* screens and less than 5 to 25 mg per kg (oral or subcutaneous) for *in vivo* screens (Fidock *et al.*, 2004). In addition, there is a general consensus that drug combinations are essential for the optimal control of malaria in developing countries and in replacing existing monotherapies or combination therapies, such as chloroquine or sulphadoxine-pyrimethamine, respectively, that have low efficacy against resistant strains (Fidock *et al.*, 2004; National Department of Health, 2010; WHO, 2013).

2.1.2 pH-Dependent sensitivity of *P. falciparum* parasites

Drug absorption is determined by the drug's physicochemical properties, formulation, and route of administration (Rang *et al.*, 2012b). Unless given intravenously, a drug must cross several semi-permeable cell membranes before it reaches the systemic circulation. These cell membranes are biologic barriers that selectively inhibit passage of drug molecules. The membranes are composed primarily of a lipid bilayer with intramembranous proteins, which

determine membrane permeability. Drugs may cross cell membranes by passive diffusion, facilitated passive diffusion, active transport, pinocytosis, or intramembranous receptors (Rang *et al.*, 2012b). A complicating factor in relation to membrane permeation is that many drugs are weak acids or weak bases, which means that depending on the pH, they exist in varying ratios in both non-ionised lipid-soluble form and ionised lipid-insoluble form when in solution (Rang *et al.*, 2012b). Approximately 95% of drugs on the market, are either weak acids (20%) or weak bases (75%) and are ionisable (Bhal *et al.*, 2007). Chloroquine (Figure 2.1), a 4-aminoquinoline schizontocidal agent and weak base is predominantly non-ionised at a neutral pH (7.0) and can therefore diffuse freely into the parasite digestive vacuole as it traverses down the pH gradient (Krogstad *et al.*, 1987; O'Neill *et al.*, 2012; Rang *et al.*, 2012a). Then at the acidic pH (4.8-5.2) of the digestive vacuole (chloroquine's site of action), chloroquine is converted to a di-protonated, membrane-impermeable form and is “trapped” inside the parasite as it cannot translocate across the vacuole membrane (Krogstad *et al.*, 1987; Rang *et al.*, 2012a).

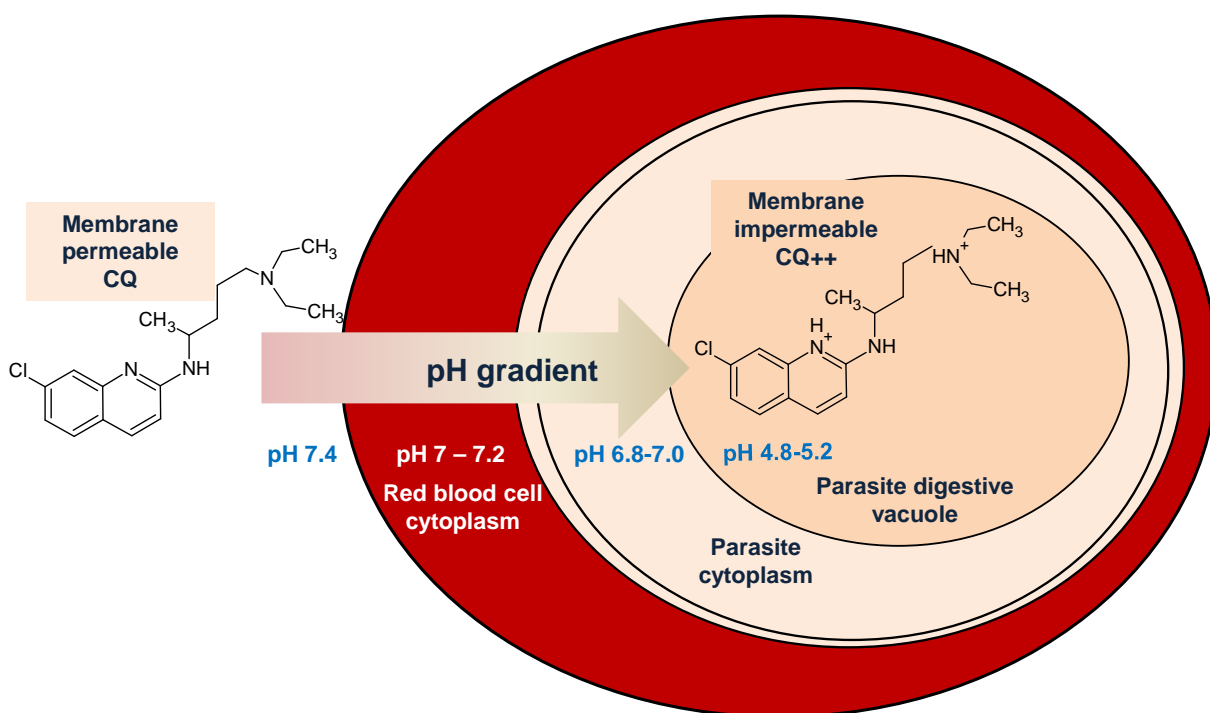


Figure 2.1 “Ion-trapping” of chloroquine within the malaria parasite digestive vacuole (adapted from O’Neill *et al.*, 2012). Non-ionised chloroquine (CQ), a weak base, diffuses through the RBC and parasite plasma membranes down the pH gradient and ionises at an acidic pH within the digestive vacuole leading to increased accumulation of the ionised or di-protonated drug (CQ⁺⁺). The secondary and tertiary amine groups both accept a single proton. The resulting quaternary amine putatively binds to β -haematin thus inhibiting haemozoin formation.

2.1.3 pK_a and degree of drug ionisation

The pH-partition hypothesis of Shore *et al.* (1957) proposed that highly ionised drugs are either poorly absorbed or not absorbed at all, as illustrated with chloroquine in Figure 2.1 (Shore *et al.*, 1957; Disanto and Wagner, 1972). The relative concentrations of the ionic and molecular forms of the drug depend on the pK_a (relative acid-base strength) of the drug and the pH of the medium (Knittel and Zavod, 2008). In addition, most drugs are absorbed by passive diffusion of the non-ionised form (Rang *et al.*, 2012b), therefore the degree of ionisation of a drug at a certain pH is of great importance. Based on the Brønsted-Lowry Theory, a drug that is a weak acid can reversely dissociate into an anion (negatively charged) and a proton (H⁺) and a weak base forms a cation (positively charged) by accepting a proton (Rosenthal, 2007). The Henderson-Hasselbalch equation (Equation 2.1) relates the ratio of protonated (conjugate acid) to unprotonated (conjugate base) species of weak acids or bases to the drug's pK_a (negative logarithm of the dissociation constant, K_a) and the pH (negative logarithm of the H⁺ or acid concentration) of the medium (Aulton, 2002; Rosenthal, 2007).

$$\text{pK}_a = \text{pH} + \log \frac{[\text{acid}]}{[\text{base}]}$$

Equation 2.1 The Henderson-Hasselbalch equation.

There is therefore a direct link between the degree of ionisation of a drug and its solubility in aqueous medium (Figure 2.2). In addition, the degree of ionisation of a drug (Section 2.3.14) in a solution can be derived from the Henderson-Hasselbach equation (Equation 2.1) if the pK_a value of the drug and the pH of the solution are known (Aulton, 2002). The pK_a of a drug influences solubility, protein binding and permeability, which in turn directly affects pharmacokinetic characteristics such as absorption, distribution, metabolism and excretion (ADME) (Manallack, 2007). The strong association between pK_a and the pharmacokinetics of most drugs has resulted in measurement of pK_a values as a regulatory requirement by the Food and Drug Administration in the USA (Manallack, 2007). It is however conceded that pK_a values in isolation maybe limited. Therefore an estimate of likely ADME characteristics can be obtained using pK_a values in combination with other physicochemical properties such as molecular weight (MW), logarithm of partition coefficient or octanol (organic)-water distribution coefficient of a compound (log P), number of hydrogen donors and hydrogen bond acceptors, as well as the polar surface (the total number of hydrogen bonds) of the drug molecule (Lipinski *et al.*, 1997; Manallack, 2007). A variety of computational approaches exist and a number of algorithms and qualitative structure-activity relationship (QSAR)

models are used within commercial software packages such as ACD/Labs that identify ionisable groups and predict principal pK_a (acid or base) values (Manallack, 2007). So taking pK_a values into account when screening compounds, allows for early ADME profiling during the drug discovery process.

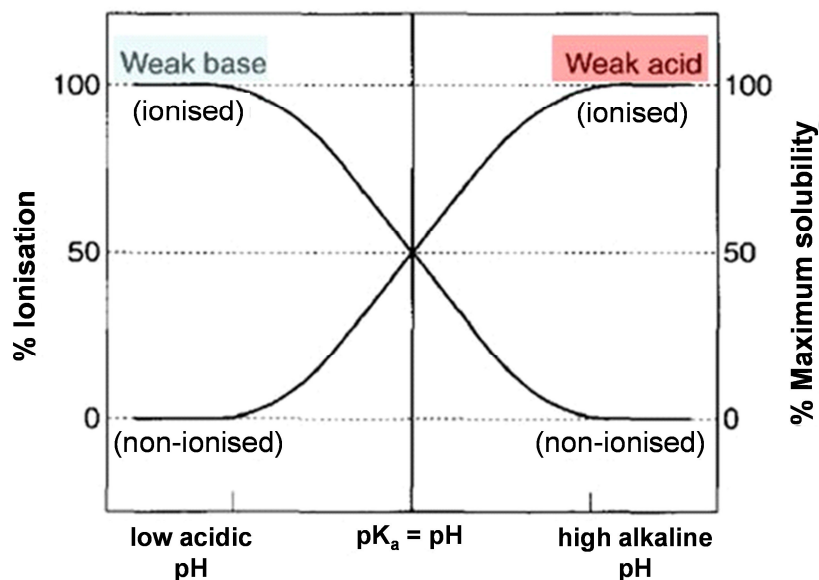


Figure 2.2 Change in ionisation and relative solubility of weakly acidic and weakly basic drugs as a function of pH (adapted from Aulton, 2000).

2.1.4 Lipinski's Rule of 5 as a measure of 'drug-likeness'

The drug-like properties of the most active test compounds were assessed using a non-empirical, *in silico* or computational approach, known as the Lipinski's Rule of Five (Ro5), first published by Lipinski *et al.* (1977). This approach was adopted by the Pfizer Research Centre and is widely accepted by the pharmaceutical industry for drug-likeness profiling of orally administered therapeutics that are passively transported to the site of action (Lipinski *et al.*, 2001; Bhal *et al.*, 2007). With the advent of computational high-throughput screening (HTS) techniques, it has become feasible to screen hundreds of compounds using the Ro5 and other new profiling tools and quickly eliminate lead candidates that have poor physicochemical properties for oral bioavailability (Lipinski, 2004; Bhal *et al.*, 2007). The term "drug-likeness" specifically refers to drug-like permeability properties (Lipinski, 2004; Bhal *et al.*, 2007). High oral bioavailability is a critical factor when developing therapeutic agents and it is enhanced when there is a balance between the compound's solubility and lipid-solubility (Lipinski, 2004; Salahuddin *et al.*, 2013). Bioavailability is influenced by good intestinal absorption, reduced molecular flexibility (or low number of rotatable bonds),

low polar surface area (Salahuddin *et al.*, 2013). The four key physicochemical parameter ranges used to describe drug-likeness using the Ro5 are the molecular weight (MW) < 500, the logarithm value of the partition coefficient (log P) < 5, hydrogen bond donors (HBDs) < 5, hydrogen bond acceptors (HBAs: a sum of nitrogen and oxygen atoms) < 10, in this case 10 being a multiple of 5 (Lipinski *et al.*, 1997, 2001). Although the Lipinski's Ro5 has no range limit for log P, negative log P value (log P < 0) implies the compound is hydrophilic, the larger the log P value (log P > 0) the greater its lipophilicity (Khanna and Ranganathan, 2009). Therefore, log P is often taken into consideration with the molecular weight of the compound since smaller molecules (MW < 500) may diffuse across cellular membranes (Leeson and Springthorpe, 2007). The log P, octanol/water partition coefficient of a compound, is a predictor of lipid-solubility and widely accepted as having a significant impact on the ADME properties of compounds (Bhal *et al.*, 2007). However, the application of log P is limited to compounds in their neutral state. The changing pH environment for orally administered drugs along the gastrointestinal tract varies from the stomach to the colon, meaning that compounds will often be in a mixture of ionic species (Bhal *et al.*, 2007). Oral drug absorption occurs in the small intestines at approximately pH 5.5. In order to account for the mixture of ionic species, log D (distribution constant) a pH-dependant parameter is often used in physiological systems (Bhal *et al.*, 2007).

2.2 Objectives

The objectives were to evaluate: the antimalarial activity of all test compounds, the combined effect of the most active synthetic and natural colourants with quinine, and to assess possible mechanism(s) of action and cytotoxicity of all the lead compounds. Initially, the antimalarial activity of the test compounds was screened at a maximum final concentration of 100 μM for synthetic compounds and 100 $\mu\text{g/ml}$ for natural compounds. The IC_{50} values for the active compounds, that inhibited parasite growth by at least 80% or more, were determined. The active compounds (IC_{50} values < 100 μM for synthetic compounds and 100 $\mu\text{g/ml}$ for natural compounds) were included for further pharmacological action studies.

Although the screening concentration of a 100 μM used in the current study was above the 1-5 μM concentration range stated by Fidock *et al.* (2004), the objective was to narrow down the search for more active compounds since there was a chance that a large number of the test compounds could be inactive and as such further studies could be done to determine the IC_{50} values on these select compounds.

2.3 Methodology

2.3.1 Preparation of test compounds

A total of 56 test compounds were screened in the current study. The azo dyes (28) were acquired from Dr Laurent Meijer (Station Biologique de Roscoff, France) as a gift and the other synthetic colourants (3) including methylene blue, safranin O and mercury orange were acquired commercially from Sigma-Aldrich. The novel nucleoside analogues (8) and imidazopyridines (8) were donated by Professor Charles De Koning (School of Chemistry, University of the Witwatersrand). The novel nucleoside analogues (Appendix A1) based on purine (guanosine and inosine) pyrimidine (uridine and cytosine) nucleobases, were synthesised using the ring closing metathesis methodology and fully characterised by spectroscopic methods by Dr Jenny-Lee Panayides under the supervision of Professor Willem A.L. van Otterlo at the School of Chemistry, University of the Witwatersrand (van Otterlo *et al.*, 2003; Panayides, 2012). The structure-activity relationship strategy approach for the JLP series compounds was based on a pyrimidine scaffold with substitutions of various reactive groups. The imidazopyridine analogues (Appendix A2), designated IP, were synthesised using a multicomponent coupling reaction by Dr Amanada L. Rousseau under the supervision of Professor Charles De Koning (Rousseau *et al.*, 2007). A cyclohexane ring at position R¹ in compounds IP-2 to IP-4 of the imidazopyridine analogue series was substituted with a 1,3-dimethylbenzene ring in IP-5 to IP-8.

Natural colourants (9): curcumin, paprika powder extract, beet-P3006 powder extract, beet-0611, carbon black, safflower, annatto, cochineal and carmine, were donated by Phytone (Ltd.). Stock solutions of 10 mg/ml for natural compounds and 10 mM of all synthetic test compounds including quinine hydrochloride (Sigma-Aldrich) were prepared in 100% (v/v) dimethyl sulfoxide (DMSO) (Sigma-Aldrich). Serial dilutions of test compounds were prepared using experimental medium. The final % DMSO used in the experiments did not exceed 1% such as not to have an inhibitory effect on the *P. falciparum* parasites.

2.3.2 *P. falciparum* parasite culture maintenance

The chloroquine-sensitive (3D7) strain of *P. falciparum* was cultured (Biosafety clearance number: 20090503, Appendix B1) aseptically according to the method of Trager and Jensen (1976) and departmental protocol modified by Van Zyl *et al.* (2010). Parasitised human RBCs were maintained *in vitro* at 5-10% parasitaemia and 5% leukocyte and platelet-free haematocrit in Rosewell Park Memorial Institute (RPMI)-1640 culture medium (Section 2.3.3). The culture (20 ml) was flushed with a gas mixture of 5% CO₂, 3% O₂ and 92% N₂

(Afrox) and incubated at 37°C in a 75 cm³ culture flask. Spent culture medium was replaced daily and uninfected RBCs added every 48 h when the parasites were in trophozoite to schizont stages. All experiments were conducted using cultures synchronised (Section 2.3.8) in the ring stage (Trager and Jensen, 1976; Freese *et al.*, 1988; Van Zyl *et al.*, 2010).

2.3.3 Preparation of culture medium

The incomplete RPMI-1640 (Gibco) culture medium was prepared as directed by dissolving 5.9 g/l 4-(2-hydroxyethyl)-1-piperazineethanesulfonic acid (HEPES) buffer (Merck), 4.0 g/l D-glucose (Merck), 44.0 mg/l hypoxanthine (Sigma-Aldrich) and 0.01% (v/v), 50 mg/l gentamicin sulphate (Sigma-Aldrich) into 1 litre of Milli-Q[®] water. The incomplete culture medium was sterilised by filtration through a 0.22 µm pore size Millipore[™] membrane (Merck) and stored at 4°C. Aliquots of this culture medium were incubated at 37°C for 48 h to ensure there was no contamination prior to use. The culture medium used to maintain the parasites was completed by adding 10% (v/v) human plasma (Section 2.3.4) and 4.2 % (v/v) sterile filtered NaHCO₃ (Merck), to give a final pH of 7.4. The experimental medium did not contain hypoxanthine and gentamycin. Incomplete experimental medium (used for serial dilutions of test compounds) excluded human plasma, hypoxanthine and gentamycin.

2.3.4 Preparation of human plasma

Human plasma was acquired from the South African National Blood Service (SANBS) (Ethical clearance number: WCJ-131030-1, Appendix B2). At least three bags of plasma were aseptically pooled and heat-inactivated at 56°C in a pre-heated water bath for 2 h, whilst agitating every 10-15 min. The heat-inactivated plasma was centrifuged at 1,877 x g (SORVALL[®] T6000D) for 10 min and the supernatant aliquoted and stored at -20°C. Prior to use, the plasma was thawed and pre-warmed to 37°C.

2.3.5 Preparation of buffered solution

Phosphate-buffered saline (PBS, pH 7.4) contained 8.0 g/l NaCl (Merck), 0.3 g/l KCl, 0.73 g/l Na₂HPO₄.2H₂O (Merck) and 0.2 g/l KH₂PO₄ (Merck) in Milli-Q[®] water and sterilised by autoclaving at 120°C for 20 min.

2.3.6 Preparation of red blood cells

Whole blood was drawn from healthy human donors (Ethical clearance number: M090532, Appendix B3) and stored at 4°C for at least two weeks in blood tubes (BDH) containing citrate phosphate dextrose adenosine to prevent coagulation. The blood was centrifuged at 834 x g for 5 min and the plasma and buffy coat discarded. The packed RBCs were washed three times by centrifugation with PBS (Section 2.3.5). The RBCs were diluted to 50% (v/v) with

incomplete experimental medium (Section 2.3.3). The RBC suspension was used for at least a week to maintain the parasite culture before being discarded.

2.3.7 Blood smear slide preparation and parasite assessment

The percentage parasitaemia and erythrocytic developmental growth stages were assessed daily using light microscopy. A thin blood smear was prepared and air-dried prior to staining with a rapid Giemsa stain kit, RapiDiff™ staining kit (Global Diagnostics), containing a fixative solution (thiazine dye in methanol), eosin Y in phosphate buffer to stain the cytoplasm, and Giemsa to stain the parasites' nuclei. The slide was examined with a light microscope (Nikon) at 1000x magnification under oil immersion. Infected RBCs and uninfected RBCs from ten fields of view were counted and the average percentage parasitaemia calculated.

2.3.8 Synchronisation of parasite culture

The parasite culture was synchronised using 5% (w/v) D-sorbitol lysis when in the ring stage (Lambros and Vanderberg, 1979). The D-sorbitol solution was sterile filtered through a 0.22 µm pore size Millipore™ filter unit and stored at 4°C. Cultures were centrifuged at 469 x g for 5 min and the spent medium discarded. The pellet was re-suspended in 10 volumes of pre-warmed 5% D-sorbitol and left for 20 min at room temperature. The more permeable RBCs infected with mature parasites were lysed, killing trophozoite and early-to-mid schizont stages. The culture was centrifuged at 469 x g for 5 min and the D-sorbitol discarded. The culture was re-suspended in pre-warmed complete culture medium, gassed with 5% CO₂ and maintained routinely without addition of erythrocytes (Section 2.3.2).

2.3.9 Tritiated hypoxanthine incorporation assay

Incorporation of [³H]-hypoxanthine into parasitic DNA provides a direct measure of the number of infected RBCs in culture and quantification of parasite growth (Desjardins *et al.*, 1979; Fidock *et al.*, 2004). This incorporation of [³H]-hypoxanthine is enhanced by the enzymatic purine salvage pathway facilitated by nucleoside transporters expressed on the *P. falciparum* parasite membrane since the parasite lacks the ability to synthesise purines *de novo* (Baldwin *et al.*, 2007).

2.3.9.1 Preparation of parasite suspension and plate layout

Test compound solutions (25 µl) were added to the first row (row-A) in triplicate and serially diluted (1:2 dilutions in incomplete experimental medium) down the 96-well microtitre plate (rows A to G), such that 4 compounds were tested per plate (Figure 2.3). Row-H was reserved for the uninfected RBCs (wells 1-4) in order to reduce isotope residue that could bind non-

selectively to the RBCs, and the 100% parasite growth (wells H5-H12) controls where the test compound was substituted with 25 μ l incomplete experimental medium. The synchronised parasite culture was adjusted to 0.5% parasitaemia and 1% haematocrit in complete experimental medium. The parasite suspension (200 μ l) was transferred to all the wells excluding the uninfected RBC control wells. The microtitre plate was incubated for a total period of 48 h at 37°C under micro-aerobic conditions in a humidified desiccated candle jar. Within the initial 24 h incubation period, 25 μ l of 5 mCi/ml [3 H]-hypoxanthine isotope (Amersham), pre-diluted at a ratio of 1:270 in incomplete experimental medium, was added to a final concentration of 1.85 μ Ci/ml per well. The microtitre plate was then incubated for a further 24 h period. The classic antimalarial drug quinine (Sigma-Aldrich) was used as a reference drug (Trager and Jensen, 1976; Desjardins *et al.*, 1979).

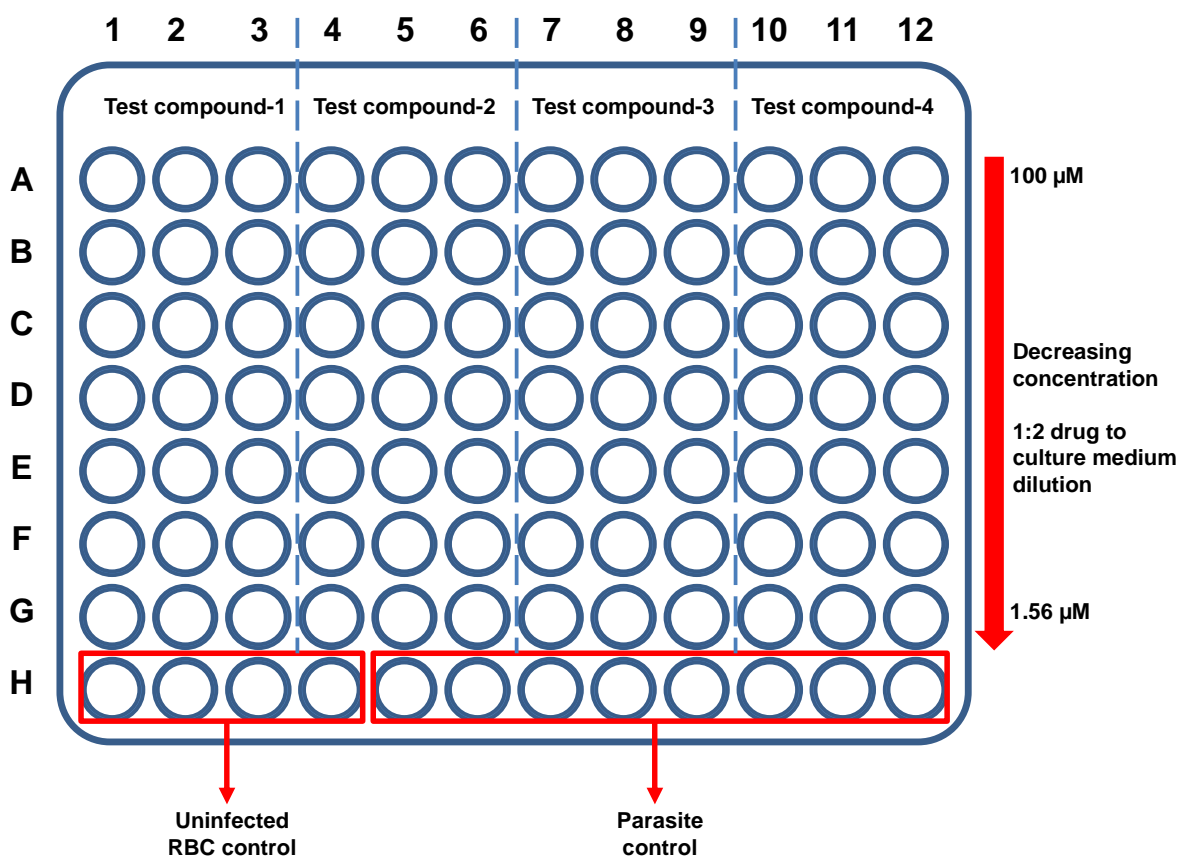


Figure 2.3 Design of [3 H]-hypoxanthine assay in a 96-well microtitre plate (adapted from Desjardins *et al.*, 1979).

2.3.9.2 Harvesting parasitic 3 H-labelled DNA

The parasitic 3 H-labelled DNA was harvested onto Wallac™ Betaplate glass fibre filter mats using a multichannel Titertek™ semi-automatic cell harvester. The filter mats were allowed to air-dry overnight at room temperature.

2.3.9.3 Scintillation counting of radiolabelled DNA

The mats were transferred to plastic sample bags containing 10 ml of Betaplate™ scintillation liquid (Perkin-Elmer) and the sample bags heat-sealed. In order to measure the [³H]-hypoxanthine incorporation into the parasitic DNA, β-emissions from the tritiated hypoxanthine were counted in the Wallac™ 1205 Betaplate scintillation counter. The counts per minute (cpm) generated were expressed as percentage of surviving parasites taking the controls into account (Equation 2.2).

$$\% \text{ Parasite growth} = \frac{\text{cpm}_{\text{treatment}} - \text{cpm}_{\text{RBC control}}}{\text{cpm}_{\text{parasite control}} - \text{cpm}_{\text{RBC control}}} \times 100$$

Equation 2.2 Percentage parasite growth.

2.3.10 Drug combination study

In accordance with WHO treatment guidelines, combination therapies should be used to avoid treatment failure and drug resistance (WHO, 2013). A synergistic combination of antimalarial agents is more favourable as it would allow for lower doses of the individual drugs and still maintain the antimalarial effect, as well as minimise side-effects (Bell, 2005). Whereas, combination therapy with two drugs that demonstrate an antagonistic interaction should be avoided, as it would result in treatment failure (Bell, 2005). Therefore drug combination studies provide new information that may be used in the choice of new drug combinations and potentiation of existing classical antimalarial drugs. The interactions of the most active colourants against malaria in combination with quinine, were determined by using the modified [³H]-hypoxanthine incorporation assay (Section 2.3.9) and the interaction interpreted with the construction of isobolograms (Berenbaum, 1978; Berenbaum *et al.*, 1980). Taking a 20-fold dilution factor into account, two compounds were combined in various concentration ratios (10:0, 9:1, 8:2, 7:3, 6:4, 5:5, 4:6, 3:7, 2:8, 1:9 and 0:10), such that the concentration of quinine decreased whilst that of the test compound increased. The test compounds were 2-fold serially diluted in incomplete experimental medium in duplicate wells.

2.3.10.1 Determination of fractional inhibitory concentrations

The IC₅₀ values were determined from log sigmoid dose-response curves using the Enzfitter® software. The fractional inhibitory concentration (FIC) value was calculated as the concentration of the inhibitor present in the combination divided by the concentration of the inhibitor alone that gives the same effect (Elion *et al.*, 1954; Bell, 2005). Therefore, the FIC₅₀ values for each test compound were calculated from the IC₅₀ values of the compound in combination and the IC₅₀ value of the compounds alone (Equation 2.3).

$$\text{FIC}_{50} = \frac{\text{IC}_{50} \text{ of compound in combination with quinine}}{\text{IC}_{50} \text{ value of compound alone}}$$

Equation 2.3 Fractional inhibitory concentrations.

2.3.10.2 Analysis of drug interactions using isobolograms

The FIC_{50} values of quinine were plotted on the x-axis and the test compound on the y-axis in an isobologram using GraphPad Prism® version 5.0. A line of best fit or additive isobole (solid straight line in Figure 2.4) intersected the x-axis and y-axis at $\text{FIC}_{50} = 1$, representing the IC_{50} of quinine alone and the IC_{50} of the test compound alone, respectively (Bell, 2005).

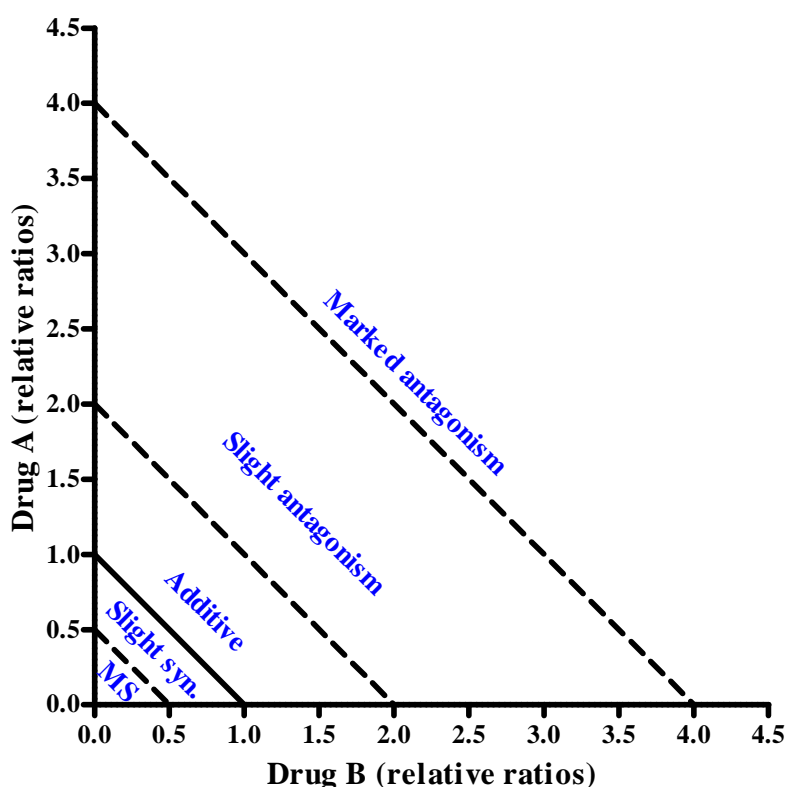


Figure 2.4 A general isobologram with classification of possible interactions between two drugs (adapted from Gupta *et al.*, 2002). The dotted lines denote cut-off values for marked synergism (MS); slight synergism (Slight syn.); additive, slight and marked antagonism (Gupta *et al.*, 2002; Bell, 2005).

Generally, the FIC_{50} data points distributed along the solid straight line indicate additivity, points displaced to the bottom, synergism and points above the additive isobole, antagonism. However, the strength of synergism or antagonism is indicated by the degree of deviation from the additive isobole. This was achieved by calculating the mean of the FIC_{50} values of each compound in combination and then adding the mean sum of the FIC_{50} values and using the ΣFIC_{50} value to classify the overall drug interaction (Equation 2.4) according to cut-offs defined by Gupta *et al.* (2002).

$$\Sigma\text{FIC}_{50} = \text{mean FIC}_{50} \text{ of Quinine} + \text{mean FIC}_{50} \text{ of Test compound}$$

Equation 2.4 Sum of mean fractional inhibitory concentrations.

Based on the sum of the mean FIC_{50} values, the drug interactions were defined as: marked synergism ($0 > \Sigma\text{FIC}_{50} < 0.5$), slight synergism ($0.5 \geq \Sigma\text{FIC}_{50} < 1$), additive interaction ($1 \geq \Sigma\text{FIC}_{50} < 2$), slight antagonism ($2 \geq \Sigma\text{FIC}_{50} < 4$) and marked antagonism ($2 \geq \Sigma\text{FIC}_{50} < 4$) (Gupta *et al.*, 2002; Bell, 2005).

2.3.11 Haemolysis assay

RBCs consist of skeletal proteins underlying a lipid bilayer with inter-membrane proteins and haemoglobin for oxygen delivery to the tissues (Mohandas and Gallagher, 2008). Anaemia is one of the multiple pathologies of human malaria and along with increased lipid peroxidation that affects the plasma membrane integrity of both infected and uninfected RBCs. As such, one has to be cautious of an increased risk of haemolysis when new compounds are administered (Becker *et al.*, 2004; WHO, 2012). Therefore, it was prudent to assess whether the antimalarial activity demonstrated by the lead compounds, was due to a selective inhibitory effect on the intra-erythrocytic parasite, or due to their haemolytic potential. To achieve this, the compounds were screened for haemolytic activity using healthy human RBCs (Section 2.3.6). This involved spectrophotometrically measuring free haemoglobin released due to haemolysis at a wavelength of 412 nm (Hayat *et al.*, 2011). Consistent with the [^3H]-hypoxanthine incorporation assay (Section 2.3.9), a 1% human haematocrit was prepared from freshly washed blood in complete experimental medium. Fresh blood (or less than 4 days old) was used to ensure cell membrane integrity of the RBCs. The test and reference compounds were screened at a maximum concentration of 100 μM (or 100 $\mu\text{g/ml}$). The experimental controls included: a positive control with 1% haematocrit and 0.2% Triton X-100 (Sigma-Aldrich) in order to achieve 100% haemolysis; a background colour control with 250 μl complete experimental media; a colour control for the coloured compounds (25 μl compound with 200 μl complete experimental media; as well as a negative control (25 μl incomplete experimental media with 200 μl RBC suspension). Test compounds (25 μl) and the RBC suspension (200 μl) were transferred to sterile microcentrifuge tubes and incubated at 37°C for 48 h in a humidified candle jar. After the initial 24 h period, 25 μl of incomplete experimental medium was added to all the microcentrifuge tubes followed by further 24 h incubation. After 48 h, the RBCs were incubated at room temperature for 10 min. The microcentrifuge tubes were gently agitated and centrifuged at 284 x g (SANYO[®] microcentrifuge) for 5 min. The supernatant (20 μl) from all the microcentrifuge tubes was transferred to duplicate wells in a 96-well microtitre plate and diluted in 80 μl PBS (pH 7.4)

and the absorbance read at 412 nm using the iEMS microplate reader (Labsystems) operated with Ascent software (version 2.4). The % haemolysis (Equation 2.5) was determined from the absorbance (Abs) values.

$$\% \text{ Haemolysis} = \frac{\text{mean Abs}_{\text{treatment}} - \text{mean Abs}_{\text{negative control}}}{\text{mean Abs}_{100\% \text{ haemolysis}} - \text{mean Abs}_{\text{treatment}}} \times 100$$

Equation 2.5 Percentage haemolysis equation.

2.3.11.1 Modified haemolysis assay procedure for the colourants

In the case of the colourants, the 200 µl supernatant was discarded and the remaining RBCs were washed three times with PBS of the same volume. The supernatant from the third wash was used as a colour control for the test compound. The remaining pellets of RBCs were treated with 0.2% (v/v) Triton X-100 in order to achieve 100% haemolysis. The supernatant (20 µl) from all the microcentrifuge tubes was transferred to duplicate wells in a non-sterile 96-well microtitre plate with 80 µl PBS (pH 7.4) and absorbance read at 412 nm using the iEMS Microplate Reader MF (Labsystems) operated with Ascent software (version 2.4) and the % haemolysis was determined using the modified % haemolysis equation (Equation 2.6).

$$\% \text{ Haemolysis} = \frac{[100 - (\text{mean Abs}_{\text{treatment}} - \text{Abs}_{\text{colour control}})] - \text{mean Abs}_{\text{negative control}}}{\text{mean Abs}_{100\% \text{ haemolysis}} - \text{mean Abs}_{\text{negative control}}} \times 100$$

Equation 2.6 Modified % haemolysis equation for colourants.

To ensure that haemolysis did not contribute to the antimalarial activity of the most active test compounds, the selectivity index (Equation 2.7) was calculated, where a selectivity index ≥ 10 indicated that the compound's mechanism of action was selective to the malaria parasite and not only toxic to uninfected human RBCs to effect parasite death (Pink *et al.*, 2005).

$$\text{Selectivity index} = \frac{\text{Haemolytic activity (HLC}_{50})}{\text{Antimalarial activity (IC}_{50})}$$

Equation 2.7 Selectivity index for *P. falciparum* compared to uninfected human RBC.

2.3.12 Beta-haematin formation inhibition assay

The pathway involving the biocrystallisation of oxidised free haem (Fe³⁺-protoporphyrin IX) into an inert substance, haemozoin in *P. falciparum* is a validated drug target (Egan, 2003; Kumar *et al.*, 2007). The quinoline family of drugs including chloroquine, quinine and related 4-aminoquinoline drugs, accumulate into the parasite's food vacuole and form adducts with redox-active free haem molecules, inhibiting the aggregation of haemozoin (Egan, 2006).

Failure of the parasite to sequester the increasing haem molecules overwhelms the parasite's detoxification system, causing oxidative stress and parasite membrane damage, which leads to parasite death (Section 1.11) (Wright *et al.*, 2001). The synthetic counterpart of haemozoin, β -haematin, can be synthesised *in vitro* from haemin chloride (Cl-Fe³⁺-protoporphyrin) by the acid-catalysed method which proceeds in an aqueous solution (Slater *et al.*, 1991; Egan, 2008b). In the current study, the assay was modified according to Chemaly *et al.* (2007). Briefly, haemin chloride (Sigma-Aldrich) stock solution (1 mg/ml) was prepared in DMSO. Test compound solutions were diluted in DMSO and used at a maximum concentration ratio of 1:4 (haem to drug). The test compounds (25 μ l), haemin (25 μ l), 50 μ l of Milli-Q[®] water and 100 μ l of acetate buffer (pH 4.4), were consecutively transferred to a 96-well microtitre plate. This was to simulate the acidic conditions prevalent in the digestive vacuole (pH 5-5.2) of the malaria parasite. The plate was placed in a humidified, sealed container and incubated at 37°C for 24 h. Quinine and chloroquine were used as reference drugs. The β -haematin crystals were isolated by centrifugation at 1,877 x g for 10 min and washed three times with DMSO to remove un-reacted haemin followed by two washes with Milli-Q[®] water. These DMSO-insoluble crystals were dissolved in 100 μ l 2 M NaOH and diluted four-fold in 1 M NaOH. The absorbance of the β -haematin formed was measured using the iEMS Microplate Reader MF (Labsystems) operated with Ascent software (version 2.4) at a wavelength of 405 nm (Chemaly *et al.*, 2007). The percentage of β -haematin formed (Equation 2.8) was calculated using appropriate controls. IC₅₀ values of test compounds that inhibited β -haematin formation by at least 80% were determined using Enzfitter[®].

$$\% \beta\text{-Haematin formed} = \frac{\text{mean Abs}_{\text{treatment}}}{\text{mean Abs}_{100\% \text{ haematin formation}}} \times 100$$

Equation 2.8 Percentage β -haematin formation.

2.3.13 Drug-sensitivity of erythrocytic stages of *P. falciparum*

It has been established that specific plasmodial developmental stages show enhanced sensitivity to some antimalarial drugs. In order to determine the stage-specific activity of the test compounds against the erythrocytic stages of *P. falciparum* (Figure 1.2), parasitaemia counts and stage identification of the parasites were examined microscopically. The parasite suspension (200 μ l) adjusted to 2% parasitaemia and 2% haematocrit, prepared in complete experimental culture media was aliquoted into 25 cm³ flasks when the parasite were in the early-ring stage and treated with 25 μ l test compound or quinine at an inhibitory concentration yielding 90% parasite kill (IC₉₀). A drug-free control was included and cultures were incubated at 37°C for 48 h. The parasitaemia count (all stages), parasite stage, and

morphological observations were recorded at 8 h intervals over the 48 h period. Samples were taken from the flasks using sterile pasteur pipettes and the cultures flushed with a gas mixture of 5% CO₂, 3% O₂ and 92% N₂ (Afrox) and returned to the incubator (37°C). The Giemsa stained thin blood smears of each culture were microscopically examined at 1000x magnification under oil immersion using a digital microscope with a mounted camera (Olympus®) operated with CellSens Dimension software (version 1.7), and images captured.

2.3.14 Measurement of drug-likeness using physicochemical properties

For the purpose of this study, log P (partition coefficient) was used as a predictor of lipid-solubility of the most active compounds compared to reference drugs in an *in vitro* context. The application of the Ro5 (Figure 2.5) included the construction of two-dimensional chemical structures of the compounds in their oxidative state (that is excluding the salt moiety of the compound). Thereafter, solubility and permeability property predictions were performed using the ChemSpider chemical database (www.chemspider.com) accessed from the ACD/ChemSketch (freeware version) software application that was used to draw the chemical structures. Compounds that violated one or more of the Ro5 parameters were classified as non ‘drug-like’ or having poor pharmacokinetic properties for oral administration (Figure 2.5) (Bhal *et al.*, 2007).

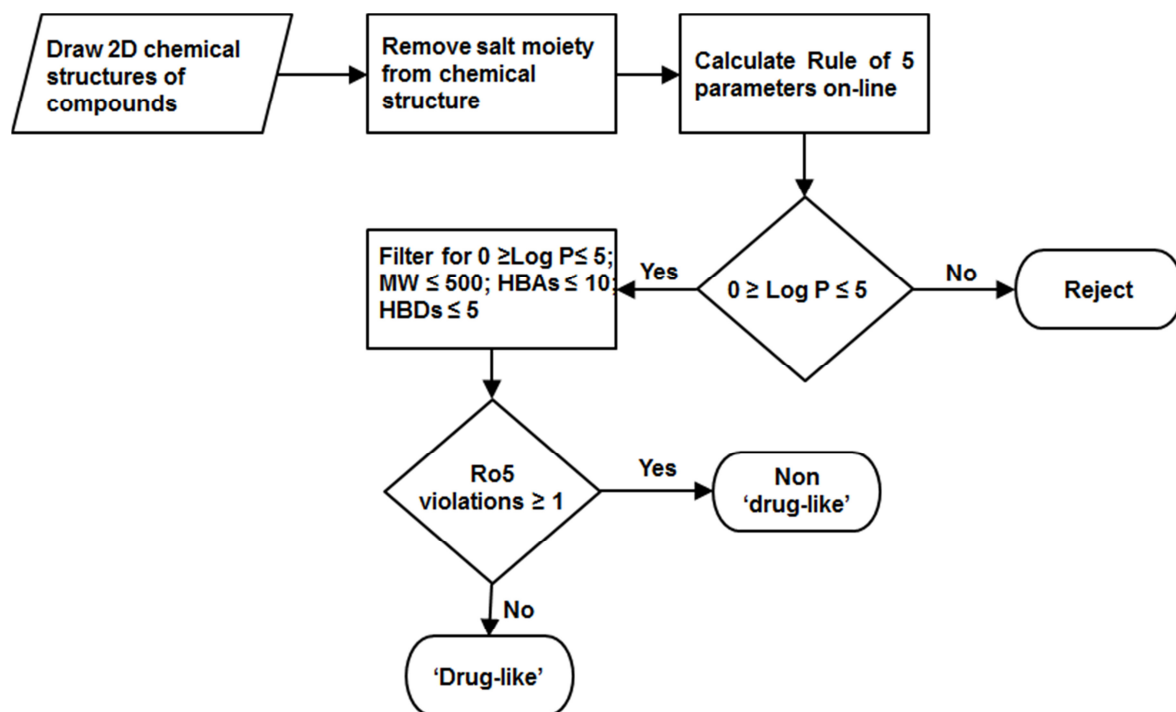


Figure 2.5 Workflow of *in silico* methodology applying the Lipinski Rule of 5 (adapted from Bhal *et al.*, 2007). The Ro5 parameters for the most active synthetic compounds and reference drugs were predicted using the ChemSpider chemical database (www.chemspider.com) accessed from the ACD/ChemSketch (freeware version) software application.

The ionisation constants (pK_a values) of the test compounds were predicted *in silico* using ACD/iLab version 2.0 (<http://ilab.acdlabs.com/iLab2>) (pH 7.0 and 25°C). The estimated percentage of ionised drug during second stage ionisation (Equation 2.9) for weak acids ($pK_a - \text{pH}$) and for weak bases ($\text{pH} - pK_a$) at physiological pH 7.4 (RBC cytosol) and pH 5.0 (parasite's acidic digestive vacuole), was derived from the Henderson-Hasselbalch equation (Equation 2.1) (Knittel and Zavod, 2008).

$$\% \text{ Ionisation} = \frac{100}{1 + \text{anti-log}(pK_a - \text{pH})}$$

Equation 2.9 Percentage ionisation for weak acids and weak bases ($\text{pH}-pK_a$).

2.4 Data analysis

The IC_{50} values were determined from log sigmoid dose-response curves generated using the Enzfitter[®] software (version 1.05). The results are reported as the mean of at least 3 replicates with standard deviation. Statistical difference between the activity (IC_{50} values) of the test compounds and the control was determined by a one-way ANOVA test, using GraphPad Prism[®] software, version 5.0 (Motulsky, 2003; Glantz, 2005). A p -value less than 0.05 ($p < 0.05$) was considered statistically significant. A correlation between the haemolytic, β -haematin inhibitory activities of the test compounds and their antimalarial activity was determined using linear regression with a 95% confidence interval.

2.5 Results

2.5.1 Antimalarial activity

The test compounds displayed variable ability to inhibit parasite growth with 21% inhibiting more than 80% parasite growth at a concentration of 100 μM or 100 $\mu\text{g/ml}$. The *in vitro* antimalarial activity of the test compounds was classified as follows (Clarkson *et al.*, 2004; Gathirwa *et al.*, 2008): highly active, IC_{50} value $\leq 5 \mu\text{g/ml}$; promising activity, IC_{50} value 6-10 $\mu\text{g/ml}$; moderate activity, IC_{50} values 11-50 $\mu\text{g/ml}$; low activity, IC_{50} values 51-100 $\mu\text{g/ml}$; inactive, IC_{50} values $> 100 \mu\text{g/ml}$. The same classification was applied for all the synthetic compounds in molar concentration (μM).

2.5.1.1 Synthetic colourants

Only 3 of the 28 colourants inhibited more than 50% of parasite growth. The synthetic colourants, safranin O, methylene blue and mercury orange demonstrated *in vitro* parasite growth inhibition of more than 90% at a maximum final concentration of 100 μM (Table 2.1). Para red and methyl red showed inhibitory activity below 50%, whilst the least active (inhibition $< 5\%$) was acid orange 8.

Table 2.1 The *in vitro* antimalarial activity of synthetic colourants and reference drugs chloroquine and quinine.

Compound	Antimalarial activity	
	IC ₅₀ ± S.D. (µM)	% Parasite growth inhibition at 100 µM
Methylene blue	0.004 ± 0.00*	99.63 ± 0.11
Safranin O	0.087 ± 0.00	99.88 ± 0.09
Mercury orange	0.664 ± 0.01	99.44 ± 0.19
Para red	> 100	44.74 ± 0.14
Methyl red	> 100	29.22 ± 0.19
Palatine chrome black 6BN	> 100	16.01 ± 0.05
Eriochrome black R	> 100	10.82 ± 0.11
Sudan III	> 100	10.81 ± 0.01
Trypan blue	> 100	9.60 ± 0.02
Sunset yellow	> 100	9.34 ± 0.06
Xylidine ponceau 2R	> 100	8.05 ± 0.01
Breibrich scarlet	> 100	7.94 ± 0.03
Ethyl orange	> 100	7.80 ± 0.02
Acid red 88	> 100	7.31 ± 0.03
Dimethyl yellow	> 100	7.11 ± 0.04
Ponceau 4R	> 100	6.63 ± 0.06
Eriochrome blue black B	> 100	6.57 ± 0.05
Orange II	> 100	6.15 ± 0.01
Acid red 151	> 100	5.30 ± 0.01
Sudan I	> 100	4.03 ± 0.05
1-Naphthol-4-sulfonic acid	> 100	3.97 ± 0.05
Crocein orange G	> 100	3.71 ± 0.03
Amaranth	> 100	3.30 ± 0.04
Indigo carmine	> 100	2.99 ± 0.03
Tartrazine	> 100	2.84 ± 0.01
Orange G	> 100	2.47 ± 0.03
Eriochrome black T	> 100	2.33 ± 0.01
Tropaeolin O	> 100	2.31 ± 0.01
4-Phenylazophenol	> 100	1.81 ± 0.01
Orange I	> 100	1.72 ± 0.00
Toluidine red	> 100	1.04 ± 0.00
Acid orange 8	> 100	0.60 ± 0.00
Quinine	0.10 ± 0.01	99.59 ± 0.01
Chloroquine	0.01 ± 0.00	99.99 ± 0.32

* $p < 0.05$ significantly more potent compared to quinine.

The highly active compounds, methylene blue, safranin O and mercury orange, inhibited parasite growth in a dose-dependent manner (Figure 2.6), in the nanomolar (10^{-9}) range. Methylene blue was significantly ($p < 0.05$) more potent than quinine. Safranin O was comparable, whilst mercury orange was significantly ($p < 0.05$) less potent than quinine. The rest of the synthetic colourants were inactive (IC_{50} values $\geq 100\mu\text{M}$).

The *in vitro* inhibitory activity of the reference drugs; quinine (IC_{50} : 103.92 ± 8.29 nM) and chloroquine (IC_{50} : 12.10 ± 1.71 nM) against the *P. falciparum* chloroquine-sensitive 3D7-strain in the current study, was comparable to published IC_{50} values (quinine IC_{50} : 9.73 ± 5.11 nM; chloroquine IC_{50} : 102.34 ± 31.56 nM) (Vivas *et al.*, 2007).

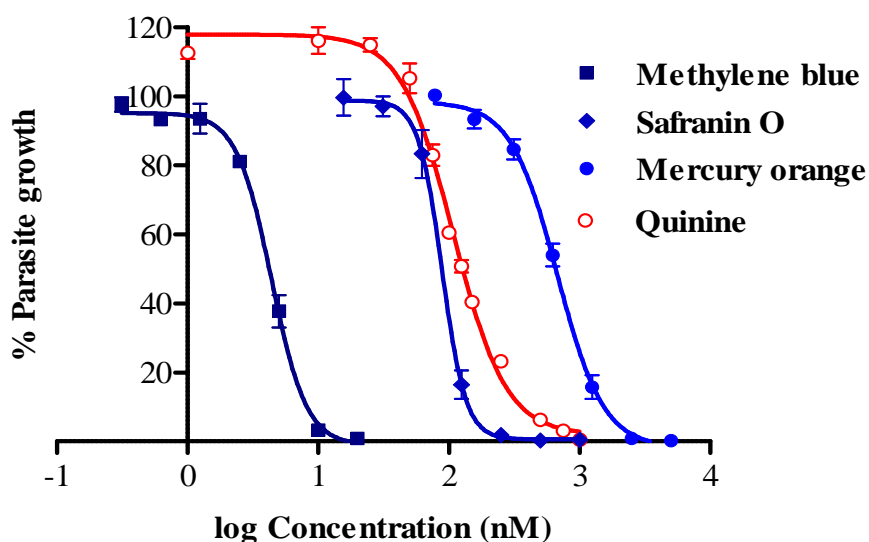


Figure 2.6 *In vitro* antimalarial activity of synthetic colourants on *P. falciparum*. Percentage parasite growth (mean \pm s.d.) based on 3-treatment replicates on the microtitreplate, from three separate experiments ($n = 3$).

2.5.1.2 Natural colourants

All the natural colourants, except for curcumin and carbon black (that showed inhibition above 99%), were inactive with *in vitro* parasite growth inhibition below 20% at a screening concentration of $100 \mu\text{g/ml}$ (Table 2.2). Curcumin was highly active, whilst carbon black showed moderate activity against *P. falciparum*, where both were significantly ($p < 0.05$) less potent compared to quinine (Figure 2.7). However, curcumin extract was significantly ($p < 0.05$) more potent than carbon black.

Table 2.2 Antimalarial activity of natural colourants on *P. falciparum*.

Compound	Antimalarial activity	
	IC ₅₀ ± S.D. (µg/ml)	% Parasite growth inhibition at 100 µg/ml
Curcumin	2.290 ± 0.18	99.72 ± 0.40
Carbon black	22.73 ± 2.36	99.63 ± 0.19
Annatto	> 100	16.26 ± 3.70
Paprika	> 100	9.51 ± 3.08
Carmine	> 100	9.09 ± 0.91
Cochineal	> 100	6.24 ± 2.57
Beet (0611) liquid extract	> 100	4.87 ± 2.25
Beet (P3006) powder extract	> 100	1.88 ± 0.22
Safflower	> 100	1.33 ± 0.67
Quinine	0.04 ± 0.00	100 ± 0.00
Chloroquine	0.01 ± 0.00	100 ± 0.00

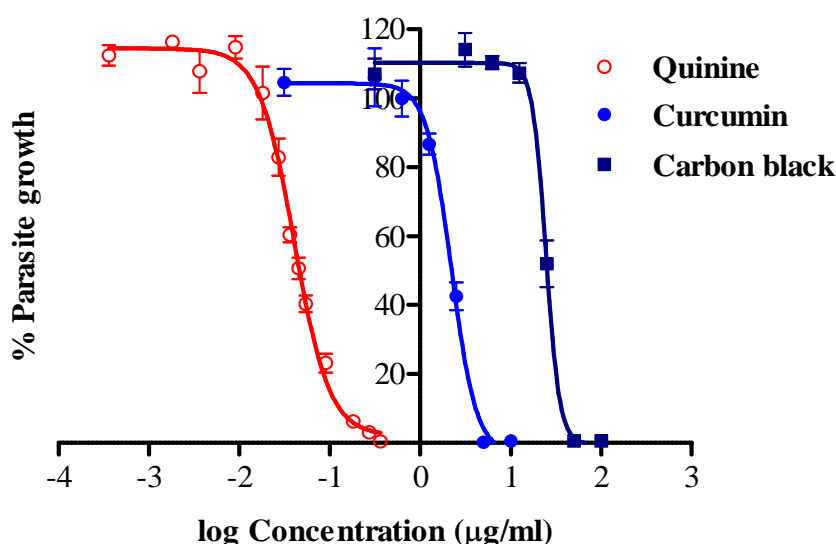


Figure 2.7 Antimalarial activity of curcumin and carbon black on the growth of *P. falciparum* parasite compared to quinine. Percentage parasite growth (mean ± s.d.) based on 3-treatment replicates on the microtitreplate, from three separate experiments (n = 3).

2.5.1.3 Nucleosides and analogues

Of the 8 nucleosides analogues, only the pyrimidine-based analogues JLP118.1 and JLP093 inhibited parasite growth by more than 80% at a screening concentration of 100 µM (Table 2.3). JLP118.1 and JLP093 were highly active (Figure 2.8), although these compounds were all significantly ($p < 0.05$) less potent compared to quinine.

Table 2.3 Antimalarial activity of nucleosides analogues.

Compound	Antimalarial activity	
	IC ₅₀ ± S.D. (µM)	% Parasite growth inhibition at 100 µM
JLP118.1	1.79 ± 0.12	91.81 ± 0.13
JLP093	2.38 ± 0.11	82.60 ± 2.79
JLP095.2	> 100	42.24 ± 5.19
JLP077.1	> 100	40.63 ± 1.63
JLP089	> 100	20.08 ± 8.11
JLP090.3	> 100	9.45 ± 3.52
JLP117.1	> 100	9.23 ± 4.92
JLP087	> 100	0.50 ± 0.00
Quinine	0.10 ± 0.01	99.59 ± 0.01
Chloroquine	0.01 ± 0.00	99.99 ± 0.32

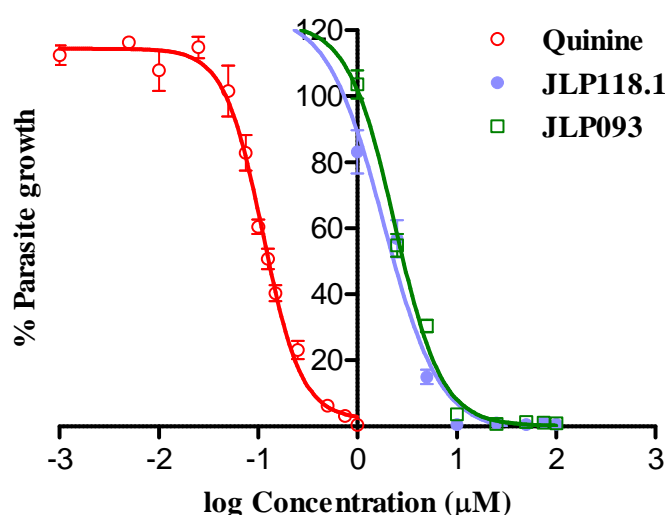


Figure 2.8 Inhibitory activity of nucleoside analogues on the *P. falciparum* parasite growth compared to quinine. Percentage parasite growth (mean ± s.d.) based on 3-treatment replicates on the microtitreplate, from three separate experiments (n = 3).

2.5.1.4 Imidazopyridine analogues

Five of the eight imidazopyridines analogues screened at 100 µM, inhibited malaria parasite growth by more than 90%, which was comparable to quinine (Table 2.4). Test compounds IP-3, -4 and -5 showed moderate antimalarial activities with IC₅₀ values between 10 and 50 µM, whilst IP-6 and -7 showed low activity (IC₅₀ values: 51-100 µM). All the most active imidazopyridine analogues were significantly ($p < 0.05$) less potent compared to quinine.

Table 2.4 Antimalarial activity of imidazopyridine analogues on *P. falciparum*.

Compound	Antimalarial activity	
	IC ₅₀ ± S.D. (µM)	% Parasite growth inhibition at 100 µM
IP-2	> 100	11.20 ± 2.11
IP-3	20.77 ± 0.72	98.90 ± 0.38
IP-4	15.30 ± 0.41	99.42 ± 0.64
IP-5	36.30 ± 1.19	99.91 ± 0.34
IP-6	67.20 ± 3.05	99.79 ± 0.46
IP-7	55.30 ± 1.90	99.63 ± 0.51
IP-8	> 100	27.40 ± 3.22
Quinine	0.10 ± 0.01	99.59 ± 0.01
Chloroquine	0.01 ± 0.00	99.99 ± 0.32

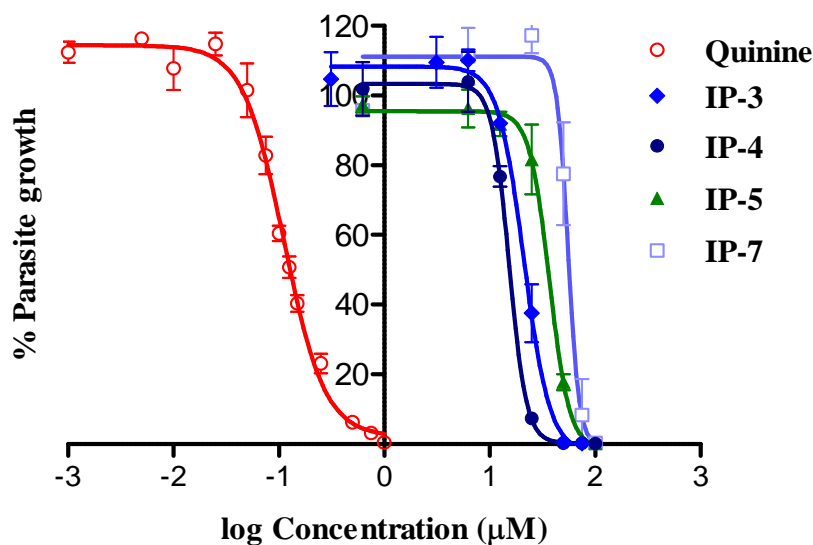


Figure 2.9 Antimalarial activity of the most active imidazopyridine analogues on the *in vitro* growth of *P. falciparum* parasite compared to quinine. Percentage parasite growth (mean ± s.d.) based on 3-treatment replicates on the microtitreplate, from three separate experiments (n = 3).

2.5.2 Haemolytic activity

The haemolysis assay results are summarised in Table 2.5 (for synthetic compounds) and Table 2.6 (for natural colourants). Of all the compounds tested, mercury orange was the only compound to induce haemolysis (99.8 ± 0.56%) significantly ($p < 0.05$) compared to quinine (0.15 ± 0.01%) at the screening concentration of 100 µM. Mercury orange demonstrated a

haemolytic activity (HLC_{50} : $16.81 \pm 0.56 \mu M$) in a dose dependent manner. The selectivity index (S.I. = 25.32) of mercury orange was above 10, which is the minimum concentration ratio (1:10, antimalarial activity IC_{50} to haemolytic activity IC_{50}) for a non-toxic compound (Pink *et al.*, 2005). Therefore, mercury orange was selective to *P. falciparum* at nanomolar concentrations (IC_{50} : $0.664 \pm 0.01 \mu M$), but demonstrated RBC lysis at higher, micromolar concentrations which would in that case contribute to its antimalarial activity.

Although methylene blue ($13.92 \pm 0.03\%$) showed minimum haemolytic activity at a screening concentration (100 μM), it was significantly higher ($p < 0.05$) compared to both quinine and chloroquine (Table 2.5). Curcumin and carbon black (Table 2.6) did not show haemolytic activity, although the degree of haemolysis ($6.24 \pm 0.18\%$) caused by curcumin at the screening concentration (100 $\mu g/ml$) was significantly ($p < 0.05$) higher than quinine. The nucleoside analogues did not show any haemolytic activity similarly to quinine.

Table 2.5 Haemolytic activity of the most active synthetic compounds.

Compound class	Compound	Haemolytic activity $HLC_{50} \pm S.D.$ (μM)
Synthetic colourants	Methylene blue	>100 ($13.92 \pm 0.03\%$)
	Safranin O	>100 ($0.31 \pm 0.01\%$)
	Mercury orange	16.81 ± 0.56
Nucleoside analogues	JLP093	>100 ($0.35 \pm 0.05\%$)
	JLP118.1	>100 ($0.92 \pm 0.04\%$)
Nucleosides	Guanosine	>100 ($0.21 \pm 0.03\%$)
	Inosine	>100 ($0.1 \pm 0.01\%$)
Imidazopyridine analogues	ND	ND
Reference drugs	Quinine	>100 ($0.15 \pm 0.01\%$)
	Chloroquine	>100 ($0.01 \pm 0.01\%$)

ND, not determined due to limited quantity of compounds.

Table 2.6 Haemolytic activity of natural colourants.

Compound class	Compound	Haemolytic activity $HLC_{50} \pm S.D.$ ($\mu g/ml$)
Natural colourants	Curcumin	>100 ($6.24 \pm 0.18\%$)
	Carbon black	>100 ($0.22 \pm 0.04\%$)
Reference drugs	Quinine	>100 ($0.40 \pm 0.01\%$)
	Chloroquine	>100 ($0.02 \pm 0.01\%$)

2.5.3 β -Haematin inhibition activity

The β -haematin assay results are summarised in Table 2.7 (synthetic compounds) and Table 2.8 (natural colourants). The synthetic colourants did not inhibit β -haematin formation at a maximum concentration of 800 μM . In comparison to quinine, there was no inhibitory

activity by methylene blue ($0.001 \pm 0.02\%$) and safranin O ($10.80 \pm 1.07\%$) at a maximum concentration of $800 \mu\text{M}$ (Table 2.7).

Table 2.7 β -Haematin formation inhibition of the most active synthetic compounds.

Compound class	Compound	β -haematin inhibition $\text{IC}_{50} \pm \text{S.D.} (\mu\text{M})$
Synthetic colourants	Methylene blue	$> 800 (0.001 \pm 0.02\%)$
	Safranin O	$> 800 (10.8 \pm 1.07\%)$
	Mercury orange	$> 800 (0.001 \pm 0.01\%)$
Nucleoside analogues	JLP093	$> 800 (5.80 \pm 3.35\%)$
	JLP118.1	$> 800 (0.001 \pm 0.02\%)$
Nucleosides	Guanosine	$> 800 (24.48 \pm 12.08\%)$
	Inosine	$> 800 (65.66 \pm 7.50\%)$
Imidazopyridine analogues	ND	ND
Reference drugs	Quinine	68.3 ± 4.17
	Chloroquine	38.4 ± 4.77

ND, not determined due to limited quantity of compounds.

The natural colourant, curcumin inhibited β -haematin formation in a dose-dependent manner, but was about 12 to 16-fold less active ($p < 0.05$) than quinine and chloroquine. Whilst, carbon black natural extract, inhibited $40.47 \pm 0.83\%$ of β -haematin formation at the screening concentration ratio of 1:4 (haem to drug), and thus the IC_{50} value was $> 4,000 \mu\text{g/ml}$.

Table 2.8 β -Haematin formation inhibition activity of natural colourants.

Compound class	Compound	β -haematin inhibition $\text{IC}_{50} \pm \text{S.D.} (\mu\text{g/ml})$
Natural colourants	Curcumin	320 ± 0.01
	Carbon black	$> 4000 (40.47 \pm 0.83\%)$
Reference drugs	Quinine	24.65 ± 1.28
	Chloroquine	19.60 ± 2.46

2.5.4 Drug interactions

The most active synthetic colourants demonstrated additive interactions with quinine, except for methylene blue ($\sum\text{FIC}_{50} < 1$) that was synergistic (Figure 2.10a). Methylene blue demonstrated a synergistic interaction ($\sum\text{FIC}_{50} < 1.0$), whilst safranin O and mercury orange showed additive interactions with $\sum\text{FIC}_{50}$ values between 1.0 and 2.0 (Table 2.9). The methylene blue/quinine curve showed a concave shape around the straight line. Most of the points in the safranin O/quinine and mercury orange/quinine curves were along and above the

straight line. However the ΣFIC_{50} values between 1.0 and 2.0 were observed for safranin O and mercury orange when in combination with quinine. Natural colourants, curcumin and carbon black, demonstrated additive interactions, with ΣFIC_{50} values between 1.0 and 2.0, in combination with quinine (Figure 2.10b). The carbon black/quinine curve showed a more convex shape than the curcumin/quinine curve, which borders on partial antagonism ($\Sigma\text{FIC}_{50} \geq 2$ and < 4).

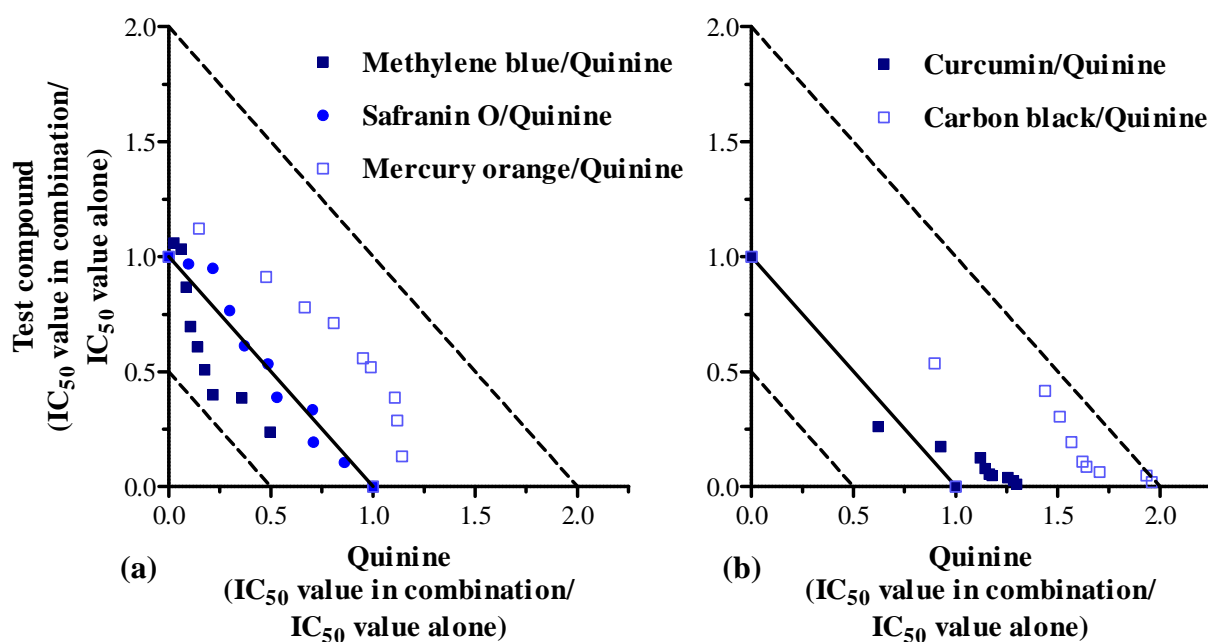


Figure 2.10 Isobolograms showing the drug interactions between quinine and the most active (a) synthetic and (b) natural compounds.

Table 2.9 Drug interactions of the most active colourants in combination with quinine.

Compound class	Combinations with quinine	ΣFIC_{50} (mean \pm S.D.)	Interaction classification
Synthetic colourants	Methylene blue	0.64 ± 0.31	Slightly synergistic
	Safranin O	1.01 ± 0.09	Additive
	Mercury orange	1.42 ± 0.08	Additive
Natural colourants	Curcumin	1.20 ± 0.07	Additive
	Carbon black	1.78 ± 0.20	Additive

2.5.5 Morphology and drug-sensitivity of development stages

The Giemsa-stained (Section 2.3.7) parasitised RBC control (Figure 2.11a) demonstrated the distinct morphological features of different stages of the erythrocytic life-cycle of the *P. falciparum* malaria parasite. The ring form was early-to-mid stage at 8 h, whilst at 24 and 32 h the trophozoite form contained yellow-brown haemozoin crystals, and schizont form showed

blue-stained merozoites. The early-ring stage was observed at 48 h, post-invasion of merozoites into human RBCs. In contrast, the development of the parasites exposed to quinine, was arrested at the late trophozoite stage (Figure 2.11b). Parasites treated with methylene blue (Figure 2.11c) progressed up to the schizont stage, which was consistent with the parasitised RBC control. However degenerate or ‘crisis form’ parasites were observed at 48 h, suggesting that the schizont stage was most sensitive. The trophozoite stage was particularly sensitive to nucleoside derivative, JLP118.1 (Figure 2.11d) as the parasite did not proceed to the schizont stage. The IP-4 treated parasites (Figure 2.11e) underwent morphological change from ring to trophozoite stage, but did not proceed to schizont stage and appeared vacuolated.

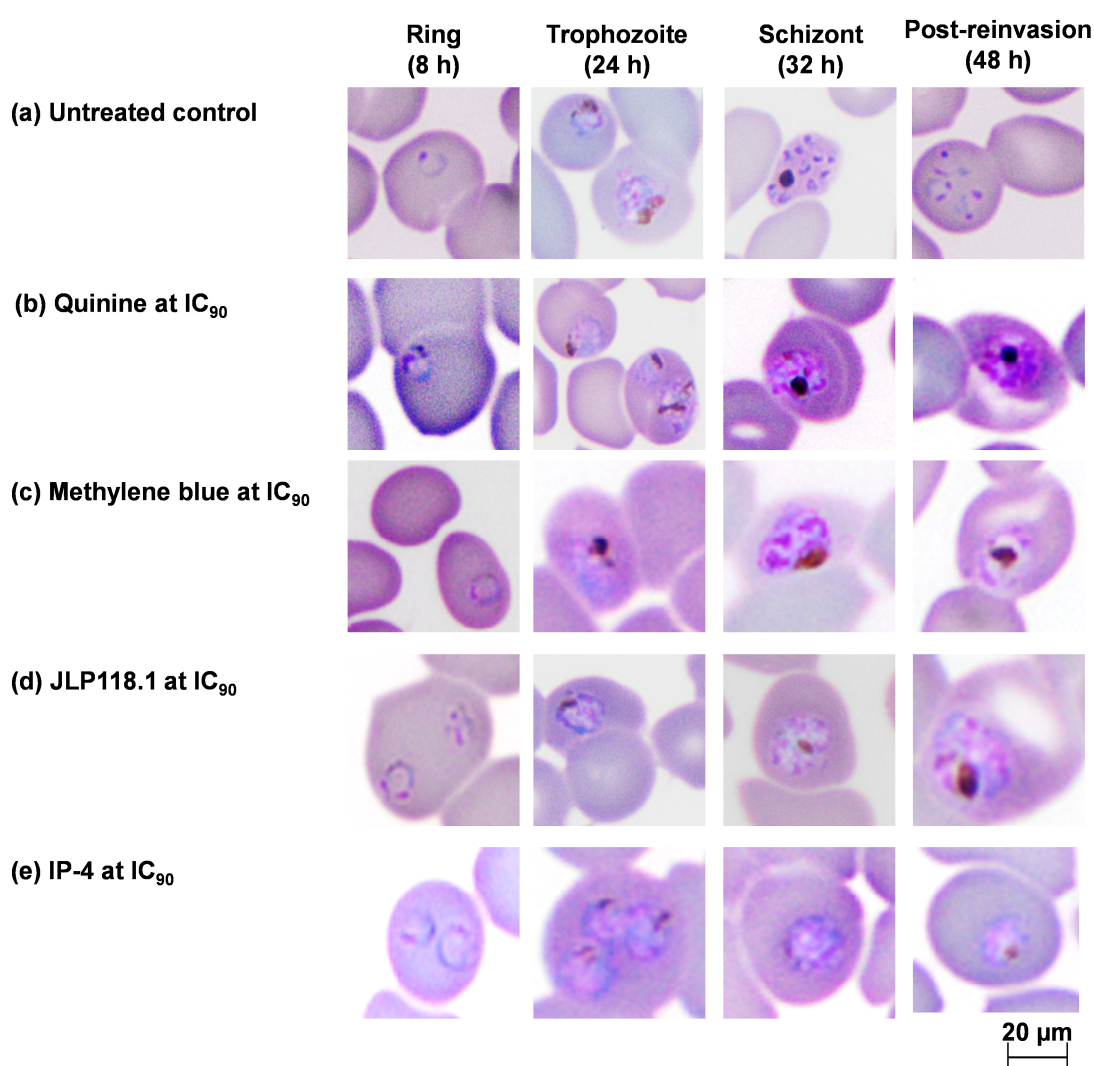


Figure 2.11 Morphological changes and stage-sensitivity of the *P. falciparum* parasites to the most active compounds. The parasites were exposed to: (b) Quinine (IC₉₀: 0.525 μM), MB (IC₉₀: 8.4 nM), (c) JLP118.1 (IC₉₀: 3.5 μM) and (d) IP-4 (IC₉₀: 23 μM) being the most active compounds from each class compound. The images were taken at 1000x magnification under oil immersion.

The effect of the test compounds on the total parasitaemia of the cultures over a 48 h exposure period is shown in Figure 2.12. Dead parasites were noted as condensed, darkly stained with un-differentiated morphological features and were excluded in the parasite count. The increase from the 2% parasitaemia seeded in the ring form to 4-6% within the 0-8 h period, was attributed to the presence of late schizonts in the culture. The decrease to the total parasitaemia after 8 h of exposure to quinine could be due to the sensitivity of the mature forms of the parasites. After 16 h post-exposure, JLP118.1 and IP-4 reduced total parasitaemia by 1.5-2% compared to the control, whilst the ring forms survived until trophozoite stage at 24 h with the quinine and methylene blue treatments (Figure 2.12). The inhibitory effect methylene blue and quinine again showed a similar pattern with the total parasitaemia decreasing and plateauing around 3-3.5% during schizont stages (32-40 h); whilst the control culture's total parasitaemia increased to about 6.85% during the same period. JLP118.1 and IP-4 showed a different inhibitory pattern showing a marked decrease pre-invasion stage resulting in reduced parasitaemia (JLP118: 1.8%, IP-4: 3%) during the ring stage at 48 h compared to 7.5% observed with the control culture (Figure 2.12). The effect of an IC₉₀ concentration of quinine demonstrated a parasitaemia below 10% against the laboratory *P. falciparum* strain TM29 (Monatrakul *et al.*, 2010). In the current study, the parasitaemia was ≤ 4% at an IC₉₀ concentration of quinine over the 48 h exposure period.

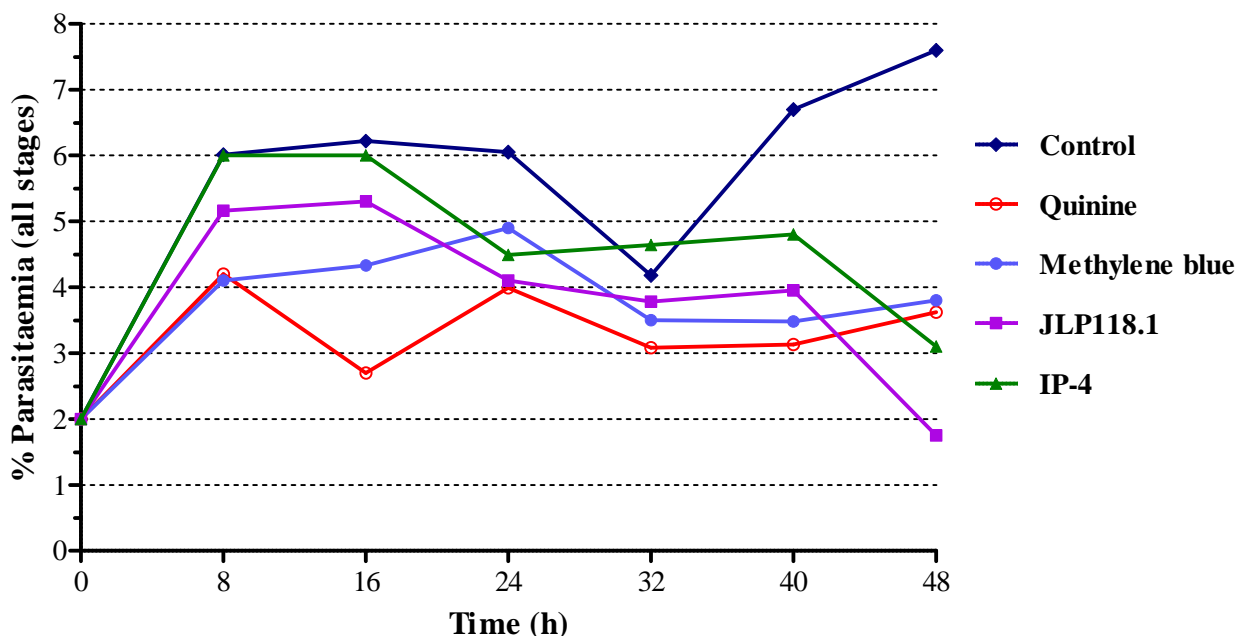


Figure 2.12 Effect of methylene blue, JLP118.1 and IP-4 in comparison to quinine at an IC₉₀ value on *P. falciparum* parasite growth over a single 48 h-cycle. Dead parasites were noted as condensed, darkly stained with un-differentiated morphological features and were excluded in the parasite count.

2.5.6 Structure-activity relationship of analogue compounds

The chemical structures of the synthetic colourants, both active and inactive were too diverse to make structural comparisons that may be related to their antimalarial activity. However, structural analysis of the most active synthetic colourants, all the nucleoside analogues as well as the imidazopyridine analogue series of compounds, was performed.

2.5.6.1 Nucleoside analogues

The overall antimalarial activity of the most active nucleoside analogues was classified as highly active ($\leq 5 \mu\text{M}$). Of all the nucleoside analogues tested, only the pyrimidine-based nucleoside analogues, JLP118.1 (contained uracil base) and JLP093 (contained cytosine base) were highly active against *P. falciparum*. The substitution of the tert-butyl-dithiomethyl-hydroxyl group at R¹ and acetate groups at R³ and R⁴ positions in JLP118.1, with the tert-butyl-diphenylsilyl and hydroxyl groups (-OH) in JLP093, did not improve the antimalarial potency (Table 2.10). When the cytosine base in JLP093 was substituted with uracil at R² in JLP089 it resulted in JLP089 becoming inactive ($\text{IC}_{50} > 100 \mu\text{M}$). The single substitution of the tert-butyl-diphenylsilyl group at R¹ position in JLP089 with the tert-butyl-dithiomethyl-hydroxyl group in JLP090.3 did not improve the antimalarial activity as both compounds were inactive. Similarly, the R¹ substitution with tert-butyl-diphenylsilyl in JLP118.1 resulted in JLP117.1 being inactive. JLP087 contained a uniquely modified uracil nucleobase (at R² position) and an acetaldehyde group at R¹, but was inactive although the sugar group in JLP118.1 was retained. The purine-based nucleosides JLP095.2 (R¹ = tert-butyl-diphenylsilyl, R² = adenine) and JLP077.1 (R¹ = tert-butyl-dithiomethyl-hydroxyl, R² = modified hypoxanthine) were structurally diverse to compare with only the ribose structure similar in both compounds, but were inactive. All the purine-based nucleoside analogues tested against *P. falciparum* were inactive.

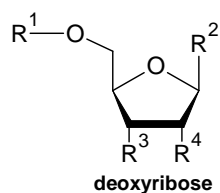
2.5.6.2 Imidazopyridine analogues

Overall the antimalarial activity of the most active imidazopyridine analogues was classified as low (50-100 μM) to moderate (10-50 μM). The cyclohexane (-C₆H₁₂) ring at position R¹ in compounds IP-2 to -4 was substituted by a 1,3-dimethylbenzene ring in compounds IP-5 to -8 (Table 2.11). Within the R¹ cyclohexane ring containing group of compounds, IP-3 and IP-4, were the most active of all the imidazopyridines. The increase in compound size and lipid-solubility with the benzyloxy (-C₇H₈O) side chains at positions R³ and R⁴ did not improve the antimalarial activity as observed in IP-2. However, replacing of the benzyloxy groups with hydroxy groups at R³ and R⁵ as well as the removal of the formamide (-CH₃NO) group at R² from IP-3, increased the antimalarial activity of IP-4 by 1.4-fold. On comparing the two

hydroxy substituted compounds, IP-4 and IP-5, the only difference between the two compounds is the R¹ substitute, where the 1,3-dimethylbenzene ring decreased the antimalarial activity of IP-5 by 2-fold compared to the cyclohexane ring (Table 2.11).

All the imidazopyridine analogues (except for IP-3) were significantly ($p < 0.05$) less potent compared to IP-4 (IC₅₀: 15.3 ± 0.41 μM). Of the test compounds that contained a 1,3-dimethylbenzene ring, IP-5 (IC₅₀: 36.3 ± 1.19 μM) was the most active. IP-5 was similar to IP-4 in structure with both compounds possessing hydroxyl groups at positions R³ and R⁵, however, IP-5 was found to be at least 2-fold less active than IP-4. The substitution of *N,N*-dihydroxymethanamine with a methyl group in IP-7 at R² decreased the antimalarial activity of IP-8 (IC₅₀ > 100 μM) by over 2-fold.

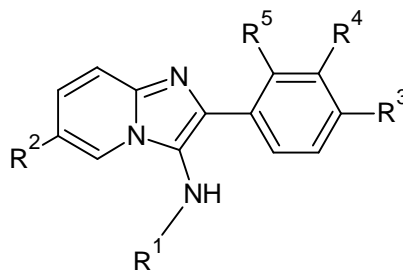
Table 2.10 Chemical structure and antimalarial activity of nucleoside analogues.



Compound	R ¹	R ²	R ³	R ⁴	Antimalarial activity IC ₅₀ (μM)
JLP118.1					1.79 ± 0.12
JLP093					2.38 ± 0.11
JLP089					> 100 (20.08 ± 8.11%)
JLP090.3					> 100 (9.45 ± 3.52%)
JLP117.1					> 100 (9.23 ± 4.92%)
JLP087					> 100 (0.50 ± 0.00%)
JLP095.2					> 100 (42.24 ± 5.19%)
JLP077.1					> 100 (40.63 ± 1.63%)

The red stick (•) shows the site of attachment to the parent structure. Inhibitory activity of the test compound with IC₅₀ value > 100 μM is in parentheses as % parasite growth inhibition.

Table 2.11 Chemical structure and antimalarial activity of imidazopyridine analogues.



Compound	R ¹	R ²	R ³	R ⁴	R ⁵	Antimalarial activity IC ₅₀ (μM)
IP-2					-H	> 100 (11.20 ± 2.11%)
IP-3				-H		20.77 ± 0.72
IP-4		-H	-OH	-H	-OH	15.30 ± 0.41
IP-5		-H	-OH	-H	-OH	36.30 ± 0.19
IP-6		Br-	-CH ₃ OH	-H	-CH ₃ OH	67.20 ± 3.05
IP-7			-CH ₃ OH	-H	-CH ₃ OH	55.30 ± 1.90
IP-8		-CH ₃	-CH ₃ OH	-H	-CH ₃ OH	> 100 (27.40 ± 3.22%)

The red stick (→) shows the site of attachment to the parent structure. Inhibitory activity of the test compound with IC₅₀ value > 100 μM is in parentheses as % parasite growth inhibition.

Overall, the antimalarial activities of the imidazopyridine analogues as a class was significantly varied ($p < 0.0001$) and the individual antimalarial activities were all significantly ($p < 0.05$) less potent compared to quinine.

2.5.7 Drug-like properties

At least three violations of the Lipinski's Ro5 may be allowed depending on the nature of the compound, its permeability and transport to its specific target for a compound to be considered drug-like (Lipinski *et al.*, 1997). However, no assumptions were made regarding the permeability of the parasites to the test compounds or how they were transported *in vitro*. Therefore, for the purpose of the study, the test compounds had to comply with all the Ro5

physicochemical properties, in their non-ionised or neutral states, in order to be considered as drug-like. The log P value was predicted for the test compounds in their natural or non-ionised state. A positive log P value (10:1, organic to aqueous ratio) reflected a lipophilic property of the test compound, a negative log P value (1:10 ratio) indicated a hydrophilic property and log P = 0 (1:1 ratio) meant the compound was soluble or partitioned equally in both lipophilic organic and aqueous phases (Khanna and Ranganathan, 2009).

Table 2.12 Predicted solubility and permeability properties of most active synthetic test compounds based on the Lipinski's Rule of 5 (Lipinski, 2004).

Compound class	Compound	MW < 500	HBA < 10	HBD < 5	0 ≥ Log P ≤ 5	# of Ro5 violations
Synthetic colourants	Methylene blue	319.85	3	0	4.09 ± 1.51	0
	Safranin O	315.39	4	4	-0.68 ± 1.46	1
	Mercury orange	483.31	3	1	3.98 ± 1.04	0
Natural colourants	Curcumin ¹	368.38	6	3	2.85 ± 0.41	0
	Carbon black	ND	ND	ND	ND	ND
Nucleoside analogues	JLP093	481.62	8	4	3.03 ± 0.57	0
	JLP118.1	630.64	12	1	5.13 ± 0.55	3
Imidazopyridine analogues	IP-3	546.66	7	3	6.05 ± 0.99	2
	IP-4	323.39	5	3	3.26 ± 0.60	0
	IP-5	345.40	5	3	3.87 ± 0.88	0
	IP-6	452.34	5	1	5.68 ± 1.44	1
	IP-7	418.45	8	1	4.75 ± 1.43	0
Reference drugs	Quinine	324.42	4	1	2.82 ± 0.43	0
	Chloroquine	319.87	3	1	4.41 ± 0.76	0

¹The chemical structure of curcumin was sourced from Bernabé-Pineda *et al.* (2004). MW, molecular weight; HBA, hydrogen bond acceptors; HBD, hydrogen bond donors; # of Ro5 violations, Number of Rule of five violations. All parameters including log P were predicted using ACD/ChemSketch software (freeware version). ND, not determined.

All the synthetic test compounds that complied with the Lipinski's Rule of 5 (Ro5 violations = 0) had MWs in the range of 300-484 g/mol and log P values between 0 and 5, comparable to quinine (Table 2.12). Nucleoside analogue, JLP118.1, showed the most violations (Ro5 violations = 3) compared to all the test compounds and did not comply the drug-likeness test. IP-3 and -6 showed one to two violations and were excluded as drug-like compounds (Table 2.12). The negative log P value of safranin O reflected significantly ($p < 0.05$) poor-solubility compared to quinine and chloroquine, and was regarded as not 'drug-like'. However safranin O had a significantly ($p < 0.05$) smaller molecular size (MW: 315.39) compared to quinine and chloroquine. Curcumin complied with the Lipinski's Ro5 for drug-likeness and was highly active ($IC_{50} < 5 \mu\text{g/ml}$) against *P. falciparum* (Table 2.12). Both quinine and

chloroquine demonstrated drug-like properties and complied with the Lipinski's Ro5. The predicted log P and antimalarial activity (IC_{50} values) data of the most active synthetic compounds, was plotted on a linear graph (Figure 2.13) to determine if there was a correlation between the lipid-solubility and activity of the compounds.

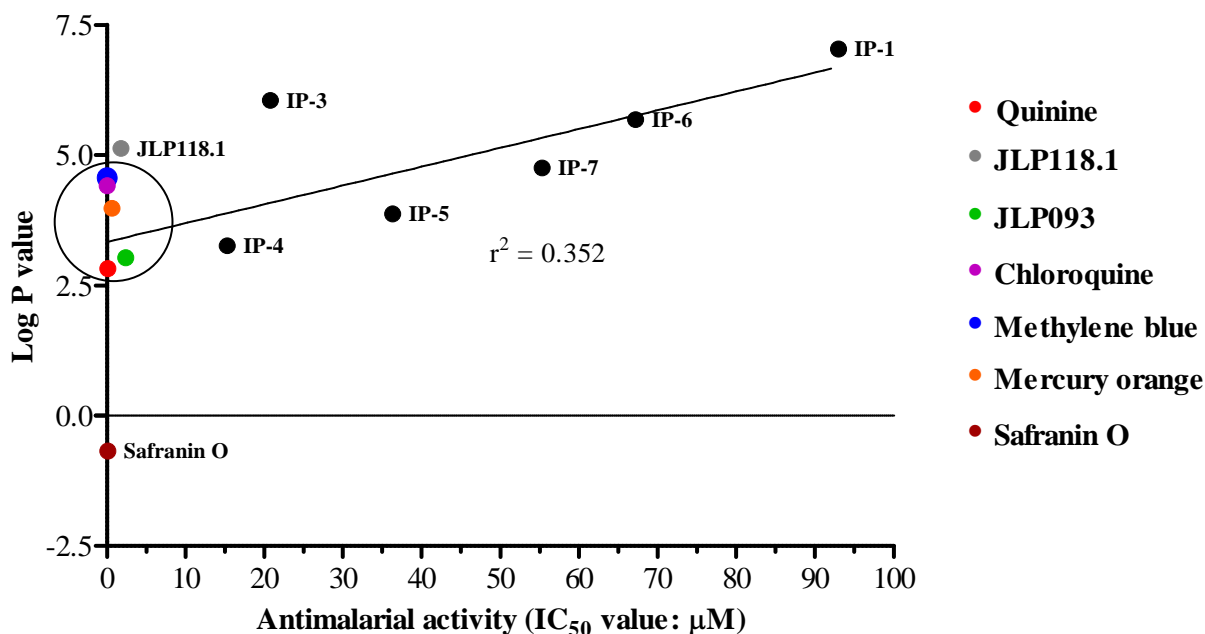


Figure 2.13 Correlation between predicted log P values and antimalarial activity IC_{50} values. The encircled compounds that complied with all the Ro5 parameters were: quinine, JLP093, chloroquine, methylene blue and mercury orange showed high antimalarial activity ($\leq 5 \mu M$) and log P values were in the 0-5 range.

No significant correlation was observed ($r^2 = 0.352$). However, the compounds that are encircled (Figure 2.13) complied with all the Ro5 parameters, and were highly active ($IC_{50} \leq 5 \mu M$) against *P. falciparum*. In addition, the compounds quinine, JLP093, mercury orange, chloroquine and methylene blue complied with the Lipinski's Ro5 parameters (Figure 2.13). Although safranin O was highly active ($IC_{50} < 5 \mu M$), it showed a negative log P value, which implied it was a hydrophilic compound.

2.5.8 Predicted ionisation and absorption as a function of pH

The predicted pK_a and (%) ionisation values at physiological pH 7.4 (similar to RBC cytosol) and acidic pH 5.0 (similar to the parasite's digestive vacuole environment) of the most active compounds are summarised in Table 2.13.

Table 2.13 Predicted percentage ionisation of most active test compounds.

Compound class	Compound	pK _a	% Ionisation		% Absorption at pH 7.4
			pH 7.4	pH 5	
Synthetic colourants	Methylene blue	-0.60, 0.00	0.00	0.00	100
	Safranin O	5.80	2.45	86.32	97.55
	Mercury orange	-1.86, -5.32	0.00	0.00	100
Natural colourants	Curcumin ¹	10.50, 8.38	0.08	0.00	99.92
	Carbon black	ND	ND	ND	ND
Nucleoside analogues	JLP093	4.20	0.06	13.68	99.94
	JLP118.1 ²	8.90	3.07	0.01	96.93
Imidazopyridine analogues	IP-3	6.00	3.83	90.91	96.17
	IP-4	4.10	0.05	11.18	99.95
	IP-5	4.70	0.02	33.39	99.80
	IP-6	5.80	2.45	86.32	97.55
	IP-7	4.90	0.32	44.27	99.68
Reference drugs	Quinine ³	9.70, 5.07	0.47	54.02	99.53
	Chloroquine ⁴	10.10, 8.10	83.34	99.92	16.63

¹pK_a value for ionisable acidic group from Bernabé-Pineda *et al.* (2004); ²Only pK_a value for ionisable acidic group was predicted; ³pK_a values from O'Neil *et al.* (2001); ⁴pK_a values from O'Neill *et al.* (2012).

2.5.8.1 Synthetic colourants

Methylene blue (MB⁺) and safranin O (SO⁺) are cationic (positively charged) basic dyes and usually stabilised with chloride (Cl⁻) salts (Vennerstrom *et al.*, 1995). In its cationic form, methylene blue (pK_{a1} = 0.00, pK_{a2} = -0.60) did not show a degree of ionisation (% ionisation: 0.00) at pH 7.4 and 5.0. The absorption and accumulation into the parasite of methylene blue could not be attributed to its weak acid-base properties. In contrast, safranin O (pK_a = 5.80) showed increasing ionisation down the pH gradient from 2.45% at pH 7.4 to 86.32% at pH 5.0 and a substantial amount (97.55%) of the non-ionised compound could be absorbed into the digestive vacuole. Mercury orange (pK_{a1} = -1.86, pK_{a2} = -5.32), a neutral azo dye also showed no degree of ionisation at both pH levels, thus a high absorption rate (100%) in both the RBC and digestive vacuole compartments was predicted. Quinine (pK_{a1} = 9.70, pK_{a2} = 5.07) showed 54.02% ionisation at pH 5.0 and although chloroquine showed an absorptive rate of 16.63% at pH 7.4, all of the non-ionised species were almost completely ionised at pH 5 (% ionisation: 99.92) leading to increased drug accumulation into the parasite (O'Neil *et al.*, 2001; O'Neill *et al.*, 2012).

2.5.8.2 Natural colourants

Curcumin is a polyprotic acid (an acid that can donate more than one proton) with three ionised states giving pK_{a1} = 8.38, pK_{a2} = 9.88 and pK_{a3} = 10.50 (Bernabé-Pineda *et al.*, 2004). However, it only showed a low degree of ionisation of 0.08% at pH 7.4, thus yielding a high concentration (% ionisation: 99.92) of non-ionised, but acidic compound (Table 2.13). Curcumin did not show any degree of ionisation at acidic pH 5.0.

2.5.8.3 Nucleosides and nucleosides analogues

Only the pKa value (8.9) for the acidic group of JLP118.1 was predicted *in silico*. From this, JLP118.1 showed a low ionisation value of 3.1% at basic pH 7.4 and was non-ionised at acidic pH 5 (Table 2.13). Overall the absorption rate of the nucleoside analogues was more than 90% at basic pH 7.4 and JLP093 showed a significant ($p < 0.05$) ionisation of 13.7% at an acidic pH 5.0 within the compound class.

2.5.8.4 Imidazopyridine analogues

The imidazopyridines showed absorption rates (96-100%) comparable to quinine (99.5%) (Table 2.13). However, only IP-3 showed a % ionisation value (91%) comparable to chloroquine (99%) suggesting good “ion-trapping” within the digestive vacuole compartment at acidic pH of 5. IP-6 also showed a high ionisation value of 86.3% at pH 5.0.

2.6 Discussion

2.6.1 Antimalarial activity of synthetic colourants

The results (summarised in Table 2.14) confirmed the potent antimalarial activity of the thiazine colourant, methylene blue and phenazinium colourant, safranin O that have been previously investigated (Vennerstrom *et al.*, 1995; Atamna *et al.*, 1996; Schirmer *et al.*, 2003; Meissner *et al.*, 2006). Vennerstrom *et al.* (1995) reported similar findings that showed a significantly potent ($p < 0.05$) antimalarial activity of methylene blue (IC_{50} : 3.58 ± 2.22 nM) and a significantly ($p < 0.05$) less potent antimalarial activity of safranin O (IC_{50} : 43.3 ± 29.3 nM) against the Sierra Leone (D6) chloroquine-sensitive strain in comparison with chloroquine (IC_{50} : 24.0 ± 4.92 nM). In the current study, the antimalarial potency of methylene blue (IC_{50} : 4.19 ± 0.16 nM) was at least 25-fold more potent than the reference drug, quinine (IC_{50} : 103.90 ± 8.30 nM). The morphological studies on parasites treated with methylene blue, however suggest that the parasites' development was arrested at the trophozoite stage (Figure 2.11c). In contrast, methylene blue was active against all developmental stages but, 8-fold less active against the schizont stage of both chloroquine-sensitive (3D7) and chloroquine-resistant (K1) strains of *P. falciparum* (Akoachere *et al.*, 2005). In the current study, Safranin O (IC_{50} : 86.50 ± 2.61 nM) was significantly ($p < 0.05$) more active, whereas mercury orange was approximately six-fold less active compared to quinine. Methylene blue and safranin O showed minimal toxicity to uninfected human RBCs, as did quinine (Table 2.14). In contrast, the azo colourant mercury orange, showed significant haemolytic activity ($p < 0.05$) in a dose-dependent manner. However, mercury orange showed a selectivity index (S.I.: 25.32) significantly higher ($p < 0.05$) than 10. In general, a

compound that demonstrates a toxic concentration 10-fold ($S.I. \geq 10$) or more than its effective concentration yielding a 50% response, is regarded as non-toxic (Pink *et al.*, 2005).

Table 2.14 Summary of antimalarial, haemolytic and β -haematin formation inhibitory activity of the most active synthetic colourants.

Compound	Antimalarial activity $IC_{50} \pm S.D.$ (μM)	Haemolytic activity $HLC_{50} \pm S.D.$ (μM) ^a	β -Haematin inhibition $IC_{50} \pm S.D.$ (μM) ^a
Methylene blue	0.004 ± 0.00	>100 ($13.92 \pm 0.03\%$)	>800 ($0.001 \pm 0.02\%$)
Safranin O	0.087 ± 0.00	>100 ($0.31 \pm 0.01\%$)	>800 ($10.8 \pm 1.07\%$)
Mercury orange	0.664 ± 0.01	16.81 ± 0.56 [$S.I. = 25.32$] ^b	>800 ($0.001 \pm 0.01\%$)
JLP118.1	1.79 ± 0.12	>100 ($0.92 \pm 0.04\%$)	>800 ($0.01 \pm 0.02\%$)
JLP093	2.38 ± 0.11	>100 ($0.35 \pm 0.05\%$)	>800 ($5.8 \pm 3.35\%$)
Quinine	0.10 ± 0.01	>100 ($0.15 \pm 0.01\%$)	68.3 ± 4.17
Chloroquine	0.01 ± 0.00	>100 ($0.01 \pm 0.01\%$)	38.4 ± 4.77

^aHaemolytic activity of test compounds that demonstrated HLC_{50} values above $100 \mu M$, and ^a β -haematin formation inhibition IC_{50} values above $800 \mu M$ (or $> 4 \text{ mg/ml}$) were reported as percentage (%) values. ^bS.I.: Selectivity index.

However, significant haemolysis induced by a compound in comparison to quinine and chloroquine, should be considered with caution especially in the context of malaria, which increases the risk of anaemia (Müller *et al.*, 2013). The chloro-mercuri reactive group in mercury orange is known to have a high binding affinity to non-protein sulfhydryl (thiols) groups in glutathione (O'Connor *et al.*, 1988). This would greatly reduce the capability of both uninfected and infected RBC, and the parasite itself to prevent oxidative stress, resulting in peroxidation of the cell membrane lipids and increased haemolysis, as well as parasite death. The risk of methylene blue-induced haemolysis (from four randomised controlled trials in Burkina Faso, West-Africa) has been found to be clinically insignificant in glucose-6-phosphate dehydrogenase (G6PD)-deficient children (below five years of age) with uncomplicated *P. falciparum* malaria (Müller *et al.*, 2013). In the latter study, methylene blue did not show haemolysis as a major side-effect in any of the individuals, as was the finding in the current *in vitro* study (Table 2.14). Similarly in another study, healthy adults with class III G6PD-deficiency were given a three day oral regimen of a total of 780 mg of methylene blue. No occurrence of haemolysis was reported and haemoglobin levels remained stable (Mandi *et al.*, 2005). Methylene blue may be combined with classical antimalarial drugs to prevent resistance or even sensitise drug-resistant strains of *P. falciparum* to existing antimalarial agents (Schirmer *et al.*, 2003). In the current study, methylene blue interacted in a slight synergistic (ΣFIC_{50} : 0.64 ± 0.31) manner with quinine (Figure 2.10a). In contrast, Akoachere

et al. (2005) reported an additive interaction (mean Σ FIC₅₀: 1) between methylene blue (IC₅₀: 6.5 ± 1.8 nM) and quinine (IC₅₀: 90 ± 39 nM) when tested against the chloroquine-resistant (K1) strain of *P. falciparum*, whilst Garavito *et al.* (2007) reported a synergistic effect between methylene blue and quinine against the chloroquine-resistant *P. falciparum* strain FcM29 (Garavito *et al.*, 2007). Therefore the discrepancy could be attributed to the difference in strains and in some cases the type of assay used and the classification of drug interaction applied. The combinations of methylene blue with chloroquine, and all the other quinolines tested, as well as with pyrimethamine were antagonistic (Akoachere *et al.*, 2005). Antagonistic interactions between methylene blue and quinoline drugs tested in the latter study, have been suggested to increase the likelihood of cross-resistance in *P. falciparum* (Akoachere *et al.*, 2005).

Safranin O and mercury orange demonstrated an additive interaction with quinine (Figure 2.10a). Although the interactions of methylene blue and safranin O were additive when combined with quinine, the latter combinations may have potential to prevent cross-resistance as the thiazine and phenazinium colourants are putatively effective inhibitors of *P. falciparum* glutathione reductase (*PfGR*), thus complementing the β -haematin formation inhibitory activity of quinine (Färber *et al.*, 1998; Lüönd *et al.*, 1998; Akoachere *et al.*, 2005).

The rest of the azo, naphthalene and sulfonated synthetic colourants were inactive at a screening concentration of 100 μ M against the *P. falciparum* parasites. However, anionic sulfonated azo dyes such as trypan blue (IC₅₀: 41.3 μ M) have been found to inhibit the activity of the recombinant triose phosphate isomerase enzyme involved in ATP production during glycolysis in *P. falciparum* (Joubert *et al.*, 2001). In the current study, trypan blue was inactive (IC₅₀ > 100 μ M) against the whole-parasite.

2.6.1.1 Physicochemical properties of synthetic colourants

On analysing the physicochemical properties of synthetic colourants, methylene blue (pK_{a1} = 0.0; pK_{a2} = -0.6) complied with the Lipinski's Ro5, but did not demonstrate any degree of ionisation at a pH of 5 and 7.4 in its cationic form (Table 2.13). However, there was no correlation between the log P and antimalarial activity of all the most active test compounds (Figure 2.13). Vennerstrom *et al.* (1995) has suggested that the relative lipid-solubility of the thiazine colourants such as methylene blue, may be rather unimportant compared to their reduced, neutral forms. This is further evidence to support the hypothesis that the potent antimalarial activity of methylene blue and most thiazine analogues is not due to its acid-base properties (Vennerstrom *et al.*, 1995). Although methylene blue maintains its positively

charged cationic form in a wide pH range (1 to 8), it has demonstrated good absorption in humans after oral administration with leucomethylene blue being the only urinary metabolite to be isolated (Disanto and Wagner, 1972; Vennerstrom *et al.*, 1995). In fact vital colourants such as methylene blue are often classified as “basic” dyes, referring to their cationic nature and not their weak-base properties, even though methylene blue is indeed an extremely weak base (Vennerstrom *et al.*, 1995). In addition, methylene blue concentrates selectively in parasitised RBC although the mechanism that leads to this sequestration is not clear (Akoachere *et al.*, 2005).

Based on the theory of histochemical staining techniques, coloured cations of basic dyes stain tissue structures rich in anions, such as phosphated DNA and RNA, and carboxylated or sulphated mucosubstances due to electrostatic or Coulombic attractions (Horobin, 2002). Although mature RBCs lack DNA, selective staining of malaria parasites by methylene blue is well established (Wainwright, 2008). An alternative hypothesis to the stain-tissue affinity theory proposed by Buchholz *et al.* (2012) was based on the redox properties of methylene blue. Upon entry into the parasitised RBC, methylene blue is electron-reduced to its neutral form, leucomethylene blue, a reaction catalysed by the human glutathione reductase or by a spontaneous reaction with NADPH (Buchholz *et al.*, 2008). The more lipid-soluble leucomethylene blue would then freely diffuse through the parasite and digestive vacuole membranes and be auto-oxidised to the methylene blue cation, and thus be trapped in the digestive vacuole (Buchholz *et al.*, 2008). Therefore, the accumulation of MB⁺ in the digestive vacuole would not be a weak base effect, but a redox mechanism. In contrast, safranin O (pK_a = 5.8), a cationic basic dye showed a negative log P value (-0.68 ± 1.46) suggesting poor lipid-solubility compared to quinine (log P: 2.82 ± 0.43) (Table 2.12). In addition, safranin O showed an increasing degree of ionisation (from 2.5% to 86.3%) down the pH gradient and demonstrated the “ion-trapping” effect at an acidic pH 5.0 (Table 2.13). The latter further confirms that the log P value is only an indicator of lipid-solubility of compounds and that the pH of the environment, acid-base properties and molecular weight are other contributing factors for effective drug absorption (Lipinski, 2004; Bhal *et al.*, 2007). Safranin O is putatively a strong reversible, uncompetitive inhibitor (K_i = 0.5 mM) of glutathione reductase similarly to methylene blue (Lüönd *et al.*, 1998). Mercury orange (pK_{a1} = -1.86, pK_{a2} = -5.8), a neutral azo compound, did not show ionisation at either basic pH 7.4 or acidic pH 5.0 level (Table 2.13). In addition, mercury orange showed compliance with the Lipinski’s Ro5 (Table 2.12). The log P (< 5) and non-ionisation (% ionisation: 0.00%) of mercury orange suggested high lipid-solubility and possible diffusion into the RBC, as well as

the parasite's digestive vacuole; although there was no strong correlation between the log P and the antimalarial activity (IC₅₀) of all the most active compounds (Figure 2.13).

2.6.1.2 Pharmacological effects of methylene blue

Methylene blue may have multiple modes of action against *P. falciparum* including inhibition of haemozoin formation, increased hexose monophosphate shunt, selective inhibition of the malaria parasites' glutathione reductase enzyme or may be due to its redox activity. Whereas the photoactivation therapeutic application of methylene blue, may be more suitable for localised skin malignancies and infections (Atamna *et al.*, 1994; Färber *et al.*, 1998; Tardivo *et al.*, 2005; Blank *et al.*, 2012). The latter modes of action are discussed within the context of the study although methylene blue has been extensively studied - the classical review by Clark *et al.* (1925) that cited 400 references being a case in point (Buchholz *et al.*, 2008).

2.6.1.2.1 β -Haematin formation inhibition

The current study showed that none of the most active synthetic colourants inhibited β -haematin formation and all showed IC₅₀ values greater than 800 μ M in comparison to known β -haematin inhibitors namely, chloroquine (IC₅₀: $38 \pm 4.77 \mu$ M) and quinine (IC₅₀: $68.30 \pm 20.39 \mu$ M). However, the antimalarial mechanism of action of methylene blue and its analogues has been proposed to involve the inhibition of haemozoin formation by forming haem-complexes in the parasite's digestive vacuole, similarly to 4-aminoquinoline drugs such as quinine (Atamna *et al.*, 1996; Ginsburg *et al.*, 1998; Schirmer *et al.*, 2003; Kumar *et al.*, 2007). In contrast, the current study showed that methylene blue, safranin O and mercury orange were not inhibitory to β -haematin crystal formation (Table 2.14).

The main difference that could account for this discrepancy in the results is the methodology that was used to assess the inhibition of β -haematin formation under *in vitro* conditions. In the study conducted by Atamna *et al.* (1996), the ability of methylene blue to complex with haem was done by monitoring a 'red-shift' or a peak absorption (at $\lambda = 605$ nm) using a UV-Vis spectrophotometer. Therefore, the method used in the latter study did not directly measure β -haematin formation as compared to the current study, where methylene blue did not show inhibition of β -haematin crystal formation, subsequent to incubation under acidic conditions (pH 4.4) similar to those in the parasite's food vacuole (Deharo *et al.*, 2002). The conditions of the current assay were not influenced by Cl⁻ salts (used to stabilise methylene blue) as may have been proposed earlier (Basilico *et al.*, 1998; Parapini *et al.*, 2000). In addition, β -haematin formation inhibitory activities previously reported by Hawley *et al.* (1998) for quinine (IC₅₀: 64.8μ M) and chloroquine (IC₅₀: 24.4μ M) were almost comparable to those

found in the current study (Hawley *et al.*, 1998). Quinine (IC_{50} : 68.3 ± 4.17) and chloroquine (IC_{50} : 38.4 ± 4.77) demonstrated β -haematin crystal formation inhibition in the current study and a strong correlation ($r^2 = 0.89$ and $r^2 = 0.99$, respectively) to the antimalarial activity was observed. However, an alternative hypothesis has been proposed by Blank *et al.* (2012) on the mechanism by which methylene blue may inhibit β -haematin formation (Figure 2.14).

According to Blank *et al.* (2012), methylene putatively acts as a pro-drug of redox-active molecules that are cycled in and out of the acidic digestive vacuole in infected RBCs, thereby oxidising major intracellular reductants (NADPH) and subsequently reducing haematin (Fe^{3+} -PPIX) into Fe^{2+} -PPIX (Figure 2.14) (Blank *et al.*, 2012). The stacking of iron porphyrins (haem) decreases their active surface and consequently decreases pro-oxidant capacity (Blank *et al.*, 2012). Therefore, redox-active compounds such as methylene blue, that display the ability of reducing Fe^{3+} -PPIX to Fe^{2+} -PPIX could inhibit haemozoin formation and lead to increased oxidative stress and subsequent death of *P. falciparum* parasites (Blank *et al.*, 2012). In addition, with methylene blue acting as a redox-cycling substrate of *P. falciparum* glutathione reductase, each reaction cycle catalysed by *P. falciparum* glutathione reductase leads to the consumption of NADPH and oxygen, and to the production of toxic reactive oxygen species, predominantly hydrogen peroxides, which interact with iron in the Fenton reaction and result in Fe^{3+} -PPIX decomposition (Figure 2.14) (Blank *et al.*, 2012).

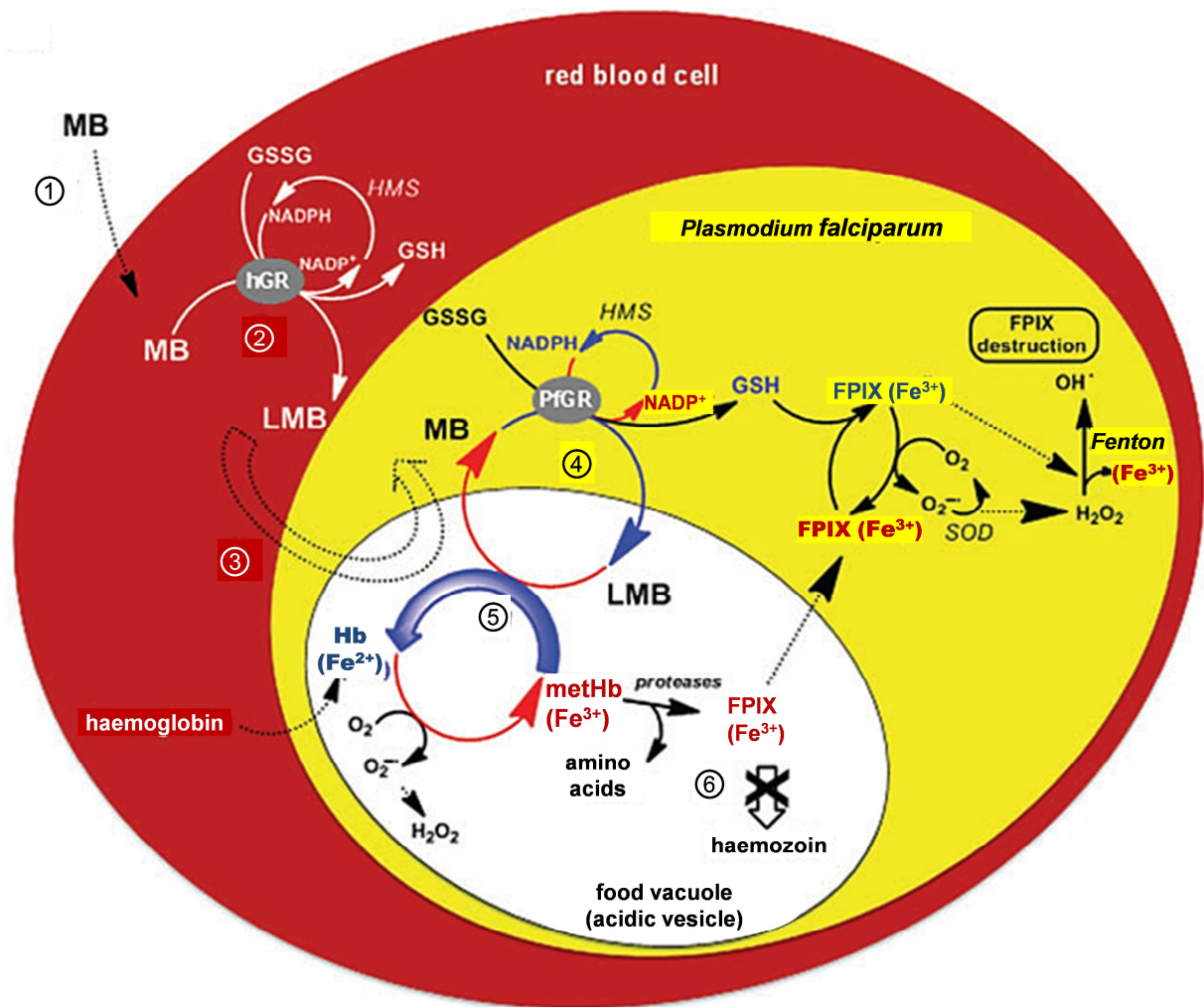


Figure 2.14 Putative redox-cycling of methylene blue affecting anti-oxidant systems in *P. falciparum*-infected RBC attributed to antimalarial activity (adapted from Blank *et al.* 2012). MB, methylene blue; LMB, leucomethylene blue; HMS, hexose monophosphate shunt; GSH, glutathione; GSSG, glutathione disulfide; PfGR, *P. falciparum* glutathione reductase; NADPH, nicotinamide adenine dinucleotide phosphate; NADP⁺, oxidised form of NADPH; FPIX, ferriprotoporphyrin IX; Hb, haemoglobin; metHb, Hb with iron in the ferric (Fe³⁺); SOD, superoxide dismutase; Fenton, Fenton's reaction step that produces hydroxyl radical (OH[•]) from hydrogen peroxide (H₂O₂) in the presence of Fe³⁺.

2.6.1.2.2 Activation of hexose monophosphate shunt

Although depletion of NADPH via the hexose monophosphate shunt (Figure 2.15) has been proposed as a plausible mechanism of action for methylene blue, this pathway is not the main cause of parasite death, but a contributing factor (Atamna *et al.*, 1994). The hexose monophosphate shunt is a source of pentose sugars required for nucleotide synthesis and for the reduction of NADP⁺ to NADPH (Atamna *et al.*, 1994). *P. falciparum* parasites are highly dependent on glucose for optimal growth and are very sensitive to oxidative stress (Preuss *et al.*, 2012). In fact, human glucose-6-phosphate dehydrogenase (G6PD)-deficiency (G6PD being the key enzyme in the hexose monophosphate shunt) protects the human host to a certain degree from malaria infections (Preuss *et al.*, 2012). Both the parasites and human

RBCs possess a complete hexose monophosphate shunt, but there are major differences between the parasite and human G6PD enzyme (Preuss *et al.*, 2012). Studies on the ability of methylene blue to recycle methaemoglobin (metHb, Fe³⁺) to normal haemoglobin (Hb, Fe²⁺), revealed that methylene blue enters RBCs, where it is enzymatically reduced by NADPH-dependant glutathione reductase to leucomethylene blue (Figure 2.14) at the cost of NADPH, and in turn leucomethylene blue then reduces metHb to Hb (Atamna *et al.*, 1996). Consequently, NADPH depletion activates the hexose monophosphate shunt pathway (Figure 2.15) which replenishes NADPH by activation of G6PD, which is the rate limiting enzyme of the pathway (Preuss *et al.*, 2012).

NADPH has been reported to spontaneously reduce methylene blue and as a result cytosolic NADPH was be depleted at a rate of about 1-5 $\mu\text{M}/\text{min}$ if not replenished under *in vitro* conditions (Schirmer *et al.*, 2003). Indeed, hexose monophosphate shunt activity in infected RBCs has been found to be 78-fold higher than that of healthy uninfected RBCs (Atamna *et al.*, 1994). In addition, the hexose monophosphate shunt activity increased with parasite maturation from the ring stage towards the trophozoite stage, and declined at the schizont stage (Atamna *et al.*, 1994). This correlates with findings of the current study that showed that the parasites were mostly sensitive to methylene blue during the trophozoite stage (Figure 2.11c). Activation of the hexose monophosphate shunt may be a mode of action of methylene blue and not necessarily indicative of toxicity. Methylene blue has been found to be safe in adults and children with and without G6PD-deficiency when administered to subjects at an established dose of 12 mg/kg, over a three day period in combination with chloroquine (Meissner *et al.*, 2006). Under *in vitro* conditions, sodium nitrite, a hexose monophosphate shunt stimulant, has been shown to elevate hexose monophosphate shunt activity 15-fold with significant proteolysis in mature RBCs. Even though methylene blue elevated hexose monophosphate shunt activity by as much as 45-fold, it did not cause proteolysis (Baird, 1984). Therefore, proteolysis could not have contributed to methylene blue's mechanism of action against *P. falciparum*.

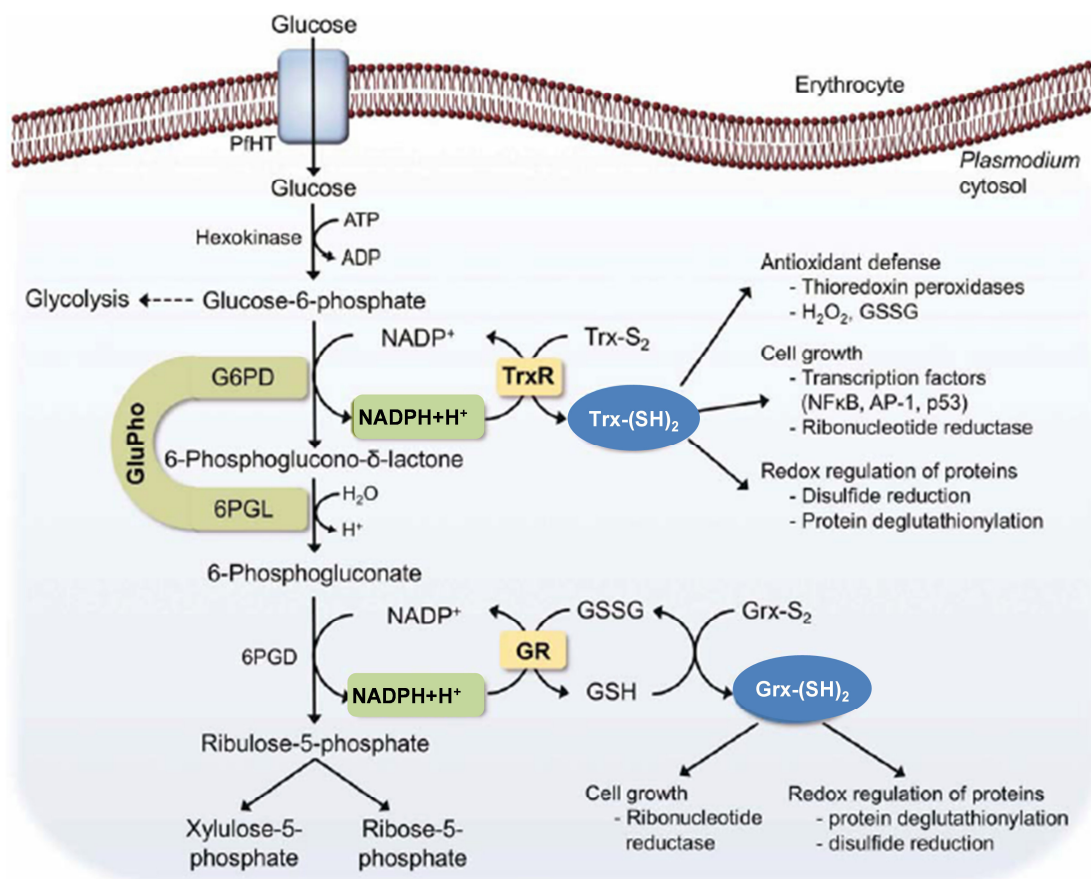


Figure 2.15 The hexose monophosphate pathway in *P. falciparum* (adapted from Preuss *et al.* 2012). The hexose monophosphate pathway replenishes NADHP for the glutathione (GSH) and thioredoxin (Trx) detoxification systems in *P. falciparum*. NADPH formed by GluPho (glucose-6-phosphate dehydrogenase 6-phosphogluconolatonase) and 6PGD (6-phosphogluconate dehydrogenase) are used by both Trx-reductase (TrxR) and glutathione reductase (GR) for the reduction of their substrates, thioredoxin (Trx) and glutaredoxin (Grx). Trx and Grx can reduce a broad range of protein substrates and are thus involved in the redox regulation of many cellular processes. 6PGL, 6-phosphogluconolactonase; G6PD, glucose-6-phosphate dehydrogenase; *PfHT*, *P. falciparum* hexose transporter (Preuss *et al.*, 2012).

There is further evidence to suggest that “methylene blue-like” drugs activate the hexose monophosphate shunt in the presence of a glutathione reductase inhibitor, and that “ascorbate-like” compounds fail to do so under the same conditions (Baird, 1984). However, in a study by Atamna *et al.* (1994), antimalarial drugs (chloroquine and quinine, both at 5 μM) and radical oxidative species scavengers (uric acid and benzoic acid, both at 4 μM) reduced hexose monophosphate shunt activity by 20-44% in infected RBCs (Atamna *et al.*, 1994). The latter findings contribute to the argument that the *in vitro* activation of the hexose monophosphate shunt observed in eukaryotic cells and parasites in the presence of methylene blue, does not increase to appreciable levels to cause cell death. Therefore, parasite death as a result of oxidative stress due to NADPH depletion via the hexose monophosphate shunt

within the infected RBC may not be a plausible, singular mechanism of action of methylene blue, but may be a secondary contributing factor to parasite death.

2.6.1.2.3 Inhibition of recombinant *P. falciparum* glutathione reductase enzyme

Methylene blue has been shown to inhibit a recombinant *P. falciparum* glutathione reductase (*PfGR*) enzyme in a non-competitive manner (Färber *et al.*, 1998). *PfGR* was the first molecule to be identified as a target of methylene blue in the parasite. In a study by Färber *et al.* (1998), the enzymatic activity of recombinant *PfGR* (optimal pH 6.9-7.2) was reduced by 60% when exposed to methylene blue (10 μM), but the inhibition was reversible by dilution. Whilst a later study by Buchholz *et al.* (2008) showed that methylene blue inhibited *PfGR* (IC_{50} : 5.4 μM) more potently compared to human glutathione reductase (hGR) (IC_{50} : 16.4 μM). Glutathione reductase, a dimeric flavoenzyme, catalyses the conversion of reduced glutathione, GSSG into GSH, which is necessary for cellular protection against oxidative stress, whereby NADPH is oxidised to NADP^+ (Preuss *et al.*, 2012). In the RBC cytosol, glutathione reductase maintains a concentration ratio of 1:100 for GSSG:GSH (Färber *et al.*, 1998). Both *PfGR* and hGR play a crucial role in maintaining the redox homeostasis for the intra-erythrocytic growth of the parasite (Färber *et al.*, 1998). Therefore the inhibition of *PfGR* is likely to contribute significantly to the toxicity of methylene blue to the parasite and oxidative stress.

2.6.1.2.4 Methylene blue photo-activation

Methylene blue activity may be induced by photo-activation to cure infections. In the current study, the treated parasites were incubated in the dark and photoactivation did not form part of the study. However, as early as the 1930's, it was shown that phages and viruses stained with phenothiazium dyes, such as methylene blue, were killed by light illumination (Tardivo *et al.*, 2005). However, new therapeutic concepts include locally applied methylene blue for treatment of basal carcinoma, Kaposi's sarcoma, melanoma, viral and fungal infections, and subsequent radiation with a light source in the red spectrum region (600-750 nm). When, methylene was delivered intravenously, it was found to be reduced and excreted far more rapidly than when topically applied (Tardivo *et al.*, 2005). Therefore, although methylene blue may be useful in photodynamic therapy, with low toxicity and minimal side-effects, it has a limited therapeutic spectrum and as such is not ideal for *P. falciparum* infections.

2.6.2 Antimalarial activity of natural colourants

All the natural colourants, except for curcumin and carbon black, were inactive and showed *in vitro* parasite growth inhibition below 20% at a screening concentration of a 100 $\mu\text{g/ml}$ (Table 2.2). Curcumin (diferuloylmethane) was highly active, whilst carbon black showed moderate

activity against *P. falciparum*, but were both significantly less potent ($p < 0.05$) compared to quinine (Figure 2.7). Curcumin was however, significantly more potent ($p < 0.05$) than carbon black. The findings of the current study (Table 2.15) confirmed the antimalarial potency of curcumin (IC_{50} : $2.29 \pm 0.18 \mu\text{g/ml}$), although significantly more potent ($p < 0.05$) than previously reported to be in the range of 7-11 $\mu\text{g/ml}$ against both chloroquine-sensitive (IC_{50} : $\sim 9.1 \mu\text{g/ml}$ against the 3D7 strain) and resistant strains (Cui *et al.*, 2007).

Table 2.15 Summary table showing antimalarial, haemolytic activity and β -haematin formation inhibition IC_{50} values of the most active natural compounds.

Compound	Antimalarial activity $IC_{50} \pm \text{S.D.} (\mu\text{g/ml})$	Haemolytic activity $HLC_{50} \pm \text{S.D.} (\mu\text{g/ml})$	β -Haematin inhibition $IC_{50} \pm \text{S.D.} (\mu\text{g/ml})$
Curcumin	2.29 ± 0.18	$>100 (6.24 \pm 0.18\%)$	320 ± 0.01
Carbon black	22.73 ± 2.36	$>100 (0.22 \pm 0.04\%)$	$>1:4 (40.47 \pm 0.83\%)$
Quinine	0.04 ± 0.01	$>100 (0.41 \pm 0.01\%)$	24.65 ± 1.28
Chloroquine	0.01 ± 0.01	$>100 (0.02 \pm 0.01\%)$	19.6 ± 2.46

Haemolytic activity of test compounds that demonstrated HLC_{50} values $> 100 \mu\text{M}$, and β -haematin formation inhibition IC_{50} values above $800 \mu\text{M}$ (or $> 4 \text{ mg/ml}$) were reported as percentage (%) values.

Curcumin showed slight haemolytic activity although significantly higher compared to quinine (Table 2.15). This may be of minor clinical significance since at least three different Phase I clinical trials involving mice and humans have indicated curcumin's safety and tolerance at maximum doses of 12 g per day (Anand *et al.*, 2007). Peak plasma concentration (C_{max}) of curcumin has been detected at 300 ng/ml in rats, after oral administration (100 mg/kg) (Liu *et al.*, 2006). Whereas in human subjects, the C_{max} value was $2.30 \pm 0.26 \mu\text{g/ml}$ after a single oral dose of 10 g curcumin (Vareed *et al.*, 2008). Of the two natural colourants, only curcumin inhibited β -haematin formation significantly ($p < 0.05$) compared to quinine (Table 2.15). Curcumin interfered with the differential staining of the RBC and the parasite; as such observations could not be made for the morphology and stage sensitivity studies. The excessive staining or high affinity of curcumin to the infected RBC indicated probable, targeted antimalarial activity. In the treatment of malaria, combination therapy is essential in preventing treatment failure and drug resistance (WHO, 2012). In the current study, both curcumin and carbon black showed an additive interaction with quinine (Figure 2.10b). Similarly, in a study by Nandakumar *et al.* (2006), the combination of curcumin and quinine showed an additive *in vitro* effect on *P. falciparum* (FCK strain) parasites. In the same study, an additive *in vivo* interaction was observed when a combination of curcumin (three day oral regimen of 5mg) and artemisinin was administered to *P. berghei*-infected mice (Nandakumar *et al.*, 2006). Although there is no resistance data that has been reported for curcumin, a

clinical and parasitological failure of quinine mono-treatment associated with IC₅₀ values up to 0.4 µg/ml against isolates originating from South America has been reported (Bertaux *et al.*, 2011). The resistance cut-off values for quinine are IC₅₀ values greater than 0.3 µg/ml (Bertaux *et al.*, 2011). Therefore, curcumin used in combination with classical antimalarial drugs has the potential of delaying the onset of resistance of these drugs and of possibly increasing the susceptibility of the parasites. For instance, a single dose of artemether (750 µg) in combination with curcumin (5 mg) has been shown to give complete protection in *P. berghei*-infected mice (Nandakumar *et al.*, 2006).

Although curcumin has been found to have a low bioavailability and rapid clearance rate in humans, a low dose of piperine from pepper can substantially enhance curcumin uptake in humans and the combination is well tolerated (Nandakumar *et al.*, 2006). In addition a polyethylene glycol or PEGylated liposome formulation loaded with a molar ratio of 0.6:1 (artemisinin to curcumin), showed a higher efficacy (60% parasitaemia reduction) in *P. berghei*-infected mice in just three days compared to 80% reduction in parasitaemia over 7 days with free artemisinin alone (Isacchi *et al.*, 2012). This increased efficacy of artemisinin and curcumin combination in the latter study may be attributed to increased bioavailability of both drugs. A combination study by Nandakumar *et al.* (2006) has demonstrated an additive interaction between free artemisinin and curcumin against *P. berghei*. Despite its pharmacokinetic properties, curcumin shows potential as a template for new antimalarial agents and warrants further research.

2.6.2.1 Physicochemical properties of natural colourants

Curcumin (pK_{a1} = 10.51; pK_{a2} = 9.88; pK_{a3} = 10.5), a polyprotic acid as determined by Bernabé-Pineda *et al.* (2004), showed drug-like properties and complied with the Lipinski's Ro5 (Table 2.12). At pH 7.4 curcumin showed a low degree of ionisation (0.1%) and was non-ionised at pH 5.0 (Table 2.13). This suggests that curcumin would be absorbed across the pH gradient with a low degree of ionisation of accumulation especially at the acid pH 5.0. However, poor bioavailability due to poor absorption, rapid metabolism, rapid elimination and a half-life of 1-2 h, has been a major drawback in the approval of curcumin as a therapeutic agent (Anand *et al.*, 2007; Isacchi *et al.*, 2012). The physicochemical properties of carbon black were not determined.

2.6.2.2 Pharmacological effects of curcumin

Curcumin (diferuloylmethane), a natural polyphenolic compound, has demonstrated diverse pharmacological properties including anti-inflammatory, anti-carcinogenic, anti-bacterial and

anti-protozoal activities (Cui *et al.*, 2007). Curcumin demonstrates both anti-oxidant and pro-oxidant activities which are concentration-dependent (Cui *et al.*, 2007). Its cytotoxicity on various cancer cell lines is attributed to its pro-oxidant activity through the generation of reactive oxygen species (ROS). The generation of ROS as well as the inhibition of acetylation of chromosomal proteins, histones, have been proposed as possible mechanisms of action of curcumin (Cui *et al.*, 2007; Croken *et al.*, 2012). Notwithstanding that curcumin has multiple therapeutic effects, in addition has a variety of protein targets and inhibits the activity of various kinases (Goel *et al.*, 2008).

2.6.2.2.1 Oxidative damage through increased reactive oxygen species

According to Cui *et al.*, (2007), at low concentrations (< 1 μM), curcumin appears to reduce intracellular ROS levels, whereas at higher concentrations (> 20 μM), it promoted intracellular ROS in a concentration-dependent manner. In the latter study, incubation of *P. falciparum* parasites with a combination of curcumin (50 μM) and the anti-oxidants, mannitol (at a 1:6 to 8 curcumin to mannitol concentration ratio) or 1 mM ascorbic acid, significantly reduced ROS levels and restored parasite growth almost to the parasitaemia of untreated controls (Cui *et al.*, 2007). The nucleic and mitochondrial DNA damage observed in the same study may be attributed to the generation of ROS by curcumin. As such, the latter results and the reported antimalarial activity suggest that ROS generation plays a key role in killing malaria parasites (Cui *et al.*, 2007). Curcumin as an anti-oxidant, has the potential to interfere with the inhibitory effects of macrophage-induced nitric oxide *in vivo* and thus exacerbate the malaria infection (Cui *et al.*, 2007). Therefore, curcumin's concentration levels may have to be optimally adjusted in order to favour its pro-oxidant activity.

2.6.2.2.2 Inhibition of histone acetylation and histone acetyltransferase activity

The inhibitory effects of curcumin on the activity of histone acetyltransferases (HATs), may partially account for its antimalarial activity (Cui *et al.*, 2007). In eukaryotic cells, genomic DNA is packaged into chromatin (Alberts *et al.*, 2004). Chromatin is a complex of DNA and chromosomal proteins, predominantly histones, which condenses into mitotic chromosomes (Alberts *et al.*, 2004). The DNA is wrapped around the histone proteins in a "bead on a string" pattern, forming nucleosomes (Figure 2.16); the basic units of the chromatin fibre (Alberts *et al.*, 2004). The nucleosome consists of about 150 base pairs of DNA wound twice around an octameric histone core (Croken *et al.*, 2012). The nucleosome 'bead' consists of two copies of histones H2A, H2B, H3 and H4 (Cui *et al.*, 2007). The nucleosomes are packed tightly by H1-H1 histone protein interaction. Chromatin exists in a condensed form with transcription silencing and in an expanded form associated with active gene transcription (Goodman, 1998;

Miao *et al.*, 2006). However, histone acetylation (Figure 2.16), which is catalysed by HATs, alters the chromatin structure, exposing DNA sequences to allow for gene expression, DNA replication or repair (Alberts *et al.*, 2004; Cui *et al.*, 2007). The latter process is reversed by histone deacetylases or HDACs (Cui *et al.*, 2007).

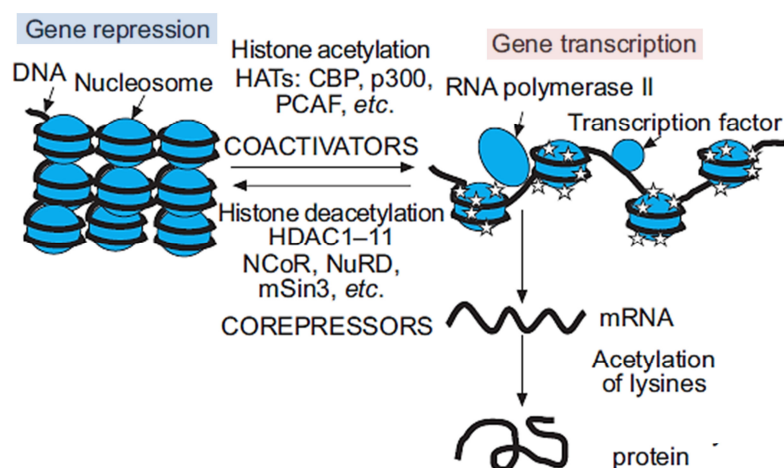


Figure 2.16 Regulation of gene activation and repression by acetylation of histones (adapted from Barnes *et al.*, 2005). Histone acetylation is mediated by co-activators that have intrinsic histone acetyltransferase (HAT) activity. Acetylation of histones opens the chromatin structure exposing the DNA strands, thus allowing binding of RNA polymerase II and transcription factors. The latter process is reversed by co-repressors, which include histone deacetylases (HDACs) that reverse acetylation and causing gene silencing or repression. CBP, CREB-binding protein; PCAF, p300/CBP-associated factor; NCoR, nuclear receptor co-repressor (Barnes *et al.*, 2005).

Similarly, malaria parasites have a typical chromatin structure, which plays a key role in epigenetic (“heritable changes that alter gene expression levels”) regulation of gene expression (Cui *et al.*, 2007; Croken *et al.*, 2012). Cui *et al.* (2007) previously demonstrated that curcumin (25-100 μM) has the ability to reduce nuclear HAT activity of the parasite *in vitro*, as well as to inhibit the HAT activity of the recombinant *P. falciparum* general control non-depressed 5 (*PfGCN5*) histone acetyltransferase (IC_{50} : $\sim 48 \mu\text{M}$). In addition, curcumin has demonstrated specific inhibition of the HAT p300/CREB-binding protein and related transcriptional activity (Balasubramanyam *et al.*, 2004). Thus, *P. falciparum* HATs are plausible targets for curcumin (Cui *et al.*, 2007).

2.6.3 Antimalarial activity of nucleoside and analogues

The most active nucleoside analogues, JLP118.1 (IC_{50} : $1.79 \pm 0.12 \mu\text{M}$) and JLP093 (IC_{50} : $2.38 \pm 0.11 \mu\text{M}$), demonstrated antimalarial activity within the micromolar range, but were significantly less potent ($p < 0.05$) than quinine (Table 2.15). The overall antimalarial activity of the most active nucleoside analogues was classified as highly active ($\leq 5 \mu\text{M}$). Of all the

nucleoside analogues tested, only the pyrimidine-based nucleoside analogues, JLP118.1 and JLP093 were highly active against *P. falciparum*. Both compounds showed negligible toxicity to human RBCs and showed no ability to inhibit β -haematin crystal formation as a possible mechanism of action (Table 2.15). The trophozoite stage was particularly sensitive to nucleoside analogue, JLP118.1 as the parasite did not proceed to the schizont stage (Figure 2.11d).

2.6.3.1 Physicochemical properties of nucleoside analogues

JLP118.1 (MW: 630.64 g/mol) a pyrimidine-based analogue, was the bulkiest compound and violated three of the Lipinski's Ro5 parameters (MW > 500, HBA > 10 and log P > 5), compared to all the other most active compounds (Table 2.12), yet it demonstrated the most potent antimalarial activity in its class. Overall, the absorption rate of both the nucleoside analogues was more than 95% at basic pH 7.4 in their un-ionised state. JLP093 showed some significant ($p < 0.05$) ionisation (13.7%) at an acidic pH 5.0, compared to JLP118.1 (Table 2.13). This suggests that the activity of this class of compounds was not due to their acid-base properties, except for JLP093 which could possibly over time accumulate within the digestive vacuole's acidic environment based on the "ion-trapping" effect described earlier by Shore *et al.* (1957). However, nucleosides must first be phosphorylated within the parasite to their respective nucleotides in order to be pharmacologically active (Gero *et al.*, 2003). In addition, nucleotides are anionic compounds which are unable to translocate cell membranes, whereas nucleosides and some analogues are neutral molecules that can cross through cellular membranes (Gero *et al.*, 2003). Indeed, the *P. falciparum* equilibrative nucleoside transporter (*PfENT1*) has been found to facilitate the uptake of both purine and pyrimidine nucleosides and nucleobases (Baldwin *et al.*, 2007). When compared to natural nucleosides that are transported into cells, nucleoside analogues are often modified to enable passive diffusion or a combination of passive diffusion and facilitated transport via nucleoside transporters (Li *et al.*, 2008).

Structurally, JLP118.1 was the only uracil-derived analogue tested with a combination of the tert-butyl-dithiomethyl-hydroxyl group and the modified ribose structure containing acetaldehyde groups. Whilst JLP093 was the only cytosine-derived analogue with the tert-butyl-diphenylsilyl group and un-modified ribose structure in the nucleoside analogue series (Table 2.10).

Table 2.16 Summary of antimalarial, haemolytic and β -haematin formation inhibitory activity of the most active nucleoside analogues.

Compound	Antimalarial activity IC ₅₀ \pm S.D. (μ M)	Haemolytic activity HLC ₅₀ \pm S.D. (μ M)	β -Haematin inhibition IC ₅₀ \pm S.D. (μ M)
JLP118.1	1.79 \pm 0.12	>100 (0.92 \pm 0.04%)	>800 (0.01 \pm 0.02%)
JLP093	2.38 \pm 0.11	>100 (0.35 \pm 0.05%)	>800 (5.8 \pm 3.35%)
Quinine	0.10 \pm 0.01	>100 (0.15 \pm 0.01%)	68.3 \pm 4.17
Chloroquine	0.01 \pm 0.00	>100 (0.01 \pm 0.01%)	38.4 \pm 4.77

Haemolytic activity of test compounds that demonstrated HLC₅₀ values > 100 μ M, and β -haematin formation inhibition IC₅₀ values above 800 μ M (or > 4 mg/ml) were reported as percentage (%) values.

2.6.3.2 Pharmacological effects of nucleoside analogues

Unlike purines that are in abundance in human RBCs, pyrimidines exist in small concentrations (Cassera *et al.*, 2011). As a result *P. falciparum* has retained its capacity for *de novo* synthesis of pyrimidines and developed pathways for the salvage of purines from the host RBC, but lacks pyrimidine salvage enzymes (Reyes *et al.*, 1982; Cassera *et al.*, 2011). In the current study, pyrimidine-based analogues, JLP118.1 and JLP093 demonstrated comparable activity to the purine nucleoside, inosine. In addition, the trophozoite stage was particularly sensitive to JLP118.1 since the parasite did not proceed to the schizont stage. DNA synthesis in synchronised *P. falciparum* cultures has been found to peak mostly during the trophozoite stage, which has been compared to the S-phase of the cell cycle in mammalian cells (Figure 1.3), 28-31 h after merozoite invasion and the DNA content increases for 8-10 h (Arnot and Gull, 1998; Downie *et al.*, 2008; Arnot *et al.*, 2011).

Therefore the pyrimidine nucleoside analogues, JLP118.1 and JLP093, may have interfered with the nucleic acid synthesis during the trophozoite stage. Although PfENT1, facilitates the transport of both purine and pyrimidine nucleosides and nucleobases, the uptake of pyrimidines into the RBCs does not benefit the parasites as they lack *de novo* pyrimidine salvage pathways (Baldwin *et al.*, 2007). However, PfENT1 does provide a route for the uptake of cytotoxic pyrimidine drugs such as 5-fluoroorotate, which inhibits the *de novo* pyrimidine synthesis pathway of *P. falciparum* directly (Baldwin *et al.*, 2007). In contrast, earlier studies have shown that parasites in *P. knowlesi*-infected monkeys, failed to incorporate ¹⁴C-labelled exogenous pyrimidines (thymine, thymidine, uracil and uridine) into their nucleic acids (Downie *et al.*, 2008). Natural inosine, one of the purines salvaged from the host RBC, is a direct precursor of hypoxanthine (Cassera *et al.*, 2011). Nevertheless, the morphology and stage sensitivity studies, confirmed the inhibitory effects of the JLP118.1

pyrimidine-based nucleoside analogue as demonstrated in the [³H]-hypoxanthine incorporation assay (Figure 2.11, Table 2.16).

2.6.4 Antimalarial activity of imidazopyridine analogues

IP-2 to IP-4 of the imidazopyridines analogue series chemical structures contained a cyclohexane ring and the other half of the series, IP-5 to IP-8 contained a 1,3-dimethylbenzene ring (Table 2.11). The most active imidazopyridine analogues (Figure 2.9), IP-3 (IC₅₀: 20.77 ± 0.72 μM) and IP-4 (IC₅₀: 15.30 ± 0.41 μM), that contained the cyclohexane ring, were generally more potent than IP-5, -6 and -7, that contained the 1,3-dimethylbenzene ring, but all were about 200 to 300-fold less potent than quinine (IC₅₀: 0.10 ± 0.01 μM). The most active imidazopyridines showed low (50-100 μM) to moderate (10-50 μM) antimalarial activity and were significantly (*p* < 0.05) less potent compared to quinine. The parasite morphology and stage sensitivity studies, suggest sensitivity of the trophozoite stage to IP-4 as they degenerated after the initial 24 h period and failed to proceed to the subsequent schizont stage (Figure 2.11e). These compounds were however not tested for haemolytic activity and β-haematin formation inhibition in the study due to limited stock. Therefore it was not apparent whether parasite death was related to any of these aforementioned mechanisms.

2.6.4.1 Physicochemical properties of imidazopyridine analogues

Of the most active imidazopyridine analogues only 2 and 1 violations of the Lipinski's Ro5 principles were noted for IP-3 and IP-6, respectively. The MWs of the imidazopyridine analogue were greater than 500 g/mol, except for IP-4 and IP-5 which were below 400 g/mol. So the Ro5 violations were mostly on the MWs and the log P values that were greater than 5. However, no correlation pattern was observed between the Ro5 number of violations and antimalarial activity; although IP-4, the most active of the class complied with Lipinski's drug-likeness, Ro5 criteria.

2.6.4.2 Pharmacological effects of imidazopyridines

The antimalarial activity of the imidazopyridines may be associated with the inhibition of CDKs. A high-throughput screen of the AstraZeneca compound library identified a series of imidazo[1,2-a]pyridines as a class of potent inhibitors of cyclin-dependent kinase CDK4 with the lead analogue demonstrating an IC₅₀ value of 8 μM (Anderson *et al.*, 2003; Enguehard-Gueiffier and Gueiffier, 2007). In the latter study, the binding mode of these compounds by X-ray crystallography of the compound complex with CDK2, led to the synthesis of 100-fold more potent compounds against CDK2 (Anderson *et al.*, 2003). The various chemical structures tested against *P. falciparum* demonstrated varying degrees of activity, but were all

relatively non-toxic to RBCs except for mercury orange. Curcumin acted by inhibiting β -haematin crystal formation. The most active compounds could be used as templates for new antimalarial agents and further derivatisation.

Chapter 3 Mammalian cell toxicity

3.1 Introduction

Toxicology is concerned with the deleterious effects of chemical agents on all living systems. In humans, adverse effects resulting from exposure to drugs, their safety or potential toxicity associated with their use is of critical importance (Plaa, 2005). *In vitro* cytotoxicity assays allow for rapid evaluation of potential toxicity of large numbers of test compounds on cell lines, reducing the need for animal experimentation, during the initial stages of drug development (Ekwall *et al.*, 1990). For instance, the tritiated ($[^3\text{H}]$)-thymidine incorporation assay in particular, measures cell growth from the amount of $[^3\text{H}]$ -thymidine incorporated into dividing cells (Wagner *et al.*, 1999). The toxic potential of any substance, be it natural or chemically synthesised, always remains a concern. The adverse effect profile and efficacy of all drugs are known and constantly updated (WHO, 2008). The potentiation of these adverse effects as concentrations or dosages reach toxic levels, are documented as well. The potential toxic properties of compounds or drugs administered to humans are constantly monitored by the WHO and country regulatory bodies such as the Food and Drug Administration (USA) and the Medicines Control Council (South Africa) through pharmacovigilance (WHO, 2008; National Department of Health, 2013). The safety margin or therapeutic index of administered drugs is based on the ratio between the therapeutic dose and the toxic dose (Muller and Milton, 2012).

3.1.1 Selectivity index and *in vitro* toxicology

In drug development, the selectivity index, which is the ratio between *in vitro* efficacy (IC_{50}) and *in vitro* cytotoxicity is used as an early indicator of the toxicity of the test compounds (Muller and Milton, 2012; Najahi *et al.*, 2013). It is conceded that the extent of efficacy and safety data only increases as a candidate compound progresses from *in vitro*, to animal and then to human studies (Muller and Milton, 2012). *In vivo* rodent malaria models are an ideal starting point for elucidation of toxicology, pharmacokinetic and pharmacodynamic data during antimalarial drug discovery (Fidock *et al.*, 2004). In addition, *in vitro* toxicology assays often make use of mammalian cancer cell lines and not naturally dividing cells (Pink *et al.*, 2005). However, there has been consideration for a transition from animal screens to more *in vitro* systems and predictive toxicology methods within the 21st century (National Toxicology Program, 2004). The vision of the National Toxicology Program and the FDA (U.S.A.) is to strive to address the “3Rs” effectively that include: the reduction of the number of animals used in research programs, refining the end-points to derive the maximum amount

of information with minimum amount of pain and suffering, and replacement of species currently used with lower species or *in vitro* systems (National Toxicology Program, 2004). Therefore *in vitro* cytotoxicity assays with their limitations, do however provide a high-throughput screening method to determine selectivity of candidate compounds for *P. falciparum* parasites (Fidock *et al.*, 2004; Pink *et al.*, 2005; Muller and Milton, 2012). For pure compounds, biological efficacy must have a selectivity index of at least 10 or more (Pink *et al.*, 2005). Whereas for crude plants extracts it is more difficult to establish the selectivity index value, especially if the specific concentration and identity of the active ingredient is unknown and the extract may contain other constituents that contribute to the cytotoxicity (Valdés *et al.*, 2008). The attrition rate of new compounds in pre-clinical and clinical phases of drug development is largely due to poor efficacy and/or toxicity (McKim, 2010). Therefore, it was critical to test the compounds for potential toxicity in the current study.

3.2 Objectives

- To evaluate the *in vitro* cytotoxicity of the test compounds with the most antimalarial activity against the transformed human embryonic kidney epithelial (HEK293 cells, ATCC CRL11268) and the human chronic myelogenous leukaemic (K562 cells, ATCC CCL243) cell lines.
- Determine the selectivity index of the most active test compounds for *P. falciparum* and their effect on the HEK293 and K562 human cell lines.

3.3 Methods

3.3.1 Cell lines

The K562 human cancer cell line (Highveld Biological) was established in 1970 from a pleural effusion of a 53-year old patient with chronic myelogenous leukaemia in blastic crisis (Lozzio and Lozzio, 1979). This suspension cell line is of erythroleukaemia type and is characterised as a highly undifferentiated cell resembling granulocytes and erythrocytes (Lozzio and Lozzio, 1979). The monolayer HEK293 cell line (Highveld Biological), was immortalised and derived from the transformation of primary cultures of human embryonic kidney (HEK293) cells by exposing cells to sheared fragments of adenovirus type 5 DNA (Graham *et al.*, 1977; Shaw *et al.*, 2002).

3.3.2 Preparation of culture medium

Sterile-filtered Dulbecco's Modified Eagle's Medium (DMEM) and RPMI-1640 growth media were used to maintain the HEK293 and K562 cells in culture, respectively. DMEM (500 ml; Sigma-Aldrich) was supplemented with 4.5 g/L glucose, 110 mg/L sodium pyruvate

and 0.584 g/L L-glutamine. RPMI-1640 (Sigma-Aldrich) was supplemented with 4.5 g/L glucose, 0.3 g/L L-glutamine and 2 g/L NaHCO₃. The growth media was completed by adding 5% (v/v) heat-inactivated (56°C for 1 h) foetal calf serum (Sigma-Aldrich), antibiotics: 0.1% (v/v) penicillin (5000 units/100 ml) and streptomycin (5 mg/100 ml) (Sigma-Aldrich). Complete experimental medium was supplemented with 5% (v/v) heat-inactivated foetal calf serum, but excluded antibiotics to prevent any interaction with the test compounds; whilst the incomplete experimental medium (for serial dilutions of test compounds) excluded both the foetal calf serum and antibiotics.

3.3.3 Preparation of test compounds and control drugs

Stock solutions of the natural (10 mg/ml) and synthetic (10 mM) test compounds, the reference drugs, quinine (Sigma-Aldrich) and camptothecin (Sigma-Aldrich) were prepared in 100% (v/v) DMSO (Sigma-Aldrich). Appropriate serial dilutions of test compounds were prepared using incomplete experimental medium. The final % DMSO used in the experiments did not exceed 1% such as to minimise an inhibitory effect on the cell viability.

3.3.4 General cell culture maintenance

The cell lines were aseptically maintained in culture according to cell culture methods described by Freshney (1988). A waiver was obtained from the Human Research Ethics Committee for use of both cell lines in *in vitro* studies (Ethical clearance waiver reference number: W-CJ-090425-12; Appendix B3). Culture maintenance was carried out in a Class II biosafety laminar flow hood. The cultures were incubated at 37°C in a humidified incubator (Heraeus Cell) with an atmosphere containing 5% CO₂, to maintain the pH (7.44) of the culture (Wagner *et al.*, 1999). Sub-culturing of both cell cultures was carried out every 2-3 days when cells reached confluency and the culture flasks returned to the incubator. The cell cultures within the flasks were examined for confluency and morphology using an inverted phase contrast microscope (Olympus-CK2) at 200 x magnification. Based on this observation the cultures were either prepared for re-seeding of the culture or for experimentation.

3.3.5 Sub-culturing of HEK293 monolayer cells

The adherent, monolayer HEK293 cells were re-suspended by treatment with trypsin (Freshney, 1988). Spent culture media was discarded and the adherent cells washed twice with 2 ml pre-warmed (37°C) PBS (pH 7.4). Pre-warmed, 2 ml 0.25% trypsin/0.1% versene ethylene diamine-tetracetic acid (EDTA, Sigma-Aldrich) was added to the culture flask and incubated at 37°C for 3-5 minutes or until the adherent cells detached from the flask surface. Thereafter, 4 ml complete DMEM culture medium was added in order to neutralise the

proteolytic activity of trypsin. The cell suspension was centrifuged at 834 x g for 5 min, the supernatant aspirated and the cell pellet resuspended in fresh complete culture medium.

3.3.6 Sub-culturing of K562 suspension cells

The K562 cells grown in suspension were centrifuged at 834 x g for 5 min. Thereafter, 90% (v/v) spent culture medium was aspirated, leaving 10% v/v to retain sufficient growth factors and the remaining cell pellet was re-suspended with fresh pre-warmed complete culture medium.

3.3.7 Determination of cell number

Cells were counted with a Neubauer haemocytometer and cell viability was determined using the trypan blue exclusion assay (Freshney, 1988; Strober, 2001). According to the method described by Freshney (1988), viable cells with intact membranes do not stain blue with trypan blue, whilst dead cells take up the dye and stain blue as observed under a light microscope. Briefly, cultures were transferred into a 50 ml centrifuge tube, centrifuged at 834 x g for 5 min and re-suspended in 20 ml complete experimental medium. A 20 µl sample of cell suspension was transferred to a microcentrifuge tube and stained in a 1:1 volume ratio with 20 µl, 0.2% (v/v) trypan blue prepared in PBS (pH 7.4) (Section 2.3.5). The cell suspension was transferred into the haemocytometer and covered with a coverslip. Unstained viable cells within the central grid were counted and the mean cell count from the two chambers was used to determine the number of cells per volume (ml) (Equation 3.1).

$$\text{Cell density (cells/ml)} = (\text{Mean number of viable cells} \times 10^4) \times 2 \text{ dilution factor}$$

Equation 3.1 Cell density.

3.3.8 Tritiated thymidine incorporation assay

The inhibitory effect of the test compounds on the *in vitro* cell growth was determined using the [³H]-thymidine incorporation assay (Sondak *et al.*, 1984; Coward *et al.*, 1998). Based on the principle of the assay, live replicating cells incorporate [³H]-thymidine into their DNA and the percentage cell growth is determined by measuring the radioactivity from the precipitated [³H]-thymidine.

3.3.8.1 Seeding of cells

Cells were seeded into a 96-well microtitre plate at a density of 50,000 cells per well in 180 µl cell suspension prepared in complete experimental medium. All assays included untreated cells as a negative control containing 20 µl of PBS, along with quinine and camptothecin as

the reference drugs. Cells were exposed to serial dilutions (100 μM – 1.56 μM) of the compounds and incubated for 72 h at 37°C in a humidified incubator in 5% CO_2 atmosphere. The [^3H]-thymidine (20 Ci/mmol) isotope was added to a final concentration of 0.5 Ci/ml per well after 48 h incubation. The cells were incubated for a further 24 h to allow incorporation of the [^3H]-thymidine into the DNA of proliferating cells (Sondak *et al.*, 1984).

3.3.8.2 Cell harvesting

The cellular [^3H]-labelled DNA harvested onto WallacTM Betaplate glass fibre filter mats using a multichannel TitertekTM semi-automatic cell harvester. The isotope incorporated into the cellular DNA was measured using the WallacTM 1205 Betaplate scintillation counter (Perkin-Elmer) (Section 2.3.9.2). The scintillation counter results (cpm) were expressed as percentage cell growth compared to untreated control (Equation 3.2) and the concentration of the test compound causing a 50% cytotoxic effect (IC_{50}) was calculated from log sigmoid dose-response curves generated using Enzfitter[®] software.

$$\% \text{ Cell growth} = \frac{\text{mean cpm}_{\text{treated cells}}}{\text{mean cpm}_{\text{untreated control}}} \times 100$$

Equation 3.2 Percentage cell growth determination.

3.4 Data analysis

The IC_{50} values were determined from log sigmoid dose-response curves generated by the Enzfitter[®] software (version 1.05). The results are reported as the mean of at least 3 replicate experiments with standard deviation (mean \pm s.d.). Statistical difference between the activity (IC_{50} values) of the test compounds and the reference drugs was determined by a one-way ANOVA test, using GraphPad Prism[®] software, version 5.0 (Motulsky, 2003; Glantz, 2005). A p -value less than 0.05 ($p < 0.05$) was considered statistically significant. The anti-proliferative activity of the test compounds against both the HEK293 epithelial and K562 erythroleukaemic cell lines were compared using a two-way ANOVA test. A p -value less than 0.05 ($p < 0.05$) was considered statistically significant (Motulsky, 2003; Glantz, 2005).

3.5 Selectivity index

The selective activity of the most active compounds against the *P. falciparum* parasites compared to their cytotoxicity was determined by calculating the S.I. (Equation 3.3). Both synthetic and natural compounds with S.I. values of ≥ 10 were regarded as non-toxic (Pink *et al.*, 2005).

$$\text{Selectivity index} = \frac{\text{Cytotoxicity (IC}_{50})}{\text{Antimalarial activity (IC}_{50})}$$

Equation 3.3 Selectivity index for *P. falciparum* compared to human cancer cell lines.

3.6 Results

3.6.1 Cytotoxic effect of synthetic colourants

The cytotoxicity results of the synthetic colourants are depicted in Figure 3.1. HEK293 cells were more sensitive to all the test compounds compared to the K562 cells. The positive control, camptothecin, was potently inhibitory to the HEK293 cell line (IC₅₀: 16.75 ± 1.22 nM) than the K562 cell line (IC₅₀: 41.64 ± 2.34 nM). The reference drug, quinine was the least inhibitory against both cell lines compared to all the synthetic test compounds and more than 900-fold less active compared to camptothecin (Figure 3.1).

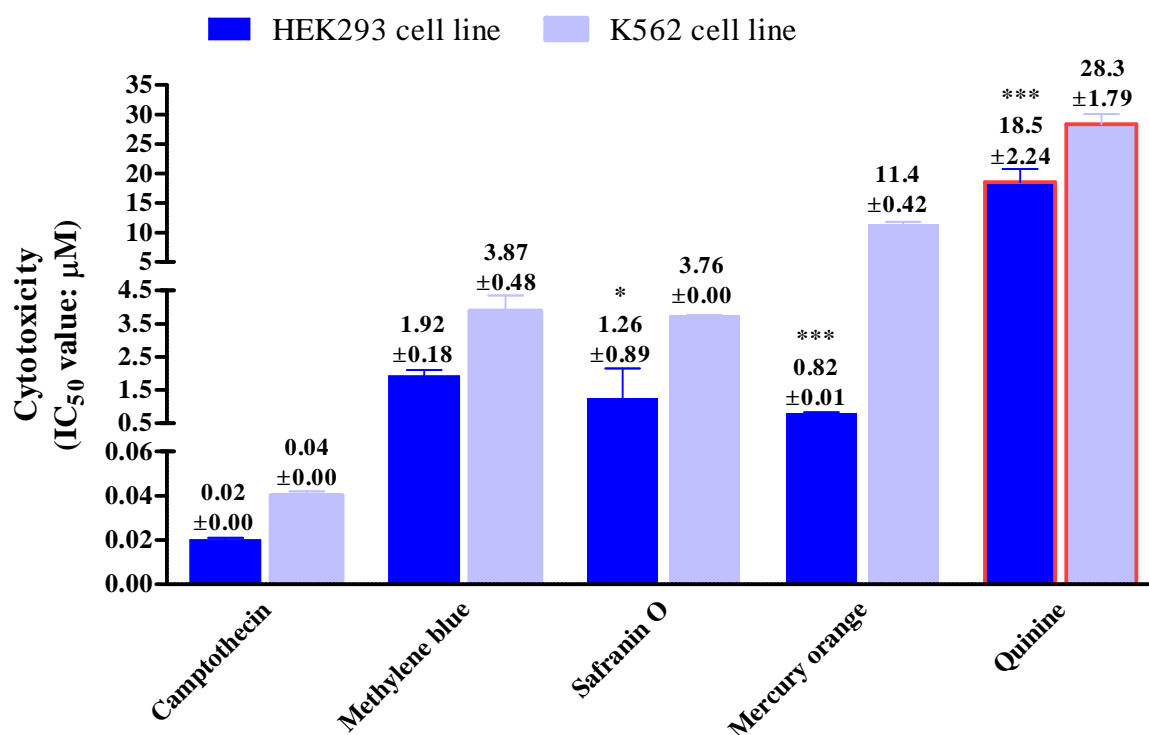


Figure 3.1 Cytotoxic effect of synthetic colourants on the HEK293 and K562 cell lines. IC₅₀ data was obtained using the [³H]-thymidine incorporation assay (n = 3). Two-way ANOVA test showed significant (*p* < 0.05, *; *p* < 0.001, ***) cell growth inhibitory activity against the HEK293 cell line compared to the K562 cell line.

Mercury orange (IC₅₀: 0.82 ± 0.01 μM) was the most potent test compound against the HEK293 cell line, whilst methylene blue (IC₅₀: 1.92 ± 0.02 μM) was the least effective. Safranin O (IC₅₀: 1.26 ± 0.2 μM) inhibited HEK293 cells significantly (*p* < 0.05) compared

to quinine, but was 63-fold less active than camptothecin. The cytotoxicity of mercury orange (IC_{50} : $0.82 \pm 0.00 \mu\text{M}$) on HEK293 cells was comparable to that of safranin O and methylene blue (Figure 3.1). The K562 cell line was generally less sensitive to all the test compounds. Methylene blue and safranin O showed comparable cytotoxicity against K562 cells and were both significantly ($p < 0.05$) potent compared to mercury orange. Quinine was more than 7-fold less active compared to methylene blue and safranin O, 2.5-fold less active compared to mercury orange against the K562 cells.

3.6.2 Cytotoxic effect of natural colourants

The cytotoxicity results of the natural compounds are depicted in Figure 3.2 and presented in mass molarity units ($\mu\text{g/ml}$) since all the most active natural colourants were in a liquid paste form when acquired. For comparative analysis, the IC_{50} values for quinine and camptothecin were converted to mass molarity. Camptothecin was equally, significantly ($p < 0.05$) more potent against both cell lines than curcumin, carbon black and quinine.

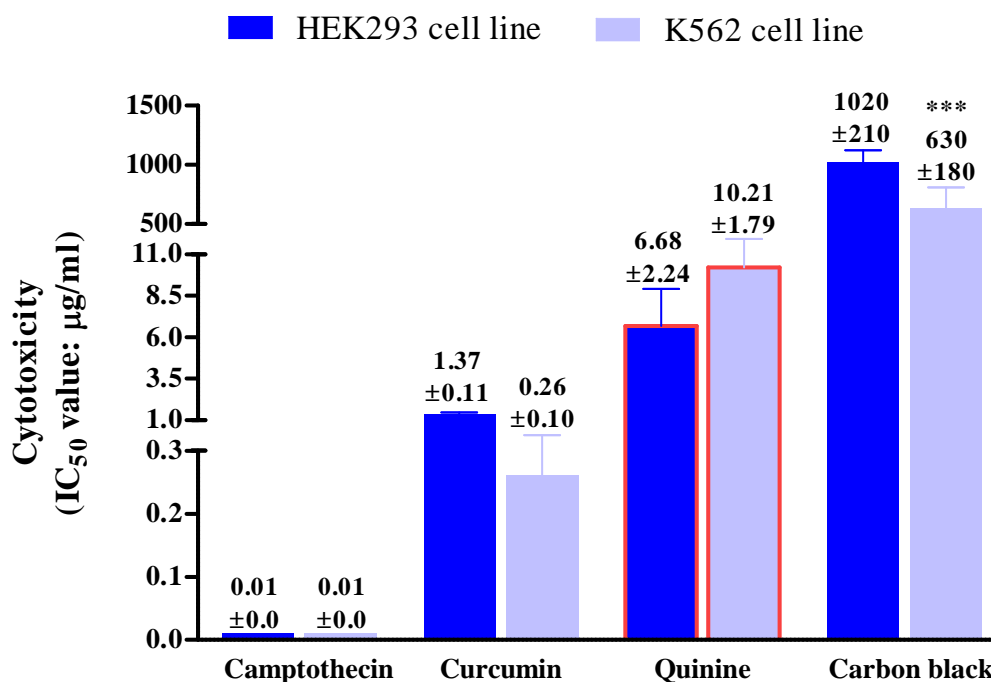


Figure 3.2 Cytotoxic effect of natural colourants on the HEK293 and K562 cell lines. IC_{50} values were obtained using the [^3H]-thymidine incorporation assay ($n = 3$). The two-way ANOVA test showed significant ($p < 0.001$, ***) differences in sensitivity of HEK293 and K562 cell line to carbon black.

Curcumin was highly cytotoxic (IC_{50} : $1.37 \pm 0.11 \mu\text{g/ml}$) and 745-fold more potent than carbon black and significantly ($p < 0.05$) more potent compared to quinine (IC_{50} : $6.68 \pm 2.24 \mu\text{g/ml}$) against the HEK293 cells. In comparison, curcumin was 137-fold less potent compared to camptothecin (IC_{50} : $5.84 \pm 0.28 \text{ ng/ml}$) against the HEK293 cells, whilst quinine

(IC₅₀: 6.68 ± 2.24 µg/ml) was 668-fold less active compared to camptothecin. There was a significant difference ($p < 0.001$) in the cytotoxic effect of carbon black between the two cell lines with K562 being the most sensitive at an IC₅₀ value of 630 ± 180 µg/ml. The cytotoxicity activity of curcumin against the K562 cell line was significantly ($p < 0.05$) more potent compared to quinine and carbon black, but 26-fold less active than camptothecin (IC₅₀: 14.51 ± 0.43 ng/ml).

3.6.3 Cytotoxicity of nucleoside and imidazopyridine analogues

The cytotoxic activity results of the nucleoside and imidazopyridine analogues are shown in Figure 3.3. The two-way ANOVA test showed that the HEK293 cells were significantly ($p < 0.001$) more sensitive specifically to JLP093, IP-4, IP-3 and IP-7 compared to the K562 cells (Figure 3.3).

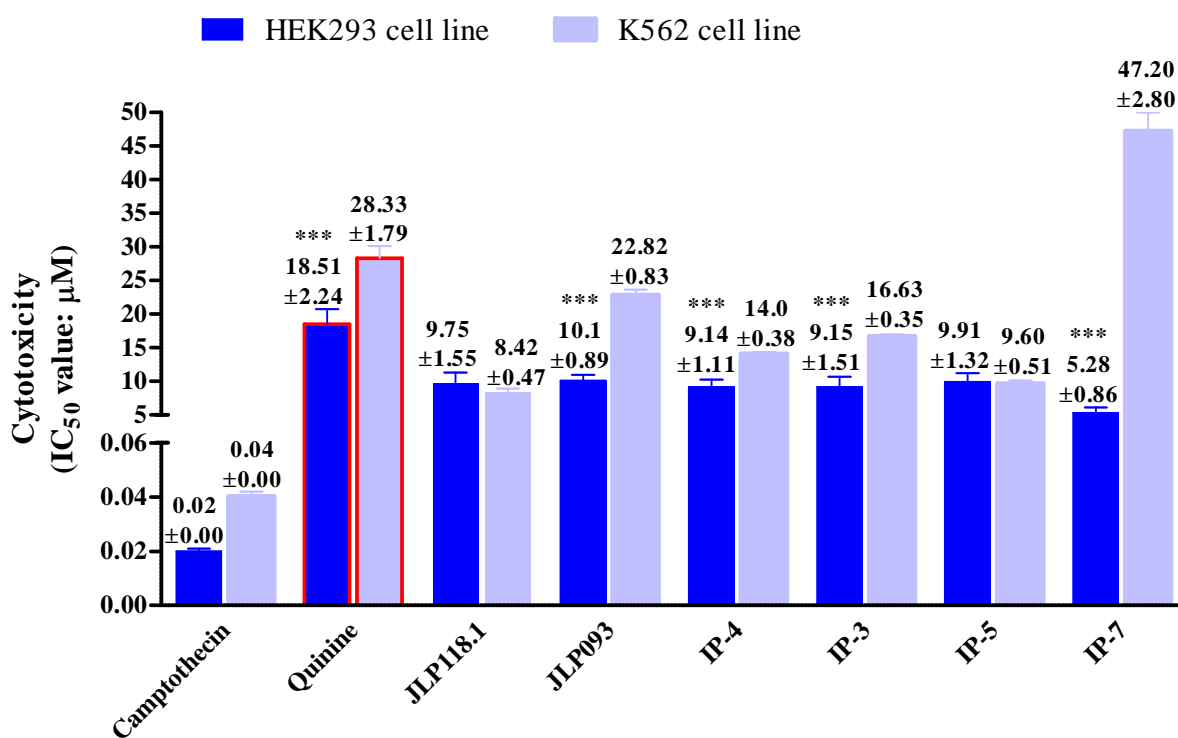


Figure 3.3 Cytotoxic effect of nucleoside and imidazopyridine analogues against the HEK293 and K562 cell lines. IC₅₀ values were obtained using the [³H]-thymidine incorporation assay (n = 3). The two-way ANOVA test showed significant ($p < 0.001$, ***) differences in sensitivity of the HEK293 and K562 cell line to specific compounds.

The cytotoxic effect of the nucleoside (JLP118.1, JLP093) and imidazopyridine analogues (IP-4, IP-3, IP-5) against the HEK293 cells was comparable at IC₅₀ values between 9-10 µM, except for IP-7 (IC₅₀: 5.28 ± 0.86 µM) which was most potent (Figure 3.3). The test compounds were all significantly ($p < 0.05$) more toxic to HEK293 cells compared to quinine

(IC_{50} : $18.51 \pm 2.24 \mu\text{M}$). IP-7 was 3.5-fold more potent compared to quinine, but 264-fold less active compared to camptothecin. The K562 cells showed the least sensitivity to IP-7 (IC_{50} : $47.20 \pm 2.80 \mu\text{M}$) compared to all the test compounds (Figure 3.3). The cytotoxic effect of JLP118.1 on K562 cells was comparable to that on the HEK293 cells, whilst JLP093 (IC_{50} : $22.82 \pm 0.83 \mu\text{M}$) was significantly less inhibitory to K562 cells compared to HEK293 cells. The K562 cells were significantly ($p < 0.05$) less sensitive to both IP-4 and IP-3 compared to HEK293 cells. IP-5 did not show any specific activity between the K562 and HEK293 cell lines and the IC_{50} values were comparable (Figure 3.3).

3.6.4 Selectivity indices of most active test compounds for *P. falciparum*

The selectivity of the most active compounds for *P. falciparum* compared to human cell lines (HEK293 and K562) is depicted in Figure 3.4.

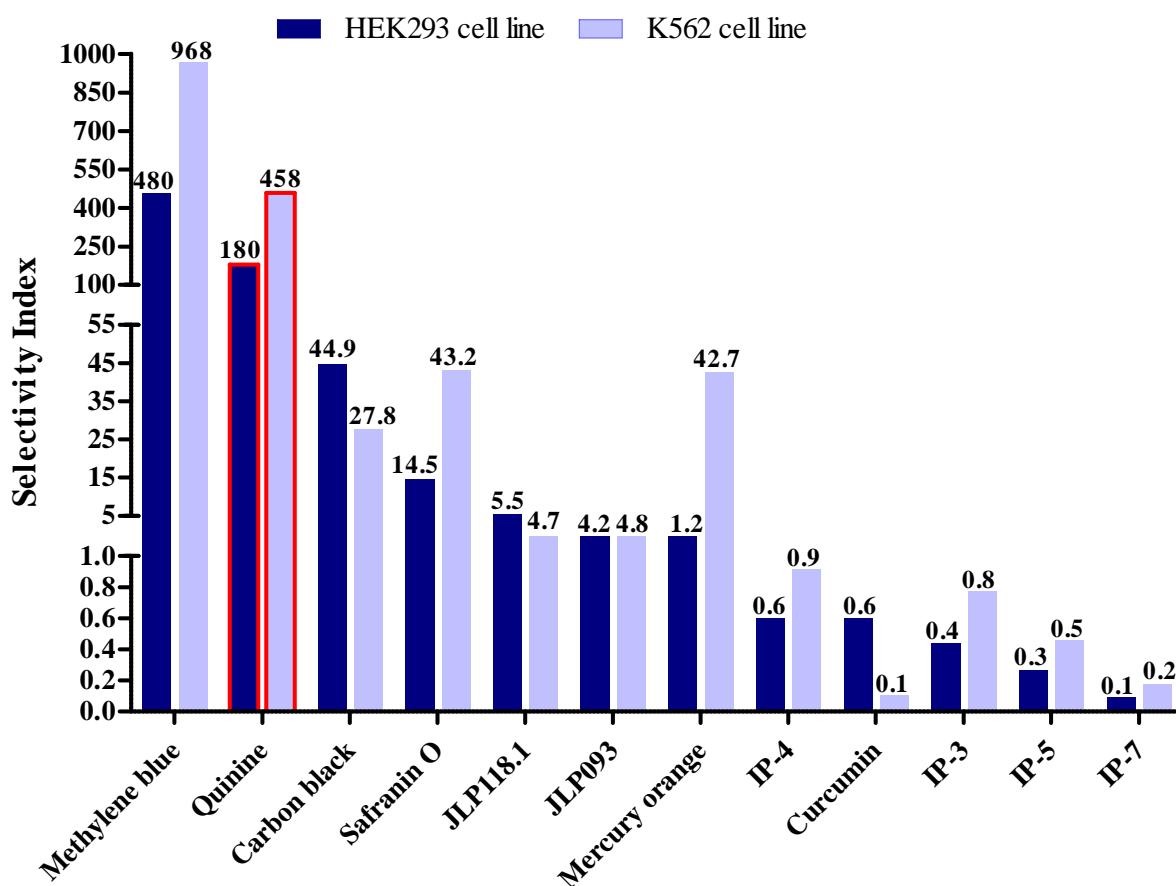


Figure 3.4 Selectivity indices of the most active compounds for *P. falciparum*. The S.I. was calculated by dividing the cell growth inhibitory IC_{50} values with the antimalarial IC_{50} values. Test compounds that showed S.I. values > 10 were regard as non-toxic or showing more selectivity for *P. falciparum* compared to the human HEK293 and K562 cell lines.

Test compounds with a selectivity index > 10 were regarded as more specific to *P. falciparum* or non-toxic to the human cell lines (Pink *et al.*, 2005). Methylene blue showed markedly high selectivity indices, for both the HEK293 (S.I.: 480) and K562 (S.I.: 968) cell lines compared to all the test compounds and the S.I. values were almost 2-fold higher than quinine (S.I.: 180 for HEK293 and S.I.: 458 for K562 cell lines). The imidazopyridine analogues showed the lowest selectivity indices (S.I. range: 0.1-0.9). The nucleoside analogues showed selectivity indices below 10 (S.I. range: 1.2-5.5) across both cell lines. The natural colourant, curcumin (S.I. range: 0.1-0.6) was poorly selective for *P. falciparum* compared to carbon black (S.I. range: 27.8-44.9), which was significantly ($p < 0.05$) less toxic to both cell lines. Overall, quinine showed a significantly ($p < 0.05$) high selectivity indices compared to all the test compounds with the exception of methylene blue which was more selective to *P. falciparum* compared to both cell lines.

3.7 Discussion

The selectivity indices of the active compounds were calculated by dividing the cytotoxicity IC_{50} value by the antimalarial IC_{50} value. The cut-off selectivity index was ≥ 10 , meaning that the cytotoxicity IC_{50} value had to be at least 10 times more than the antimalarial IC_{50} , in order for the compounds to be regarded selective for the *P. falciparum* parasite. The cytotoxicity of the active compounds was tested on transformed human kidney epithelial cells (HEK293) and the chronic myelogenous leukaemia cell line (K562).

3.7.1 Selectivity of synthetic colourants for *P. falciparum*

3.7.1.1 Methylene blue

Although methylene blue showed significant ($p < 0.05$) cytotoxic effect (Figure 3.1) on both the HEK293 and K562 cell lines compared to quinine, methylene blue was 25-fold more potent against *P. falciparum* parasites compared to quinine (Table 2.14). Methylene blue demonstrated the highest selectivity indices for *P. falciparum* (S.I.: 480, HEK293 cells; S.I.: 968, K562 cells) compared to all the test compounds and more than 2-fold selective compared to quinine. However, the chemotherapeutic agent, camptothecin (IC_{50} : $0.02 \pm 0.01 \mu\text{M}$, HEK293 cells; IC_{50} : $0.04 \pm 0.01 \mu\text{M}$, K562 cells) was significantly ($p < 0.05$) more potent than methylene blue (Figure 3.1). In a previous study, Vennerstrom *et al.* (1995) reported a cytotoxic effect of methylene blue (IC_{50} : $1.61 \mu\text{M}$) on the KB cell line using the sulforhodamine B assay (derived from the human epidermoid carcinoma of the mouth) comparable to the cytotoxic effect observed on HEK293 cells (IC_{50} : $1.92 \pm 0.2 \mu\text{M}$) in the current study.

The current study confirmed that methylene blue was selective for *P. falciparum*. In addition, methylene blue showed negligible haemolytic activity at a screening concentration of 100 μM (Table 2.5). Moreover, the spontaneous cycling of the oxidised and reduced methylene blue makes it an effective redox reagent for reducing cellular oxidative stress (Atamna and Kumar, 2010). The latter chemical property has been taken advantage of in the management of methaemoglobinaemia and for the prevention of ifosfamide-induced encephalopathy (Schirmer *et al.*, 2003; Atamna and Kumar, 2010).

An open-label randomised controlled Phase II study in children (aged 6-10 years) with uncomplicated malaria, demonstrated the efficacy of methylene blue in accelerating parasite clearance in artemisinin-based therapies, as well as its tolerability after oral administration of methylene blue with artesunate (20 mg/kg: 4 mg/kg drug ratio daily) or methylene blue with amodiaquine (20 mg/kg : 10 mg/kg drug ratio daily) over a three day period (Zoungrana *et al.*, 2008). After more than a century since the antimalarial activity of methylene blue was first described, there has been a renewed interest in methylene blue as an antimalarial agent. The chemical structure of methylene blue may also serve as a template for the development of newer, safer and cheaper drugs, which can also be used synergistically or additively in combination therapy with other antimalarial drugs such as artemisinin or quinine.

3.7.1.2 Safranin O

Compared to quinine, safranin O was 14.69-fold and 7.53-fold more toxic to HEK293 and K562 cells, respectively (Figure 3.1). Although, camptothecin was significantly ($p < 0.05$) more cytotoxic to both HEK293 and K562 cells lines than safranin O. Vennerstrom *et al.* (1995) previously reported comparable cytotoxicity activity (IC_{50} : 0.57 μM) for safranin O on KB epidermoid carcinoma cells, as compared to the cytotoxic effect on the HEK293 cells (IC_{50} : $1.26 \pm 0.89 \mu\text{M}$) (Figure 3.1). The selectivity indices for *P. falciparum* were > 10 but significantly ($p < 0.05$) less than quinine. Importantly, safranin O and other phenazinium dyes have been found to bind and intercalate DNA strands selectively at guanine-cytosine nucleotide sequences with a higher affinity compared to the adenine-thymine nucleotides sequences, thus causing DNA breakage (Saha *et al.*, 2010). In addition, replicating cells in the late S-phase or early G₂-phase of the cell cycle are most susceptible to DNA intercalators compared to non-replicating cells which are more resistant (Ralph *et al.*, 1983). In the current study safranin showed more toxicity to the transformed HEK293 epithelial cells than the K562 leukaemic cells, but less selective to *P. falciparum* when compared to quinine.

3.7.1.3 Mercury orange

Mercury orange was 22.57-fold more toxic to HEK293 cells and about 2.48-fold more toxic to K562 cells compared to quinine. Although in comparison to camptothecin, mercury orange was 41-fold and 285-fold less toxic to HEK293 and K562 cells, respectively (Figure 3.1). Nevertheless, mercury orange showed significantly ($p < 0.05$) low selectivity indices compared to quinine and demonstrated poor selectivity for *P. falciparum* based on the selectivity index of HEK293 cells (S.I.: 1.2). Mercury orange was the only compound that demonstrated marked haemolysis against uninfected human RBCs in the current study (Table 2.14). The K562 erythroleukaemic cell line has striking similarities to normal erythrocytes such as the cell surface glycoproteins, however mercury orange was about 13-times more toxic to the HEK293 cells than to the K562 cells (Andersson *et al.*, 1979). The cytotoxicity mechanism of mercury orange may well be attributed to its chloro-mercuri reactive group. Mercury containing compounds denature proteins by breaking di-sulphide bonds in proteins and inactivate glutathione by binding to thiols, thus reducing the protective role of glutathione within the epithelial cells against oxidative stress (O'Connor *et al.*, 1988; Byrns and Penning, 2011). Amongst other pathologies, acute exposure to mercury salts leads to tubular necrosis in kidneys, often resulting in renal failure (Byrns and Penning, 2011). Although mercury salts were once used in anti-septics, anti-diuretics, skin-lightening creams and laxatives, they have since been replaced with safer and more effective drugs (Byrns and Penning, 2011).

3.7.2 Selectivity of natural colourants for *P. falciparum*

3.7.2.1 Curcumin

Curcumin (diferuloylmethane), the active natural pigment of the rhizome of *Curcuma longa*, is well known for its diverse therapeutic actions including anti-inflammatory and anti-cancer properties (Bhaumik *et al.*, 1999; Goel *et al.*, 2008). Curcumin showed a significantly more potent ($p < 0.05$) cytotoxic effect (IC₅₀ range: 0.26-1.37 µg/ml) on both the HEK293 and K562 cell lines compared to quinine (IC₅₀ range: 6.7-10.2µg/ml) (Figure 3.2). Compared to camptothecin, curcumin was significantly ($p < 0.05$) less cytotoxic against both HEK293 and K562 cells lines, although curcumin showed a potent cytotoxic IC₅₀ < 1µg/ml against the K562 cells. The current study showed that curcumin was poorly selective (S.I.: 0.6 and 0.1, HEK293 and K562 cells, respectively) for *P. falciparum* and toxic to human cells (Figure 3.4). Curcumin has been found to have both anti-oxidant and pro-oxidant properties depending on its concentration (Cui *et al.*, 2007). For instance in *P. falciparum* parasites, curcumin was found to slightly reduce ROS levels at concentrations less than 1 µM and promoted ROS levels at higher concentrations. In addition, it has been suggested by Cui *et al.*

(2007) that *P. falciparum* parasites are more sensitive to curcumin than mammalian cells, since the induction of ROS has been found to be a major effector of curcumin in killing malaria parasites. The pro-apoptotic, anti-oxidant and anti-inflammatory characteristics of curcumin are however, implicated in its anticancer activity (Parsai *et al.*, 2014). For instance, *in vitro* studies by Parsai *et al.* (2014) have identified several enzymes such as: aldo-keto reductase family 1 member B10, serine/threonine-protein kinase, protein kinase C, matrix metalloproteinase, cyclooxygenase and epidermal growth factor receptor, to be involved in the initiation and progression of cancer as targets for curcumin.

Curcumin has been found to be safe in humans and tolerated at high doses. For instance, in a Phase I clinical trial involving 25 adults, up to 8 g/day was administered for three months to patients with pre-malignant lesions without any toxic side-effects (Chen *et al.*, 2001; Nandakumar *et al.*, 2006). The mean peak serum concentration was $1.77 \pm 1.87 \mu\text{M}$, occurring 1-2 hours after oral intake of the effective dose, and urinary excretion of curcumin was undetectable. The results of the latter study, suggested a chemopreventative effect of curcumin on cancer (Chen *et al.*, 2001). The main disadvantages of curcumin are its chemical instability (under neutral and basic pH conditions), poor aqueous solubility and low systemic bioavailability (Nandakumar *et al.*, 2006; Goel *et al.*, 2008; Parsai *et al.*, 2014). However, curcumin's efficacy against *P. berghei* has been shown to improve when delivered in a liposomal formulation (Nandakumar *et al.*, 2006).

3.7.2.2 Carbon black

Carbon black showed significantly ($p < 0.05$) higher cytotoxicity against the K562 cell line (IC_{50} : $1020 \pm 210 \mu\text{g/ml}$) compared to the HEK293 cell line (IC_{50} : $630 \pm 180 \mu\text{g/ml}$) (Figure 3.2), but was significantly ($p < 0.05$) less cytotoxic compared to camptothecin, curcumin and quinine. However, carbon black still showed significantly ($p < 0.05$) better selectivity indices (S.I.: 27.8, 44.9 for HEK293 and K562, respectively) on both cell lines compared to curcumin (Figure 3.4). The potential mode of action involved is not clear, but the IARC has classified carbon black under group 2B category, meaning that it is a possible carcinogenic to humans (Wellmann *et al.*, 2006). Carbon black or vegetable black is an EU approved food colourant (E153) derived from carbonised plant material of vegetable origin (European Food Safety Authority, 2012). However, benzo[*a*]pyrene, a polycyclic aromatic hydrocarbon found in carbon black, charred food, environmental and tobacco smoke can be enzymatically metabolised into mutagenic and highly carcinogenic metabolites possibly associated with colon and lung cancers (Denissenko *et al.*, 1996; Le Marchand *et al.*, 2002; Jiang *et al.*, 2007).

In the current study, the selectivity indices were 2 to 4-fold higher than the cut-off selectivity index of 10, indicating a reasonable selectivity for *P. falciparum* compared to human cell lines. The measurement of benzo[α]pyrene content in the carbon black test compound was outside the scope of the project.

3.7.3 Selectivity of nucleoside analogues for *P. falciparum*

The nucleosides analogues, JLP093 (IC₅₀: 10 ± 0.9 µM) and JLP118.1 (IC₅₀: 9.8 ± 1.6 µM) demonstrated comparable cytotoxicity to each other on the HEK293 cell line. However, JLP118.1 (IC₅₀: 8.4 ± 0.5 µM) was significantly ($p < 0.05$) more cytotoxic on the K562 cell line than JLP093 (IC₅₀: 22.8 ± 0.8 µM) (Figure 3.3). Overall, both nucleoside analogues were more cytotoxic than quinine, but significantly ($p < 0.05$) less cytotoxic compared to camptothecin. The selective indices of both nucleoside analogues were < 10 and significantly ($p < 0.05$) poorly selective (37 to 109-fold less selective towards *P. falciparum*) compared to quinine, which showed more selectivity or toxicity towards the parasites than the cell lines (Figure 3.4). A potential mode of action would be the interference of DNA synthesis. Nucleoside analogues are closely related to normal intermediates or precursors metabolised in DNA synthesis and therefore can act as anti-metabolites (Neal, 2005). These agents exert their cytotoxic activity by incorporating into and altering DNA and RNA. Nucleoside analogues interfere with the function of various enzymes, such as DNA polymerases, ligases and endonucleases, involved in synthesis of nucleic acids (Galmarini *et al.*, 2002). This contributes to the hypothesis of DNA synthesis inhibition in human cells. In addition, nucleoside analogues require specialised nucleoside transporter proteins to enter the cell (Galmarini *et al.*, 2002; King *et al.*, 2006). Mammalian cells express nucleoside transporters that have been associated with drug transport and activity of nucleoside analogues (Galmarini *et al.*, 2002). Intracellular penetration or accumulation of nucleosides may be directly affected or limited by the level of expression of nucleoside transport facilitating proteins such as the hENT1 protein (Galmarini *et al.*, 2002).

The most active of the nucleoside analogues tested in the current study, the purine-derived JLP118.1, exerted its effect on the trophozoite stage of the parasite, where DNA synthesis is elevated (Table 2.12). However, other purine analogues such as fludarabine have cytotoxic effects on non-dividing cells, but preferentially target the cells' DNA repair mechanism (Galmarini *et al.*, 2002).

3.7.4 Selectivity of imidazopyridine analogues for *P. falciparum*

The imidazopyridine analogues: IP-3 (IC_{50} : $9.15 \pm 1.5 \mu\text{M}$), IP-4 (IC_{50} : $9.14 \pm 1.1 \mu\text{M}$), and IP-7 (IC_{50} : $5.28 \pm 0.9 \mu\text{M}$) were significantly ($p < 0.05$) more cytotoxic on HEK293 cells than the K562 cells, whilst IP-5 showed consistent cytotoxic effect on both cell lines (IC_{50} : $9.91 \pm 1.3 \mu\text{M}$, HEK293 cells; IC_{50} : $9.6 \pm 0.5 \mu\text{M}$, K562 cells) (Figure 3.3). Of all the imidazopyridine analogues, IP-7 showed the lowest selective indices, indicating poor selectivity for *P. falciparum* compared to human cancer cell lines. All the imidazopyridine analogues were significantly ($p < 0.05$) less cytotoxic compared to camptothecin, but more cytotoxic than quinine. The imidazopyridine analogues demonstrated poor selectivity for *P. falciparum* with S.I. values < 1 , significantly less than quinine (S.I.: 180-458) (Figure 3.4). The known pharmacological activity of imidazopyridine analogues is very diverse with their activities including the inhibition of enzymes involved in cell cycle regulation, receptor ligands of eukaryotic cells, anti-viral and anti-protozoal activity (Enguehard-Gueiffier and Gueiffier, 2007; Jones *et al.*, 2008). Some imidazopyridine analogues inhibit cyclin-dependent kinases, in particular CDK2 and have progressed to clinical trials (Jones *et al.*, 2008). In an *in vitro* study by Dahan-Farkas *et al.* (2011) using the tetrazolium dye assay, a range of 6-substituted imidazo[1,2 α]pyridines were able to induce apoptosis in HT-29 and Caco-2 colon cancer cell lines after a 24 hr exposure. Moreover, the anti-proliferative activity (IC_{50} values) of the imidazo[1,2 α]pyridines against the HT-29 and Caco-2 cell lines ranged from 6-22 μM (Dahan-Farkas *et al.*, 2011), comparable to the cytotoxicity activities against both the HEK293 and K562 cell lines which ranged from 5-17 μM (except for IP-7 cytotoxicity on K562 cells), observed in the current study (Figure 3.3).

Overall, methylene blue showed the highest S.I. values demonstrating high selectivity for *P. falciparum* and cytotoxicity effects comparable to safranin O. The natural curcumin colourant, was very potent against both the HEK293 and K562 cell lines, and showed potential anticancer activity. Carbon black was significantly less cytotoxic and showed selective indices 278 to 449-times higher than curcumin. The nucleoside analogues demonstrated poor selectivity for *P. falciparum* (S.I. values < 10), whilst, the imidazopyridine analogues were the most poorly selective compounds (S.I. values < 1).

Chapter 4 Potential inhibition of *PfNek-4* protein kinase by test compounds

4.1 Introduction

Gametocytes, which are the initial stages of the sexual cycle of *P. falciparum*, are responsible for its transmission back to the mosquito vector from the human host. The latter is critical for the maintenance of the malaria life-cycle between host and vector (Drakeley *et al.*, 2006). Preventing parasite transmission between host and the mosquito vector is recognised as a potential strategy to control malaria (Doerig *et al.*, 2010). All the merozoites from a schizont are committed to either the sexual or asexual pathway (Doerig and Meijer, 2007; Dixon *et al.*, 2008). Protein kinases play a key role in regulation of the parasite developmental life-cycle and have been identified as possible drug targets (Doerig *et al.*, 2010). Analysis of the *Plasmodium* kinome revealed divergence compared to the counterpart enzymes found within the human host, in terms of amino acid sequence and biochemical properties (Doerig and Meijer, 2007). Never-in-mitosis *Aspergillus nidulans* (NIMA)-related kinase, *PfNek-4*, has been identified and is postulated to regulate gametocytogenesis and the maturation of the zygote of the *P. falciparum* parasite (Reininger *et al.*, 2012). *PfNek-4* is a serine/threonine protein kinase, consists of 310 amino acids, has a molecular mass (M_r) of 36.35 kDa, and an isoelectric point of 9.7 (Reininger *et al.*, 2009).

4.1.1 Catalytic activity of protein kinases

Protein kinases are critical in the regulation of biochemical processes in eukaryotic cells, including cell growth, enzymatic activity, gene expression, metabolism, motility, membrane transport, apoptosis and cell signalling (Pollard and Earnshaw, 2004; Alberts *et al.*, 2008c). Phosphorylation can either activate or inhibit specific proteins involved in cellular processes. In eukaryotes phosphorylation occurs on serine, threonine or tyrosine residues or side chains. When linked in series, different kinases form a signalling cascade that amplifies a response to a stimulus (Pollard and Earnshaw, 2004). The catalytic domain (Figure 4.1) of eukaryotic protein kinases is conserved across species and has highly conserved amino acids and motifs (Hanks, 2003).

The catalytic domain of eukaryotic protein kinases (ePK's) (Figure 4.1) is characterised by a highly conserved amino acids distributed in 12 subdomains (Hanks and Hunter, 1995; Hanks, 2003). The three glycine (G) residues in subdomain I form a hairpin-like structure which encloses part of the ATP molecule (Hanks, 2003). A lysine (K) residue in subdomain II,

orientates the ATP molecule through contacts with the α - and β -phosphates (Hanks, 2003). A glutamate (E) residue in subdomain III forms a salt bridge with the G residue in subdomain I (Hanks, 2003). Aspartate (D) and asparagine (N) residues are found within the signature motif of ePKs in subdomain VIB, where D is suggested to be the catalytic residue acting as a base acceptor (Hanks, 2003). The D residue in the DFG motif of subdomain VII, binds to the magnesium (Mg^{2+}) or manganese (Mn^{2+}) cation associated with ATP (Hanks, 2003). Whereas the E residue in subdomain VIII, forms a salt bond with the arginine (R) in subdomain XI which provides structural stability of the carboxyl (C)-terminal lobe (Hanks, 2003). The D residue in in subdomain IX is involved in stabilising the catalytic loop of subdomain IV through hydrogen bonds with the backbone (Hanks, 2003).

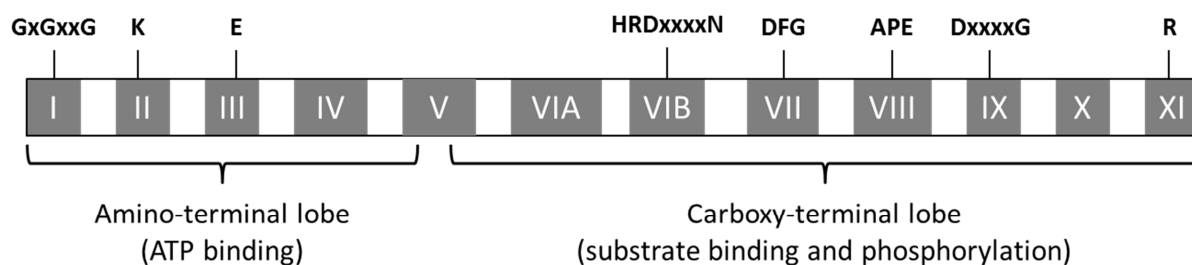


Figure 4.1 The catalytic domain of eukaryotic protein kinases consisting of 12 conserved subdomains (adapted from Hanks, 2003). The 12 conserved subdomains are indicated by Roman numerals. The positions of amino acid residues and motifs highly conserved throughout the eukaryotic protein kinase superfamily are indicated above the subdomains, using the single-letter amino acid code with “x” as any amino acid. Important for catalytic function are the invariant K (lysine) in subdomain II and the invariant aspartate in subdomain VII that function to anchor and orient ATP, and the invariant aspartate in subdomain VIB which is the catalytic base in the phosphotransfer reaction. G, glycine; E, glutamine; D, aspartate; N, asparagine; F, phenylalanine; A, alanine; P, proline; R, arginine(Hanks, 2003).

4.1.2 *PfNek-4* and the *P. falciparum* sexual cycle

Once committed, the gametocytes undergo five distinct morphological stages (Figure 4.2). Only once the gametocytes have reached maturity stage (after 9-23 days depending on the species) can they undergo sexual reproduction after being taken up by the feeding mosquito (Dixon *et al.*, 2008). A study using green fluorescent protein (GFP) reporter, detected the expression of the GFP-fused *PfNek4* in stages II to V of the gametocytes (Figure 4.2), as well as in asexual erythrocytic stage parasites undergoing schizogony, suggesting involvement in both stages (Reininger *et al.*, 2012).

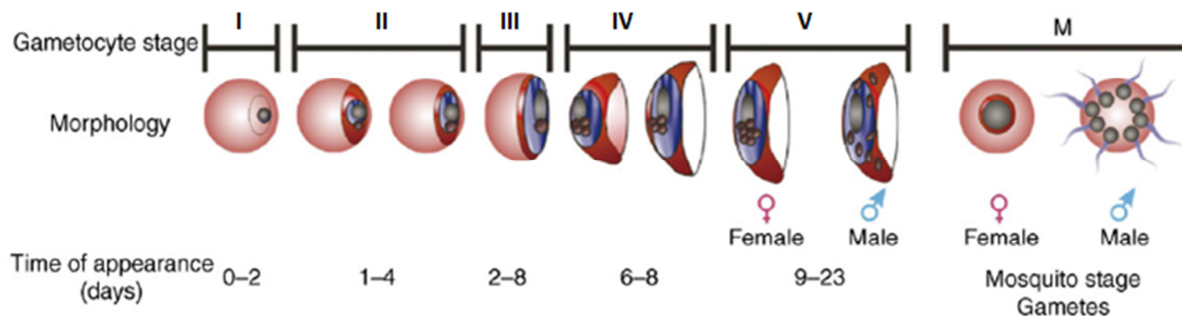


Figure 4.2 *P. falciparum* erythrocytic stage gametocytes development (adapted from Dixon *et al.*, 2008). Stages I-II: early stage gametocytes are morphologically indistinguishable from ring stage asexual parasites; stages II-III: gametocytes become elongated due to the formation of a network of polar microtubules; stages III-IV: gametocytes have the characteristic crescent shape of the *P. falciparum* gametocyte; stage V: gametocytes lose the polar microtubule network and become more rounded, assuming a 'sausage' shape; M-stage: mosquito stage gametes before egress from the RBCs. The male gametes (microgametes) have flagella. Red = RBCs, blue and grey = parasite and brown = haemozoin deposits (Dixon *et al.*, 2008).

4.1.3 *Plasmodium* NIMA-related kinases and the sexual cycle completion

The kinome analysis of *P. falciparum* has revealed a cluster of structurally related serine-threonine kinases belonging to the Nek family (Doerig *et al.*, 2008). The NIMA-related kinase (Nek) family is represented by four members in the *P. falciparum* kinome, *PfNek*-1 to 4 (Doerig *et al.*, 2008). *PfNek*-1 clusters within the *Aspergillus* NIMA/human Nek-2 branch in phylogenetic trees however this orthology cannot be confirmed with the other three *PfNek* enzymes (Doerig *et al.*, 2008; Reininger *et al.*, 2009). In addition, *PfNek*-1 is expressed in both asexual and sexual stages of the plasmodium development cycle. In contrast, mRNA encoding for *PfNeks* 2, 3 and 4 are exclusively detectable in gametocytes, suggesting a possible role in the sexual development of the parasite (Reininger *et al.*, 2009). The *P. berghei* orthologue of *PfNek*-1, *PbNek*-4, is only present in male gametocytes and has shown to be essential in ookinetes maturation (Doerig *et al.*, 2008). Previous studies have indeed confirmed this theory where *P. berghei*, rodent malaria parasites, lacking the Nek-4 enzyme were unable to complete the DNA replication cycles in the zygote before meiosis (Reininger *et al.*, 2009). There is sufficient evidence to suggest that cell cycle progression in the zygote is identified as a precondition for its morphological transition to the ookinete and for the successful malaria infection in the mosquito (Reininger *et al.*, 2009; Doerig *et al.*, 2010). However, in a recent study, *PfNek*-4 has been found that it is not strictly gametocyte-specific, and is expressed in a small subset of asexual parasites displaying high rate of conversion to sexual development (Reininger *et al.*, 2012). In addition, *PfNek*-4 is not responsible for switching erythrocytic schizogony to gametocytogenesis, but rather a molecular marker of sexually committed schizonts (Reininger *et al.*, 2012). The identification of compounds that

can potentially inhibit *PfNek-4* activity may further elucidate the role of *PfNek-4* in the *P. falciparum* sexual as well as asexual life cycle.

4.2 Aim

The aim was to determine the effect of the most active compounds on the kinase activity of recombinant *PfNek-4*.

4.3 Methodology

4.3.1 *PfNek-4* expression plasmid

An expression plasmid containing the full-length *PfNek-4* gene was a gift from Dr Luc Reininger and Professor Christian Doerig (INSERM U609, Wellcome Centre for Molecular Parasitology, University of Glasgow, Glasgow G12 8TA, Scotland, U.K.). Competent *Escherichiacoli* (BL21 strain) cells were transformed with the pGEX-*PfNek-4* plasmid by Dr L.J. Harmse (University of the Witwatersrand) (Biosafety clearance: 201220701, Appendix B4). The pGEX-*PfNek-4* plasmid codes for a *PfNek-4* protein, fused to glutathione S-transferase (GST). The predicted molecular weight of the GST-*PfNek-4* fusion protein was 62.35 kDa. The GST-fusion protein was constructed by enzymatically inserting the *PfNek-4* gene into the multiple cloning site of the pGEX-4T-3 vector containing the GST gene upstream of the *PfNek-4* gene, and the ampicillin-resistant gene (downstream) as described by Reininger *et al.* (2009). Expression in the *PfNek-4* GST fusion protein is regulated by a *tac* promoter, which can be induced by the lactose analogue, isopropyl β -D thiogalactoside (IPTG) (Studier, 2005). An internal *lacI^q* gene encodes for a repressor protein that binds to the operator region of the *tac* promoter, preventing target protein expression until induction by IPTG. The pGEX-4T-3 vector has been engineered so that the GST can be cleaved from the fusion protein by digestion with site-specific thrombin protease (Smith and Johnson, 1988).

4.3.2 2YT broth preparation

Plasmid containing *E. coli* bacterial culture was grown in double-strength yeast and tryptone (2YT) broth according to methods described by Sambrook, *et al.* (1989). The broth was prepared to 1 litre with 16 g Bacto-tryptone, 10 g Bacto-yeast extract and 5 g NaCl dissolved in Milli-Q[®] water and sterilised by autoclaving. All media was stored at 4°C until use. Before use of the broth, carbenicillin was added as a selector to a final concentration of 50 μ g/ml.

4.3.3 Preparation of carbenicillin selector agar plates

The agar solution was prepared by adding 12 g agar to 1 litre 2YT broth, followed by stirring to disperse the agar, sterilised by autoclaving for 10 min at 121°C and allowed to cool down

to 60°C (Sambrook *et al.*, 1989). Carbenicillin was added to a final concentration of 50 µg/ml to the agar selector plates (carbenicillin-positive) to permit only ampicillin-resistant bacterial colonies to grow (Sambrook *et al.*, 1989). The agar solution was allowed to cool and solidify in a laminar flow cabinet before replacing the lids. The agar plates were stored inverted, at 4°C in sealed plastic bags in order to prevent dehydration. Carbenicillin was used instead of ampicillin because it is more resistant to β-lactamase produced by *E. coli* bacteria.

4.3.3.1 Overnight culture preparation

Pre-warmed (37°C) 2YT broth (5 ml) was transferred to culture tubes and inoculated with *E. coli* BL21 (DE3) thawed stock cultures containing the plasmid constructs. A control tube containing the 2YT broth only was included. The cultures were grown overnight (16-18 h) at 37°C in a shaking incubator (200 rpm).

4.3.3.2 Inoculation of agar plates

In order to obtain isolated colonies on the agar plate, the standard streak technique commonly applied in microbiology was used (Sambrook *et al.*, 1989). Carbenicillin-negative plates were used as a positive control. The plates were sealed, inverted and incubated overnight at 37°C and then stored at 4°C.

4.3.4 Expression of GST-PfNek-4 fusion protein

4.3.4.1 Induction of GST-fusion protein expression

The principle of induced protein expression is based on the inactivation of the repressor protein, *lacI*^q, bound to the *tac* promoter. Adding a lactose analogue, IPTG, during the log phase of bacterial growth, allows RNA polymerase to bind to the *tac* promoter, and expression of the genes which synthesise the GST-fusion protein (Sambrook *et al.*, 1989; Studier, 2005). Protein expression was induced with the addition of IPTG (1 mM, final concentration) to a culture in the log phase of growth. A 10 mM stock of IPTG was prepared in Milli-Q[®] water, sterile filtered and stored frozen. The 2YT broth (100 ml) supplemented with carbenicillin (50 µg/ml), was inoculated with 100 µl overnight cultures grown from single colonies harvested from the agar selector plates. The cultures were grown for 4 h at 37°C and shaken at 200 rpm, until the culture reached optical density at 600 nm (OD₆₀₀) of 0.5-0.7, which indicated that the bacterial growth was in log phase. Protein expression was induced by adding IPTG to a final concentration of 1 mM to the cultures and further incubation overnight (15-18 h).

4.3.4.2 Harvesting of bacteria

Bacteria were harvested by splitting the cultures into two 50 ml tubes and centrifugation at 421 x g for 5 min at 4°C and the supernatant discarded. The bacterial cells were re-suspended and washed twice with PBS, and the supernatant discarded.

4.3.4.3 GST-PfNek-4 fusion protein purification by affinity chromatography

The packed bacterial cells were re-suspended in complete BugBuster[®] Master Mix (Novagen) protein extraction reagent (5 ml per gram of wet cell paste), supplemented with phenylmethanesulfonyl fluoride (phenylmethanesulfonyl fluoride (PMSF), Sigma-Aldrich) and a single Complete[™] tablet (Roche) that contained a cocktail of protease inhibitors. Protease inhibitors are required to prevent degradation of the isolated target protein by proteolytic enzymes once the bacteria are lysed. The cell suspension was incubated on a rotating mixer at room temperature. The bacterial lysate was centrifuged at 10 528 x g for 30 min at 4°C in 15 ml culture tubes to remove insoluble cell debris. The soluble extract (supernatant) was transferred into clean 15 ml culture tubes using a pipette and the pellet discarded. A sample (60 µl) of soluble extract was transferred into microcentrifuge tubes and mixed with 40 µl sample loading buffer for later analysis by sodium dodecyl sulphate-polyacrylamide gel electrophoresis (SDS-PAGE) (Section 4.3.5.1).

GST-fusion proteins were purified from the soluble extracts by affinity chromatography using glutathione immobilised to a Sepharose matrix (Amersham-Biosciences, 2002). GST-PfNek-4 fusion proteins bind to the beads, allowing purification of the GST-PfNek-4 proteins by centrifugation and several washing steps as discussed below (Amersham-Biosciences, 2002). The Glutathione Sepharose[™] 4B beads (Amersham) suspension (133 µl) were washed three times by centrifugation (SANYO[®] MSE centrifuge) at 284 x g for 1 min with 1 ml PBS and then loaded directly to 5 ml of soluble bacterial lysate.

The lysates and beads were incubated at 4°C overnight on a blood tube rotator to bind the GST-PfNek4 fusion protein to the Sepharose beads. The lysates were centrifuged at 284 x g for 2 min to sediment the Sepharose beads and the supernatant was discarded. This was repeated three times. The GST-fusion protein was eluted from the Sepharose beads using 200 µl of elution buffer which consisted of 40 mM reduced glutathione in 50 mM Tris, pH 8.0 and the sepharose bead suspension centrifuged at 284 x g for 2 min before use of the eluates and stored at 4°C in microcentrifuge tubes.

4.3.5 Analysis of the GST-PfNek-4 protein

4.3.5.1 SDS-polyacrylamide gel electrophoresis

The purified GST-tagged PfNek-4 protein samples were analysed by discontinuous SDS-PAGE (Laemmli, 1970). In principle, SDS confers a negative charge to denatured proteins which then separate in the gel matrix according to their molecular weights. (Sambrook *et al.*, 1989). These proteins migrate within a moving boundary of leading high-mobility chloride ions (Cl⁻) and trailing glycine ions (Gly⁻), created by an electric current passed between the negative cathode and positive anode electrodes (Sambrook *et al.*, 1989). The SDS-polypeptide complexes then concentrate into a very thin stack of on the surface of the resolving gel. The higher pH of the resolving gel increases the charge of Gly⁻ ions that migrate past the stacked polypeptides and travel through the resolving gel. The polypeptides move through the resolving gel in a zone of uniform voltage and pH and separate according to size by sieving. The ability of the discontinuous stacking and resolving buffer systems to concentrate all the polypeptide complexes into a small volume greatly increases the resolution of SDS-PAGE gels. (Laemmli, 1970; Sambrook *et al.*, 1989).

- **Preparation of SDS-Polyacrylamide gels**

The SDS-PAGE discontinuous gel system consisted of a 12% resolving gel overlaid by a 5% stacking gel. The resolving gel was buffered to pH 8.8 with 1.5 M Tris and the stacking gel to pH 6.8 with 0.5 M Tris using 12% (v/v) HCl. Both stacking and resolving gels were prepared using Milli-Q[®] water and contained 30% (w/v) total acrylamide (Bio-Rad Laboratories), 2.7% (w/v) bisacrylamide (Bio-Rad Laboratories), 10% SDS (Sigma-Aldrich), 10% ammonium persulfate (Bio-Rad Laboratories) and N,N,N',N'-tetramethylethylenediamine (TEMED, Promega). TEMED accelerates the polymerisation of acrylamide and bisacrylamide by catalysing the formation of free radicals from ammonium persulfate (Sambrook *et al.*, 1989). The gels were cast on a vertical casting apparatus (Bio-Rad Laboratories) and allowed to polymerise.

- **Protein sample loading and running the gel**

Proteins were denatured by heating protein extract samples in SDS gel-loading buffer (100mM dithiothreitol or DTT, 2% w/v SDS, 0.1% w/v bromophenol blue, 10% v/v glycerol in 50 mM Tris, pH 6.8). Heating protein samples in SDS, confers a negative charge to the polypeptide backbone (Sambrook *et al.*, 1989). DTT, a reducing agent, further denatures the protein sample by reducing the disulphide bonds preventing tertiary folding and denaturing quaternary structures. The eluted protein samples (20 µl) were mixed with 10 µl loading buffer in labelled microcentrifuge tubes and kept on ice. Milli-Q[®] water (300 ml) was brought

to a boil in a glass beaker and protein samples were denatured in the boiling water for 5 min and returned to ice for 10 min to prevent re-folding of the linear, polypeptide. Protein samples (10 µl per well) were loaded into the gel assembly mounted onto a Bio-Rad mini-gel electrophoresis tank filled with electrophoresis buffer (0.025 M Tris pH 8.3, 0.192 M glycine, 0.1% w/v SDS), and pre-cooled to 4°C. The gel was run at 200 Volts until the bromophenol blue tracking dye reached the bottom of the gel. Thereafter, the glass plates were removed and pried apart using a clean plastic wedge (Bio-Rad Laboratories). The orientation of the gels was marked by cutting from the bottom-right corner of the gel. Two gels were run simultaneously: the one gel was equilibrated for Western blotting whilst the other gel was routinely stained with coomassie blue.

4.3.5.2 Coomassie blue gel staining

The gels were fixed and stained by immersion into Coomassie blue staining solution (0.125% w/v Coomassie blue R-250, 50% v/v methanol, 10% v/v acetic acid) for 2 h with gentle agitation (Sambrook *et al.*, 1989). The Coomassie stain solution was filtered through Whatman[®] grade 2 filter papers before use. The gels were placed in 20 ml destain solution-I (50% v/v methanol, 10% v/v acetic acid) and thereafter in destain solution-II (7% v/v acetic acid, 5% methanol) for 1 h in each, in order to visualise the protein bands on the gel.

4.3.5.3 Western blotting of separated proteins

Western blotting, as described by Towbin *et al.* (1979), is an electrophoretic technique used to detect specific proteins immobilised on a membrane by using antibodies as probes (Sambrook *et al.*, 1989). The technique, frequently referred to as immunoblotting, involves the transfer of proteins separated by SDS-PAGE to an adsorbent membrane like polyvinylidene fluoride (PVDF) or nitrocellulose, forming a replica of the SDS-polyacrylamide gel. The proteins immobilised on the membrane are then detected using enzyme-labelled or radiolabelled antibodies specific to the protein antigen (Towbin *et al.*, 1979). Therefore, the aim of assaying the proteins using the Western blotting technique was to confirm if the *PfNek-4* GST-tagged protein band identified by size and mobility during SDS-PAGE is the protein of interest by probing with an anti-GST antibody conjugated to horse-radish peroxidase enzyme (Kurien and Scofield, 2006).

- ***Post-electrophoresis wet protein transfer***

Following electrophoresis the unstained SDS-polyacrylamide gel was equilibrated in transfer buffer (48 mM Tris, pH 8.3, 39 mM glycine, 0.1% SDS and 20% v/v methanol). At pH 8.3, the proteins would not blot or transfer to the membrane therefore 0.1% SDS was added to the transfer buffer to increase the negative charge of the denatured proteins. The PVDF

membrane (Millipore) was pre-wetted in 100% methanol before equilibration in transfer buffer. The PVDF membrane, two pieces of filter paper (cut to the size of the SDS-gel) and the two fibre pads were soaked in transfer buffer for 10 min. The gel “sandwich” (Figure 4.3) was assembled without trapping air bubbles. The assembly was transferred to the Mini-Trans Blot™ Cell (Bio-Rad Laboratories) with ice cold transfer buffer and a frozen cooling unit. The apparatus was placed on a magnetic stirrer and transfer took place at a constant voltage of 100 Volts and 350 mA for at least 1 h.

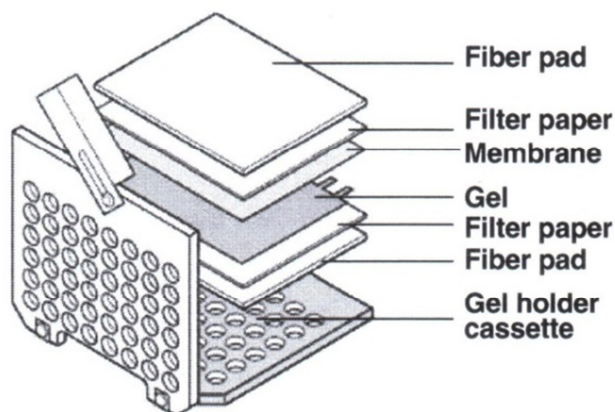


Figure 4.3 Assembly of the “gel-sandwich” for electrophoretic protein transfer to a PVDF membrane (Bio-Rad, 2013).

- ***Blocking of the PVDF membrane***

In order to prevent unspecific binding of horse-radish peroxidase conjugated anti-GST primary antibodies, the membrane was incubated in 20 ml blocking buffer for 1 h at room temperature on a rocker (Sambrook *et al.*, 1989). The blocking buffer contained 5% bovine serum albumin (BSA, Sigma-Aldrich) dissolved in Tris buffered saline-Tween-20 solution (TBST) prepared from 50 mM Tris, 150 mM NaCl, 0.1% (v/v) Tween-20, adjusted to a pH of 7.5 using 12% HCl.

- ***Immuno-detection***

The membrane was then washed once for 5 min with TBST followed by overnight incubation at 4°C with HRP-conjugated goat anti-GST polyclonal antibodies (Amersham) diluted to 1:15 000 by adding 2 µl antibody serum in 30 ml blocking buffer, diluted to 2% (v/v) BSA in TBST. This was to allow the antibodies to bind to the GST-fusion protein that is immobilised on the membrane for visualisation later using chemiluminiscent detection. The membrane was washed 6 times for 10 min with 25 ml TBST in order to reduce the background. Filter paper

was used to blot excess reagent from the membrane before subjecting it to chemiluminescence.

- **Chemiluminescence**

The membrane was incubated for 60 seconds in 3 ml Western Lightning™ (Perkin-Elmer) chemiluminescence reagent (luminol reagent and oxidising reagent mixed in 1:1 ratio). The principle of the method (Figure 4.4) is that the HRP-conjugated to the anti-GST antibody, oxidises the luminol substrate (whilst the oxidising agent is reduced), emitting blue luminescence (Sambrook *et al.*, 1989). The chemiluminiscent signal was visualised by exposing the PVDF membrane to Hyperfilm®-MP multipurpose film (Amersham) for differential periods of 0.5, 1 and 2 min in a dark room. The film was developed at the Charlotte Maxeke Hospital, Radiography Department, using an automated X-ray processor.

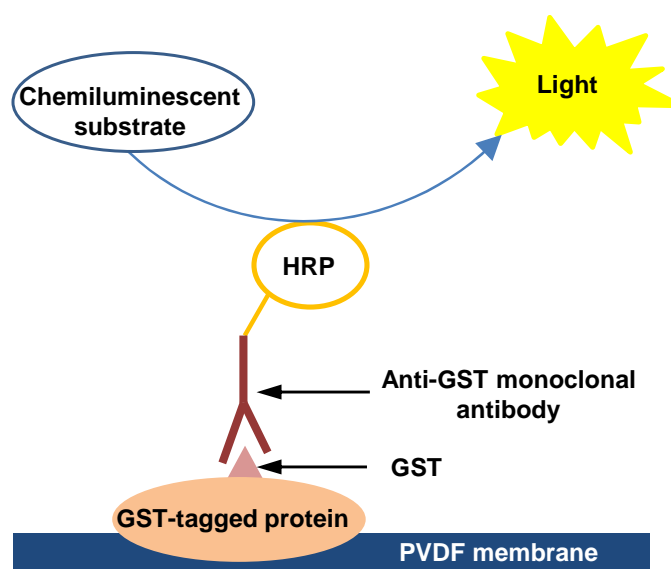


Figure 4.4 Chemiluminiscent visualisation of the GST-tagged proteins using horseradish peroxidase conjugated primary antibodies. HRP-conjugated anti-GST primary antibodies recognise and bind to a compatible GST site expressed on the target GST-tagged protein that was immobilised on the PVDF membrane. Once a chemiluminescent substrate is added, the HRP enzyme oxidises the substrate. This oxidation reaction emits luminescent signal that can be detected and visualised by exposure to X-ray film.

4.3.5.4 Determination of the protein molecular weight

The MW of the expressed GST-tagged *PfNek-4* protein was determined from the SDS-PAGE gel. The protein sample was separated alongside a set of MW Perfect™ protein standards (Qiagen) by electrophoresis. A linear graph of log MW versus relative migration distance, or retention factor (R_f), was generated, using GraphPad Prism (version 5.0) software. An r^2 value

≥ 0.99 was regarded a significant correlation between the control variable (x-values) and response variable (y-values) and for interpolating y-values. The R_f values were determined from the ratio of the migration distance of the protein and the migration distance of dye front. The linear curve was described by the equation $y = mx + c$ where, where y is the log MW, m is the slope, x is the R_f value, and c is the y-intercept. Therefore, in order to verify that the protein expressed was the correct size, the MW was calculated by expressing the linear equation as the anti-log of MW, such that $MW = 10^y$.

4.3.5.5 Determination of the protein concentration

The concentration of the GST-fusion protein eluted from the GST Sepharose beads was determined by using the Bio-Rad Protein Assay, which is based on the dye-binding method and described by Bradford *et al* (1976). The Bradford assay involves a differential colour change of Coomassie blue-G dye as it binds to protein. Accordingly, the peak absorbance wavelength of the acidic Coomassie dye shifts from 465 nm to 595 nm when protein binding occurs. Briefly, six dilutions of standard BSA between 200 and 1400 $\mu\text{g/ml}$ were prepared in triplicates in Milli-Q[®] water. The protein standards and recombinant protein samples were mixed with the Bio-Rad dye reagent and incubated for 5 min at room temperature. The reaction solutions (1 ml) were transferred to a plastic cuvette and the absorbance of the protein-dye complex measured using a Perkin-Elmer[™] UV-Visible spectrophotometer at a wavelength of 595 nm (Bradford, 1976). A standard curve of Abs_{595} versus concentration ($\mu\text{g/ml}$) of protein standards was constructed using GraphPad Prism 3.0 software program. The absorbance values of the recombinant protein samples were expressed in $\mu\text{g}/\mu\text{l}$ using the standard curve and used to determine the amount of protein in the protein extracts prior to kinase assays.

4.3.6 Kinase assay

The kinase activity of GST-*PfNek-4* was measured according to the method described by Reininger *et al.* (2009). The kinase assays were performed in a standard 30 μl reaction containing 20 mM Tris-Cl (pH 7.4), 20 mM MgCl_2 , 10 mM NaF, 10 mM glycerol 2-phosphate, 2 mM MnCl_2 , 54 mg/ml casein from bovine milk as substrate, in the presence of 10 μM ATP (reagents purchased from Sigma-Aldrich), 5 mCi/ml [γ -³²P]-ATP (American Radiolabeled Chemicals) and 0.5-3 μg recombinant kinase (Table 4.1). Co-factors, MgCl_2 and MnCl_2 activate and enhance kinase activity, whilst NaF and glycerol 2-phosphate inhibit phosphatases. Non-radioactive labelled ATP was added as an additional substrate to prevent substrate depletion. The final concentration of the isotope in the 30 μl standard kinase reaction was 0.08 $\mu\text{Ci}/\mu\text{l}$. The GST-*PfNek-4* enzyme was exposed to final concentrations of

10 μM of the synthetic compounds or 10 $\mu\text{g/ml}$ final concentrations of the natural compounds for 30 min at 37°C. The reaction was started by adding the GST-*PfNek-4* enzyme last. Separate casein (without enzyme and test compound) and GST-*PfNek-4* kinase (without test compound) controls were performed in order to detect kinase activity and incorporation of ^{32}P into the casein substrate by phosphorylation. Standard precautions when working with ^{32}P radioisotope were observed. The kinase reaction was terminated by adding 10 μl , SDS-loading buffer (Section 4.3.5.1) and the reaction tubes placed on a pre-heated (100°C) metal heating block for 5 min to denature the protein. The reaction tubes were incubated on ice for 10 min and 20 μl reaction samples were subjected to SDS-PAGE (Section 4.3.5.1). The gels were stained with coomassie blue and dried before exposure to Hyperfilm[®]-MP autoradiographic film (Amersham).

Table 4.1 List of stock reagents and volumes of the 30 μl single kinase reaction solution.

Stock reagents	Volume
20 mM Tris-Cl (pH 7.4) Kinase buffer	3 μl
20 mM MgCl_2	3 μl
10 mM NaF	3 μl
10 mM Glycerol 2-phosphate	3 μl
2 mM MnCl_2	3 μl
54 mg/ml Casein substrate	0.5 μl
0.5-3 μg Recombinant kinase	5 μl
10 μM ATP ^a	0.5 μl ^a
100 μM or 100 $\mu\text{g/ml}$ Test compound	3 μl
5mCi/ml ATP [γ - ^{32}P]	0.5 μl
Milli-Q [®] water	5.5 μl

^aNon-radioactive ATP was added to prevent limitation of the kinase reaction.

- ***Drying of SDS-polyacrylamide gels and autoradiography***

SDS-polyacrylamide gels containing proteins radiolabelled with ^{32}P were dried before autoradiography to prevent quenching (Sambrook *et al.*, 1989). The stained gels were placed and oriented on a piece of Whatman[™] paper and the gel was covered with plastic wrap. The sandwich of filter paper, gel and plastic wrap was placed on the gel dryer slab with the plastic wrap being the uppermost layer. The gels were dried under vacuum for 40 min at 50°C using the Slab Gel Dryer (Hoefer Scientific Instruments). The dried gels were removed from the dryer and the kinase activity was visualised by exposing the gels to Hyperfilm[®]-MP autoradiographic film (Amersham) overnight (16-18 h) in a dark room. The autoradiographic films were developed at the Charlotte Maxeke Hospital, Radiography Department, using an automated X-ray processor.

4.3.7 Plasmid isolation

Plasmid DNA was isolated and purified from bacterial cells by using the QIAprep[®] Spin Miniprep Kit (Qiagen) by following the manufacturer's instructions. The kit provided buffers optimized for efficient isolation of plasmid DNA and removal of contaminants from a pellet of bacterial cells. The RNase enzyme activity was monitored by a colour change of Lyseblue indicator, from blue to colourless-cloudy appearance. The DNA was adsorbed to a silica-membrane in spin-columns, whilst the contaminants passed through the column during centrifugation. Impurities were washed away, and the plasmid DNA was eluted into microcentrifuge tubes using nuclease-free water.

4.3.8 Restriction digest of *PfNek-4* containing plasmids

A sample of plasmid (3 μ l) was subjected to restriction digest master-mix solution (17 μ l) with *SalI* and *BamHI* at 37°C for 3 h. The restriction digest master-mix solution was prepared with 138 μ l nuclease-free water, 2 μ l acetylated BSA and 20 μ l buffer D (that consisted of 60 mM Tris-Cl pH 7.9, 1.5 M NaCl, 60 mM MgCl₂ and 10 mM DTT) (Promega). The restriction enzymes, *SalI* and *BamHI* (Promega) were added (5 μ l each) into the restriction digest master-mix solution, with *BamHI* added last. The reaction was terminated by denaturing the restriction enzymes by heat-inactivation at 65°C for 15 min. The restriction products were analysed by agarose gel electrophoresis (Sambrook *et al.*, 1989) or stored at -20°C.

4.3.9 Agarose gel electrophoresis of restriction products

Agarose gel electrophoresis as described by Sambrook *et al.* (1989) was used to analyse the products from the restriction digest of the plasmid. A 1.5% agarose gel was prepared by adding 0.45 g agarose (Promega) to 30 ml tris-acetate EDTA (TAE) buffer (40 mM Tris, 20 mM acetic acid, and 1 mM EDTA, pH 8.0) and heating until the agarose was in solution. The gel mixture was heated in a microwave oven and swirled until all of the translucent agarose particles were dissolved. The molten agarose solution was allowed to cool to 50-60°C and 3 μ l of 1 μ g/ml ethidium bromide (EtBr) was added and the gel solution mixed thoroughly before the gel was cast. EtBr intercalates DNA at the major grooves and under UV light, EtBr fluoresces giving an intense orange colour, thus allowing for visualisation of DNA.

The agarose gel was cast in a horizontal agarose gel casting unit (Bio-Rad) with a 15-toothed plastic comb, and allowed to solidify. The gel was submerged in TEA buffer in the electrophoresis tank. Bromophenol blue tracking dye (2 μ l) was added to restriction digest reaction samples (10 μ l), control reactions, 50 base pair (bp) DNA ladder (1 μ l) (New

England BioLabs). All the samples were loaded into the wells using a pipette. The gel was run at 25 Volts until the bromophenol blue tracking dye reached the end of the gel.

4.3.10 DNA sequencing

DNA sequencing involves establishing the order of nucleotides or deoxynucleotide triphosphates (dNTP) in the DNA fragment of interest. The most widely used DNA sequencing method, referred to as the chain termination method was earlier described by Sanger *et al.* (1977). In the current study, the sequencing of the full-length DNA sequence of the plasmids was outsourced to Inqaba Biotech. The aim was to verify the DNA sequence of the inserts and exclude any base sequence errors. Sequencing was performed using an ABI 3500XL genetic analyser (Applied Biosystems), which is a fully automated, capillary electrophoresis instrument for high quality base calling, assembly and single base change detection. The ABI BigDye[®] Terminator V 3.1 Cycle Sequence kit (Applied Biosystems) containing primers, polymerases, fluorescent-dideoxynucleotides and deoxynucleotide triphosphates, in a 6:1 ratio, was used together with pGEX single primers (pGEX3: GGAGCTGCATGTGTCAGAGG; pGEX5: GGCAAGCCACGTTTGGTG). Agar plates containing single colonies of *PfNek4-A* and B clones were provided to Inqaba Biotech for plasmid isolation, primer design and automated sequencing. The resulting consensus DNA sequences were subjected to bioinformatics analysis.

4.3.11 Bioinformatics

The DNA sequence obtained from Inqaba Biotech was subjected to bioinformatic analysis to verify the integrity of the sequence. Nucleotide sequence alignment and the amino acid sequence prediction were performed *in silico* using the basic local alignment search tools (BLAST's) designed by Altschul *et al.*, (1990). BLAST's are algorithms, that allow comparison and alignment of primary biological sequences of the molecule of interest such as proteins (by using blastp or blastx) or nucleotide sequences DNA (by using blastn), against a library of sequences or database (Altschul *et al.*, 1990). The query sequence was used as input in text format and the indexed library sequences can be accessed with an identifier number. Sequences showing similarity to the query sequence were reported in order of similarity scores, identity % and E-values. The native gene record was accessed by performing a text search on the *PfNek-4* gene (identifier: PF3D7_0719200) from the PlasmoDB database (www.plasmodb.org). The National Centre for Biotechnology Information database (www.ncbi.nlm.nih.gov) provides access to biomedical and genomic information as well as BLAST tools. The consensus nucleotide sequence of *PfNek4-A* DNA was used to retrieve the amino acid sequence of the polypeptide chain by using blastx.

4.4 Results

4.4.1 Expression of *PfNek4*

The coomassie blue stained SDS gel (Figure 4.5) showed that IPTG-induced overnight protein expression at 37°C (lane 2), was much more efficient (demonstrated by the darker bands) compared to the IPTG-induced overnight protein expression at 30°C (lanes 3-6). The protein concentration yield from the expression induced overnight with 1mM IPTG at a higher temperature (37°C), was on average higher (1.7 µg/µl) compared to expressions carried out at 30°C, which yielded on average, 1.3 µg/µl. SDS-polyacrylamide electrophoresis showed at least two distinct bands of proteins, which corresponded to the predicted sizes of the GST-*PfNek-4* and GST proteins. The smaller bands in lanes 2-6 are most likely truncated GST protein. The pGEX-4T-3 expression vector yields fusion proteins with the GST-tag on the amino-terminus and the protein of interest, in this case, *PfNek-4* at the carboxyl-terminus.

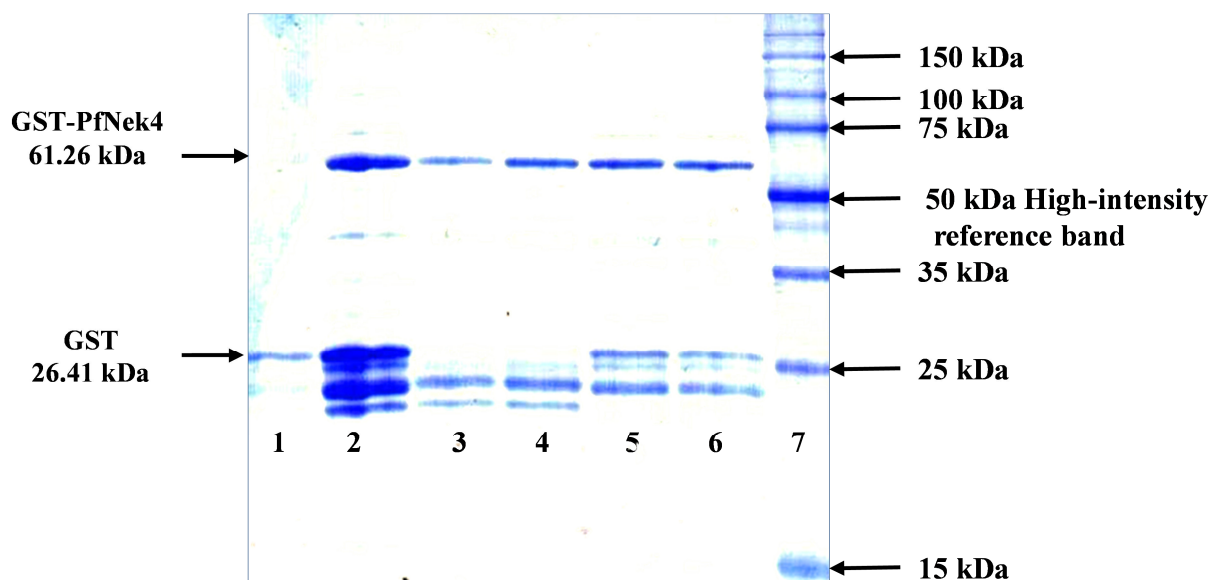


Figure 4.5 Coomassie blue-stained SDS-PAGE gel depicting the isolated GST-*PfNek-4* (clone A) protein bands alongside molecular weight markers. Lane1: non-induced control, lane 2: overnight IPTG-induced protein expression at 37°C, lanes 3-6: overnight IPTG-induced protein expression at 30°C and lane MW: Perfect™ protein standards (15-150 kDa). The isolated 26 kDa GST protein in all the lanes, suggest cleavage of the GST tag by the *E. coli* host enzymes from the fusion protein and/or basal level expressions from the *lac*.

The linear curve (Figure 4.6) of log MW versus R_f was plotted by using the migration distances of the Perfect™ protein standards and of the expressed protein bands (GST-*PfNek-4* and GST) measured from the SDS-PAGE gel (Figure 4.5). The log MW values of the unknown protein were interpolated by applying the linear equation using Prism 5.0 software. The MW's were calculated by expressing the linear equation as a function of the anti-log of

Y. The R_f values for Protein X ($R_f = 0.23$) and Protein Y ($R_f = 0.88$) were substituted into as x-values into the linear equation. The strong linear relationship ($r^2 > 0.99$) between the proteins' MW and R_f values demonstrates the reliability of the elucidated MW values of the expressed proteins. The calculated MW's 61.26 kDa and 26.41 kDa, corresponded to the predicted sizes of the GST-*PfNek-4* and GST proteins, respectively.

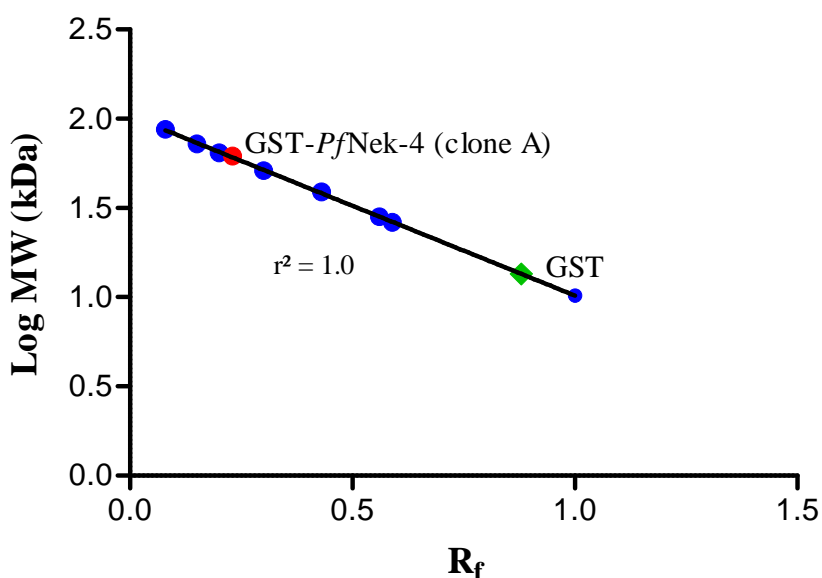


Figure 4.6 A linear curve of the log MW versus R_f values used to determine the MW of expressed proteins.

4.4.2 Western blot

Protein transfer to the PVDF membrane was successful by inclusion of 0.1% SDS in the transfer buffer, to confer a negative charge to the proteins. SDS is usually not added to the transfer buffer, however in this case the predicted isoelectric point (pI: 8.9) of the expressed GST-*PfNek-4* fusion protein whilst the pH of the transfer buffer was 8.2, thereby reducing the net charge on the GST-*PfNek-4* fusion protein for effective protein transfer. Upon probing the expressed proteins, two GST-tagged proteins were detected on the PVDF membrane using polyclonal anti-GST HRP-conjugated antibodies, and visualised on the Hyperfilm[®]-MP films (Figure 4.7). In addition, GST (26.41 kDa) encoded by the *Schistosoma japonicum* gene (NCBI identifier: P08515.3) and GST-*PfNek-4* (36.35 kDa) encoded by the gene PF3D7_0719200 (www.plasmodb.org), have been previously characterised and published. The expressed Protein Y (26.41 kDa) separated during SDS-PAGE, correlated with the GST protein detected on the Western blot. Therefore, by immuno-detection and arithmetic inference, Protein X (61.26 kDa), was confirmed to be the GST-*PfNek-4* protein since its total

MW would include the GST protein: $MW_{PfNek-4}(34.85 \text{ kDa}) = MW_{GST-PfNek-4 \text{ protein}}(61.26 \text{ kDa}) - MW_{GST}(26.41 \text{ kDa})$.

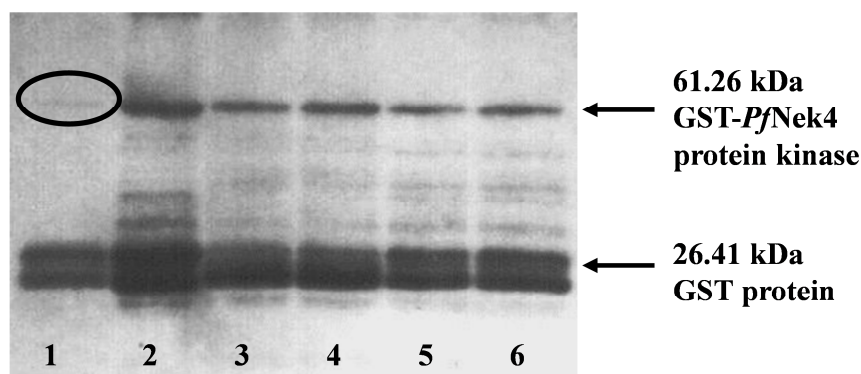


Figure 4.7 Western Blot of the GST-*PfNek4* (A) protein kinase. Lane1: non-induced sample control, lane 2: overnight IPTG-induced protein expression at 37°C, lanes 3-6: overnight IPTG-induced protein expression at 30°C. The circled area in lane 1 showed a faint band with the same migration distance as the 61 kDa protein and a 26 kDa GST protein suggest cleavage of the GST tag by the *E. coli* host enzymes from the fusion protein and/or possible basal level expressions from the *lac* promoter.

4.4.3 Protein concentration

The concentration of the GST-*PfNek4* protein expressed was determined using the Bio-Rad Protein Assay. The sample of the expressed protein used in the kinase assay gave a mean absorbance value of 1.19 at a wavelength of 595 nm. The Y-value (protein concentration), was interpolated from the standard curve (Figure 4.8) by entering the X-value ($\text{absorbance}_{595\text{nm}} = 1.19$) in the data table in GraphPad Prism version 5.0. The kinase protein concentration value computed was 1.63 $\mu\text{g}/\mu\text{l}$. Therefore, taking into consideration a dilution factor of 7, the final amount of the GST-*PfNek4* in the kinase assay reaction was 1.16 μg . The strong linear relationship ($r^2 = 0.99$) between the $\text{absorbance}_{595\text{nm}}$ values and the concentrations ($\mu\text{g}/\text{ml}$) of the BSA protein standards demonstrated the reliability in predicting the concentration of the GST-*PfNek4* (A) protein sample.

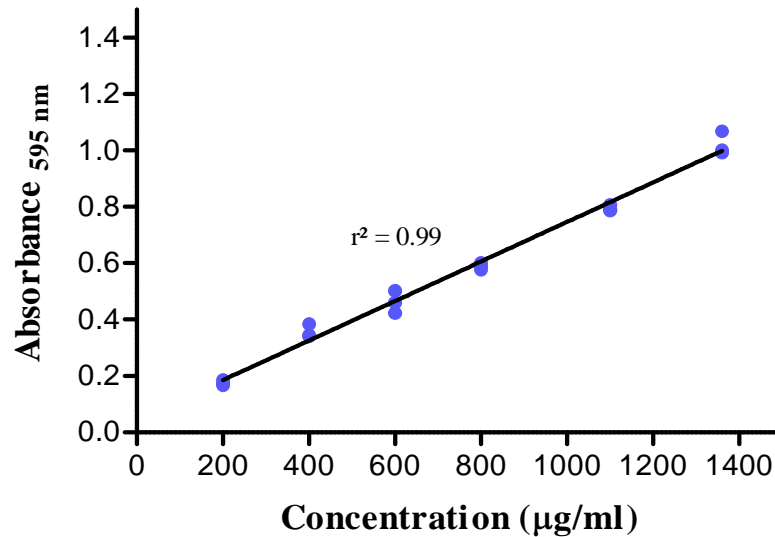
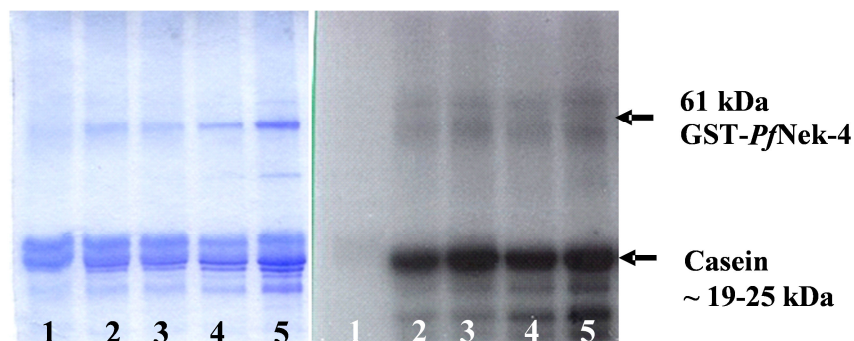


Figure 4.8 Standard curve of BSA protein standard concentrations and absorbance_{595nm} values.

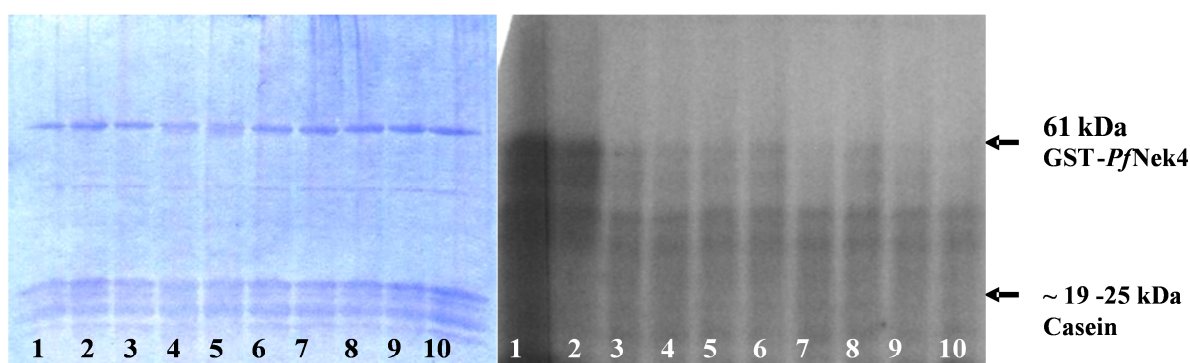
4.4.4 Kinase activity and inhibition

The kinase activity of the various GST-fusion protein kinase isolates were screened without the test compounds. The GST-*PfNek4* fusion protein stained blue with coomassie blue on the SDS-PAGE gel. The phosphorylated casein substrate is demonstrated as a dark band on the autoradiograph (Figure 4.9).



(a) SDS-PAGE gel of the kinase assay. **(b) Autoradiogram.**

Figure 4.9 Kinase activity of various isolates of the recombinant GST-*PfNek-4* protein kinase. Both the (a) Coomassie stained SDS-PAGE gel and the (b) autoradiogram of the coomassie stained gel: Lane 1: casein control; Lanes 2-5: various isolates of the recombinant GST-*PfNek-4* kinase with the casein substrate.



(a) SDS-PAGE gel of the kinase assay. (b) Autoradiogram.

Figure 4.10 The kinase assays with most active compounds. Panels (a) Dried SDS-PAGE gel and (b) autoradiograph, Lane 1: casein control (without enzyme), lane 2: kinase control (without test compound). Panel (b), lane 3: methylene blue, lane 4: safranin O, lane 5: mercury orange, lane 6: JLP118.1, lane 7: JLP093, lane 8: Guanosine, lane 9: inosine, lane 10. Not shown are: carbon black, lane 11: curcumin, lanes 12-19: IP 1-8 and lane 20: quinine, which were on a separate gel.

However at the time of performing the kinase inhibition assay, phosphorylation of the casein substrate was not visualised in the kinase control (lane 2: without test compound) suggesting that the isolated recombinant protein had no kinase activity (Figure 4.10a). The casein protein was visualised in the coomassie stained SDS-PAGE gel (Figure 4.10a), however there was no corresponding band in the autoradiograph (Figure 4.10b). This indicates that the GST-*PfNek4* recombinant protein kinase had no enzymatic activity. The kinase assay was repeated in three separate experiments using different GST-*PfNek4* isolates, and all were inactive.

4.4.5 Plasmid isolation and restriction analysis of *PfNek4*

As a first step to determine the reason for the loss of kinase activity, plasmids were isolated from six different colonies and then subjected to restriction digest to allow analysis of the *PfNek4* DNA insert. Restriction digests of isolated plasmid were carried out by exposure to *Bam*HI and *Sal*I restriction enzymes. Agarose gel electrophoresis of the product samples demonstrated the presence of a band corresponding to the size of the *PfNek4* insert which is 933 bp. Included was the undigested plasmid control which shows the undigested plasmid (Figure 4.11). Although the 50 bp low molecular DNA ladder electrophoresed along the plasmid extracts did not resolve well, the 1,350 bp and 916 bp high-intensity bands were visualised. *PfNek4* DNA insert band with a predicted size of 933 bp was positioned between 1,350 bp and 916 bp bands. The additional smaller fragments seen in Figure 4.11 (lanes 2-7) indicate potential “star” (non-specific) activity of the restriction enzymes or may be an indication of plasmid instability (Godiska *et al.*, 2010). Although both *Bam*HI and *Sal*I were supplied with pH 7.4 buffers (25°C), the optimum pH levels for 100% activity are pH 8.0 for

*Bam*HI and pH 7.5 for *Sal*I at 37°C. The restriction digest reactions in the current study were performed at pH 7.9, 37°C.

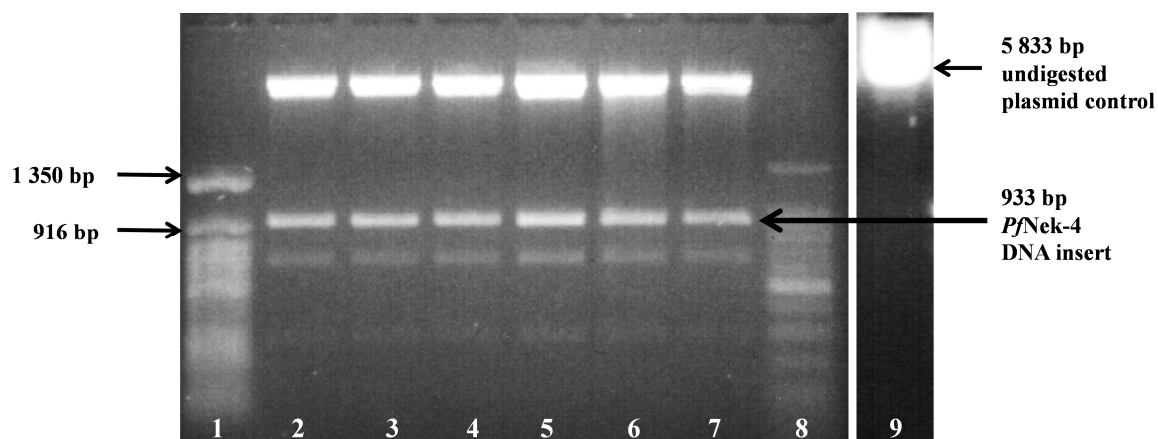


Figure 4.11 Agarose gel electrophoresis of plasmid extracts fragmented with site-specific restriction digest enzymes, *Bam*HI and *Sal*I. Lane1: 50 bp DNA ladder, lanes 2-4: *PfNek*-4 (A) plasmid restriction digest, lanes 5-7: *PfNek*-4 (B) plasmid restriction digests and lane 8: 100 bp DNA ladder undigested plasmid control, lane 9: *PfNek*-4 (A) undigested plasmid control.

4.4.6 Nucleotide sequence analysis

Since the restriction digestion showed a band of the correct size of 933 bp, the DNA sequence of the insert and surrounding plasmid was determined. The plasmid was sequenced across the insert sites in order to determine if the reading frame of the *PfNek*-4 sequence was maintained. The *PfNek*-4 insert DNA nucleotide sequence was compared to the plasmid sequence as well as the published *PfNek*-4 complete coding sequence. The chromatographs (Appendix B4) show the nucleotide sequencing results of both *PfNek*-4 A and B clones produced by Inqaba Biotec. Consensus sequence data from both forward and reverse sequences of *PfNek*-4 (clones A and B) was edited and generated by Inqaba Biotec and was used for sequence analysis.

The BLASTn results for the *PfNek*-4 (clone-A) nucleotide sequence (Figure 4.12) showed that the plasmid was inserted in the correct orientation with the start codon (ATG) in the correct position (23rd position, after the primer sequence). In addition the *PfNek*-4 (clone-A) insert sequence was 100% identical to the published sequence. The open reading frame (ORF) and restriction sites (*Bam*HI and *Sal*I) identified and annotated using the CLC Main Workbench (version 6.8.1) software, further confirmed that the *PfNek*-4 DNA insert was in frame (Figure 4.13).

Score	Expect	Identities	Gaps	Strand
1724 bits(933)	0.0()	933/933(100%)	0/933(0%)	Plus/Plus
Clone-A 11		ATGAATAAATATGAAAAGATTAGAGATATAGGAAAAGGAAATTATGGAAATACAATACTT		70
PfNek-4 1		ATGAATAAATATGAAAAGATTAGAGATATAGGAAAAGGAAATTATGGAAATACAATACTT		60//
Clone-A 851		CCTTTAAAAGAAAAGCCAGCTATTGAAAATGAAAATTCAGGAGCCAACGAACAAGAAGTA		910
PfNek-4 841		CCTTTAAAAGAAAAGCCAGCTATTGAAAATGAAAATTCAGGAGCCAACGAACAAGAAGTA		900
Clone-A 911		AAAACATTACTTCTGGATGTTGTTGATACTTAA		943
PfNek-4 901		AAAACATTACTTCTGGATGTTGTTGATACTTAA		933

Figure 4.12 Nucleotide sequence alignment of *PfNek-4* (clone-A) consensus sequence. BLASTn results of *PfNek-4* (clone-A) showing 100% alignment with the coding sequence of *PfNek-4* on the NCBI database. The pipe (|) shows nucleotide alignment. *PfNek-4* (A) 5' sequence showing **ATG** = start codon (1st position), **TAA** = stop codon (position 930). Results are truncated (//), the full results are shown in Appendix D1.

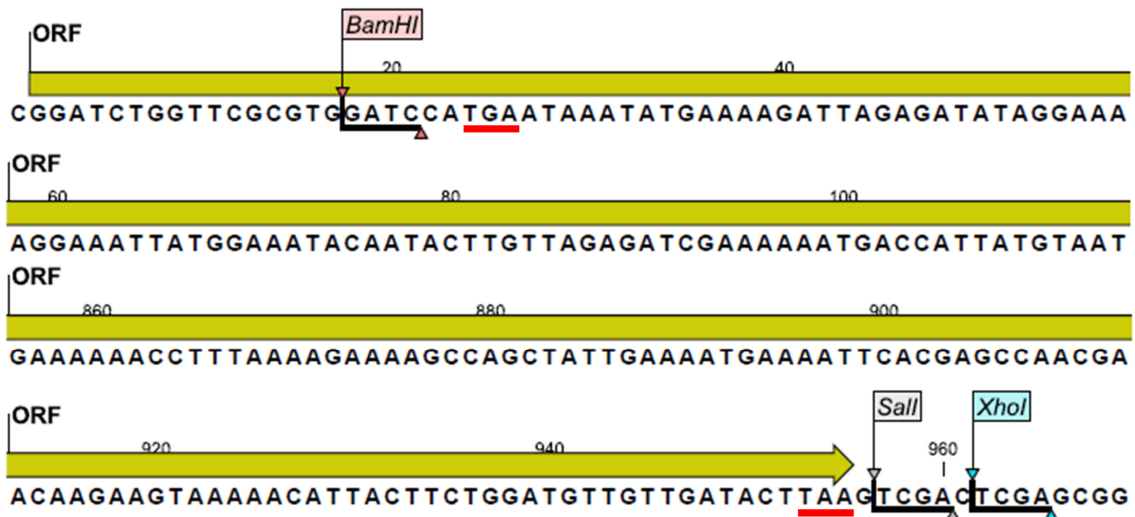


Figure 4.13 Open Reading Frame showing the DNA insert of *PfNek-4* (clone-A) and restriction sites. The restriction sites for the *PfNek-4* were *BamHI* and *SalI*. The start and stop codon are underlined in red.

Similarly, *PfNek-4* (clone-B) BLASTn results showed a 100% nucleotide sequence alignment with the coding sequence for *PfNek-4* gene (Figure 4.14). The insert sequence was identified within the ORF (Figure 4.15).

	Score	Expect	Identities	Gaps	Strand
	1724 bits(933)	0.0()	933/933(100%)	0/933(0%)	Plus/Plus
Clone-B	21	ATGAATAAATATGAAAAGATTAGAGATATAGGAAAAGGAAATTATGGAAATACAATACTT	80		
PfNek-4	1	ATGAATAAATATGAAAAGATTAGAGATATAGGAAAAGGAAATTATGGAAATACAATACTT	60//		
Clone-B	861	CCTTTAAAAGAAAAGCCAGCTATTGAAAATGAAAATTCAGGAGCCAACGAACAAGAAGTA	920		
PfNek-4	841	CCTTTAAAAGAAAAGCCAGCTATTGAAAATGAAAATTCAGGAGCCAACGAACAAGAAGTA	900		
Clone-B	921	AAAACATTACTTCTGGATGTTGTTGATACTTAA	953		
PfNek-4	901	AAAACATTACTTCTGGATGTTGTTGATACTTAA	933		

Figure 4.14 Nucleotide sequence alignment of *PfNek-4* (clone-B) consensus sequence. BLASTn results of *PfNek-4* (clone-B) showing 100% alignment with the coding sequence of *PfNek-4* on the NCBI database. Results are truncated (//), the full results are shown in Appendix D2.

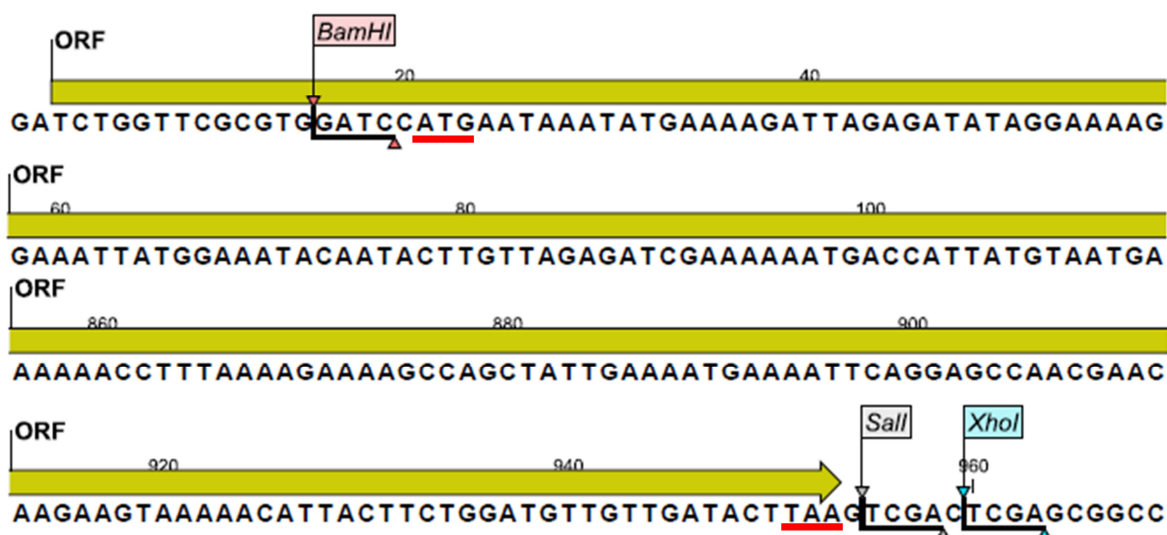


Figure 4.15 Open Reading Frame showing the DNA insert of *PfNek-4* (clone-B) and restriction sites. The restriction sites for the *PfNek-4* were *Bam*HI and *Sal*I. The start and stop codon are underlined in red.

4.4.7 Protein sequence analysis

The recombinant *PfNek-4* (clone-A) nucleotide sequence was used to obtain the predicted amino acid sequence by using the basic local alignment search tools (BLASTx) tool on NCBI. *PfNek-4* (clone-A) showed no mutations on the amino acid residues and showed 100% alignment with the *P. falciparum* Nek-4 protein kinase amino acid sequence (Figure 4.16). The BLASTx results for clone-B (Figure 4.17) matched 100% identities and no mutations were identified on the amino acid residues.

Clone-A	11	MNKYEKIRDIGKGNYGNTILVRDRKNDHYVMKIINISQMSQKEKRQCLKEVELLSKLNHP	190
		MNKYEKIRDIGKGNYGNTILVRDRKNDHYVMKIINISQMSQKEKRQCLKEVELLSKLNHP	
PfNek-4	1	MNKYEKIRDIGKGNYGNTILVRDRKNDHYVMKIINISQMSQKEKRQCLKEVELLSKLNHP	60
Clone-A	191	FIVKYIESYIEGDTLRIVMKHCKGGDLYHYIQNKKKQNTPIKEKRILIWLTOILTALKFL	370
		FIVKYIESYIEGDTLRIVMKHCKGGDLYHYIQNKKKQNTPIKEKRILIWLTOILTALKFL	
PfNek-4	61	FIVKYIESYIEGDTLRIVMKHCKGGDLYHYIQNKKKQNTPIKEKRILIWLTOILTALKFL	120
Clone-A	371	HSNHILHRDMKSLNILIDSDKRVRLCDFGISKVLENTLDYANTLIGTPYYLSPELCKDKK	550
		HSNHILHRDMKSLNILIDSDKRVRLCDFGISKVLENTLDYANTLIGTPYYLSPELCKDKK	
PfNek-4	121	HSNHILHRDMKSLNILIDSDKRVRLCDFGISKVLENTLDYANTLIGTPYYLSPELCKDKK	180
Clone-A	551	YSWPSDVWATGCLIIYELATFRTPFHSTKGIQQLCYNIRYAPIPDLPNISKELNNIYKSM	730
		YSWPSDVWATGCLIIYELATFRTPFHSTKGIQQLCYNIRYAPIPDLPNISKELNNIYKSM	
PfNek-4	181	YSWPSDVWATGCLIIYELATFRTPFHSTKGIQQLCYNIRYAPIPDLPNISKELNNIYKSM	240
Clone-A	731	LIREPSYRATVQQLLVSDIVQRQLKLLIEEKIREKQSMKKPLKEKPAIENENSGANEQEV	910
		LIREPSYRATVQQLLVSDIVQRQLKLLIEEKIREKQSMKKPLKEKPAIENENSGANEQEV	
PfNek-4	241	LIREPSYRATVQQLLVSDIVQRQLKLLIEEKIREKQSMKKPLKEKPAIENENSGANEQEV	300
Clone-A	911	K 913	
		K	
PfNek-4	301	K 301	

Figure 4.16 Alignment of translated amino acid sequence of clone-A to *PfNek-4*. The BLASTx results showed no mutations on amino acid residues. The amino acid sequence was represented in a single-letter amino acid code (Appendix E).

Clone-B	21	MNKYEKIRDIGKGNYGNTILVRDRKNDHYVMKIINISQMSQKEKRQCLKEVELLSKLNHP	200
		MNKYEKIRDIGKGNYGNTILVRDRKNDHYVMKIINISQMSQKEKRQCLKEVELLSKLNHP	
PfNek-4	1	MNKYEKIRDIGKGNYGNTILVRDRKNDHYVMKIINISQMSQKEKRQCLKEVELLSKLNHP	60
Clone-B	201	FIVKYIESYIEGDTLRIVMKHCKGGDLYHYIQNKKKQNTPIKEKRILIWLTOILTALKFL	380
		FIVKYIESYIEGDTLRIVMKHCKGGDLYHYIQNKKKQNTPIKEKRILIWLTOILTALKFL	
PfNek-4	61	FIVKYIESYIEGDTLRIVMKHCKGGDLYHYIQNKKKQNTPIKEKRILIWLTOILTALKFL	120
Clone-B	381	HSNHILHRDMKSLNILIDSDKRVRLCDFGISKVLENTLDYANTLIGTPYYLSPELCKDKK	560
		HSNHILHRDMKSLNILIDSDKRVRLCDFGISKVLENTLDYANTLIGTPYYLSPELCKDKK	
PfNek-4	121	HSNHILHRDMKSLNILIDSDKRVRLCDFGISKVLENTLDYANTLIGTPYYLSPELCKDKK	180
Clone-B	561	YSWPSDVWATGCLIIYELATFRTPFHSTKGIQQLCYNIRYAPIPDLPNISKELNNIYKSM	740
		YSWPSDVWATGCLIIYELATFRTPFHSTKGIQQLCYNIRYAPIPDLPNISKELNNIYKSM	
PfNek-4	181	YSWPSDVWATGCLIIYELATFRTPFHSTKGIQQLCYNIRYAPIPDLPNISKELNNIYKSM	240
Clone-B	741	LIREPSYRATVQQLLVSDIVQRQLKLLIEEKIREKQSMKKPLKEKPAIENENSGANEQEV	920
		LIREPSYRATVQQLLVSDIVQRQLKLLIEEKIREKQSMKKPLKEKPAIENENSGANEQEV	
PfNek-4	241	LIREPSYRATVQQLLVSDIVQRQLKLLIEEKIREKQSMKKPLKEKPAIENENSGANEQEV	300
Clone-B	921	K 923	
		K	
PfNek-4	301	K 301	

Figure 4.17 Alignment of translated amino acid sequence of clone-B to *PfNek-4*. The amino acid sequence was represented in a single-letter amino acid code (Appendix E).

A protein search (BLASTp) on the *PfNek-4* (clone-A) predicted amino acid sequence returned 100 hits. Of the 100 matches, only four from the *Plasmodium* species showed a maximum score (difference of the sum of identities/mismatches and sum of gap penalties) greater than or equal to 1000 (Table 4.2). The highest ranking match (100% identities) was

with *Plasmodium falciparum* (3D7) Nek-4 protein kinase (maximum score: 1618), with the lowest expect (E) value. The *Homo sapiens* Nek4 (hNek4) showed the least orthology (42%) which shows differences or uniqueness of the *P. falciparum* NimA-related protein kinase structures as compared to the hNek4 protein kinase. The results (Table 4.2) again ruled out any mutations within the nucleotide sequence of the recombinant *PfNek-4* DNA.

Table 4.2 Homologous protein sequences to *PfNek-4* (clone-A).

Accession	Source	Length	Score	Identities (%)	E-value
XP_002808785.1	Protein kinase, <i>Plasmodium falciparum</i> (isolate 3D7), <i>PfNek-4</i>	310	1618	100.0	0.0
XP_677620.1	Serine/threonine protein kinase 2, putative, <i>Plasmodium berghei</i> (strain ANKA)	310	1571	96.0	0.0
XP_001612826.1	Serine/threonine protein kinase NEK4, putative, <i>Plasmodium vivax</i> (strain Salvador I)	310	1570	96.0	0.0
GAB64821.1	Serine/threonine protein kinase NEK4, <i>Plasmodium cynomolgi</i> strain B	361	1508	82.0	0.0
XP_002261112.1	Serine/threonine protein kinase 2, putative, <i>Plasmodium knowlesi</i> (strain H)	307	1372	87.0	0.0
AAH15515.1	NEK4, <i>Homo sapiens</i>	451	228	42.0	8×10^{-67}

Protein sequences that showed a maximum score ≥ 1000 and lowest E-values, are listed from a 100 hits generated from a BLASTp protein search on the NCBI database.

4.5 Discussion

The SDS-PAGE gels confirmed the MW of the GST-*PfNek-4* fusion protein in line with the predicted size and the MW of the GST and *PfNek-4* protein, by elucidation (Figure 4.6). The GST-tagged *PfNek-4* (clones A and B) protein were identified and visualised by Western immunoblotting (Figure 4.7). Since the GST-*PfNek-4* fusion protein did not show any kinase activity, the plasmids were isolated and the *PfNek-4* DNA insert analysed in order to determine factors that may have contributed the kinase inactivity. Restriction enzyme digest products analysed using agarose electrophoresis showed plasmid inserts with the correct size (933 bp) as well as smaller fragments, due to potential star activity of restriction enzymes or plasmid instability (Godiska *et al.*, 2010). Thereafter, agar plates with bacterial cells

containing the plasmids with the *PfNek-4* DNA insert were submitted to Inqaba Biotech, for nucleotide sequencing of the plasmids. The nucleotide sequence alignment of the *PfNek-4* DNA insert with the published coding sequence for the *PfNek-4* gene (PlasmoDB identifier: PF3D7_0719200, formerly MAL7P1.100), confirmed the match to the native gene (Figure 4.12). Therefore no mutations were identified in the nucleotide residues. The kinase assay results, however, did not demonstrate any kinase activity of *PfNek-4* (A) on the casein substrates (Figure 4.10b). As a result, the inhibitory activity of test compounds could not be evaluated. The functionality of a recombinant protein can be affected by post-transcriptional modifications of the protein itself. These modifications include folding of the newly formed polypeptide chain into its tertiary, three-dimensional and quaternary (spatial arrangements of subunits) structures and are critical to the functioning of a protein (Pollard and Earnshaw, 2004). Protein folding is determined by the amino acid sequence of the protein. Efficient protein folding requires additional factors called chaperones, which bind to newly formed and misfolded proteins to stabilise partially folded polypeptides and assist in their folding or refolding. (Pollard and Earnshaw, 2004). Although the *E. coli* BL21 expression vector was the most efficient vector for the expression of *PfNek-4* protein kinase, it was still not identical to the *P. falciparum* organism.

However, basal level expression (expression in the absence of an inducer, in this case IPTG) of the *PfNek-4* enzyme was detected on the Western Blot (Figure 4.7), meaning that the expression of the *PfNek-4* enzyme was not tightly regulated by the repressor and promoter genes. Some, basal level expression is associated with most inducible promoters (Amersham-Biosciences, 2002). This basal level expression has been shown to affect the outcome of cloning experiments for toxic inserts by selecting against inserts cloned in the proper orientation (Amersham-Biosciences, 2002). However, in the current study, the *PfNek-4* DNA insert was in frame and the fusion protein was expressed.

The casein protein was visualised with coomassie staining of the SDS-gel (Figure 4.10a), although it would have been detected on the autoradiograms provided the *PfNek-4* was functionally capable of phosphorylating the protein. Casein from bovine milk consists of four subunits: α -s1, α -s2, β -casein and κ -casein and their MWs range from 19-25 kDa, and *PfNek-4* has the ability to autophosphorylate and phosphorylate exogenous β -casein substrate, with the exception of myelin basic protein and histone-1 substrates as previously reported (Pardo and Natalucci, 2002; Reininger *et al.*, 2009). However, no kinase activity was detected.

The test compounds were not tested on the whole gametocytes of the *P. falciparum* parasites as it was beyond the scope of the current study and it would have only been considered if any of the test compounds were shown to inhibit GST-PfNek-4 kinase activity. A study by Reininger *et al.* (2012), suggests that PfNek-4 is not responsible for switching erythrocytic schizogony to gametocytogenesis, but rather a molecular marker of sexually committed and sexually pre-committed schizonts (Reininger *et al.*, 2012). Nevertheless, NimA-related kinases putatively involved in the regulation of the gametocyte stages, are still critical drug targets to prevent human host-vector transmission.

In order to ensure protein kinase activity, future studies could include re-transformation of the *E. coli* cells with the pGEX-4T-3 vectors containing the PfNek-4 DNA insert. In addition the kinase assay conditions such as pH can be optimised, taking into consideration the isoelectric point of the protein kinase.

Chapter 5 Conclusions

The aim of the study was to investigate the *in vitro* antimalarial activity of 56 select compounds against the intra-erythrocytic stages of *P. falciparum*, alone and in combination with the classical antimalarial drug, quinine using the [³H]-hypoxanthine incorporation assay. Drug interactions were classified as marked synergism ($0 > \Sigma\text{FIC}_{50} < 0.5$), slight synergism ($0.5 \geq \Sigma\text{FIC}_{50} < 1$), additive interaction ($1 \geq \Sigma\text{FIC}_{50} < 2$), slight antagonism ($2 \geq \Sigma\text{FIC}_{50} < 4$) and marked antagonism ($2 \geq \Sigma\text{FIC}_{50} < 4$) (Gupta *et al.*, 2002; Bell, 2005). The screening concentration of compounds was at 100 μM for synthetic compounds and at 100 $\mu\text{g/ml}$ for natural compounds. The malaria parasites were exposed over a 48 h single-cycle to the test compounds which included synthetic and natural colourants, novel nucleoside analogues and imidazopyridine analogues. Stage and morphology studies were carried out in order to determine which parasite stages were most sensitive to the most active test compounds from each compound class. The haemolytic activity was investigated to test whether the host RBC cell membrane's integrity was affected by most active test compounds, thereby eliminate haemolysis as a mechanism of action. The ability of the most active test compounds to inhibit the haemozoin formation pathway, which is an ideal drug target similarly to classical antimalarial drugs such as quinine and chloroquine, was investigated.

In order to identify test compounds with low toxicity, the selectivity of the most active compounds for *P. falciparum* rather than human cells was investigated. The selectivity index was calculated by dividing the antimalarial IC_{50} by the cytotoxicity IC_{50} values (obtained using the [³H]-thymidine incorporation assay) against the transformed human HEK293 and leukaemic K562 cell lines. A test compound that demonstrated a selectivity index greater than 10 was regarded as more selective to *P. falciparum* relative to human cell lines. The study also aimed to investigate the inhibitory activity of the most active compounds against the recombinant NIMA-related *PfNek-4* protein kinase activity.

5.1 Synthetic colourants

Methylene blue was significantly ($p < 0.05$) more potent against *P. falciparum* compared to quinine (Table 5.1). Both methylene blue and safranin O displayed negligible toxicity to uninfected human RBCs (Table 2.5). Combination studies with methylene blue and quinine demonstrated a synergistic interaction, whilst safranin O showed an additive interaction with quinine (Table 5.1). Therefore, there is potential for the latter compounds to be used in combination with quinine without compromising the overall antimalarial activity. Both

methylene blue and safranin O did not demonstrate inhibitory activity against the *in vitro* formation of β -haematin crystal formation, although literature has reported that methylene blue can inhibit β -haematin formation within the parasite's food vacuole (Atamna *et al.*, 1996). The schizont stage (32-40 h) was most sensitive to methylene blue at IC₉₀ concentration, indicating that it may have other modes of action, which need to be explored further. Methylene blue demonstrated the highest selectivity indices (480-968, 2-fold selective compared to quinine) indicating low toxicity to human cells but selective inhibitory effects on *P. falciparum* (Table 5.1). In comparison, safranin O was 33 to 22-fold less selective than methylene blue, although both selective indices were above 10 (Table 5.1). Both methylene blue and safranin O showed 'drug-like' properties based on the Lipinski's Rule of Five (Ro5). The predicted % ionisation values at pH 5.0, showed that safranin O would accumulate within the parasite's digestive vacuole similarly to chloroquine and quinine, whilst methylene blue was not ionisable at the same acidic environment (Table 2.13). Therefore, methylene blue's mode of action could not have been facilitated by its acid-base properties. The current study confirmed the potent antimalarial activity of methylene blue and its selectivity for *P. falciparum*. In addition, the chemical structure of methylene blue may serve as a template for the development of safer and affordable drugs, which can be used in combination therapy with other antimalarial drugs such as artemisinin or quinine.

5.2 Curcumin

The natural colourant, curcumin (diferuloylmethane) was significantly ($p < 0.05$) less potent against *P. falciparum* than quinine (Table 5.2) and showed slight haemolytic activity (at 100 $\mu\text{g/ml}$) although this haemolysis was significantly ($p < 0.05$) higher than for quinine (Table 2.6). However, curcumin's haemolytic activity is of no clinical significance since a low peak plasma concentration (C_{max} : $2.30 \pm 0.26 \mu\text{g/ml}$ after a single oral dose of 10 g) has previously been reported without adverse events in human subjects (Vareed *et al.*, 2008). The antimalarial activity of curcumin in combination with quinine, showed an additive interaction, which did not compromise the drug potency of quinine (Table 5.2). Curcumin was 78-fold more active in inhibiting β -haematin formation than quinine, indicating a possible mechanism of action. Study findings by Cui *et al.* (2007) suggest that curcumin has the potential to disable gene transcription within the *P. falciparum* parasite, by inhibiting nuclear histone acetyltransferase activity, as well as inhibit parasite growth by generating ROS. The predicted % ionisation of curcumin showed that it would be absorbed down the pH gradient of 7.4-5.0 with a low degree of ionisation or accumulation in the parasite's digestive vacuole (Table 2.13). In comparison to quinine, curcumin was significantly ($p < 0.05$) toxic to both HEK293

and K562 cell lines and showed selectivity indices below 1, indicating poor selectivity for *P. falciparum* (Table 5.2). The current study confirmed the antimalarial potency of curcumin similarly to that reported in a previous study on the chloroquine-sensitive 3D7 strain of *P. falciparum* (Cui *et al.*, 2007). In addition, curcumin showed potential as an anticancer agent as it significantly ($p < 0.05$) inhibited the *in vitro* growth of the K562 leukaemic cell line compared to the HEK293 transformed epithelial cells and was only 26-times less potent than the anticancer drug, camptothecin, as compared to quinine at 1021-times less cytotoxicity.

5.3 Nucleoside analogues

The most active pyrimidine-based nucleoside analogues, JLP118.1 and JLP093 (cytosine nucleobase), demonstrated inhibitory activities ($IC_{50} < 3 \mu\text{M}$) significantly ($p < 0.05$) less potent than quinine and both showed negligible haemolytic activity (Table 5.1). The trophozoite stage of *P. falciparum* parasites was particularly sensitive to JLP118.1, but not as a result of the inhibition of β -haematin crystal formation (Table 2.16). The uracil nucleobase containing JLP118.1, had a tert-butyl-dithiomethyl-hydroxyl group and a modified deoxyribose sugar containing acetate groups, whilst on the JLP093 chemical structure (with a cytosine nucleobase), there were tert-butyl-diphenylsilyl and hydroxyl group substitutions (Table 2.10). Both nucleosides were significantly ($p < 0.05$) more toxic to HEK293 and K562 cells than quinine and showed selectivity indices below 6, indicating poor selectivity for *P. falciparum* parasites (Table 5.1). The promising antimalarial activity of the nucleoside analogues, JLP118.1 and JLP093, warrants further investigation and targeted compound design in order to enhance antimalarial potency, as well as reduce toxicity to human cells.

5.4 Imidazopyridine analogues

The most active imidazopyridine analogues, IP-3 and IP-4, demonstrated the least potent antimalarial activity (IC_{50} range: 15-21 μM) of all the synthetic compounds tested and were significantly ($p < 0.05$) less active than quinine (Table 5.1). IP-4 arrested the development of the intra-erythrocytic parasites at the trophozoite stage. The imidazopyridine analogues were not tested for haemolytic activity and β -haematin crystal formation inhibition due to limited availability of stock. IP-3 and -4 were significantly ($p < 0.05$) more toxic to HEK293 and K562 cell lines than quinine. However, the K562 leukaemic cell line was significantly ($p < 0.05$) less sensitive to both IP-3 and -4 (Table 5.1). In addition, the selective indices of IP-3 and IP-4 were below 1, indicating poor selectivity for *P. falciparum* (Table 5.1). Therefore, the potential of these imidazopyridine analogues as antimalarial could not be established, but may be investigated further for their anticancer properties.

5.5 Potential inhibition of PfNek-4 protein kinase activity

The inhibitory activity of all active compounds, against the *PfNek-4* protein kinase activity, could not be determined since the kinase activity of the recombinant GST-fused *PfNek-4* protein was lost. Following troubleshooting experiments and nucleotide sequencing, the long storage period (4 days) at 4°C in the elution buffer pH 8.0 (instead of freezing in 50% glycerol), was attributed to the denaturing of the GST-*PfNek-4* protein kinase. Freezing in 50% glycerol would have retained kinase activity. However, time constraints did not permit for the establishment and optimisation of the kinase activity. Nevertheless, future screening of novel compounds targeted for protein kinases involved in gametocytogenesis and the sexual stages may yield results in blocking the transmission of *P. falciparum* from infected human hosts to the mosquito vectors. This would contribute in controlling if not eradicate the virulent malaria infections caused by *P. falciparum*.

Overall, the test compounds displayed variable ability to inhibit parasite growth with 21% of the test compounds inhibiting more than 80% parasite growth at a concentration of 100 µM or 100 µg/ml. The study highlights the potential of synthetic and natural colourants, and nucleoside analogues as antimalarial agents. Other modes of action such as lipid peroxidation and free radical scavenging activity and inhibitory activity against *PfNek-4* and other *P. falciparum* targets can be explored. (Motulsky, 2003)

Table 5.1 Summarised results of the most active synthetic compounds.

Compound	Antimalarial activity IC ₅₀ ± S.D. (µM)	Interaction with quinine ΣFIC ₅₀ ± S.D.	Cytotoxicity IC ₅₀ ± S.D. (µM)		Selectivity Index	
			HEK293	K562	HEK293	K562
Methylene blue	0.004 ± 0.00	Slightly synergistic (0.64 ± 0.31)	1.92 ± 0.18	3.87 ± 0.48	480	968
Safranin O	0.087 ± 0.00	Additive (1.01 ± 0.09)	1.26 ± 0.19	3.76 ± 0.00	14.5	43.2
JLP118.1	1.79 ± 0.12	ND	9.75 ± 1.55	8.42 ± 0.47	5.5	4.7
JLP093	2.38 ± 0.11	ND	10.1 ± 0.89	22.82 ± 0.83	4.2	4.8
IP-3	20.77 ± 0.72	ND	9.15 ± 1.51	16.63 ± 0.35	0.4	0.8
IP-4	15.30 ± 0.41	ND	9.14 ± 1.11	14.0 ± 0.38	0.6	0.9
Quinine	0.10 ± 0.01	-	18.51 ± 2.24	28.33 ± 1.79	180	458
Camptothecin	ND	ND	0.02 ± 0.01	0.04 ± 0.01	ND	ND

The fractional IC₅₀ values (ΣFIC₅₀) in parentheses were calculated by dividing the IC₅₀ value of the compound in combination with quinine by the IC₅₀ value of the compound alone. ND, not determined due to availability of stock.

Table 5.2 Summarised results of the natural curcumin colourant.

Compound	Antimalarial activity IC ₅₀ ± S.D. (µg/ml)	Interaction with quinine ΣFIC ₅₀ ± S.D.	Cytotoxicity IC ₅₀ ± S.D. (µg/ml)		Selectivity Index	
			HEK293	K562	HEK293	K562
Curcumin	2.29 ± 0.18	Additive (1.20 ± 0.07)	1.37 ± 0.11	0.26 ± 0.10	0.6	0.1
Quinine	0.04 ± 0.01	-	6.68 ± 2.24	10.21 ± 1.79	167	255
Camptothecin	ND	ND	0.01 ± 0.00	0.01 ± 0.00	ND	ND

The fractional IC₅₀ values (ΣFIC₅₀) in parentheses were calculated by dividing the IC₅₀ value of the compound in combination with quinine by the IC₅₀ value of the compound alone. ND, not determined due to availability of stock.

References

- Akoachere, M., Buchholz, K., Fischer, E., Burhenne, J., Haefeli, W.E., Schirmer, R.H., *et al.* (2005). *In Vitro* Assessment of Methylene Blue on Chloroquine-Sensitive and -Resistant *Plasmodium falciparum* Strains Reveals Synergistic Action with Artemisinins. *Antimicrobial Agents and Chemotherapy*. **49**(11), 4592-4597.
- Alberts, B., Alexander, J., Lewis, J., Raff, M., Roberts, K. and Peter, W. (2008a). The Cell Cycle. *Molecular Biology of the Cell*. 5th ed. Garland Publishing, Inc.: New York, pp. 1053, 1055, 1060-1075.
- Alberts, B., Alexander, J., Lewis, J., Raff, M., Roberts, K. and Peter, W. (2008b). DNA, Chromosomes, and Genomes. *Molecular Biology of the Cell*. 5th ed. Garland Publishing, Inc.: New York, pp. 197-220, 243-245.
- Alberts, B., Alexander, J., Lewis, J., Raff, M., Roberts, K. and Peter, W. (2008c). Proteins. *Molecular Biology of the Cell*. 5th ed. Garland Publishing, Inc.: New York, pp. 175-177.
- Alberts, B., Bray, D., Hopkin, K., Johnson, A., Lewis, J., Raff, M., *et al.* (2004). DNA and Chromosomes. *Essential Cell Biology*. 2nd ed. Garland Publishing, Inc.: New York, pp. 169-191.
- Allegra, M., Furtmüller, P.G., Jantschko, W., Zederbauer, M., Tesoriere, L., Livrea, M.A., *et al.* (2005). Mechanism of interaction of betanin and indicaxanthin with human myeloperoxidase and hypochlorous acid. *Biochemical and Biophysical Research Communications*. **332**(3), 837-844.
- Altschul, S.F., Gish, W., Miller, W., Myers, E.W. and Lipman, D.J. (1990). Basic local alignment search tool. *Journal of Molecular Biology*. **215**(3), 403-410.
- Amersham-Biosciences (2002). GST Gene Fusion System Handbook, Amersham <http://www.amershambiosciences.com> [Accessed 13/06/2011].
- Anand, P., Kunnumakkara, A.B., Newman, R.A. and Aggarwal, B.B. (2007). Bioavailability of Curcumin: Problems and Promises. *Molecular Pharmaceutics*. **4**(6), 807-818.
- Anderson, M., Beattie, J.F., Breault, G.A., Breed, J., Byth, K.F., Culshaw, J.D., *et al.* (2003). Imidazo[1,2-*a*]pyridines: A potent and selective class of cyclin-dependent kinase inhibitors identified through structure-based hybridisation. *Bioorganic & Medicinal Chemistry Letters*. **13**(18), 3021-3026.
- Andersson, L.C., Nilsson, K. and Gahmberg, C.G. (1979). K562 - A human erythroleukemic cell line. *International Journal of Cancer*. **23**(2), 143-147.
- Arnot, D.E. and Gull, K. (1998). The *Plasmodium* cell cycle: facts and questions. *Annals of Tropical Medicine & Parasitology*. **92**(4), 361.
- Arnot, D.E., Ronander, E. and Bengtsson, D.C. (2011). The progression of the intra-erythrocytic cell cycle of *Plasmodium falciparum* and the role of the centriolar plaques in asynchronous mitotic division during schizogony. *International Journal for Parasitology*. **41**(1), 71-80.

- Atamna, H., Krugliak, M., Shalmiev, G., Deharo, E., Pescarmona, G. and Ginsburg, H. (1996). Mode of antimalarial effect of methylene blue and some of its analogues on *Plasmodium falciparum* in culture and their inhibition of *P. vinckei petteri* and *P. yoelii nigeriensis* in vivo. *Biochemical Pharmacology*. **51**(5), 693-700.
- Atamna, H. and Kumar, R. (2010). Protective Role of Methylene Blue in Alzheimer's Disease via Mitochondria and Cytochrome c Oxidase. *Journal of Alzheimer's Disease*. **20**, 439-452.
- Atamna, H., Pascarmona, G. and Ginsburg, H. (1994). Hexose-monophosphate shunt activity in intact *Plasmodium falciparum*-infected erythrocytes and in free parasites. *Molecular and Biochemical Parasitology*. **67**(1), 79-89.
- Aulton, M.E. (2002). Pharmaceutics: The Science of Dosage Form Design. In: Aulton, M. E. (Ed.) *Properties of solutions*. 2nd ed. Churchill Livingstone: Edinburgh, pp. 33-40.
- Azeredo, H.M.C. (2009). Betalains: properties, sources, applications, and stability – a review. *International Journal of Food Science & Technology*. **44**(12), 2365-2376.
- Baird, J.K. (1984). Methylene blue-mediated hexose monophosphate shunt stimulation in human red blood cells *in vitro*: Independence from intracellular oxidative injury. *International Journal of Biochemistry*. **16**(10), 1053-1058.
- Baker, L. (2009). Malaria prophylaxis – make the right choice for travellers with special circumstances. *South African Journal of Epidemiology and Infection*. **24**(4), 44-49.
- Balasubramanyam, K., Varier, R.A., Altaf, M., Swaminathan, V., Siddappa, N.B., Ranga, U., et al. (2004). Curcumin, a Novel p300/CREB-binding Protein-specific Inhibitor of Acetyltransferase, Represses the Acetylation of Histone/Nonhistone Proteins and Histone Acetyltransferase-dependent Chromatin Transcription. *Journal of Biological Chemistry*. **279**(49), 51163-51171.
- Baldwin, S.A., McConkey, G.A., Cass, C.E. and Young, J.D. (2007). Nucleoside Transport as a Potential Target for Chemotherapy in Malaria. *Current Pharmaceutical Design*. **13**(6), 569-580.
- Bannister, L.H., Margos, G. and Hopkins, J.M. (2005). Making a home for *Plasmodium* post-genomics: Ultrastructural organisation of the blood stages. In: Sherman, I. W. (Ed.) *Molecular Approaches to Malaria*. ASM Press: Washington, D.C., pp. 24-45.
- Barnes, P.J., Adcock, I.M. and Ito, K. (2005). Histone acetylation and deacetylation: importance in inflammatory lung diseases. *European Respiratory Journal*. **25**(3), 552-563.
- Basilico, N., Pagani, E., Monti, D., Olliaro, P. and Taramelli, D. (1998). A microtitre-based method for measuring the haem polymerization inhibitory activity (HPIA) of antimalarial drugs. *Journal of Antimicrobial Chemotherapy*. **42**(1), 55-60.
- Bautista, A.R.P.L., Moreira, E.L.T., Batista, M.S., Miranda, M.S. and Gomes, I.C.S. (2004). Subacute toxicity assessment of annatto in rat. *Food and Chemical Toxicology*. **42**(4), 625-629.
- Becker, K., Tilley, L., Vennerstrom, J.L., Roberts, D., Rogerson, S. and Ginsburg, H. (2004). Oxidative stress in malaria parasite-infected erythrocytes: host–parasite interactions. *International Journal for Parasitology*. **34**(2), 163-189.

- Bell, A. (2005). Antimalarial drug synergism and antagonism: Mechanistic and clinical significance. *FEMS Microbiology Letters*. **253**(2), 171-184.
- Berenbaum, M.C. (1978). A method for testing for synergy with any number of agents. *Journal of Infectious Diseases*. **137**(2), 122-130.
- Berenbaum, M.C., Norden, C.W. and Jr, R.C.M. (1980). Correlations Between Methods for Measurement of Synergy. *The Journal of Infectious Diseases*. **142**(3), 476-480.
- Bernabé-Pineda, M., Ramírez-Silva, M.T., Romero-Romo, M., González-Vergara, E. and Rojas-Hernández, A. (2004). Determination of acidity constants of curcumin in aqueous solution and apparent rate constant of its decomposition. *Spectrochimica Acta Part A: Molecular and Biomolecular Spectroscopy*. **60**(5), 1091-1097.
- Bertaux, L., Taudon, N., Martelloni, M., Parzy, D., Pradines, B., Kraemer, P., *et al.* (2011). Quinine-resistant malaria in traveler returning from French Guiana, 2010. *Emerging Infectious Diseases*. <http://dx.doi.org/10.3201/eid1705.101424> [Accessed 03/02/2012].
- Bhal, S.K., Kassam, K., Peirson, I.G. and Pearl, G.M. (2007). The Rule of Five Revisited: Applying Log D in Place of Log P in Drug-Likeness Filters. *Molecular Pharmaceutics*. **4**(4), 556-560.
- Bhaumik, S., Anjum, R., Rangaraj, N., Pardhasaradhi, B.V.V. and Khar, A. (1999). Curcumin mediated apoptosis in AK-5 tumor cells involves the production of reactive oxygen intermediates. *FEBS Letters*. **456**(2), 311-314.
- Bio-Rad. (2013). Mini Trans-Blot[®] electrophoretic transfer cell: Instruction manual. <http://www.bio-rad.com/webroot/web/pdf/lsr/literature/M1703930.pdf> [Accessed 15/01/2013].
- Birkett, A.J., Moorthy, V.S., Loucq, C., Chitnis, C.E. and Kaslow, D.C. (2013). Malaria vaccine R&D in the Decade of Vaccines: Breakthroughs, challenges and opportunities. *Vaccine*. **31**, **Supplement 2**, B233-B243.
- Blank, O., Davioud-Charvet, E. and Elhabiri, M. (2012). Interactions of the Antimalarial Drug Methylene Blue with Methemoglobin and Heme Targets in *Plasmodium falciparum*: A Physico-Biochemical Study. *Antioxidants & Redox Signaling*. **17**(4), 544-554.
- Bracchi-Ricard, V., Barik, S., Del Vecchio, C., Doerig, C., Chakrabarti, R. and Chakrabarti, D. (2000). PfPK6, a novel cyclin-dependent kinase/mitogen-activated protein kinase-related protein kinase from *Plasmodium falciparum*. *Biochemical Journal*. **347**(1), 255-263.
- Bradford, M.M. (1976). A rapid and sensitive method for the quantitation of microgram quantities of protein utilizing the principle of protein-dye binding. *Analytical Biochemistry*. **72**(1-2), 248-254.
- Brigelius-Flohe, R. and Traber, M.G. (1999). Vitamin E: function and metabolism. *The FASEB Journal*. **13**(10), 1145-1155.
- Britannica. (2013a). *Beet plant*. <http://www.britannica.com/EBchecked/topic/58462/beet> [Accessed 14/01/ 2013].
- Britannica. (2013b). *Cochineal dye*. <http://www.britannica.com/EBchecked/topic/123540/cochineal> [Accessed 14/01/ 2013].

- Britannica. (2013c). *Turmeric*. <http://global.britannica.com/EBchecked/topic/610223/turmeric> [Accessed 14/01/ 2013].
- Britton, G. (1983). *The biochemistry of natural pigments*. Cambridge University Press, Cambridge. pp. 3-239.
- Bruce, A., Bertino, J., Cleary, J., Ortiz, T., Lane, A., Supko, J.G., *et al.* (2011). Cytotoxic Agents. *In: Chabner, B. A. and Knollmann, B. C. (Eds.) Goodman & Gilman's The Pharmacological Basis of Therapeutics*. 12 ed. McGraw-Hill: New York. <http://0-www.accesspharmacy.com.innopac.wits.ac.za/content.aspx?aID=16680251> [Accessed 11/11/2013].
- Buchholz, K., Schirmer, R.H., Eubel, J.K., Akoachere, M.B., Dandekar, T., Becker, K., *et al.* (2008). Interactions of Methylene Blue with Human Disulfide Reductases and Their Orthologues from *Plasmodium falciparum*. *Antimicrobial Agents and Chemotherapy*. **52**(1), 183-191.
- Byrns, M.C. and Penning, T.M. (2011). Environmental Toxicology: Carcinogens and Heavy Metals. *In: Chabner, B. A. and Knollmann, B. C. (Eds.) Goodman & Gilman's The Pharmacological Basis of Therapeutics*. 12 ed. McGraw-Hill: New York. <http://0-www.accesspharmacy.com.innopac.wits.ac.za/content.aspx?aID=16682725> [Accessed 11/12/2013].
- Cassera, M.B., Zhang, Y., Hazleton, K.Z. and Schramm, V.L. (2011). Purine and pyrimidine pathways as targets in *Plasmodium falciparum*. *Current topics in medicinal chemistry*. **11**(16), 2103-2115.
- Centers for Disease Control. (2011). *Malaria life cycle*. http://www.dpd.cdc.gov/dpdx/HTML/frames/M-R/Malaria/body_Malaria_page1.htm#LifeCycle [Accessed 25/04/2011].
- Chemaly, S.M., Chen, C.T. and van Zyl, R.L. (2007). Naturally occurring cobalamins have antimalarial activity. *Journal of Inorganic Biochemistry*. **101**(5), 764-773.
- Chen, A.L., Hsu, C.H., Lin, J.K., Hsu, M.M., Ho, Y.F., She, T.S., *et al.* (2001). Phase I clinical trial of curcumin, a chemopreventive agent, in patients with high-risk or pre-malignant lesions. *Anticancer Research*. **21**(4 B), 2895-2900.
- Chung, K.T., Stevens, S.E.J. and Cerniglia, C.E. (1992). The reduction of azo dyes by the intestinal microflora. *Critical Reviews in Microbiology*. **18**(3), 175-90.
- Clarkson, C., Maharaj, V.J., Crouch, N.R., Grace, O.M., Pillay, P., Matsabisa, M.G., *et al.* (2004). *In vitro* antiplasmodial activity of medicinal plants native to or naturalised in South Africa. *Journal of Ethnopharmacology*. **92**(2-3), 177-191.
- Coward, P., Wada, H.G., Falk, M., Chan, S.D.H., Meng, F., Akil, H., *et al.* (1998). Controlling signaling with a specifically designed Gi-coupled receptor. *Proc. Natl. Acad. Sci.* **95**, 352-357.
- Croken, M.M., Nardelli, S.C. and Kim, K. (2012). Chromatin modifications, epigenetics, and how protozoan parasites regulate their lives. *Trends in Parasitology*. **28**(5), 202-213.

- Cui, L., Miao, J. and Cui, L. (2007). Cytotoxic Effect of Curcumin on Malaria Parasite *Plasmodium falciparum*: Inhibition of Histone Acetylation and Generation of Reactive Oxygen Species. *Antimicrobial Agents and Chemotherapy*. **51**(2), 488-494.
- Dahan-Farkas, N., Langley, C., Rousseau, A.L., Yadav, D.B., Davids, H. and de Koning, C.B. (2011). 6-Substituted imidazo[1,2-a]pyridines: Synthesis and biological activity against colon cancer cell lines HT-29 and Caco-2. *European Journal of Medicinal Chemistry*. **46**(9), 4573-4583.
- Dajue, L. and Mündel, H.-H. (1996). Safflower. *Carthamus tinctorius* L. In: Heller, J., Engels, J. and Hammer, K. (Eds.) *Promoting the conservation and use of underutilized and neglected crops*. Institute of Plant Genetics and Crop Plant Research, Gatersleben/International Plant Genetic Resources Institute.: Rome, Italy, pp. 15-33.
- Deharo, E., García, R.N., Oporto, P., Gimenez, A., Sauvain, M., Jullian, V., *et al.* (2002). A non-radiolabelled ferriprotoporphyrin IX biomineralisation inhibition test for the high throughput screening of antimalarial compounds. *Experimental Parasitology*. **100**(4), 252-256.
- Denissenko, M.F., Pao, A., Tang, M.-S. and Pfeifer, G.P. (1996). Preferential Formation of Benzo[a]pyrene Adducts at Lung Cancer Mutational Hotspots in P53. *Science*. **274**(5286), 430-432.
- Desjardins, R.E., Canfield, C.J., Haynes, J.D. and Chulay, J.D. (1979). Quantitative assessment of antimalarial activity in vitro by a semiautomated microdilution technique. *Antimicrobial Agents and Chemotherapy*. **16**(6), 710-718.
- Disanto, A.R. and Wagner, J.G. (1972). Pharmacokinetics of highly ionized drugs II: Methylene blue - absorption, metabolism, and excretion in man and dog after oral administration. *Journal of Pharmaceutical Sciences*. **61**(7), 1086-1090.
- Dixon, M.W.A., Thompson, J., Gardiner, D.L. and Trenholme, K.R. (2008). Sex in *Plasmodium*: a sign of commitment. *Trends in Parasitology*. **24**(4), 168-175.
- Doerig, C., Abdi, A., Bland, N., Eschenlauer, S., Dorin-Semblat, D., Fennell, C., *et al.* (2010). Malaria: Targeting parasite and host cell kinomes. *Biochimica et Biophysica Acta (BBA) - Proteins & Proteomics*. **1804**(3), 604-612.
- Doerig, C., Billker, O., Haystead, T., Sharma, P., Tobin, A.B. and Waters, N.C. (2008). Protein kinases of malaria parasites: an update. *Trends in Parasitology*. **24**(12), 570-577.
- Doerig, C., Endicott, J. and Chakrabarti, D. (2002). Cyclin-dependent kinase homologues of *Plasmodium falciparum*. *International Journal for Parasitology*. **32**(13), 1575-1585.
- Doerig, C., Horrocks, P., Coyle, J., Carlton, J., Sultan, A., Arnot, D., *et al.* (1995). Pfrck-1, a developmentally regulated cdc2-related protein kinase of *Plasmodium falciparum*. *Molecular and Biochemical Parasitology*. **70**(1-2), 167-174.
- Doerig, C. and Meijer, L. (2007). Antimalarial drug discovery: targeting protein kinases. *Expert Opinion on Therapeutic Targets*. **11**(3), 279-290.
- Dondorp, A.M., Fairhurst, R.M., Slutsker, L., MacArthur, J.R., M.D, J.G.B., Guerin, P.J., *et al.* (2011). The Threat of Artemisinin-Resistant Malaria. *New England Journal of Medicine*. **365**(12), 1073-1075.

- Donovan, J.C.H., Slingerland, J. and Tannock, I.F. (2005). Cell proliferation and tumour growth. *In: Tannock, I. F., Hill, R. P., Bristow, R. G. and Harrington, L. (Eds.) The Basic Science of Oncology*. 4th ed. McGraw-Hill Medical Publishing Division: New York, pp. 167-189.
- Dorin-Semblat, D., Sicard, A., Doerig, C., Ranford-Cartwright, L. and Doerig, C. (2008). Disruption of the PfPK7 Gene Impairs Schizogony and Sporogony in the Human Malaria Parasite *Plasmodium falciparum*. *Eukaryotic Cell*. **7**(2), 279-285.
- Downie, M.J., Kirk, K. and Mamoun, C.B. (2008). Purine Salvage Pathways in the Intraerythrocytic Malaria Parasite *Plasmodium falciparum*. *Eukaryotic Cell*. **7**(8), 1231-1237.
- Drakeley, C., Sutherland, C., Bousema, J.T., Sauerwein, R.W. and Targett, G.A.T. (2006). The epidemiology of *Plasmodium falciparum* gametocytes: weapons of mass dispersion. *Trends in Parasitology*. **22**(9), 424-430.
- Duvoix, A., Morceau, F., Schnekenburger, M., Delhalle, S., Galteau, M.M., Dicato, M., *et al.* (2003). Curcumin-Induced Cell Death in Two Leukemia Cell Lines: K562 and Jurkat. *Annals of the New York Academy of Sciences*. **1010**(1), 389-392.
- Ecker, A., Lehane, A.M., Clain, J. and Fidock, D.A. (2012). PfCRT and its role in antimalarial drug resistance. *Trends in Parasitology*. **28**(11), 504-514.
- Egan, T.J. (2003). Haemozoin (malaria pigment): a unique crystalline drug target. *TARGETS*. **2**(3), 115-124.
- Egan, T.J. (2006). Interactions of quinoline antimalarials with hemozoin in solution. *Journal of Inorganic Biochemistry*. **100**(5-6), 916-926.
- Egan, T.J. (2008a). Haemozoin formation. *Molecular and Biochemical Parasitology*. **157**(2), 127-136.
- Egan, T.J. (2008b). Recent advances in understanding the mechanism of hemozoin (malaria pigment) formation. *Journal of Inorganic Biochemistry*. **102**(5-6), 1288-99.
- Ekwall, B., Silano, V., Paganuzzi-Stammati, A. and Zucco, F. (1990). Toxicity Tests with Mammalian Cell Cultures. *In: Boudeax, P., Somers, E., Mark Richardson, G. and Hickman, J. R. (Eds.) Short-term Toxicity Tests for Non-genotoxic Effects*. 1st ed. John Wiley & Sons Ltd.: New York, pp. 75-97.
- Elion, G.B., Singer, S. and Hitchings, G.H. (1954). Antagonists of nucleic acid derivatives: VIII. Synergism in combinations of biochemically related antimetabolites. *Journal of Biological Chemistry*. **208**(2), 477-488.
- Engel, P.S., Duan, S., He, S., Tsvaygboym, K., Wang, C., Wu, A., *et al.* (2003). The free radical chemistry of the azoxy group. *ARKIVOC*. iii, pp. 89-108. <http://www.arkat-usa.org/get-file/18842/> [Accessed 21 Nov 2013].
- Enguehard-Gueiffier, C. and Gueiffier, A. (2007). Recent Progress in the Pharmacology of Imidazo[1,2-a]pyridines. *Mini Reviews in Medicinal Chemistry*. **7**(9), 888-899.
- European Food Safety Authority. (2012). Scientific Opinion on the re-evaluation of vegetable carbon (E 153) as a food additive. *EFSA Journal*. **10**(4), pp. 2592-2626. www.efsa.europa.eu/efsajournal [Accessed 13 Dec 2013].

- Evans, W.C. (1996). Trease and Evans' Pharmacognosy. WB Saunders Company Ltd, London. pp. 456-461.
- Färber, P.M., Arscott, L.D., Williams, C.H., Becker, K. and Schirmer, R.H. (1998). Recombinant *Plasmodium falciparum* glutathione reductase is inhibited by the antimalarial dye methylene blue. *FEBS Letters*. **422**, 311-314.
- Fidock, D.A., Nomura, T., Talley, A.K., Cooper, R.A., Dzekunov, S.M., Ferdig, M.T., *et al.* (2000). Mutations in the *P. falciparum* Digestive Vacuole Transmembrane Protein PfCRT and Evidence for Their Role in Chloroquine Resistance. *Molecular cell*. **6**(4), 861-871.
- Fidock, D.A., Rosenthal, P.I., Croft, S.L., Brun, R. and Nwaka, S. (2004). Antimalarial drug discovery: efficacy models for compound screening. *Nature Reviews Drug Discovery*. **3**(6), 509-520.
- Florens, L., Washburn, M.P., Raine, J.D., Anthony, R.M., Grainger, M., Haynes, J.D., *et al.* (2002). A proteomic view of the *Plasmodium falciparum* life cycle. *Nature*. **419**(6906), 520-526.
- Freese, J.A., Sharp, B.L., Ridl, F.C. and Markus, M.B. (1988). In vitro cultivation of southern African strains of *Plasmodium falciparum* and gametocytogenesis. *South African Medical Journal*. **73**(12), 720-722.
- Freshney, R.I. (1988). Culture of animal cells: A manual of basic technique. Alan R. Liss, Inc., New York. pp. 227-229.
- Funk, J.L., Frye, J.B., Oyarzo, J.N., Zhang, H. and Timmermann, B.N. (2009). Anti-Arthritic Effects and Toxicity of the Essential Oils of Turmeric (*Curcuma longa* L.). *Journal of Agricultural and Food Chemistry*. **58**(2), 842-849.
- Galmarini, C.M., Mackey, J.R. and Dumontet, C. (2002). Nucleoside analogues and nucleobases in cancer treatment. *The Lancet Oncology*. **3**(7), 415-424.
- Garavito, G., Bertani, S., Rincon, J., Maurel, S., Monje, M.C., Landau, I., *et al.* (2007). Blood schizontocidal activity of methylene blue in combination with antimalarials against *Plasmodium falciparum*. *Parasite*. **14**(2), 135-140.
- Gathirwa, J.W., Rukunga, G.M., Njagi, E.N.M., Omar, S.A., Mwitari, P.G., Guantai, A.N., *et al.* (2008). The *in vitro* anti-plasmodial and *in vivo* anti-malarial efficacy of combinations of some medicinal plants used traditionally for treatment of malaria by the Meru community in Kenya. *Journal of Ethnopharmacology*. **115**(2), 223-231.
- Gero, A.M., Dunn, C.G., Brown, D.M., Pulenthiran, K., Gorovits, E.L., Bakos, T., *et al.* (2003). New malaria chemotherapy developed by utilization of a unique parasite transport system. *Current Pharmaceutical Design*. **9**, 867-877.
- Geyer, J.A., Prigge, S.T. and Waters, N.C. (2005). Targeting malaria with specific CDK inhibitors. *Biochimica et Biophysica Acta*. **1754**, 160-170.
- Ginsburg, H. (2013). *Malaria Parasite Metabolic Pathways*. <http://mpmp.huji.ac.il/maps/hemoglobinpolpath.html> [Accessed 19 Nov 2013].
- Ginsburg, H. and Deharo, E. (2011). A call for using natural compounds in the development of new antimalarial treatments - an introduction. *Malaria Journal*. **10**(Suppl 1), S1.

- Ginsburg, H., Famin, O., Zhang, J. and Krugliak, M. (1998). Inhibition of glutathione-dependent degradation of heme by chloroquine and amodiaquine as a possible basis for their antimalarial mode of action - Investigation of glutathione transport and metabolism in human erythrocytes infected with *Plasmodium falciparum*. *Biochemical Pharmacology*. **56**(10), 1305-1313.
- Glantz, S. (2005). Primer of Biostatistics. McGraw-Hill Medical, New York. pp. 113-353.
- Godiska, R., Mead, D., Dhodda, V., Wu, C., Hochstein, R., Karsi, A., *et al.* (2010). Linear plasmid vector for cloning of repetitive or unstable sequences in *Escherichia coli*. *Nucleic Acids Research*. **38**(6), e88-e88.
- Goel, A., Kunnumakkara, A.B. and Aggarwal, B.B. (2008). Curcumin as "Curecumin": From kitchen to clinic. *Biochemical Pharmacology*. **75**(4), 787-809.
- Golka, K., Kopps, S. and Myslak, Z.W. (2004). Carcinogenicity of azo colorants: influence of solubility and bioavailability. *Toxicology Letters*. **151**, 203-10.
- Goodman, S.R. (1998). Organelle Structure and Function. *In: Goodman, S. R. (Ed.) Medical Cell Biology*. 2nd ed. Lippincott-Raven: New York, pp. 111-123.
- Gordon, P.F. and Gregory, P. (1983). Organic chemistry in colour. Springer-Verlag, Berlin. pp. 1-8, 94-97.
- Graeser, R., Wernli, B., Franklin, R.M. and Kappes, B. (1996). *Plasmodium falciparum* protein kinase 5 and the malarial nuclear division cycles. *Molecular and Biochemical Parasitology*. **82**(1), 37-49.
- Graham, F.L., Smiley, J., Russell, W.C. and Nairn, R. (1977). Characteristics of a Human Cell Line Transformed by DNA from Human Adenovirus Type 5. *Journal of General Virology*. **36**(1), 59-72.
- Greenhawt, M., McMorris, M. and Baldwin, J. (2009). Carmine hypersensitivity masquerading as azithromycin hypersensitivity. *Allergy and Asthma Proceedings*. **30**(1), 95-101.
- Greenwood, B.M., Fidock, D.A., Kyle, D.E., Kappe, S.H.I., Alonso, P.L., Collins, F.H., *et al.* (2008). Malaria: progress, perils, and prospects for eradication. *The Journal of Clinical Investigation*. **118**(4), 1266-1276.
- Grosser, T., Smyth, E.M. and FitzGerald, G.A. (2011). Anti-inflammatory, Antipyretic, and Analgesic Agents; Pharmacotherapy of Gout. *In: Chabner, B. A. and Knollmann, B. C. (Eds.) Goodman & Gilman's The Pharmacological Basis of Therapeutics*. 12 ed. McGraw-Hill: New York. <http://0-www.accesspharmacy.com.innopac.wits.ac.za/content.aspx?aID=16670422> [Accessed 11/11/2013].
- Gupta, S., Thapar, M.M., Wernsdorfer, W.H. and Björkman, A. (2002). *In vitro* interactions of artemisinin with atovaquone, quinine, and mefloquine against *Plasmodium falciparum*. *Antimicrobial Agents and Chemotherapy*. **46**(5), 1510-1515.
- Gutteridge, J.M. and Quinlan, G.J. (1986). Carminic acid-promoted oxygen radical damage to lipid and carbohydrate. *Food Additives and Contaminants*. **3**(4), 289-293.

- Hanks, S. (2003). Genomic analysis of the eukaryotic protein kinase superfamily: a perspective. *Genome Biology*. **4**(5), 111.
- Hanks, S.K. and Hunter, T. (1995). Protein kinases 6. The eukaryotic protein kinase superfamily: kinase (catalytic) domain structure and classification. *The FASEB Journal*. **9**(8), 576-96.
- Harmer, R.A. (1980). Occurrence, chemistry and application of betanin. *Food Chemistry*. **5**(1), 81-90.
- Harmse, L., Van Zyl, R., Gray, N., Schultz, P., Leclerc, S., Meijer, L., *et al.* (2001). Structure-activity relationships and inhibitory effects of various purine derivatives on the in vitro growth of *Plasmodium falciparum*. *Biochemical Pharmacology*. **62**, 341-348.
- Hawley, S.R., Bray, P.G., Mungthin, M., Atkinson, J.D., O'Neill, P.M. and Ward, S.A. (1998). Relationship between Antimalarial Drug Activity, Accumulation, and Inhibition of Heme Polymerization in *Plasmodium falciparum* In Vitro. *Antimicrobial Agents and Chemotherapy*. **42**(3), 682-686.
- Hayat, F., Moseley, E., Salahuddin, A., Van Zyl, R.L. and Azam, A. (2011). Antiprotozoal activity of chloroquinoline based chalcones. *European Journal of Medicinal Chemistry*. **46**(5), 1897-1905.
- Horobin, R.W. (2002). Theory of staining and its practical implications. *In: Bancroft, J. D. and Gamble, M. (Eds.) Theory and practice of histological techniques*. Churchill Livingstone: Edinburg, pp. 109-113.
- IARC. (2010). IARC monographs on the evaluation of carcinogenic risks to humans Volume 99. Some aromatic amines, organic dyes, and related exposures. pp. 55-67. <http://monographs.iarc.fr/ENG/Monographs/vol99/mono99.pdf> [Accessed 11/01/2013].
- Isacchi, B., Bergonzi, M.C., Grazioso, M., Righeschi, C., Pietretti, A., Severini, C., *et al.* (2012). Artemisinin and artemisinin plus curcumin liposomal formulations: Enhanced antimalarial efficacy against *Plasmodium berghei*-infected mice. *European Journal of Pharmaceutics and Biopharmaceutics*. **80**(3), 528-534.
- Jain, A., Gupta, Y. and Jain, S.K. (2006). Azo chemistry and its potential for colonic delivery. *Crit Rev Ther Drug Carrier Syst*. **23**(5), 349-400.
- Jiang, H., Gelhaus, S.L., Mangal, D., Harvey, R.G., Blair, I.A. and Penning, T.M. (2007). Metabolism of Benzo[a]pyrene in Human Bronchoalveolar H358 Cells Using Liquid Chromatography–Mass Spectrometry. *Chemical Research in Toxicology*. **20**(9), 1331-1341.
- Jones, C.D., Andrews, D.M., Barker, A.J., Blades, K., Byth, K.F., Finlay, M.R.V., *et al.* (2008). Imidazole pyrimidine amides as potent, orally bioavailable cyclin-dependent kinase inhibitors. *Bioorganic & Medicinal Chemistry Letters*. **18**(24), 6486-6489.
- Joubert, F., Neitz, A.W.H. and Louw, A.I. (2001). Structure-based inhibitor screening: A family of sulfonated dye inhibitors for malaria parasite triosephosphate isomerase. *Proteins: Structure, Function, and Genetics*. **45**(2), 136-143.
- Kanner, J., Harel, S. and Granit, R. (2001). Betalains - a new class of dietary cationized antioxidants. *Journal of Agricultural and Food Chemistry*. **49**, 5178-5185.

- Kapadia, G.J., Azuine, M.A., Sridhar, R., Okuda, Y., Tsuruta, A., Ichiishi, E., *et al.* (2003). Chemoprevention of DMBA-induced UV-B promoted, NOR-1-induced TPA promoted skin carcinogenesis, and DEN-induced phenobarbital promoted liver tumors in mice by extract of beetroot. *Pharmacological Research*. **47**(2), 141-148.
- Khanna, V. and Ranganathan, S. (2009). Physiochemical property space distribution among human metabolites, drugs and toxins. *BMC Bioinformatics*. **10**(Suppl. 15).
- King, A.E., Ackley, M.A., Cass, C.E., Young, J.D. and Baldwin, S.A. (2006). Nucleoside transporters: from scavengers to novel therapeutic targets. *Trends in Pharmacological Sciences*. **27**(8), 416-425.
- Knittel, J.J. and Zavod, R.M. (2008). Drug design and relationship of functional groups to pharmacological activity. *In: Lemke, T. L. and Williams, D. A. (Eds.) FOYE'S Principles of Medicinal Chemistry*. 6th ed. Lippincot Williams & Wilkins: New York, pp. 26-53.
- Kong, D.-X., Li, X.-J. and Zhang, H.-Y. (2009). Where is the hope for drug discovery? Let history tell the future. *Drug Discovery Today*. **14**(3-4), 115-119.
- Kong, N., Fotouhi, N., Wovkulich, P.M. and Roberts, J. (2003). Cell cycle inhibitors for the treatment of cancer. *Drugs of the future*. **28**(9), 881.
- Krafts, K., Hempelmann, E. and Oleksyn, B. (2011). The color purple: from royalty to laboratory, with apologies to Malachowski. *Biotechnic & Histochemistry*. **86**(1), 7-35.
- Krogstad, D., Gluzman, I., Kyle, D., Oduola, A., Martin, S., Milhous, W., *et al.* (1987). Efflux of chloroquine from *Plasmodium falciparum*: mechanism of chloroquine resistance. *Science*. **238**(4831), 1283-1285.
- Kumar, S., Guha, M., Choubey, V., Maity, P. and Bandyopadhyay, U. (2007). Antimalarial drugs inhibiting hemozoin (β -hematin) formation: A mechanistic update. *Life Sciences*. **80**(9), 813-828.
- Kurien, B.T. and Scofield, R.H. (2006). Western blotting. *Methods*. **38**(4), 283-293.
- Laemmli, U.K. (1970). Cleavage of structural proteins during the assembly of the head of bacteriophage T4. *Nature*. **227**(5259), 680-685.
- Lambros, C. and Vanderberg, J.P. (1979). Synchronization of *Plasmodium falciparum* Erythrocytic Stages in Culture. *The Journal of Parasitology*. **65**(3), 418-420.
- Le Marchand, L., Hankin, J.H., Pierce, L.M., Sinha, R., Nerurkar, P.V., Franke, A.A., *et al.* (2002). Well-done red meat, metabolic phenotypes and colorectal cancer in Hawaii. *Mutation Research/Fundamental and Molecular Mechanisms of Mutagenesis*. **506-507**(0), 205-214.
- Le Roch, K., Sestier, C., Dorin, D., Waters, N., Kappes, B., Chakrabarti, D., *et al.* (2000). Activation of a *Plasmodium falciparum* cdc2-related Kinase by Heterologous p25 and Cyclin H: Functional Characterization of a *P. falciparum* Cyclin Homologue. *Journal of Biological Chemistry*. **275**(12), 8952-8958.
- Leeson, P.D. and Springthorpe, B. (2007). The influence of drug-like concepts on decision-making in medicinal chemistry. *Nature Reviews Drug Discovery*. **6**(11), 881-890.

- Li, F., Maag, H. and Alfredson, T. (2008). Prodrugs of nucleoside analogues for improved oral absorption and tissue targeting. *Journal of Pharmaceutical Sciences*. **97**(3), 1109-1134.
- Li, J.L., Robson, K.J.H., Chen, J.L., Targett, G.A.T. and Baker, D.A. (1996). Pfmrk, a MO15-related protein kinase from *Plasmodium falciparum*. Gene cloning, sequence, stage-specific expression and chromosome localization. *European Journal of Biochemistry*. **241**(3), 805-813.
- Li, L., Gao, H.W., Ren, J.R., Chen, L., Li, Y.C., Zhao, J.F., *et al.* (2007). Binding of sudan II and IV to lecithin liposomes and *E. coli* membranes: insights into the toxicity of hydrophobic azo dyes. *BMC Structural Biology*. **7**, 16.
- Lim, G.P., Chu, T., Yang, F., Beech, W., Frautschy, S.A. and Cole, G.M. (2001). The Curry Spice Curcumin Reduces Oxidative Damage and Amyloid Pathology in an Alzheimer Transgenic Mouse. *The Journal of Neuroscience*. **21**(21), 8370-8377.
- Lipinski, C.A. (2004). Lead- and drug-like compounds: the rule-of-five revolution. *Drug Discovery Today: Technologies*. **1**(4), 337-341.
- Lipinski, C.A., Lombardo, F., Dominy, B.W. and Feeney, P.J. (1997). Experimental and computational approaches to estimate solubility and permeability in drug discovery and development settings. *Advanced Drug Delivery Reviews*. **23**(1-3), 3-25.
- Lipinski, C.A., Lombardo, F., Dominy, B.W. and Feeney, P.J. (2001). Experimental and computational approaches to estimate solubility and permeability in drug discovery and development settings. *Advanced Drug Delivery Reviews*. **46**(1-3), 3-26.
- Liu, A., Lou, H., Zhao, L. and Fan, P. (2006). Validated LC/MS/MS assay for curcumin and tetrahydrocurcumin in rat plasma and application to pharmacokinetic study of phospholipid complex of curcumin. *Journal of Pharmaceutical and Biomedical Analysis*. **40**(3), 720-727.
- Lozzio, B.B. and Lozzio, C.B. (1979). Properties and usefulness of the original K-562 human myelogenous leukemia cell line. *Leukemia Research*. **3**(6), 363-370.
- Lucas, C.D., Hallagan, J.B. and Taylor, S.L. (2001). The role of natural color additives in food allergy. *Advances in Food and Nutrition Research*. Academic Press, pp. 195-216.
- Lüönd, R.M., McKie, J.H., Douglas, K.T., Dascombe, M.J. and Vale, J. (1998). Inhibitors of glutathione reductase as potential antimalarial drugs: Kinetic cooperativity and effect of dimethyl sulphoxide on inhibition kinetics. *Journal of Enzyme Inhibition*. **13**(5), 327-345.
- Manallack, D.T. (2007). The pK_a Distribution of Drugs: Application to Drug Discovery. *Perspectives in Medicinal Chemistry*. **1**, 25-38.
- Mandi, G., Witte, S., Meissner, P., Coulibaly, B., Mansmann, U., Rengelshausen, J., *et al.* (2005). Safety of the combination of chloroquine and methylene blue in healthy adult men with G6PD deficiency from rural Burkina Faso. *Tropical Medicine & International Health*. **10**(1), 32-38.
- Martin, S.K., Oduola, A.M. and Milhous, W.K. (1987). Reversal of chloroquine resistance in *Plasmodium falciparum* by verapamil. *Science*. **235**(4791), 899-901.

- McKim, J.M. (2010). Building a tiered approach to *in vitro* predictive toxicity screening: A focus on assays with *in vivo* relevance. *Combinatorial Chemistry and High Throughput Screening*. **13**(2), 188-206.
- Meissner, P., Mandi, G., Coulibaly, B., Witte, S., Tapsoba, T., Mansmann, U., *et al.* (2006). Methylene blue for malaria in Africa: results from a dose-finding study in combination with chloroquine. *Malaria Journal*. **5**(1), 84.
- Miao, J., Fan, Q., Cui, L., Li, J., Li, J. and Cui, L. (2006). The malaria parasite *Plasmodium falciparum* histones: Organization, expression, and acetylation. *Gene*. **369**(0), 53-65.
- Micale, N. (2012). Recent advances and perspectives on tropical diseases: Malaria. *World Journal of Translational Medicine*. **1**(2), 4-19.
- Miller, L.H., Baruch, D.I., Marsh, K. and Doumbo, O.K. (2002). The pathogenic basis of malaria. *Nature*. **415**, 673-679.
- Mishra, R., Mishra, B. and Hari Narayana Moorthy, N.S. (2006). Dihydrofolate reductase enzyme: a potent target for antimalarial research. *Asian Journal of Cell Biology*. **1**(1), 48-58.
- Mohandas, N. and Gallagher, P.G. (2008). Red cell membrane: past, present, and future. *Blood*. **112**(10), 3939-3948.
- Moniz, L., Dutt, P., Haider, N. and Stambolic, V. (2011). Nek family of kinases in cell cycle, checkpoint control and cancer. *Cell Division*. **6**(1), 18.
- Motulsky, H. (2003). Prism 4 Statistics Guide-Statistical analyses for laboratory and clinical researchers.: San Diego CA, GraphPad Software Inc. www.graphpad.com [Accessed 03 May 2010].
- Müller, O., Mockenhaupt, F.P., Marks, B., Meissner, P., Coulibaly, B., Kuhnert, R., *et al.* (2013). Haemolysis risk in methylene blue treatment of G6PD-sufficient and G6PD-deficient West-African children with uncomplicated *falciparum* malaria: a synopsis of four RCTs. *Pharmacoepidemiology and Drug Safety*. **22**(4), 376-385.
- Muller, P.Y. and Milton, M.N. (2012). The determination and interpretation of the therapeutic index in drug development. *Nature Reviews Drug Discovery*. **11**(10), 751-761.
- Müller, S. (2004). Redox and antioxidant systems of the malaria parasite *Plasmodium falciparum*. *Molecular Microbiology*. **53**(5), 1291-1305.
- Mullick, S., Das, S., Guha, S.K., Bera, D.K., Sengupta, S., Roy, D., *et al.* (2011). Efficacy of Chloroquine and Sulphadoxine-Pyrimethamine either alone or in combination before introduction of ACT as first-line therapy in uncomplicated *Plasmodium falciparum* malaria in Jalpaiguri District, West Bengal, India. *Tropical Medicine & International Health*. **16**(8), 929-935.
- Nagao, K. and Yanagita, T. (2005). Conjugated fatty acids in food and their health benefits. *Journal of Bioscience and Bioengineering*. **100**(2), 152-157.
- Najahi, E., Valentin, A., Téné, N., Treilhou, M. and Nepveu, F. (2013). Synthesis and biological evaluation of new bis-indolone-N-oxides. *Bioorganic Chemistry*. **48**(0), 16-21.

Nandakumar, D.N., Nagaraj, V.A., Vathsala, P.G., Rangarajan, P. and Padmanaban, G. (2006). Curcumin-Artemisinin Combination Therapy for Malaria. *Antimicrobial Agents and Chemotherapy*. **50**(5), 1859-1860.

National Department of Health (2009). Guidelines for the Treatment of Malaria in South Africa: Pretoria, South Africa, Department of Health. <http://www.kznhealth.gov.za/medicine/2009malariaguideline.pdf> [Accessed 21 May 2010].

National Department of Health (2010). Guidelines for the treatment of malaria in South Africa: Pretoria, South Africa, Department of Health. http://www.doh.gov.za/docs/policy/2011/malaria_treatment.pdf [Accessed 08 Sept 2011].

National Department of Health. (2012). *South Africa joins the world in commemorating World Malaria Day on 25 April 2012*. Pretoria, South Africa: Department of Health. <http://www.doh.gov.za/show.php?id=3563> [Accessed 03 May 2013].

National Department of Health. (2013). *Medicines Control Council*. Pretoria, South Africa: Department of Health. <http://www.doh.gov.za/show.php?id=2863> [Accessed 11 Nov 2013].

National Toxicology Program. (2004). *A National Toxicology Program for the 21st Century*. <http://ntp.niehs.nih.gov> [Accessed 15 Feb 2014].

Neal, M.J. (2005). *Medical Pharmacology at a Glance*. 5th ed. Blackwell: Oxford, pp. 92-93.

Newton, P.N., Green, M.D. and Fernández, F.M. (2010). Impact of poor-quality medicines in the 'developing' world. *Trends in Pharmacological Sciences*. **31**(3), 99-101.

Nwaka, S., Ilunga, T.B., Da Silva, J.S., Verde, E.R., Hackley, D., De Vré, R., *et al.* (2010). Developing ANDI: A Novel Approach to Health Product R&D in Africa. *PLoS Medicine*. **7**(6), 1-6.

Nwaka, S., Ramirez, B., Brun, R., Maes, L., Douglas, F. and Ridley, R. (2009). Advancing Drug Innovation for Neglected Diseases - Criteria for Lead Progression. *PLoS Neglected Tropical Diseases*. **3**(8), e440.

O'Connor, J.E., Kimler, B.F., Morgan, M.C. and Tempas, K.J. (1988). A flow cytometric assay for intracellular nonprotein thiols using mercury orange. *Cytometry*. **9**(6), 529-532.

O'Neil, M.J., Smith, A. and Heckelman, P.E. (2001). *The MERCK Index: An Encyclopedia of Chemicals, Drugs, and Biologicals*. Whitehouse Station, New Jersey. pp. 1444.

O'Neill, P., Barton, V., Ward, S. and Chadwick, J. (2012). 4-Aminoquinolines: Chloroquine, Amodiaquine and Next-Generation Analogues. *In: Staines, H. M. and Krishna, S. (Eds.) Treatment and Prevention of Malaria*. Springer Basel, pp. 19-44.

Osman, M.E., Mockenhaupt, F.P., Bienzle, U., Elbashir, M.I. and Giha, H.A. (2007). Field-based evidence for linkage of mutations associated with chloroquine (pfcrt/pfmdr1) and sulfadoxine-pyrimethamine (pfdhfr/pfdhps) resistance and for the fitness cost of multiple mutations in *P. falciparum*. *Infection, Genetics and Evolution*. **7**(1), 52-59.

Padmanaban, G., Nagaraj, V.A. and Rangarajan, P.N. (2012). Artemisinin-based combination with curcumin adds a new dimension to malaria therapy. *Current Science*. **102**(5), 704-711.

- Panayides, J.-L. 2012. *The synthesis and biological testing of nucleoside derivatives*. PhD Thesis, University of the Witwatersrand.
- Parapini, S., Basilico, N., Pasini, E., Egan, T.J., Olliario, P., Taramelli, D., *et al.* (2000). Standardization of the Physicochemical Parameters to Assess in Vitro the β -Hematin Inhibitory Activity of Antimalarial Drugs. *Experimental Parasitology*. **96**(4), 249-256.
- Pardo, M.F. and Natalucci, C.L. (2002). Electrophoretic Analysis (Tricine-SDS-PAGE) of Bovine Caseins. *Acta Farmaceutica Bonaerense*. **21**(1), 57-60.
- Parkinson, T. (2010). Malaria: the continuing battle. *The Newsletter of the British Pharmacological Society*. **3**(1), 23-24.
- Parsai, S., Keck, R., Skrzypczak-Jankun, E. and Jankun, J. (2014). Analysis of the anticancer activity of curcuminoids, thiotryptophan and 4-phenoxyphenol derivatives. *Oncology Letters*. **7**(1), 17-22.
- PATH. (2007). Accelerating Progress Toward Malaria Vaccines. The PATH Malaria Vaccine Initiative. http://www.malariavaccine.org/files/080212_MVI_portfolio_bro_mvilogo_000.pdf [Accessed 23/07/2012].
- Patwardhan, B. (2005). Ethnopharmacology and drug discovery. *Journal of Ethnopharmacology*. **100**(1-2), 50-52.
- Pink, R., Hudson, A., Mouries, M.-A. and Bendig, M. (2005). Opportunities and Challenges in Antiparasitic Drug Discovery. *Nature Reviews Drug Discovery*. **4**(9), 727-740.
- Plaa, G.L. (2005). Introduction to Toxicology: Occupational and Environmental. *In: Katzung, B. G. (Ed.) Basic & Clinical Pharmacology*. 10th ed. McGraw Hill Companies: New York, pp. 934-943.
- Pollard, T.D. and Earnshaw, W. (2004). Cell Biology. Saunders, Elsevier, Philadelphia. pp. 283-423.
- Preuss, J., Jortzik, E. and Becker, K. (2012). Glucose-6-phosphate metabolism in *Plasmodium falciparum*. *IUBMB Life*. **64**(7), 603-611.
- PubChem Compound. (2013a). *Carminic acid - compound summary (CID 11969478)*. http://pubchem.ncbi.nlm.nih.gov/summary/summary.cgi?cid=11969478&loc=ec_rcs [Accessed 19 Feb 2013].
- PubChem Compound. (2013b). *Curcumin - compound summary (CID 969516)*. http://pubchem.ncbi.nlm.nih.gov/summary/summary.cgi?cid=969516&loc=ec_rcs [Accessed 19 Feb 2013].
- PubChem Compound. (2013c). *Safranin O - compound summary (SID 539814)*. <http://pubchem.ncbi.nlm.nih.gov/summary/summary.cgi?sid=539814> [Accessed 19 Feb 2013].
- PubMed. (2014). *PubMed "Curcumin" Search*. <http://www.ncbi.nlm.nih.gov/pubmed?Term=curcumin> [Accessed 13 Feb 2014].
- Quashie, N., Ranford-Cartwright, L. and de Koning, H. (2010). Uptake of purines in *Plasmodium falciparum*-infected human erythrocytes is mostly mediated by the human

- Equilibrative Nucleoside Transporter and the human Facilitative Nucleobase Transporter. *Malaria Journal*. **9**(1), 36.
- Ralph, R.K., Marshall, B. and Darkin, S. (1983). Anti-cancer drugs which intercalate into DNA: How do they act? *Trends in biochemical sciences*. **8**(6), 212-214.
- Rang, H.P., Dale, M.M., Ritter, J.M., Flower, R.J. and Henderson, G. (2012a). Rang and Dale's Pharmacology. In: Rang, H. P. (Ed.) *Antiprotozoal Drugs*. 7th ed. McGraw Hill: New York, pp. 655-667.
- Rang, H.P., Dale, M.M., Ritter, J.M., Flower, R.J. and Henderson, G. (2012b). Rang and Dale's Pharmacology. In: Rang, H. P. (Ed.) *Drug absorption and distribution*. 7th ed. McGraw Hill: New York, pp. 99-114.
- Reddy, R.C., Vatsala, P.G., Keshamouni, V.G., Padmanaban, G. and Rangarajan, P.N. (2005). Curcumin for malaria therapy. *Biochemical and Biophysical Research Communications*. **326**(2), 472-474.
- Reininger, L., Garcia, M., Tomlins, A., Muller, S. and Doerig, C. (2012). The *Plasmodium falciparum*, Nima-related kinase Pfnek-4: a marker for asexual parasites committed to sexual differentiation. *Malaria Journal*. **11**(1), 250.
- Reininger, L., Tewari, R., Fennell, C., Holland, Z., Goldring, D., Ranford-Cartwright, L., *et al.* (2009). An Essential Role for the *Plasmodium* Nek-2 Nima-related Protein Kinase in the Sexual Development of Malaria Parasites. *Journal of Biological Chemistry*. **284**(31), 20858-20868.
- Reyes, P., Rathod, P.K., Sanchez, D.J., Mrema, J.E.K., Rieckmann, K.H. and Heidrich, H.-G. (1982). Enzymes of purine and pyrimidine metabolism from the human malaria parasite, *Plasmodium falciparum*. *Molecular and Biochemical Parasitology*. **5**(5), 275-290.
- Riley, E.M. and Stewart, V.A. (2013). Immune mechanisms in malaria: new insights in vaccine development. *Nature Medicine*. **19**(2), 168-178.
- Roestenberg, M., Teirlinck, A.C., McCall, M.B.B., Teelen, K., Makamdop, K.N., Wiersma, J., *et al.* (2011). Long-term protection against malaria after experimental sporozoite inoculation: an open-label follow-up study. *The Lancet*. **377**(9779), 1770-1776.
- Roll Back Malaria Partnership. (2008). The global malaria action plan. For a malaria-free world. <http://www.rollbackmalaria.org/gmap/gmap.pdf> [Accessed 14/12/2011].
- Rose, J.B. and Coe, I.R. (2008). Physiology of Nucleoside Transporters: Back to the Future. *Physiology*. **23**(1), 41-48.
- Rosenberg, L. (1971). Chemical Basis for the Histological Use of Safranin O in the Study of Articular Cartilage. *The Journal of Bone & Joint Surgery*. **53**(1), 69-82.
- Rosenthal, P.J. (2007). Antiprotozoal Drugs. In: Katzung, B. G. (Ed.) *Basic & Clinical Pharmacology*. 10th ed. McGraw Hill Companies: New York, pp. 845-856.
- Ross-Macdonald, P.B., Graeser, R., Kappes, B., Franklin, R. and Williamson, D.H. (1994). Isolation and expression of a gene specifying a cdc2-like protein kinase from the human malaria parasite *Plasmodium falciparum*. *European Journal of Biochemistry*. **220**(3), 693-701.

- Ross, R. and Smyth, S.-M. (1897). On Some Peculiar Pigmented Cells Found In Two Mosquitos Fed On Malarial Blood. *The British Medical Journal*. **2**(1929), 1786-1788.
- Rossiter, D. (2012). South African Medicines Formulary. Health and Medical Pub. Group, Rondebosch, South Africa. pp. 505-515.
- Rousseau, A.L., Matlaba, P. and Parkinson, C.J. (2007). Multicomponent synthesis of imidazo[1,2-a]pyridines using catalytic zinc chloride. *Tetrahedron Letters*. **48**(23), 4079-4082.
- Sachs, J. and Malaney, P. (2002). The economic and social burden of malaria. *Nature*. **415**(6872), 680-685.
- Saha, I., Hossain, M. and Suresh Kumar, G. (2010). Sequence-Selective Binding of Phenazinium Dyes Phenosafranin and Safranin O to Guanine–Cytosine Deoxyribopolynucleotides: Spectroscopic and Thermodynamic Studies. *The Journal of Physical Chemistry B*. **114**(46), 15278-15287.
- Salahuddin, A., Inam, A., van Zyl, R.L., Heslop, D.C., Chen, C.-T., Avecilla, F., *et al.* (2013). Synthesis and evaluation of 7-chloro-4-(piperazin-1-yl)quinoline-sulfonamide as hybrid antiprotozoal agents. *Bioorganic & Medicinal Chemistry*. **21**(11), 3080-3089.
- Sambrook, J., Fritsch, E.F. and Maniatis, T. (1989). Molecular Cloning: A Laboratory Manual. Cold Spring Harbor Laboratory Press, New York. pp. 3-41.
- Schirmer, R.H., Coulibaly, B., Stich, A., Scheiwein, M., Merkle, H., Eubel, J., *et al.* (2003). Methylene blue as an antimalarial agent. *Redox Report*. **8**, 272-275.
- Shapiro, T.A. and Goldberg, D.E. (2006). Chemotherapy of parasitic infections. *In: Brunton, L. L., Lazo, J. S. and Parker, K. L. (Eds.) Goodman and Gillman's The Pharmacological Basis of Therapeutics*. 11th ed. McGraw Hill Companies: New York, pp. 1021-1039.
- Sharp, B.L., Kleinschmidt, I., Streat, E., Maharaj, R., Barnes, K.I., Durrheim, D.N., *et al.* (2007). Seven years of regional malaria control collaboration - Mozambique, South Africa, and Swaziland. *American Journal of Tropical Medicine and Hygiene*. **76**(1), 42-47.
- Shaw, G., Morse, S., Ararat, M. and Graham, F.L. (2002). Preferential transformation of human neuronal cells by human adenoviruses and the origin of HEK 293 cells. *The FASEB Journal*.
- Shishodia, S., Chaturvedi, M.M. and Aggarwal, B.B. (2007). Role of Curcumin in Cancer Therapy. *Current Problems in Cancer*. **31**(4), 243-305.
- Shore, P.A., Brodie, B.B. and Hogben, C.A.M. (1957). The Gastric Secretion of Drugs: A pH Partition Hypothesis. *Journal of Pharmacology and Experimental Therapeutics*. **119**(3), 361-369.
- Skinner-Adams, T.S., Stack, C.M., Trenholme, K.R., Brown, C.L., Grembecka, J., Lowther, J., *et al.* (2010). *Plasmodium falciparum* neutral aminopeptidases: new targets for anti-malarials. *Trends in biochemical sciences*. **35**(1), 53-61.
- Slater, A.F.G., Swiggard, W.J., Orton, B.R., Flitter, W.D., Goldberg, D.E., Cerami, A., *et al.* (1991). An Iron-Carboxylate Bond Links the Heme Units of Malaria Pigment. *Proceedings of the National Academy of Sciences of the United States of America*. **88**(2), 325-329.

- Smith, D.B. and Johnson, K.S. (1988). Single-step purification of polypeptides expressed in *Escherichia coli* as fusions with glutathione S-transferase. *Gene*. **67**(1), 31-40.
- Sondak, V.K., Bertelsen, C.A., Tanigawa, N., Hildebrand-Zanki, S.U., Morton, D.L., Korn, E.L., *et al.* (1984). Clinical Correlations with Chemosensitivities Measured in a Rapid Thymidine Incorporation Assay. *Cancer Research*. **44**(4), 1725-1728.
- Strack, D., Vogt, T. and Schliemann, W. (2003). Recent advances in betalain research. *Phytochemistry*. **62**(3), 247-269.
- Strober, W. (2001). Trypan Blue Exclusion Test of Cell Viability. *Current Protocols in Immunology*. John Wiley & Sons, Inc., pp. A.3B.1-A.3B.2.
- Studier, F.W. (2005). Protein production by auto-induction in high-density shaking cultures. *Protein Expression and Purification*. **41**(1), 207-234.
- Tardivo, J.P., Del Giglio, A., de Oliveira, C.S., Gabrielli, D.S., Junqueira, H.C., Tada, D.B., *et al.* (2005). Methylene blue in photodynamic therapy: From basic mechanisms to clinical applications. *Photodiagnosis and Photodynamic Therapy*. **2**(3), 175-191.
- Tesoriere, L., Butera, D., Allegra, M., Fazzari, M. and Livrea, M.A. (2005). Distribution of betalain pigments in red blood cells after consumption of cactus pear fruits and increased resistance of the cells to *ex vivo* induced oxidative hemolysis in humans. *Journal of Agricultural and Food Chemistry*. **53**(4), 1266-1270.
- Towbin, H., Staehelin, T. and Gordon, J. (1979). Electrophoretic transfer of proteins from polyacrylamide gels to nitrocellulose sheets: procedure and some applications. *Proceedings of the National Academy of Sciences*. **76**(9), 4350-4354.
- Trager, W. and Jensen, J.B. (1976). Human Malaria Parasites in Continuous Culture. *Science*. **193**(4254), 673-675.
- Tsuda, S., Matsusaka, N., Madarame, H., Ueno, S., Susa, N., Ishida, K., *et al.* (2000). The comet assay in eight mouse organs: results with 24 azo compounds. *Mutation Research/Genetic Toxicology and Environmental Mutagenesis*. **465**(1-2), 11-26.
- Valdés, A.F.-C., Martínez, M.J., Lizama, R.S., Vermeersch, M., Cos, P. and Maes, L. (2008). *In vitro* anti-microbial activity of the Cuban medicinal plants *Simarouba glauca* DC, *Melaleuca leucadendron* L and *Artemisia absinthium* L. *Memórias do Instituto Oswaldo Cruz*. **103**, 615-618.
- van Otterlo, W.A.L., Ngidi, E.L., Coyanis, E.M. and de Koning, C.B. (2003). Ring-closing metathesis for the synthesis of benzo-fused bicyclic compounds. *Tetrahedron Letters*. **44**(2), 311-313.
- Van Wyk, B.E. and Wink, M. (2004). Medicinal Plants of the World: An Illustrated Scientific Guide to Important Medicinal Plants and Their Uses. Timber Press. pp. 80-119.
- Van Zyl, R.L., Seatlholo, S.T. and Viljoen, A.M. (2010). Pharmacological interactions of essential oil constituents on the *in vitro* growth of *Plasmodium falciparum*. *South African Journal of Botany*. **76**(4), 662-667.
- Vangapandu, S., Jain, M., Kaur, K., Pati, P., Patel, S.R. and Jain, R. (2007). Recent advances in antimalarial drug development. *Medicinal Research Reviews*. **27**(1), 65-107.

- Vareed, S.K., Kakarala, M., Ruffin, M.T., Crowell, J.A., Normolle, D.P., Djuric, Z., *et al.* (2008). Pharmacokinetics of curcumin conjugate metabolites in healthy human subjects. *Cancer Epidemiology Biomarkers & Prevention*. **17**(6), 1411-1417.
- Vathsala, P.G., Dende, C., Nagaraj, V.A., Bhattacharya, D., Das, G., Rangarajan, P.N., *et al.* (2012). Curcumin-artether combination therapy of *Plasmodium berghei*-infected mice prevents recrudescence through immunomodulation. *PLoS ONE*. **7**(1).
- Vennerstrom, J.L., Makler, M.T., Angerhofer, C.K. and Williams, J.A. (1995). Antimalarial dyes revisited: xanthenes, azines, oxazines, and thiazines. *Antimicrobial Agents and Chemotherapy*. **39**(12), 2671-2677.
- Verma, A.K., Dash, R.R. and Bhunia, P. (2012). A review on chemical coagulation/flocculation technologies for removal of colour from textile wastewaters. *Journal of Environmental Management*. **93**(1), 154-168.
- Vinetz, J.M., Clain, J., Bounkeua, V., Eastman, R.T. and Fidock, D. (2011). Chemotherapy of Malaria. In: Chabner, B. A. and Knollmann, B. C. (Eds.) *Goodman & Gilman's The Pharmacological Basis of Therapeutics*. 12 ed. McGraw-Hill: New York. <http://0-www.accesspharmacy.com.innopac.wits.ac.za/content.aspx?aID=16676038> [Accessed 11/11/2013].
- Vivas, L., Rattray, L., Stewart, L.B., Robinson, B.L., Fugmann, B., Haynes, R.K., *et al.* (2007). Antimalarial efficacy and drug interactions of the novel semi-synthetic endoperoxide artemisone *in vitro* and *in vivo*. *Journal of Antimicrobial Chemotherapy*. **59**(4), 658-665.
- Wagner, U., Burkhardt, E. and Failing, K. (1999). Evaluation of canine lymphocyte proliferation: comparison of three different colorimetric methods with the [³H]-thymidine incorporation assay. *Veterinary Immunology and Immunopathology*. **70**(3-4), 151-159.
- Wainwright, M. (2008). Dyes in the development of drugs and pharmaceuticals. *Dyes and Pigments*. **76**(3), 582-589.
- Wainwright, M. and Amaral, L. (2005). Review: The phenothiazinium chromophore and the evolution of antimalarial drugs. *Tropical Medicine & International Health*. **10**(6), 501-511.
- Wang, P., Lee, C.-S., Bayoumi, R., Djimde, A., Doumbo, O., Swedberg, G., *et al.* (1997). Resistance to antifolates in *Plasmodium falciparum* monitored by sequence analysis of dihydropteroate synthetase and dihydrofolate reductase alleles in a large number of field samples of diverse origins. *Molecular and Biochemical Parasitology*. **89**(2), 161-177.
- Wellmann, J., Weiland, S.K., Neiteler, G., Klein, G. and Straif, K. (2006). Cancer mortality in German carbon black workers 1976–98. *Occupational and Environmental Medicine*. **63**, 513-21.
- WHO (2008). A practical handbook on the pharmacovigilance of antimalarial medicines: Geneva, WHO. <http://www.who.int/malaria/publications/atoz/9789241547499/en/index.html> [Accessed 29/11/2013].
- WHO (2010). Guidelines for the treatment of malaria: Geneva, WHO. http://whqlibdoc.who.int/publications/2010/9789241547925_eng.pdf [Accessed 02/11/2012].

WHO (2012). World Malaria Report 2012: Geneva, WHO. http://www.who.int/malaria/world_malaria_report_2011/en/index.html. [Accessed 18/01/2013].

WHO (2013). World Malaria Report 2013: Geneva, WHO. http://who.int/malaria/publications/world_malaria_report_2013/report/en/index.html [Accessed 05/02/2014].

Winstanley, P.A. (2000). Chemotherapy for Falciparum Malaria: The Armoury, the Problems and the Prospects. *Parasitology Today*. **16**(4), 146-153.

Wright, A.D., Wang, H., Gurrath, M., König, G.M., Kocak, G., Neumann, G., *et al.* (2001). Inhibition of Heme Detoxification Processes Underlies the Antimalarial Activity of Terpene Isonitrile Compounds from Marine Sponges. *Journal of Medicinal Chemistry*. **44**(6), 873-885.

Zollinger, H. (1987). Color Chemistry: Syntheses, properties and applications of organic dyes and pigments. VCH Publishers, Weinheim. pp. 1-9, 84-87, 108-109, 305-315, 321-327.

Zoungrana, A., Coulibaly, B., Sie, A., Walter-Sack, I., Mockenhaupt, F.P., Kouyate, B., *et al.* (2008). Safety and Efficacy of Methylene Blue Combined with Artesunate or Amodiaquine for Uncomplicated Falciparum Malaria: A Randomized Controlled Trial from Burkina Faso. *PLoS ONE*. **3**(2), e1630.

Appendices

Appendix A Chemical structures of test compounds

Appendix A1 Nucleoside analogues

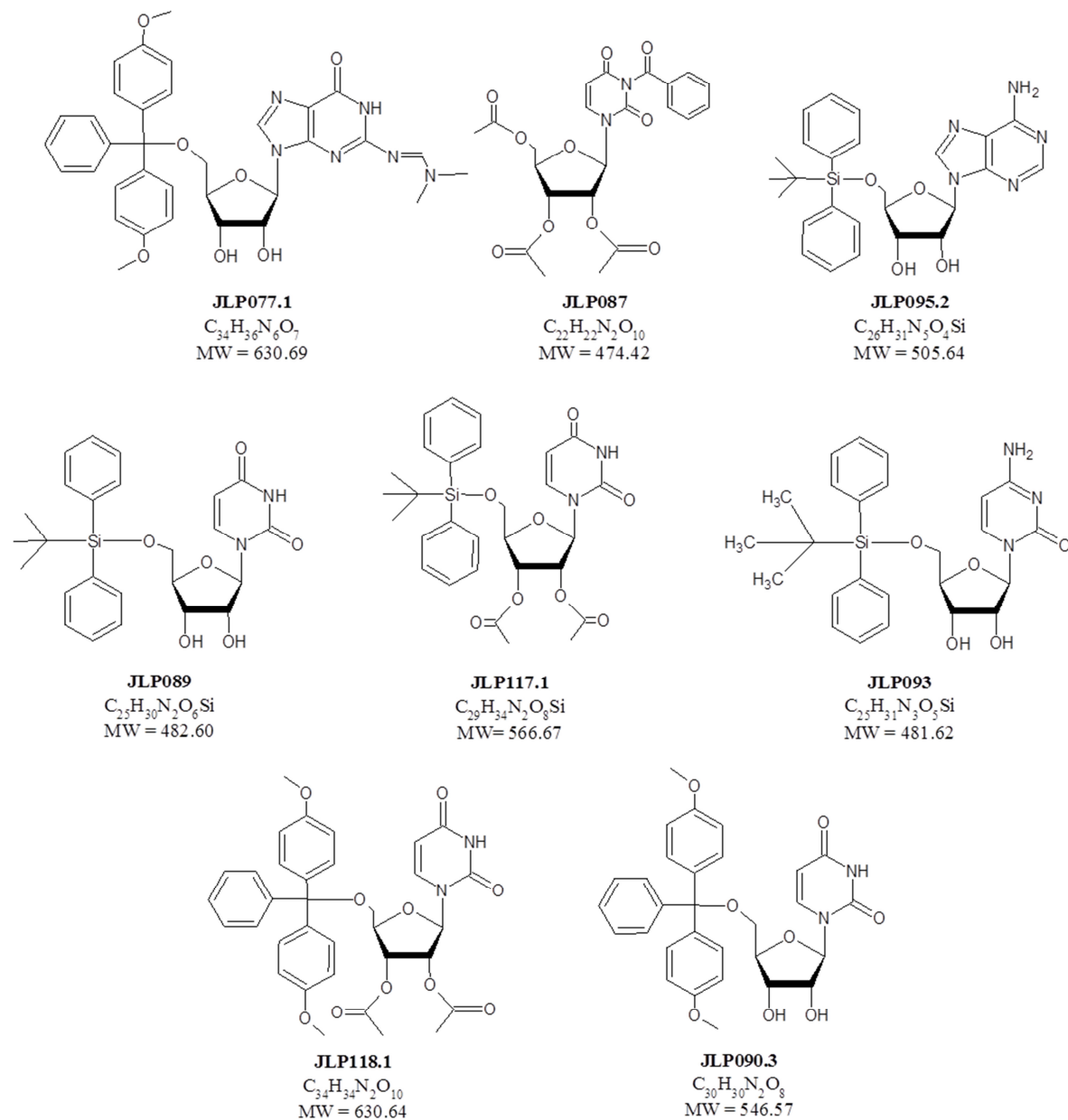


Figure A1 Chemical structures of the nucleoside analogues tested.

Appendix A2 Imidazopyridine analogues

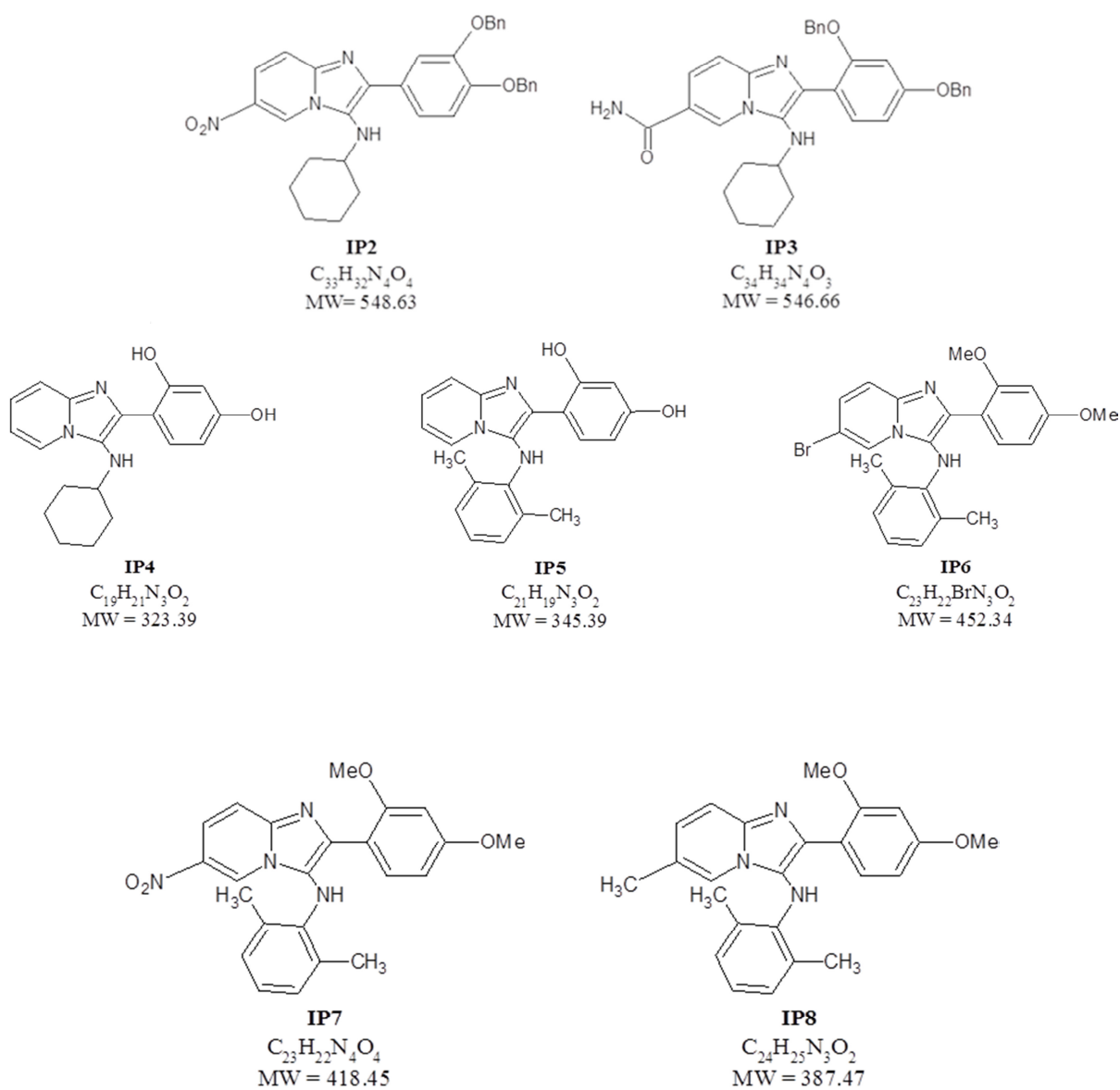


Figure A2 Chemical structures of the imidazopyridine analogues tested.

Appendix A3 Least active synthetic colourants

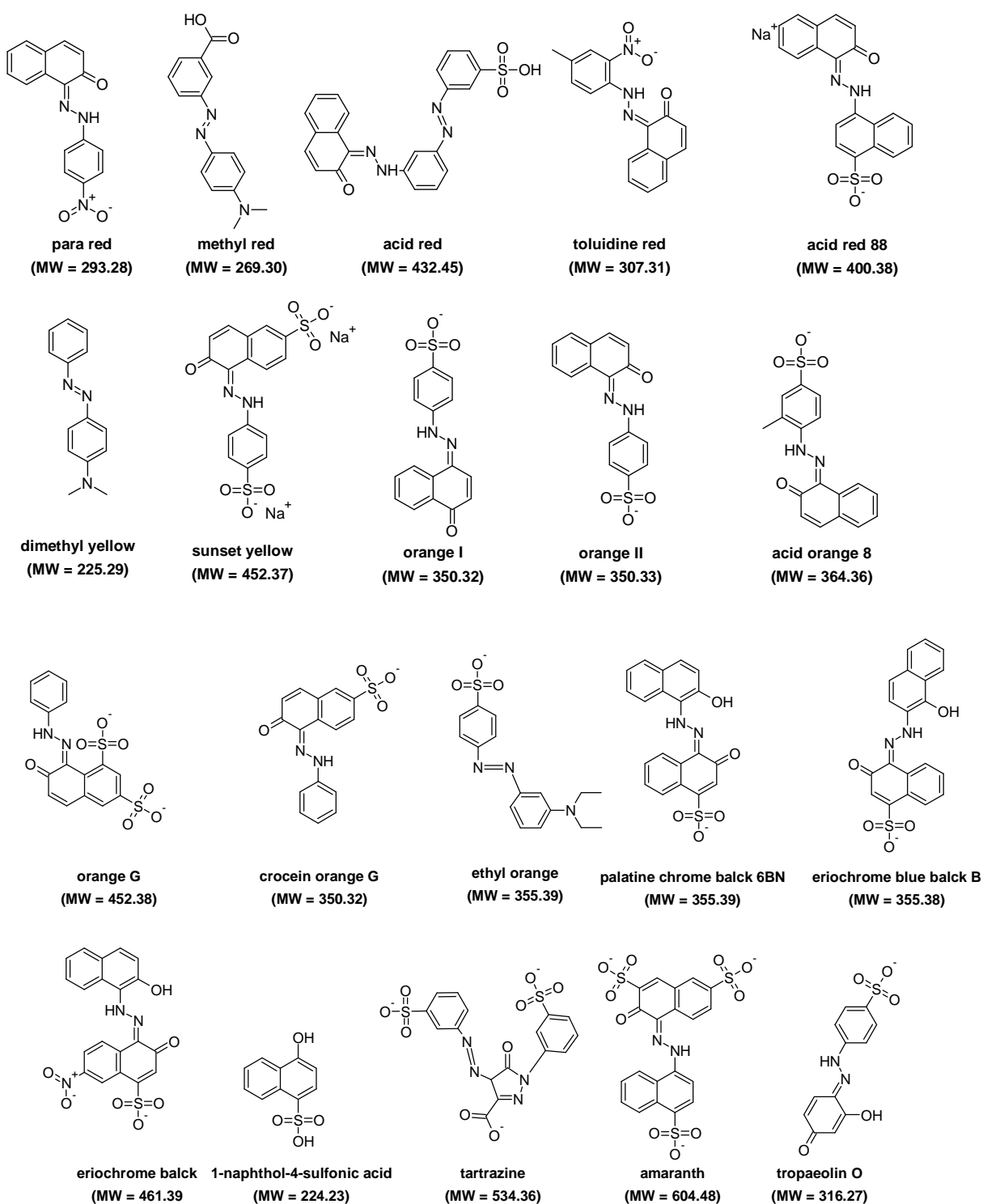


Figure A3.1 Chemical structures of the least active synthetic colourants tested.

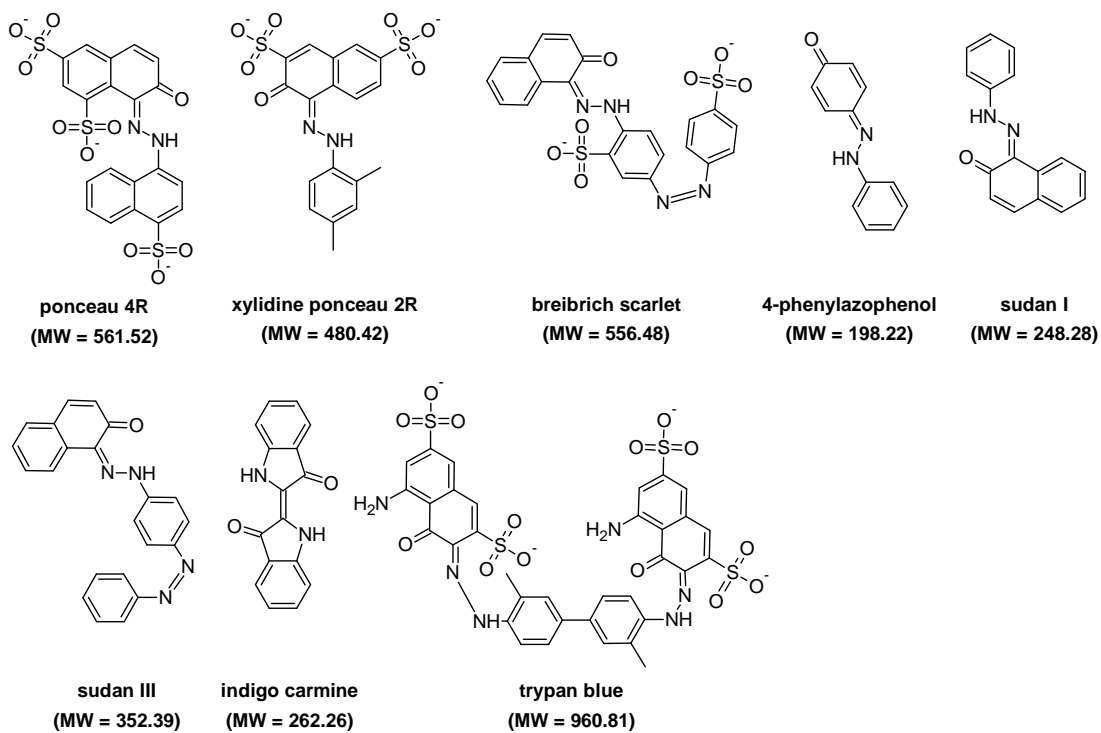


Figure A3.2 Chemical structures of the least active synthetic colourants tested.

Appendix B Biosafety and ethical clearances

Appendix B1 Biosafety clearance for use of *P. falciparum*

UNIVERSITY OF THE WITWATERSRAND, JOHANNESBURG
Research Office

INSTITUTIONAL BIOSAFETY COMMITTEE
(R 14/16)

CLEARANCE CERTIFICATE - RENEWAL

PROTOCOL NUMBER: 20090503

BRIEF DESCRIPTION OF APPLICATION:

Chemotherapeutic properties of novel synthetic and natural compounds

APPLICANT: Dr R van Zyl

SCHOOL/DEPARTMENT : Pharmacy/Pharmacology

DATE CONSIDERED: 20090528

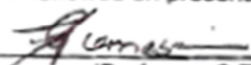
DECISION OF COMMITTEE:

Renewal approved

This clearance certificate expires on 20110501 and may be renewed on presentation of a progress report.

DATE: 20100504

CHAIRPERSON:


(Professor C Tiemessen)

DECLARATION BY APPLICANT:

To be completed in duplicate and one copy returned to the Secretary, Room 10004, 10th floor, Senate House, University.

1. I have read, understood and accepted the approval conditions above
2. I agree to submit a yearly progress report to the Committee and to submit an interim report in the event of any significant unforeseen event, e.g. suspension of a drug trial, temporary closure or relocation of my laboratory, etc
3. I note that the University Safety Officer, or his/her representative, may at any reasonable time inspect my laboratory or trial site to ensure compliance with current Health and Safety legislation. I undertake to offer my full co-operation in any such inspection.
4. I have read, understood and will comply with the *recommended standard operating procedures for the handling of biohazardous materials* posted at <http://web.wits.ac.za/Academic/Research/Biosafety.htm>
5. I declare (delete as appropriate) that:
 - a. I have all the approvals required by statute or regulation and by the funding agencies supporting this work, or
 - b. that I will not begin work until such approvals are obtained

Signed: _____

Date: _____

MSWorks2000\Nain0015\IBCClear\Renew.wps

PLEASE QUOTE THE PROTOCOL NUMBER IN ALL ENQUIRIES

Appendix B2 Ethical clearance for use of human plasma

Human Research Ethics Committee (Medical)

Research Office Secretariat: Senate House Room SH 10005, 10th floor. Tel +27 (0)11-717-1252
Medical School Secretariat: Medical School Room 10M07, 10th Floor. Tel +27 (0)11-717-2700
Private Bag 3, Wits 2050. www.wits.ac.za. Fax +27 (0)11-717-1265



Ref: W-CJ-131030-1

30/10/2013

TO WHOM IT MAY CONCERN:

Waiver: This certifies that the following research does not require clearance from the Human Research Ethics Committee (Medical).

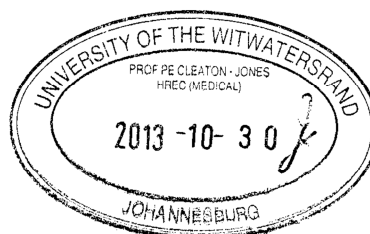
Investigator: Prof R van Zyl.

Project title: The chemotherapeutic properties of novel synthetics and natural compounds.

Reason: This is a laboratory study in which human blood and plasma for the in vitro maintenance of *Plasmodium falciparum* for experimental purposes such as drug sensitivity and toxicity studies. There are no human participants.

A handwritten signature in black ink, appearing to read 'Peter Cleaton-Jones'.

Professor Peter Cleaton-Jones



Chair: Human Research Ethics Committee (Medical)

Copy - HREC(Medical) Secretariat : Anisa Keshav, Zanele Ndlovu.

Appendix B3 Ethical clearance for drawing of human blood from volunteers

UNIVERSITY OF THE WITWATERSRAND, JOHANNESBURG

Division of the Deputy Registrar (Research)

HUMAN RESEARCH ETHICS COMMITTEE (MEDICAL)

R14/49 Dr Robyn L van Zyl

CLEARANCE CERTIFICATE

M090532

PROJECT

The Chemotherapeutic Properties of Novel Synthetic and natural Compounds (Blanket Approval)

INVESTIGATORS

Dr Robyn L. van Zyl.

DEPARTMENT

Department of Pharmacy & Pharmacology

DATE CONSIDERED

09.05.29

DECISION OF THE COMMITTEE*

Approved unconditionally

Unless otherwise specified this ethical clearance is valid for 5 years and may be renewed upon application.

DATE 09.05.29

CHAIRPERSON.....


(Professor F E Cleaton Jones)

*Guidelines for written 'informed consent' attached where applicable

cc: Supervisor : Dr RL van Zyl

DECLARATION OF INVESTIGATOR(S)

To be completed in duplicate and **ONE COPY** returned to the Secretary at Room 10004, 10th Floor, Senate House, University.

I/We fully understand the conditions under which I am/we are authorized to carry out the abovementioned research and I/we guarantee to ensure compliance with these conditions. Should any departure to be contemplated from the research procedure as approved I/we undertake to resubmit the protocol to the Committee. I agree to a completion of a yearly progress report.

PLEASE QUOTE THE PROTOCOL NUMBER IN ALL ENQUIRIES...

.....

Appendix B4 Ethical clearance waiver for use of human cell lines

Human Research Ethics Committee (Medical)
(formerly Committee for Research on Human Subjects (Medical))

Secretariat, Research Office, Room SH10005, 10th floor, Senate House • Telephone: +27 11 717-1234 • Fax: +27 11 339-6708
Private Bag 3, Wits 2050, South Africa

University
of the Witwatersrand,
Johannesburg



Ref: W-CJ-090424-12
29/04/2009

TO WHOM IT MAY CONCERN:

- Waiver:** This certifies that the following research does not require clearance from the Human Research Ethics Committee (Medical).
- Investigator:** Dr R L van Zyl & Mr T H Motau (Student no 9105478D)
- Project title:** The chemotherapeutic properties of synthetic and natural compounds.
- Reason:** This is a wholly laboratory study using commercial cell lines - Graham and K562. There are no humans involved.

A handwritten signature in black ink, appearing to read 'Peter Cleaton-Jones'.



Professor Peter Cleaton-Jones
Chair: Human Research Ethics Committee (Medical)

copy: Anisa Keshav, Research Office, Senate House, Wits

Appendix B5 Biosafety clearance for use of recombinant *Pf*Nek-4 protein kinase



Research Office

INSTITUTIONAL BIOSAFETY COMMITTEE

(R 14/16)

CLEARANCE CERTIFICATE

PROTOCOL NUMBER: 20120701

BRIEF DESCRIPTION OF APPLICATION:

The chemotherapeutic effects of synthetic and natural compounds on plasmodium falciparum

APPLICANT: Dr LJ Harmse

SCHOOL/DEPARTMENT : Therapeutic Sciences/Pharmacy

DATE CONSIDERED: By circulation

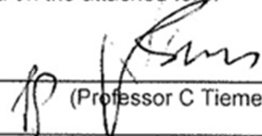
DECISION OF COMMITTEE:

Approved unconditionally

1. This clearance certificate expires on 20170719 and may be renewed on application
2. An annual report must be provided on the anniversary date of this certificate, for as long as the project continues
3. Notification of any proposed modifications must be submitted on the attached form

DATE: 20120720

CHAIRPERSON: _____


(Professor C Tiemessen)

DECLARATION OF APPLICANT:

To be completed in duplicate and **one copy** returned to the Secretary, Room 10005, 10th floor, Senate House, University.

1. I have read, understood and accepted the approval conditions above
2. I agree to submit a yearly progress report to the Committee and to submit an interim report on the form provided, in the event of any significant unforeseen event, e.g. suspension of a drug trial, temporary closure or relocation of my laboratory, etc
3. I note that the University Safety Officer, or his/her representative, may at any reasonable time inspect my laboratory or trial site to ensure compliance with current Health and Safety legislation. I undertake to offer my full co-operation in any such inspection.
4. I have read, understood and will comply with the *recommended standard operating procedures for the handling of biohazardous materials* posted at <http://web.wits.ac.za/Academic/Research/Biosafety.htm>
5. I declare (delete as appropriate) that:
 - a. I have all the approvals required by statute or regulation and by the funding agencies supporting this work, or
 - b. that I will not begin work until such approvals are obtained

Signed: _____

Date: _____

MSWorks2000/Iain0015/IBCCclear.wps

PLEASE QUOTE THE PROTOCOL NUMBER IN ALL ENQUIRIES

Appendix C pGEX 4T-3 Vector map

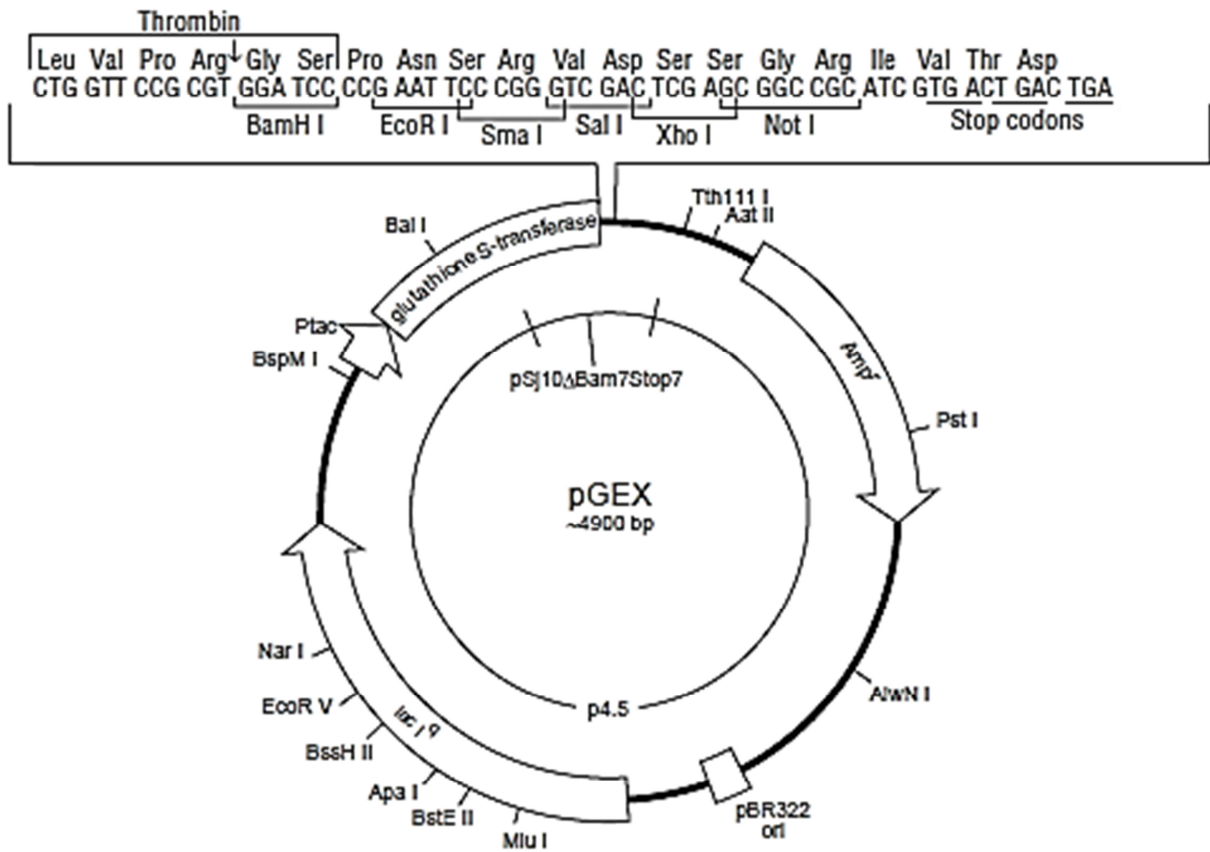


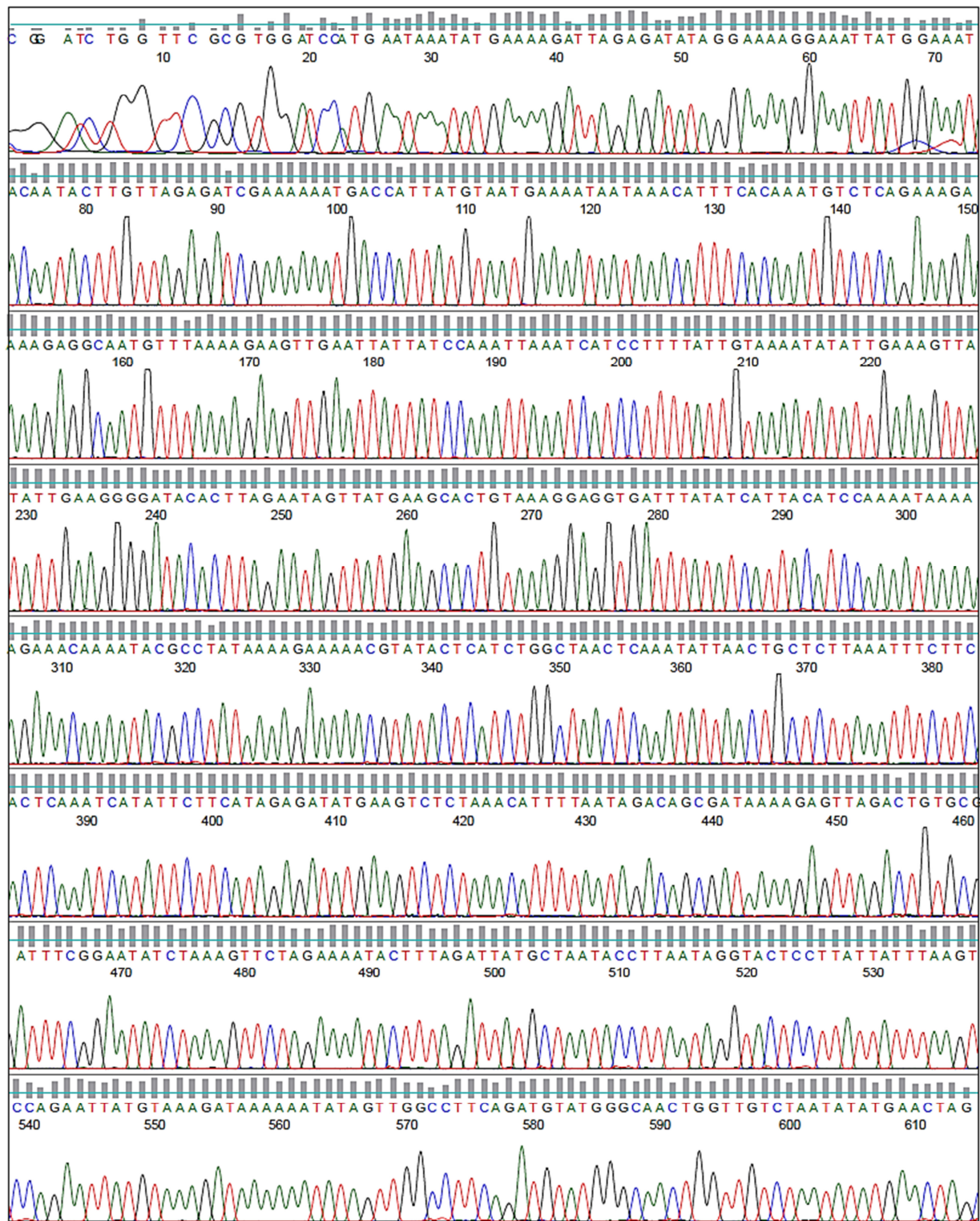
Figure C1 Vector map of pGEX 4T-3 used to construct the GST-*PfNek-4* protein. The GST gene fusion vector has: an ampicillin-resistant gene, Amp; an internal *lac*^I gene to repress expression of target protein in *E. coli* host cell; a *tac* promoter for chemically inducible high-level expression, Ptac; the GST gene; a multiple cloning site with a thrombin protease recognition site as well as *Bam*HI and *Sal*II enzyme restriction sites. (Amersham-Biosciences, 2002)

Appendix D *PfNek-4* nucleotide sequence chromatographs

Appendix D1 *PfNek-4* clone-A forward and reverse nucleotide sequences

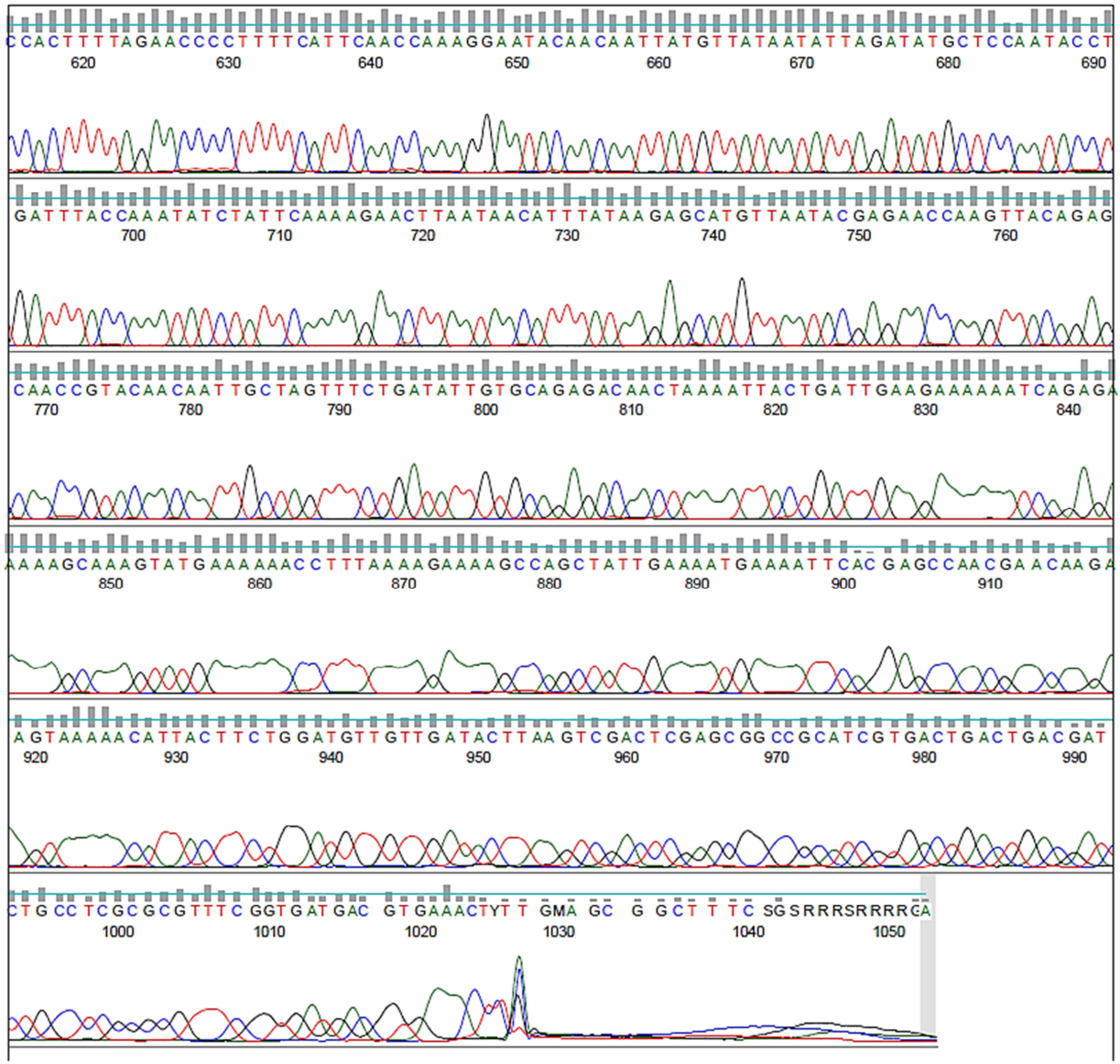
Sample Name: Pfnek4_A_pGEX_5_Seq
Mobility: KB_3500_POP7_BDTv3.mob
Spacing: 11.1984
Comment: n/a

Signal Strengths: A = 2262, C = 1096, G = 1059, T = 2115
Lane/Cap#: 20
Matrix: n/a
Direction: Native



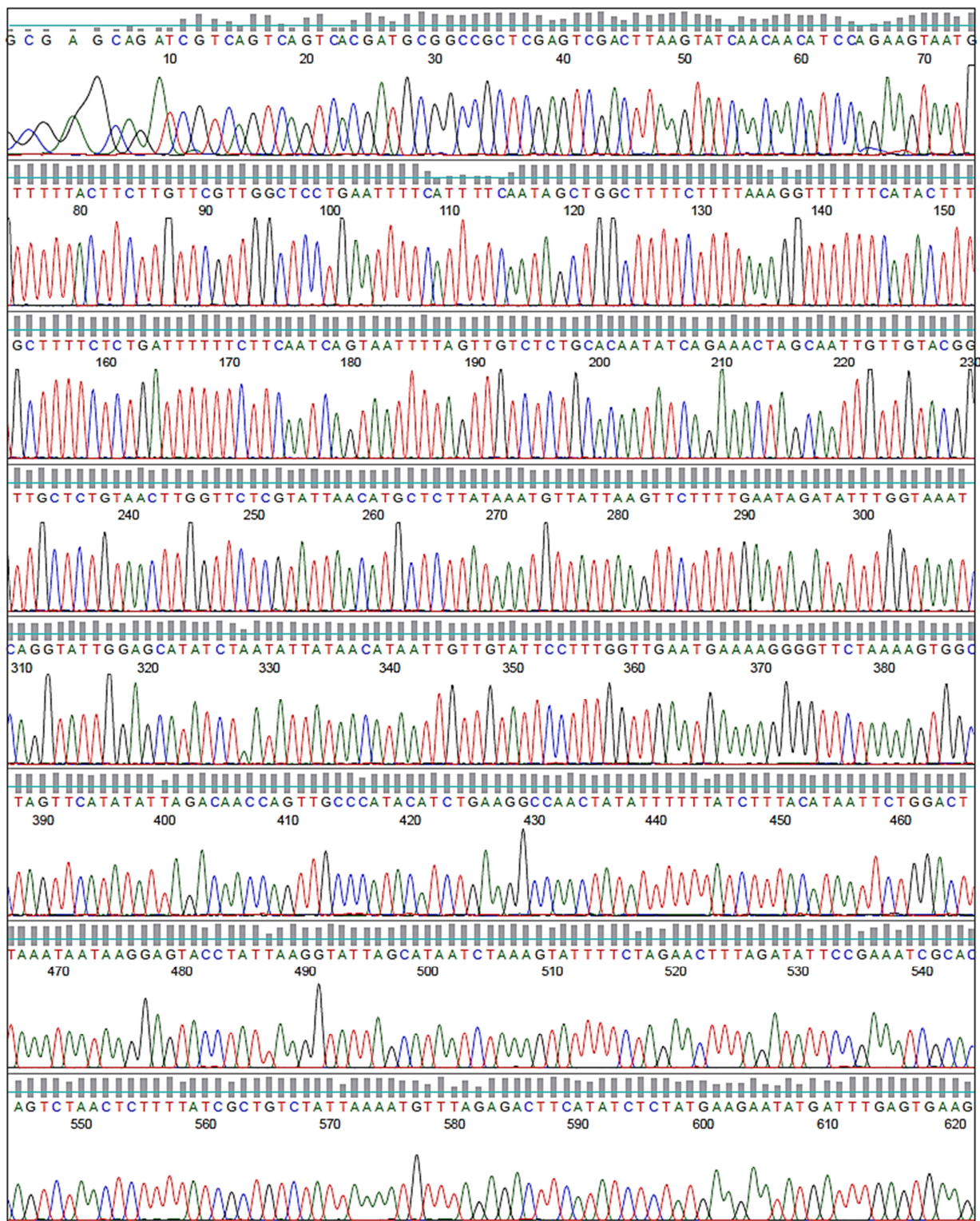
Sample Name: Pfnk4_A_pGEX_5_Seq
Mobility: KB_3500_POP7_BDTv3.mob
Spacing: 11.1984
Comment: n/a

Signal Strengths: A = 2262, C = 1096, G = 1059, T = 2115
Lane/Cap#: 20
Matrix: n/a
Direction: Native



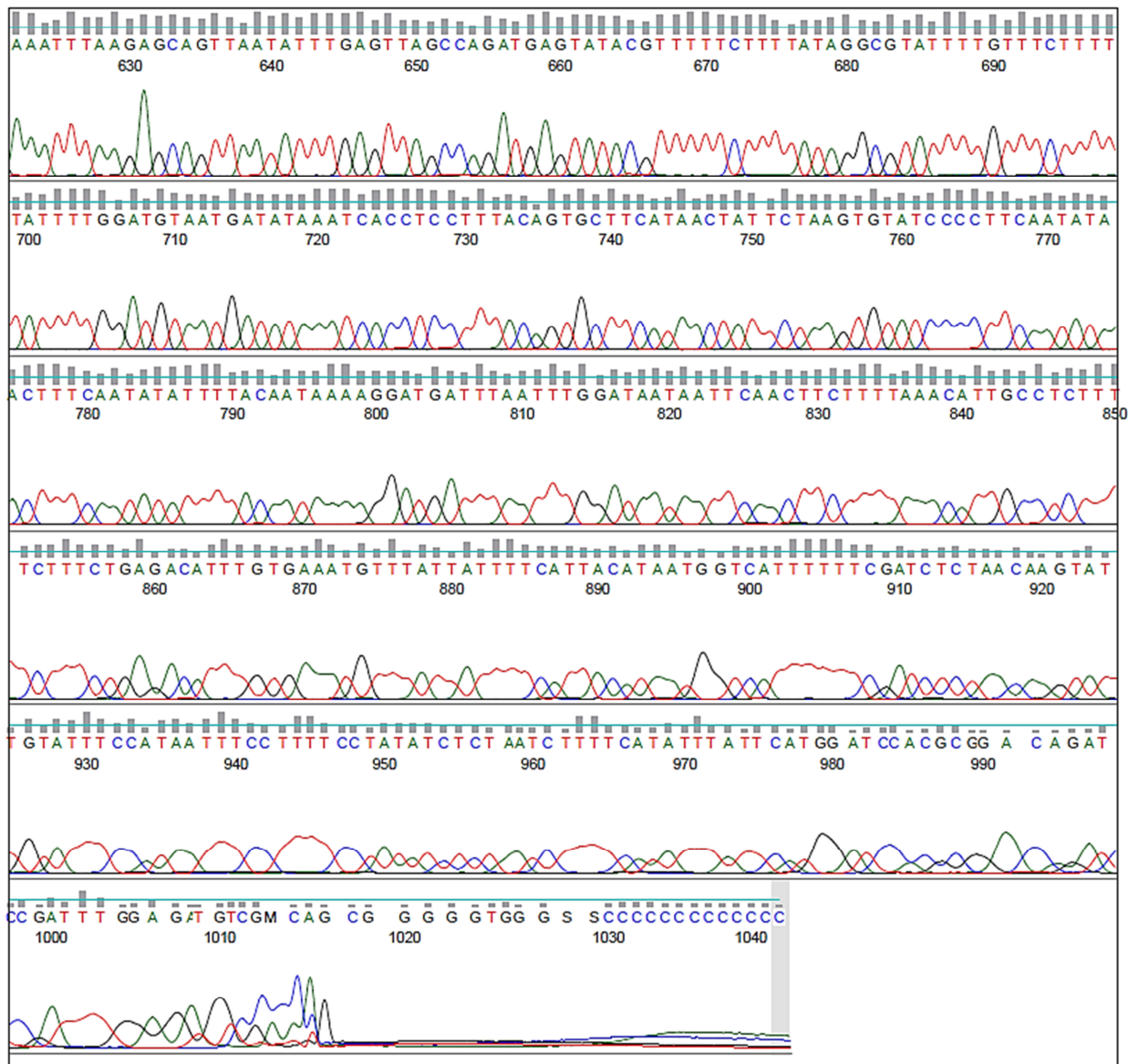
Sample Name: Pfnck4_A_pGEX_3_Seq
Mobility: KB_3500_POP7_BDTv3.mob
Spacing: 11.3788
Comment: n/a

Signal Strengths: A = 2386, C = 1679, G = 1161, T = 4455
Lane/Cap#: 3
Matrix: n/a
Direction: Native



Sample Name: Pfnck4_A_pGEX_3_Seq
Mobility: KB_3500_POP7_BDTv3.mob
Spacing: 11.3788
Comment: n/a

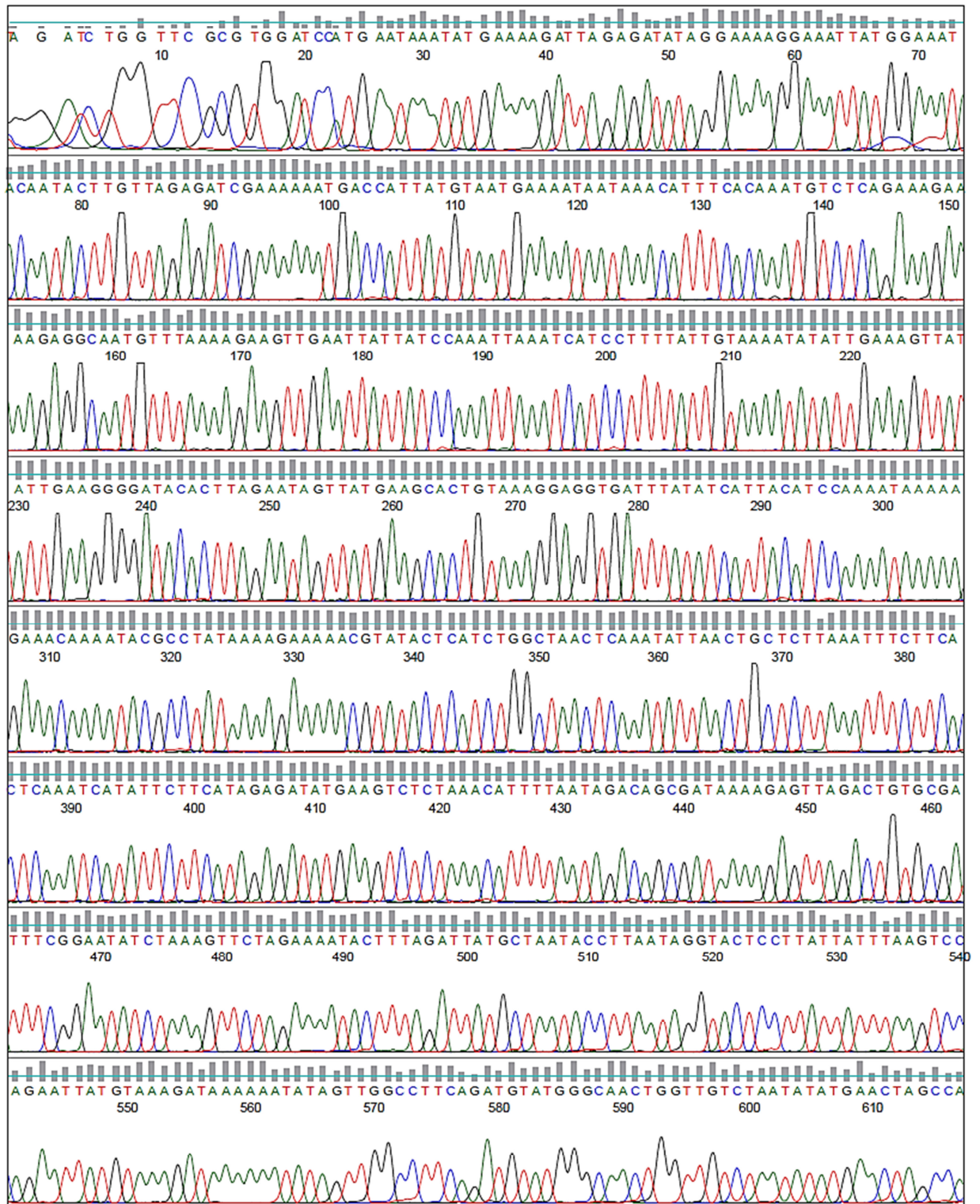
Signal Strengths: A = 2386, C = 1679, G = 1161, T = 4455
Lane/Cap#: 3
Matrix: n/a
Direction: Native



Appendix D2 *PfNek-4* clone-B forward and reverse nucleotide sequences

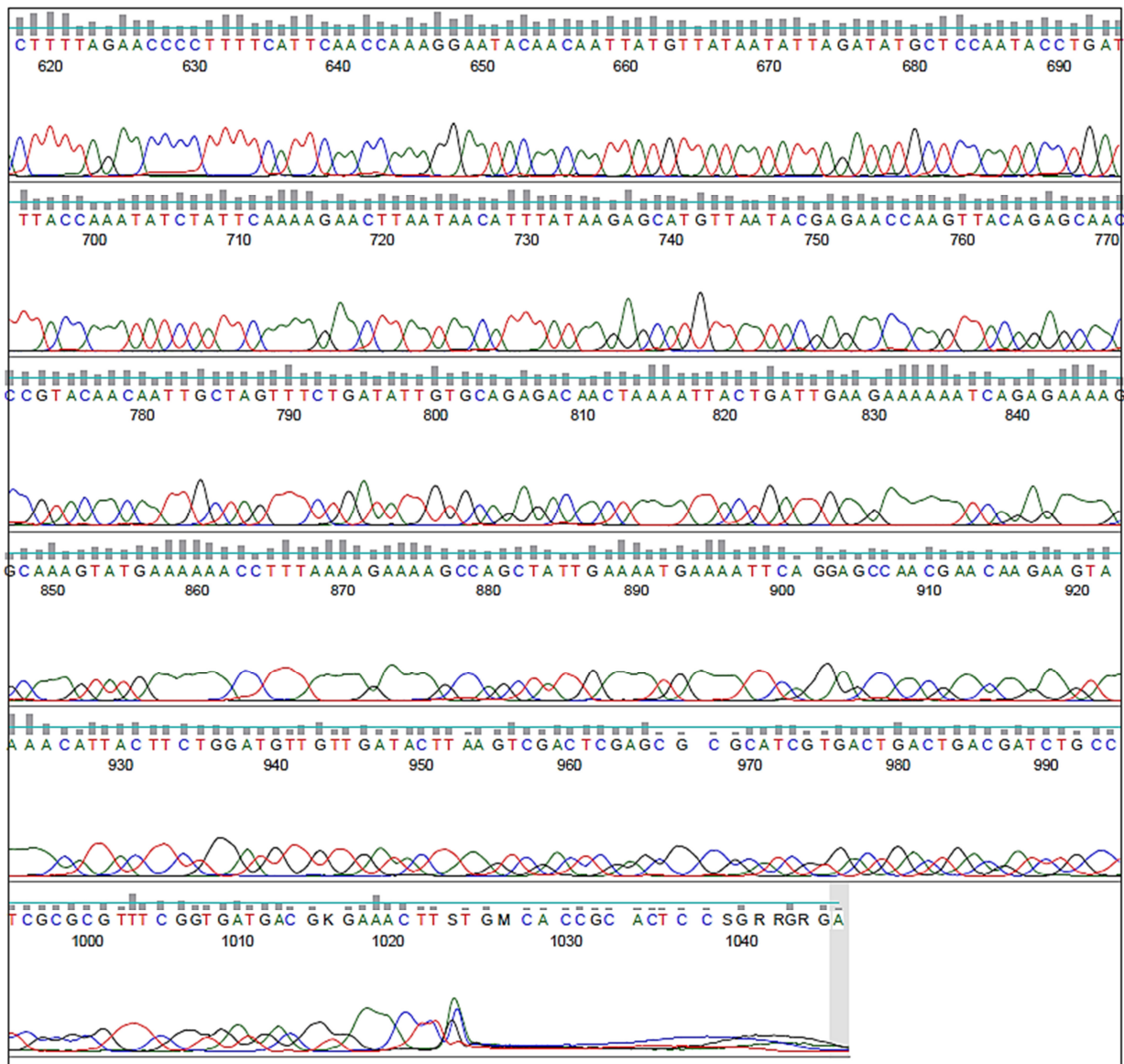
Sample Name: Pfnek4_B_pGEX_5_Seq
 Mobility: KB_3500_POP7_BDTv3.mob
 Spacing: 11.2471
 Comment: n/a

Signal Strengths: A = 1810, C = 877, G = 832, T = 1788
 Lane/Cap#: 23
 Matrix: n/a
 Direction: Native



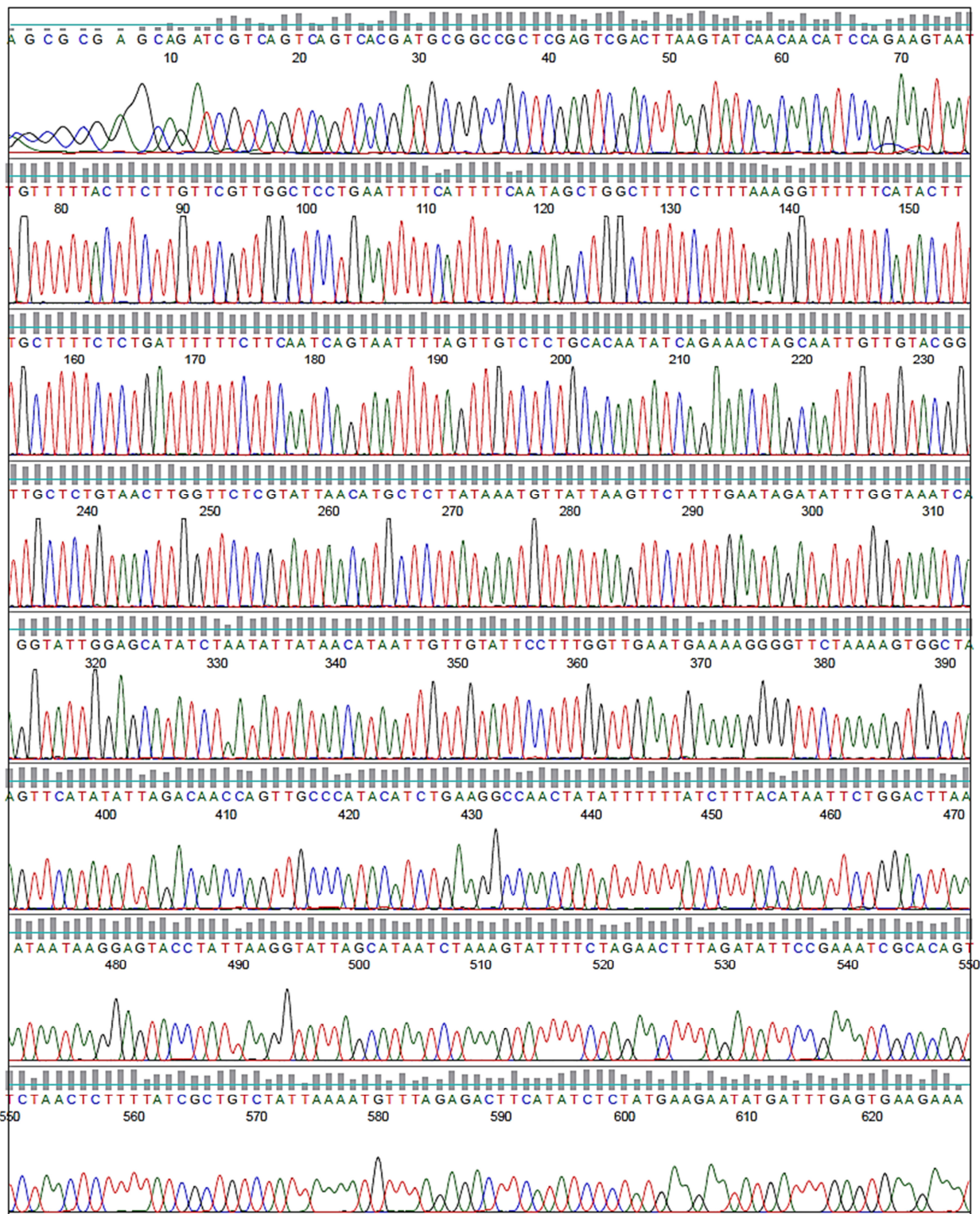
Sample Name: Pfnck4_B_pGEX_5_Seq
Mobility: KB_3500_POP7_BDTv3.mob
Spacing: 11.2471
Comment: n/a

Signal Strengths: A = 1810, C = 877, G = 832, T = 1788
Lane/Cap#: 23
Matrix: n/a
Direction: Native



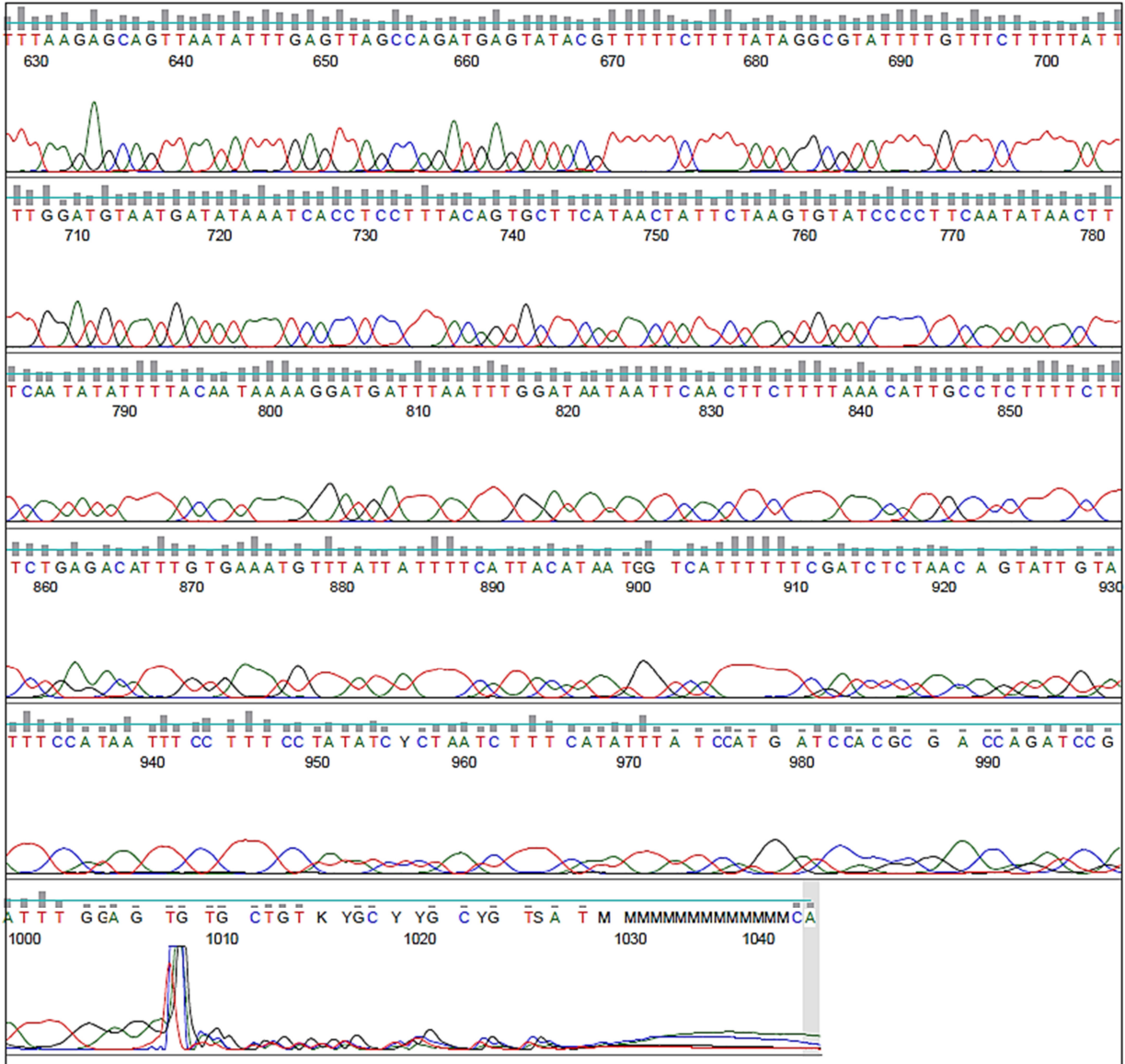
Sample Name: Pfnck4_B_pGEX_3_Seq
Mobility: KB_3500_POP7_BDTv3.mob
Spacing: 11.2867
Comment: n/a

Signal Strengths: A = 2623, C = 2048, G = 1544, T = 3862
Lane/Cap#: 6
Matrix: n/a
Direction: Native



Sample Name: Pfnck4_B_pGEX_3_Seq
Mobility: KB_3500_POP7_BDTv3.mob
Spacing: 11.2867
Comment: n/a

Signal Strengths: A = 2623, C = 2048, G = 1544, T = 3862
Lane/Cap#: 6
Matrix: n/a
Direction: Native



Appendix E *PfNek-4* nucleotide sequence alignments

Appendix E1 *PfNek-4* clone-A consensus sequence alignment

Clone-A	11	ATGAAATAAATATGAAAAGATTAGAGATATAGGAAAAGGAAATTATGGAAATACAATACTT	70
<i>PfNek-4</i>	1	ATGAAATAAATATGAAAAGATTAGAGATATAGGAAAAGGAAATTATGGAAATACAATACTT	60
Clone-A	71	GTTAGAGATCGAAAAATGACCATTATGTAATGAAAATAATAAACATTCACAAATGTCT	130
<i>PfNek-4</i>	61	GTTAGAGATCGAAAAATGACCATTATGTAATGAAAATAATAAACATTCACAAATGTCT	120
Clone-A	131	CAGAAAGAAAAGAGGCAATGTTTAAAAGAAGTTGAATTATTATCCAAATTAATCATCCT	190
<i>PfNek-4</i>	121	CAGAAAGAAAAGAGGCAATGTTTAAAAGAAGTTGAATTATTATCCAAATTAATCATCCT	180
Clone-A	191	TTTATTGTAAATATATTGAAAGTTATATTGAAGGGGATACACTTAGAATAGTTATGAAG	250
<i>PfNek-4</i>	181	TTTATTGTAAATATATTGAAAGTTATATTGAAGGGGATACACTTAGAATAGTTATGAAG	240
Clone-A	251	CACTGTAAAGGAGGTGATTTATATCATTACATCCAAAATAAAAAGAAACAAAATACGCCT	310
<i>PfNek-4</i>	241	CACTGTAAAGGAGGTGATTTATATCATTACATCCAAAATAAAAAGAAACAAAATACGCCT	300
Clone-A	311	ATAAAAGAAAACGTATACTCATCTGGCTAACTCAAATATTAAGTCTCTTAAATTTCTT	370
<i>PfNek-4</i>	301	ATAAAAGAAAACGTATACTCATCTGGCTAACTCAAATATTAAGTCTCTTAAATTTCTT	360
Clone-A	371	CACTCAAATCATATTTTCATAGAGATATGAAGTCTCTAAACATTTTAATAGACAGCGAT	430
<i>PfNek-4</i>	361	CACTCAAATCATATTTTCATAGAGATATGAAGTCTCTAAACATTTTAATAGACAGCGAT	420
Clone-A	431	AAAAGAGTTAGACTGTGCGATTTTCGGAATATCTAAAGTCTAGAAAATACTTTAGATTAT	490
<i>PfNek-4</i>	421	AAAAGAGTTAGACTGTGCGATTTTCGGAATATCTAAAGTCTAGAAAATACTTTAGATTAT	480
Clone-A	491	GCTAATACCTTAATAGGTACTCCTTATTATTTAAGTCCAGAATTATGTAAAGATAAAAAA	550
<i>PfNek-4</i>	481	GCTAATACCTTAATAGGTACTCCTTATTATTTAAGTCCAGAATTATGTAAAGATAAAAAA	540
Clone-A	551	TATAGTTGGCCTTCAGATGTATGGGCAACTGGTTGTCTAATATATGAACTAGCCACTTTT	610
<i>PfNek-4</i>	541	TATAGTTGGCCTTCAGATGTATGGGCAACTGGTTGTCTAATATATGAACTAGCCACTTTT	600
Clone-A	611	AGAACCCCTTTTCATTCAACCAAAGGAATACAACAATTATGTTATAATATTAGATATGCT	670
<i>PfNek-4</i>	601	AGAACCCCTTTTCATTCAACCAAAGGAATACAACAATTATGTTATAATATTAGATATGCT	660
Clone-A	671	CCAATACCTGATTTACCAAATATCTATTCAAAGAACTTAATAACATTTATAAGAGCATG	730
<i>PfNek-4</i>	661	CCAATACCTGATTTACCAAATATCTATTCAAAGAACTTAATAACATTTATAAGAGCATG	720
Clone-A	731	TTAATACGAGAACCAAGTTACAGAGCAACCGTACAACAATTGCTAGTTTCTGATATTGTG	790
<i>PfNek-4</i>	721	TTAATACGAGAACCAAGTTACAGAGCAACCGTACAACAATTGCTAGTTTCTGATATTGTG	780
Clone-A	791	CAGAGACAACTAAAATTAAGTATTGAAAGAAAAATCAGAGAAAAGCAAAGTATGAAAAA	850
<i>PfNek-4</i>	781	CAGAGACAACTAAAATTAAGTATTGAAAGAAAAATCAGAGAAAAGCAAAGTATGAAAAA	840
Clone-A	851	CCTTTAAAAGAAAAGCCAGCTATTGAAAATGAAAATTCAGGAGCCAACGAACAAGAAGTA	910
<i>PfNek-4</i>	841	CCTTTAAAAGAAAAGCCAGCTATTGAAAATGAAAATTCAGGAGCCAACGAACAAGAAGTA	900
Clone-A	911	AAAACATTACTTCTGGATGTTGTTGATACTTAA	943
<i>PfNek-4</i>	901	AAAACATTACTTCTGGATGTTGTTGATACTTAA	933

Appendix E2 *PfNek-4* clone-B consensus sequence alignment

Clone-B	21	ATGAATAAATATGAAAAGATTAGAGATATAGGAAAAGGAAATTATGGAAATACAATACTT	80
PfNek-4	1	ATGAATAAATATGAAAAGATTAGAGATATAGGAAAAGGAAATTATGGAAATACAATACTT	60
Clone-B	81	GTTAGAGATCGAAAAATGACCATTATGTAATGAAAATAATAAACATTCACAAATGTCT	140
PfNek-4	61	GTTAGAGATCGAAAAATGACCATTATGTAATGAAAATAATAAACATTCACAAATGTCT	120
Clone-B	141	CAGAAAGAAAAGAGGCAATGTTTAAAAGAAAGTTGAATTATTATCCAAATTAAATCATCCT	200
PfNek-4	121	CAGAAAGAAAAGAGGCAATGTTTAAAAGAAAGTTGAATTATTATCCAAATTAAATCATCCT	180
Clone-B	201	TTTATTGTAAAATATATTGAAAGTTATATTGAAGGGGATACACTTAGAATAGTTATGAAG	260
PfNek-4	181	TTTATTGTAAAATATATTGAAAGTTATATTGAAGGGGATACACTTAGAATAGTTATGAAG	240
Clone-B	261	CACTGTAAAGGAGGTGATTTATATCATTACATCCAAAATAAAAAGAAACAAAATACGCCT	320
PfNek-4	241	CACTGTAAAGGAGGTGATTTATATCATTACATCCAAAATAAAAAGAAACAAAATACGCCT	300
Clone-B	321	ATAAAAGAAAACGTATACTCATCTGGCTAACTCAAATATTAAGTCTCTTAAATTTCTT	380
PfNek-4	301	ATAAAAGAAAACGTATACTCATCTGGCTAACTCAAATATTAAGTCTCTTAAATTTCTT	360
Clone-B	381	CACTCAAATCATATTCTTCATAGAGATATGAAGTCTCTAAACATTTTAATAGACAGCGAT	440
PfNek-4	361	CACTCAAATCATATTCTTCATAGAGATATGAAGTCTCTAAACATTTTAATAGACAGCGAT	420
Clone-B	441	AAAAGAGTTAGACTGTGCGATTTTCGGAATATCTAAAGTTCTAGAAAATACTTTAGATTAT	500
PfNek-4	421	AAAAGAGTTAGACTGTGCGATTTTCGGAATATCTAAAGTTCTAGAAAATACTTTAGATTAT	480
Clone-B	501	GCTAATACCTTAATAGGTAAGTACTCCTTATTATTAAAGTCCAGAATTATGTAAAGATAAAAA	560
PfNek-4	481	GCTAATACCTTAATAGGTAAGTACTCCTTATTATTAAAGTCCAGAATTATGTAAAGATAAAAA	540
Clone-B	561	TATAGTTGGCCTTCAGATGTATGGGCAACTGGTTGTCTAATATATGAACTAGCCACTTTT	620
PfNek-4	541	TATAGTTGGCCTTCAGATGTATGGGCAACTGGTTGTCTAATATATGAACTAGCCACTTTT	600
Clone-B	621	AGAACCCTTTTTCATTCAACCAAAGGAATACAACAATTATGTTATAATATTAGATATGCT	680
PfNek-4	601	AGAACCCTTTTTCATTCAACCAAAGGAATACAACAATTATGTTATAATATTAGATATGCT	660
Clone-B	681	CCAATACCTGATTTACCAAATATCTATTCAAAAAGAACTTAATAACATTTATAAGAGCATG	740
PfNek-4	661	CCAATACCTGATTTACCAAATATCTATTCAAAAAGAACTTAATAACATTTATAAGAGCATG	720
Clone-B	741	TTAATACGAGAACCAAGTTACAGAGCAACCGTACAACAATTGCTAGTTTCTGATATTGTG	800
PfNek-4	721	TTAATACGAGAACCAAGTTACAGAGCAACCGTACAACAATTGCTAGTTTCTGATATTGTG	780
Clone-B	801	CAGAGACAACCTAAAATTACTGATTGAAGAAAAATCAGAGAAAAGCAAAGTATGAAAAAA	860
PfNek-4	781	CAGAGACAACCTAAAATTACTGATTGAAGAAAAATCAGAGAAAAGCAAAGTATGAAAAAA	840
Clone-B	861	CCTTTAAAAGAAAAGCCAGCTATTGAAAATGAAAATTCAGGAGCCAACGAACAAGAAGTA	920
PfNek-4	841	CCTTTAAAAGAAAAGCCAGCTATTGAAAATGAAAATTCAGGAGCCAACGAACAAGAAGTA	900
Clone-B	921	AAAACATTACTTCTGGATGTTGTTGATACTTAA	953
PfNek-4	901	AAAACATTACTTCTGGATGTTGTTGATACTTAA	933

Appendix F Single-letter amino acid code

Table F1 Single-letter amino acid code.

Amino acid	Abbreviation	
	Three-letter	Single-letter
Nonpolar (hydrophobic)		
Alanine	Ala	A
Proline	Pro	P
Valine	Val	V
Leucine	Leu	L
Isoleucine	Ile	I
Methionine	Met	M
Phenylalanine	Phe	F
Tryptophan	Trp	W
Polar, uncharged		
Glycine	Gly	G
Serine	Ser	S
Threonine	Thr	T
Cysteine	Cys	C
Asparagine	Asn	N
Glutamine	Gln	Q
Tyrosine	Tyr	Y
Basic		
Lysine	Lys	K
Histidine	His	H
Arginine	Arg	R
Acidic		
Aspartate	Asp	D
Glutamate	Glu	E